Synaptic Health in Alzheimer's Disease: Exploring MEG, MRI, and Neuropathology.

Jemma Pitt

St. Cross College

University of Oxford

A thesis submitted for the degree of

Doctor of Philosophy

Hilary Term 2025

Synaptic health in Alzheimer's disease: Exploring MEG, MRI, and Neuropathology.

Jemma Pitt
St. Cross College
Submitted for the degree of DPhil in Psychiatry, Hilary Term 2025

Abstract

Alzheimer's disease (AD) is a neurodegenerative disorder marked by cognitive decline and neuropathological features, including amyloid plaques and tau tangles. Early detection and monitoring are crucial for future interventions, especially given the lack of effective treatments. Traditional biomarkers like PET and lumbar puncture are invasive and do not capture the dynamic functional changes associated with the disease. This thesis explores the potential of Magnetoencephalography (MEG) as a non-invasive biomarker for AD, focusing on synaptic brain health, cognition, and neuropathology.

Utilizing the New Therapeutics in Alzheimer's Disease (NTAD) cohort, comprising biomarker-positive patients and biomarker-negative controls, I investigated resting-state MEG data. Distinct spectral patterns were observed in the eyes-open and eyes-closed conditions. In the eyes-open condition, patients exhibited increased theta activity, decreased alpha/beta activity, and a shift in alpha peak frequency. In the eyes-closed condition, there was an increase in theta activity, a shift in alpha peak frequency, and a decrease in alpha peak amplitude. Test-retest reliability was good to excellent in higher frequency bands, with the eyes-open condition showing better reliability across more sensors. Pathological analysis revealed associations between alpha peak frequency and amyloid/tau and p-tau levels. Both clinical and research-based cognitive tests were significantly associated with the MEG findings. fMRI analysis revealed differences in resting-state networks, including the Default Mode Network (DMN), with distinct relationships to neuropathology and neuropsychological measures. An exploratory analysis comparing MEG and fMRI metrics suggested that MEG may be more closely related to early AD brain alterations.

Overall, these findings provide insights into the potential use of MEG as a biomarker for AD, with the resting-state eyes-open condition emerging as the most reliable. The work contributes to the understanding of how MEG can be applied clinically in AD research, advancing its potential for monitoring disease progression, and informing therapeutic interventions.

Acknowledgements

This thesis brings to a close five busy and formative years of my life, and I am extremely grateful to those who made it possible. Firstly, I would like to thank my supervisors, Mark Woolrich, Kia Nobre, Andrew Quinn, and Mats Van Es, for their guidance and support, with special thanks to Andrew and Mats for advice and support on the MEG analysis. I am also very grateful to Nico for your help with the fMRI analysis.

I am grateful to my colleagues that made my life in Oxford so special, particularly Tony Thayanandan and Lara Bolte, who provided constant support, laughter, and encouragement. To my fabulous friend Caroline, thank you for always being there for me.

I am also thankful to Nicky Aikin and Juliet Semple for the opportunity to train as an MRI scan operator, a role I thoroughly enjoyed. I am also thankful to Anna Camera and Sven Braeutigam for the many hours we spent together in the MEG lab. I would also like to thank all the participants who took part in this research. I am deeply grateful for their time and patience.

To my parents, who have always believed in me and supported me. I have always strived to make you proud, and this achievement is at much yours as it is mine. Your love, encouragement, and belief in me has meant everything.

I would also like to acknowledge my Grandad Dampie, who always believed in my dream of studying at Oxford and even offered to drive me to the University Open Day while in hospital, despite not having driven for many years due to his dementia. I hope this work honours your support and inspiration. To my Nan Jeanie, who recently passed after suffering from Alzheimer's, I hope that future research may spare others from the same suffering. I dedicate this thesis to both of you.

Finally, to the family that came into being over the course of this thesis. To my husband, Thaine, who became part of my life just as I started my DPhil journey, thank you for your constant support, love, and patience. To our beautiful daughter, Lily. You have brought so much joy into our lives. I hope this work inspires you and reminds you that anything is possible if you put your mind to it. And to our soon-to-arrive son, welcome to a family of scientists! I can't wait to meet you and share the future with you.

Declarations

Data presented in Chapters 4, 5 & 6 were collected during my time as a research assistant and DPhil student. I completed the recruitment and data collection of all Oxford participants with support from other members of the Brain and Cognition Lab.

MEG data analysis was completed in collaboration with Dr Andrew Quinn and Dr Mats Van Es. I pre-processed and analysed NTAD data based on the metrics computed from their pipelines.

Table of Contents

List of abbreviations

Aβ	Amyloid-beta
ACE-R	Addenbrookes Cognitive Examination Revised
AChE	Acetylcholinesterase Inhibitors
AEC	Amplitude Envelope Correlation
AD	Alzheimer's disease
ADNI	Alzheimer's Disease Neuroimaging Initiative
ARSAC	Administration of Radioactive Substances Advisory Committee
ASL	Arterial Spin Labelling
ANOVA	Analysis of Variance
APP	Amyloid-Precursor Protein
APOE	Apolipoprotein E
BBB	Blood-Brain-Barrier
BET	Brain Extraction Tool
BOLD	Blood Oxygen Level Dependent
CANTAB	Cambridge Neuropsychological Test Automated Battery
CDR	Clinical Dementia Rating
COPE	Contrast of Parameter Estimate
CRF	Clinical Research Facility
CRN	Clinical Research Network
CSF	Cerebral Spinal Fluid
CT	Computed Tomography
DAN	Dorsal Attention Network
DFP	Deep and Frequent Phenotyping
DMN	Default Mode Network
ECG	Electrocardiogram
EEG	Electroencephalography
ELISA	Enzyme-Linked Immunosorbent Assay
EOG	Electrooculogram
EPAD	European Prevention for Alzheimer's Disease
ERD	Event-Related Desynchronisation
FCSRT	Free and Cued Selective Reminding Test
FDA	Food and Drug Administration
FEAT	FMRIB's Expert Analysis Tool

FIRST	FMRIB's Automated Model-Based Segmentation Tool
FIX	FMRIB's ICA-Based X-Noiseifier
FLIRT	FMRIB's Linear Image Registration Tool
fMRI	Functional MRI
FNIRT	FMRIB's Non-Linear Image Registration Tool
FOOOF	Fitting Oscillations & One-Over F
FSL	FMRIB's Software Library
GDS	Geriatric Depression Scale
GLM	General Linear Model
GPCOG	GP Assessment of Cognition
HPI	Head Position Indicator
HRA	Health Research Authority
ICA	Independent Component Analysis
ICC	Intraclass Correlation Coefficient
IWG	International Working Group
iADL	Instrumental Activities of Daily Living
JDR	Join Dementia Research
LWD	Lewy-Body Dementia
LFP	Local Field Potential
LP	Lumbar Puncture
MBI-C	Mild Behavioural Impairment Checklist
MCI	Mild Cognitive Impairment
MEG	Magnetoencephalography
MELODIC	Multivariate Exploratory Linear Optimised Decomposition into Independent Components
MMSE	Mini Mental State Examination
MOCA	Montreal Cognitive Assessment
MRC	Medical Research Council
MRI	Magnetic Resonance Imaging
MTL	Medial Temporal Lobe
NART	National Adult Reading Test
NDMA	N-Methyl-D-Aspartate
NFT	Neurofibrillary Tangles
NTAD	New Therapeutics in Alzheimer's Disease
OHBA	Oxford Centre for Human Brain Activity
OPM	Optically Pumped Magnetometers

OSL	OHBA Software Library
PET	Positron Emission Topography
PIS	Participant Information Sheet
PSD	Power Spectral Density
PSQI	Pittsburgh Sleep Quality Index
RBANS	Repeatable Battery for the Assessment of Neuropsychological Status
REC	Research Ethics Committee
ROI	Region of Interest
SHINE	Synaptic Health in Neurodegeneration
STAIT	State-Trait-Anxiety-Inventory
STFT	Short Time Fourier Transform
SUVR	Standardised Uptake Value Ratio
TE	Echo Time
TR	Repetition Time
tSSS	Temporally Extended Signal Space Separation
VAN	Ventral Attention Network
WBIC	Wolfson Brain Imaging Centre
WHO	World Health Organisation

Chapter 1: Overview and Objectives

Identifying and delaying the onset of symptoms in Alzheimer's Disease (AD) is crucial for future progress. Currently, AD remains an incurable illness that profoundly affects patients and their families, whether witnessing a loved one struggle with dementia or experiencing the anxiety of losing one's own memories. By 2050, it is projected that 139 million people worldwide will have dementia due to the aging population (WHO, 2023). AD accounts for 60–80% of these cases, making it the most prevalent form of this dementia globally (World Alzheimer's Report, 2021). Dementia is not a normal part of aging but is one of the greatest unmet medical needs, costing the economy £26 billion annually (Prince et al., 2014).

A significant challenge in AD research is the high rate of failed medication studies. Over the past 40 years, more than 100 substances investigated as potential treatments for AD have either failed or been abandoned during development (Mehta et al., 2017). This is largely because treatments have focussed on individuals already showing symptoms, despite evidence that the disease may have been present and undetected for decades (Bateman et al., 2012). Therefore, improving the ability to detect and potentially prevent AD relies on more accurate, reliable, and earlier measures of cognitive decline.

Finding biomarkers, or medical indicators of disease, is a promising area of AD research. Amyloid and tau levels in the brain, which are biological markers of AD, can be measured using Positron Imaging Topography (PET) scans and cerebrospinal fluid (CSF) analysis. Although these methods provide valuable information, they are relatively invasive as PET requires exposure to a radioactive tracer, and CSF collection involves lumbar puncture, which can be uncomfortable and carries certain risks. In contrast, Magnetic Resonance Imaging (MRI) is non-invasive and widely used to detect structural brain changes, such as hippocampal atrophy, and is incorporated into clinical diagnostic criteria in some settings (Frisoni et al., 2010). However, while PET and CSF can detect molecular changes early in the disease course, the structural changes visible on MRI typically reflect later stages of neurodegeneration, when substantial neuronal loss has already occurred. Thus, by the time abnormalities are seen on MRI, interventions aimed at the disease may be less effective. This sequence of biomarker sensitivity is demonstrated in Figure 1.1, which shows amyloid levels detectable long before the onset of atrophy and cognitive decline.

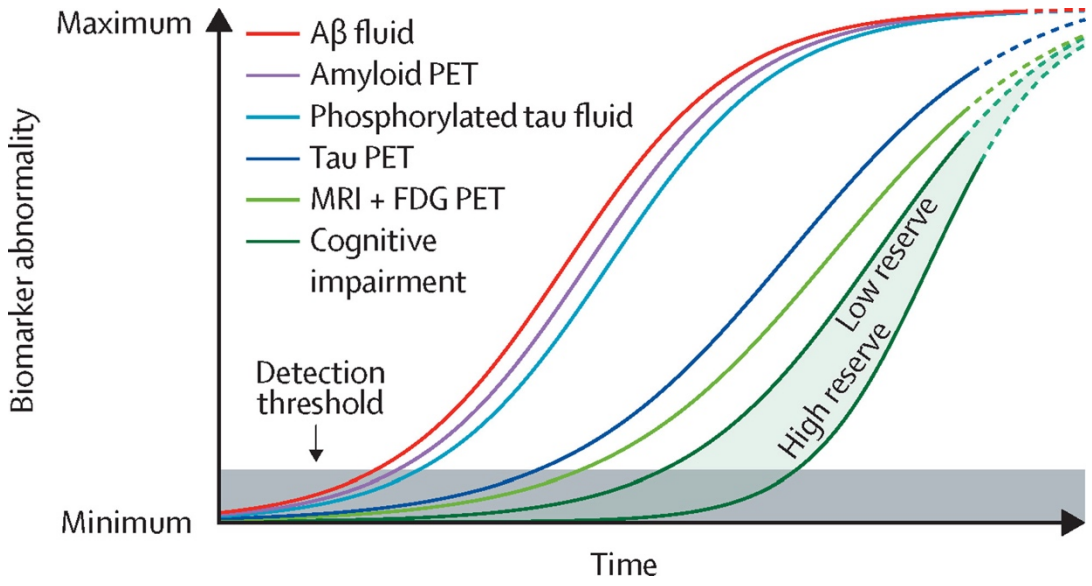

Figure 1.1. Sequence of biomarker sensitivity.

Figure from (Jack Jr et al., 2024).

Given these limitations, there is an urgent need to develop tools that can identify brain dysfunction at an earlier, preclinical stage that can detect brain changes before significant neuronal loss occurs. Magnetoencephalography (MEG) and electroencephalography (EEG) offer potential solutions as they provide direct insights into synaptic and network dynamics and can identify and track the deterioration of neuronal communication. This makes MEG particularly valuable for tracking early-stage AD progression, as it can assess synaptic dysfunction long before structural changes or cognitive decline become apparent. Increasing evidence shows that amyloid-beta and tau proteins, pathological hallmarks of AD, accumulate years before symptom onset (Long & Holtzman, 2019; Price & Morris, 1999). However, there has been limited research exploiting the physiological differences and markers of disease progression using M/EEG, and how this may fit into the sequence of biomarker sensitivity.

My DPhil will address this gap by examining AD-related brain changes and their connection to neuropathology using multi-modal MEG, MRI, and neuropathological data from the New Therapeutics in Alzheimer's Disease (NTAD) study. NTAD offers a novel opportunity to combine functional brain activity measures with neuropsychological assessments and biological measures to identify new biomarkers.

In the following chapters, I address this objective by answering five main questions:

1.1 What do we know about the neuropathology of AD?

In **Chapter 2** of this thesis, I review the existing knowledge on the neuropathology of AD and outline the key neuropathological events that characterise AD; the amyloid cascade hypothesis and the tau hyperphosphorylation hypothesis. I explore how these mechanisms can be investigated using imaging modalities such as MRI, PET, functional MRI (fMRI), and MEG. Emphasising the need for a more direct link to synaptic brain activity to understand the relationship between neuronal alterations and cognitive decline, I propose MEG as a powerful tool to achieve this. I conclude by presenting recent work that demonstrates the association between neuropathological markers and distinct MEG findings. This chapter sets the stage for my thesis by discussing the limitations of AD population research and highlighting the advantages of the NTAD study.

1.2 What study cohort could be used to investigate MEG in AD?

I provide an overview of the NTAD study participants and neuroimaging methods used in this thesis in **Chapter 3.** The NTAD study includes carefully selected biomarker-positive patients and biomarker-negative controls, addressing the limitation of including "probable AD" patients in research. This study incorporates data from multiple sites, including the University of Cambridge and University of Oxford. Notably, the data from the Oxford site was collected as part of this DPhil project. This overview provides important context for interpreting the neuroimaging findings presented in later chapters and highlights the methodological strengths of the NTAD study in the context of AD cohorts. I presented an overview of the NTAD study at the Alzheimer's Research Thames Valley Research Day and won **"Best Flash Talk"**.

1.3 What distinguishes normal ageing from AD?

Extensive literature has documented the structural and cognitive differences between AD patients and healthy controls. In **Chapter 4**, I validate the NTAD cohort and discuss the observed structural, cognitive, and pathological differences. Clinical and research-based tests are also explored, with the aim of identifying which assessments better capture AD-related

changes. This chapter presents both expected and novel findings from structural, neuropathological, and cognitive measures.

In **Chapter 5,** I focus on MEG data, introducing the power spectra and GLM-Spectrum that was used for analysis. I use resting-state data, which is when participants are not engaged in a specific task, but instead quietly resting with their eyes open or closed. This approach allows for the investigation of spontaneous neural activity. Importantly, resting-state recordings are particularly well-suited to clinical research in AD, as they are less demanding for participants. In addition, analysis focused solely on sensor-level data. Given that this thesis is grounded in the clinical application of AD research, particular attention was paid to using analysis methods that are accessible, interpretable, and ultimately translatable to clinical settings.
I evaluate the differences in the power spectra between biomarker-positive patients and biomarker negative controls and address the claim that AD patients exhibit unique brain changes distinct from general ageing. This includes how MEG metrics relate to cognitive and neuropathological markers, making it a unique and comprehensive analysis. These results have been presented in multiple conferences and won **"Best Poster"** at MEGUK.

To complement the MEG findings, **Chapter 6** presents an analysis of resting-state fMRI data from the same NTAD participants. Using Independent Component Analysis (ICA), I compare large-scale brain network connectivity between patients and controls and investigate associations with cognitive performance and biomarker profiles.

Together, these chapters aim to disentangle the effects of normal ageing from AD-specific changes, shedding light on the unique neuropathological and cognitive features of the disease. The underlying aim of all analyses is to produce clinically relevant research by combining well-established clinical methods with more exploratory, research-based approaches.

1.4 Are MEG measures of AD reliable?

An important area of MEG research in AD is assessing whether electrophysiological measures are reliable over time. Whilst structural measurements of AD-related brain changes are generally considered reliable, there is comparatively less data on the test-retest reliability of MEG metrics. Therefore, as part of my analysis in Chapter 4, I use Intraclass Correlation

Coefficient (ICC) analysis to evaluable the reliability of participants' data across a baseline and two-week follow-up scan. In addition, a key aspect of this analysis involves comparing the eyes open versus eyes closed conditions. While both of these conditions are frequently used in MEG and EEG research, their impact on the reliability of the recording remains under-explored, particularly in clinical populations such as AD patients. This is particularly important in the context of clinical research, as reliable electrophysiological measures are essential if MEG is to be used for tracking disease progression or monitoring responses to therapeutic interventions.

1.5 Are there any differences between MEG and fMRI results?

In **Chapter 6** of my thesis, I present a unique comparative analysis of MEG and fMRI data to explore how these two modalities differ in capturing functional brain changes in AD. Given that MEG and fMRI measure distinct aspects of neural activity, this comparison provides valuable insight into the complementary strengths of each technique. As this thesis centres on the potential as MEG as a biomarker tool, it was particularly important to examine how MEG and fMRI metrics relate to key neuropathological markers of AD.

Overall, this thesis aims to provide a comprehensive examination of the potential of MEG as a biomarker for AD. By integrating structural, cognitive, pathological, and neuroimaging data from the NTAD cohort, it highlights the distinctive neural and neuropathological changes associated with AD, differentiating them from normal ageing. Through my analyses, including the validation of the NTAD cohort, investigation of the resting-state MEG and fMRI data, comparison of clinical and research-based cognitive test, and exploration of the test-retest reliability of MEG data, this work contributes to the understanding and clinical application of these data in AD research.

1.6 Summary of objectives

Objective 1: To outline the neuropathology of AD and introduce the NTAD study

1. What do we know about the neuropathology of AD? Chapter 2
2. What study cohort could be used to investigate MEG in AD? Chapter 3

Objective 2: To explore MEG signatures of AD and compare with fMRI

3. What distinguishes normal ageing from AD? Chapters 4,5,6
4. Are MEG measures of AD reliable? Chapter 5
5. Are there any differences between MEG and fMRI results? Chapter 6

Chapter 2: The Neuropathology of AD

This chapter reviews the primary neuropathological events that characterise AD, the current available diagnosis recommendations and treatments, and a range of imaging modalities that can be used to measure and track the disease's progression. I conclude by addressing the importance of non-invasive imaging techniques and setting the stage for my thesis.

2.1 Introduction

Alzheimer's disease (AD) is a progressive neurodegenerative disorder primarily characterised by memory impairment, particularly affecting episodic and declarative memory (Squire et al., 2004). Episodic memory, which involves the recall of specific personal experiences, is typically more impaired early in the disease, while semantic memory, or general knowledge about the world, is relatively preserved (Moscovitch et al., 2006). Over the years, substantial research efforts have aimed to improve diagnostic accuracy and advance treatment development for AD by gaining a deeper understanding of the disease underlying neuropathological changes. Amyloid plaques and neurofibrillary tangles (NFTs) are believed to be the two main neuropathological characteristics associated with AD. Since direct neuropathological examination of brain tissue is only possible post-mortem, establishing the direct sequence of events in the disorder has been challenging. However, imaging techniques such as Magnetic Resonance Imaging (MRI) and Positron Emission Topography (PET) scans, have helped bridge this gap by measuring critical brain structures and proteins implicated in AD (Kolanko et al., 2020; McKhann et al., 2011). Additionally, cerebral spinal fluid (CSF) analysis via lumbar puncture allows for the detection of proteins surrounding the brain, including the pathological markers amyloid-beta and tau.

In 2007, the International Working Group (IWG) was the first to propose the addition of biomarkers into AD diagnostic criteria to facilitate earlier detection of the disease (Dubois et al., 2007). The availability of biomarkers through CSF and amyloid-PET significantly advanced both observational and interventional research, as these methods could confirm AD pathology. However, during the National Institute of Aging conference in 2012, neuropathologists emphasised that neuropathological changes were insufficient for a diagnosis, as many post-mortem studies show AD pathological changes in individuals who had not

exhibited cognitive or functional decline during their lifetimes (McKhann et al., 2011; J. Morris, 1997).

This perspective remained dominant until recently, when the Alzheimer's Association Working Group recently updated the criteria to base AD diagnoses solely on one core AD biomarker (amyloid or tau pathology), without requiring evidence of cognitive impairment (Jack Jr et al., 2024). In the clinical setting, this change would enable the diagnosis of cognitively normal individuals with AD, sometimes decades before symptom onset, if at all. In response, the IWG revised its approach, recommending that cognitively normal patients who test positive for amyloid but lack cognitive or functional impairment be classified as "at-risk" for AD rather than diagnosed with the disease itself.

Imaging techniques have been instrumental in advancing our understanding of AD pathology and remain central to ongoing research effects, alongside biological laboratory research. Modalities such as MRI and PET have provided invaluable insights into structural and molecular changes, including brain atrophy and the accumulation of amyloid and tau proteins. Functional MRI (fMRI) has been widely used to measure changes in brain activity by assessing blood flow, providing a functional perspective on how AD affects neural networks. However, non-invasive imaging methods like MEG and EEG have emerged as powerful tools for studying dynamic brain activity and offer a more direct measurement of neural activity with superior temporal resolution compared to fMRI. Because of this, advancements in the application of imaging modalities such as MEG and EEG, can offer new insights into the large-scale activity within specific brain regions and networks implicated in AD. Thus, this chapter explores the pathogenic processes underpinning AD, current available treatments, and how non-invasive imaging data can enhance our understanding of the disease for future research.

2.2 Pathology

Distinct macroscopic changes characterise the AD brain compared with healthy aging. Most notably, there is increased sulci spacing and atrophy of the gyri in the frontal and temporal cortices, accompanied by a reduction in overall brain size. Among these changes, the medial temporal lobe, encompassing the hippocampus and amygdala, exhibits pronounced atrophy, often accompanied by enlarged temporal horns (Apostolova et al., 2012; Jack et al., 1998). The

entorhinal cortex and hippocampus are among the earliest and most affected regions, with reduced volumes of these areas serving as sensitive predictors of AD development (Jack et al., 2011). Two fundamental hypotheses underlie these pathogenic alterations: the amyloid cascade hypothesis and the tau hyperphosphorylation hypothesis, which will be discussed in detail below.

2.2.1. The amyloid cascade hypothesis

The amyloid hypothesis, initially proposed by John Hardy and David Allsop (Hardy & Allsop, 1991), gained prominence with the discovery of beta-amyloid (Aβ) in the peptide sequence (Glenner & Wong, 1984). According to this theory, beta secretase facilitates the formation of Aβ from the amyloid-precursor protein (APP), initiating the accumulation of misfolded proteins central to AD pathology (Haass & Selkoe, 2007) (refer to Figure 2.1). The two primary Aβ polymer types, Aβ40 and Aβ42, disrupt synaptic signalling and aggregate into amyloid plaques, activating astrocytic and microglial cells, thereby triggering an inflammatory response that damages neurons and leads to cell death (Barage & Sonawane, 2015). Amyloid plaque deposition is believed to progress gradually from the neocortex, limbic regions, and subcortical areas in the early stages of the disease, and to the brainstem and cerebellar cortex in the later stages (Hampel & Teipel, 2004; Thal et al., 2002). According to the amyloid cascade hypothesis, Aβ deposition serves as the initial pathological trigger, which subsequently leads to the formation of NFTs, neuronal cell death, and ultimately, dementia.

Aβ levels can be detected using CSF and neuroimaging techniques such as amyloid-PET. Generally, low levels of CSF Aβ42 are associated with increased Aβ deposition in the brain, as confirmed by autopsies and PET scans (Blennow et al., 2001; Fagan et al., 2006; Vlassenko et al., 2012). However, Aβ42 levels are not specific to AD, as some neurologically healthy individuals may also exhibit early Aβ deposition, a phenomenon referred to as "pathological ageing" (Dickson et al., 1992). In contrast, CSF Aβ40, which is the most prevalent isoform with a lower propensity for aggregation, may represent the total Aβ levels in the brain and is often used alongside Aβ42 to aid in the diagnosis of AD (Portelius et al., 2006). The Aβ42/40 ratio was therefore introduced as a diagnostic biomarker, with a higher ratio indicating a higher risk for AD (Lewczuk et al., 2004). This ratio has consistently outperformed Aβ40 and Aβ42 alone in classifying AD patients (Baldeiras et al., 2018; Blennow & Zetterberg, 2018; Hansson

et al., 2019), likely because it accounts for a person's baseline level of total Aβ (Baldeiras et al., 2018).

In addition to CSF markers, amyloid-PET allows for the quantification Aβ levels by calculating tissue ratios between a target and reference region (SUVR ratio). These ratios are interpreted as "positive" or "negative" based on visual reads that assess Aβ binding in white and grey matter (Chapleau et al., 2022; Schöll et al., 2016). While both CSF and PET methods can detect Aβ deposition with good accuracy, these markers are not entirely specific to AD. As a result, studies suggest that combining Aβ with tau levels provides the highest diagnostic accuracy for classifying AD (Fagan et al., 2006; Lewczuk et al., 2004; Palmqvist et al., 2015; Welge et al., 2009), which is further discussed below.

Recently, plasma Aβ levels have been investigated, yielding conflicting results. Some studies have shown associations between plasma Aβ in AD patients (Cosentino et al., 2010; Mehta et al., 2001), while others have found the opposite (Hansson et al., 2019). Recent research by Palmqvist et al. (2020) explored plasma Aβ42/40 in distinguishing AD and non-AD dementias and demonstrated good diagnostic accuracy for neuropathologically confirmed cases, suggesting a relationship with CSF and PET-amyloid scans. Similarly, Verberk et al. (2020) examined plasma Aβ42/40 associations with amyloid-PET status in patients with subjective cognitive decline, MCI or AD. Results demonstrated that plasma Aβ42/40 was associated with amyloid PET status, however the results were strongest when used in combination with age and APOE status. A limitation of plasma Aβ42/40, however, is that its levels are only decreased 10-20% compared to 40-60% in CSF Aβ42/40, which may be due to plasma Aβ being metabolised outside the brain (for an overview, see Leuzy et al., 2022). As such, although plasma Aβ may be useful in clinic, combining it with other measures such as tau may provide a more robust measure of AD neuropathology.

2.2.2 Tau hyperphosphorylation hypothesis

Tau, a microtubule protein, was implicated in dementia upon discovery in the brains of AD patients by Claude Wischik in 1988 (Wischik et al., 1988). Its primary role is to maintain the microtubule structure of the neurons' axons and stabilise their integrity (Weingarten et al., 1975). When tau undergoes hyperphosphorylation, it loses its ability to uphold the cytoskeleton

and aggregates to form neurofibrillary tangles (NFTs) (refer to Figure 2.2). These tangles disrupt signal transmission, lead to synapse loss, and contribute to AD lesions and cognitive decline (Gómez-Isla et al., 1997).

NFT progression follows a spatiotemporal pattern, originating in the medial temporal lobe (entorhinal cortex and hippocampus) and progresses to the associative isocortex (Braak & Braak, 1991). The early vulnerability of the hippocampus may be explained by its high baseline tau expression and particular sensitivity to cellular stressors, such as hypoxia, which can exacerbate tau hyperphosphorylation, promote tangle formation, and contribute to early hippocampal atrophy in AD {Citation}. Studies have demonstrated a close correlation between the spatial distribution of tau pathology and the clinical manifestations of AD (Dronse et al., 2017; Ingelsson et al., 2004), underscoring the link between the accumulation of NFTs and the ensuing cognitive impairment.

The tau hyperphosphorylation hypothesis postulates that increased tau levels signify neurodegeneration, with tau tangle pathology preceding Aβ plaque formation (Blennow et al., 2001; Blennow & Zetterberg, 2018). Large population studies support this notion, demonstrating that tau pathology may commence a decade prior to amyloid plaque accumulation (Braak & Del Tredici, 2014). However, since total-tau (t-tau) levels primarily reflect the general extent of neuronal degeneration and damage, elevated levels of CSF tau are observed in many neurodegenerative diseases such as acute stroke and frontal-temporal dementia (Hampel & Teipel, 2004; Hesse et al., 2001). Indeed, it is now more widely acknowledged that Aβ is an upstream of tau in AD, prompting tau conversion into a toxic state (Bloom, 2014). Consequently, the inclusion of phosphorylated tau (p-tau) in the diagnosis of AD enhanced diagnostic specificity, particularly when compared to other forms of dementia (Andreasen et al., 2003; Hampel & Teipel, 2004). Studies have shown that the incorporation of p-tau data increases the specificity of AD diagnosis up to 94% when combined with the Aβ40/Aβ42 ratio (Welge et al., 2009). Moreover, since t-tau increases as Aβ42 decreases in AD pathology, the t-tau/Aβ42 ratio was introduced and now widely used in literature and clinical settings (Fagan et al., 2007).

Traditionally, tau levels have been assessed using CSF; however, recent advances in tau-specific PET tracers enable the in vivo detection of tau deposition (for review, see Groot et al.,

2022). To date, studies have shown little association between CSF tau levels and tau-PET scans (Gordon et al., 2016). This disparity may stem from tau-PET's closer association with brain atrophy and cognitive impairment, whereas CSF t-tau and p-tau are more closely tied to disease progression and neurodegeneration, which may precede detectability on PET scans (Blennow & Zetterberg, 2018). However, further research is needed to directly compare tau levels from CSF and PET as this remains an emerging field of study.

Furthermore, newly developed assays for plasma p-tau provide an additional avenue for tau detection. The most common assay for detecting p-tau, p-tau181, has demonstrated good diagnostic accuracy between AD and non-AD patients. For instance, Janelidze et al. (2020) compared plasma p-tau181 with tau-PET in unimpaired patients and patients with MCI, AD and non-AD dementia. It was found that plasma p-tau181 was increased in preclinical AD, and further increased in MCI and AD patients. Additionally, plasma p-tau181 correlated with CSF p-tau, predicted tau-PET results, and effectively differentiated AD from non-AD dementias. Another study examined p-tau181 in the Alzheimer's Disease Neuroimaging Initiative (ADNI) cohort (1,000 individuals including cognitively unimpaired, MCI and AD patients) and found that p-tau181 had high diagnostic accuracy and was able to distinguish between Aβ-negative and Aβ-positive patients. Additionally, higher baseline p-tau181 predicted future dementia comparably to CSF p-tau. These promising results suggest that p-tau181 may be a non-invasive biomarker for AD, offering significant clinical utility and enhancing clinical trial recruitment.

2.2.3 Genetics

Research into the genetic influences on AD risk and the role of genes in amyloid and tau pathology, has been conducted for many years. The most recognised genetic risk factor for sporadic late-onset AD is the apolipoprotein E (APOE) protein (Corder et al., 1993). APOE serves as a cholesterol transporter and plays a crucial role in neuronal growth, synaptic plasticity and membrane repair within the brain (Mahley, 1988). The three major APOE variants, ε2, ε3 and ε4, occur at varying frequencies in the Caucasian population (~7%, 80% and 13% respectively) (Myers et al., 1996). Studies consistently indicate that carriers of the APOE ε4 allele are at increased risk of AD. For example, a meta-analyses have shown elevated AD risk among individuals with one or two copies of the ε4 allele (Farrer, 1997). Recent studies have reinforced these findings, demonstrating poorer cognitive performance, particularly in episodic memory and executive function tasks among APOE ε4carriers, with these differences

accentuating with age (Wisdom et al., 2011). Longitudinal assessments considering APOE genotype and family history of AD have revealed poorer baseline cognitive scores in patients with a family history of AD, while non-carriers of the APOE ε4 allele exhibited better cognitive performance (Donix et al., 2012; Yasuno et al., 2012). Thus, the APOE ε4 allele is generally associated with synaptic processes in memory and an increased risk of AD. Conversely, individuals with the ε2 allele appear to have a lower risk and delayed onset of AD. Carriers of the ε2 allele exhibit a fourfold lower chance of developing AD (Farrer, 1997), suggesting a protective effect against late-onset AD (Corder et al., 1993). Interestingly, some immunotherapy drug trials exclude ε4 carrier due to their higher likelihood of adverse events. This increased risk is primarily due to carriers being more susceptible to amyloid-related abnormalities such as microbleeds and heightened inflammatory responses to treatment.

While ε4 status is clearly linked to increased risk and poorer performance in episodic memory, its effects on spatial cognition are less certain. A recent meta-analysis found that ε4 carriers showed only a small reduction in spatial long-term memory and had no effects on other spatial domains such as spatial working memory, navigation, or reasoning (Daly et al., 2024). These findings suggest that ε4 influence on spatial cognition is complex and remains an interesting area of research.

These genetic effects extend to studies of neuroimaging and neuropathology. Post-mortem and neuroimaging research has shown that APOE ε2 carriers have significantly less amyloid pathology and fewer Aβ plaques than non-carriers (J. C. Morris et al., 2010; Serrano-Pozo et al., 2015), suggesting a potential protective effect. In contrast, APOE ε4 carriers exhibit heightened levels of cerebral amyloid angiopathy compared to those with ε3 or ε2 alleles (Nelson et al, 2013). However, other studies suggest that APOE ε4 carriers show reduced tau deposition, but not Aβ pathology. For instance, La Joie et al. (2021) used PET to assess the global Aβ and tau load in Aβ-positive patients and found that global cerebral Aβ was unrelated to all clinical factors and showed no correlation with APOE ε4. Conversely, the presence of one of more ε4 alleles and all clinical factors were associated with global tau levels. This pattern also applied to variations in grey matter volumes, indicating that APOE ε4 had focal effects on tau distribution in the medial temporal lobe. One possible explanation is that APOE

ε4 does not influence the later stages of amyloid deposition, supporting the argument that APOE ε4 has a pleiotropic effect on both Aβ and tau (Lim et al., 2017).

In summary, AD pathology is multifaceted, influenced significantly by the interactions and effects of Aβ and tau, which are largely hereditary in nature. Individuals with an APOE ε4 allele face an increased risk of developing AD, while the ε2 allele may have a neuroprotective effect. Although the exact mechanisms underlying Aβ and tau interact remain unclear, these genetic insights offer promising avenues for AD treatment, as discussed below.

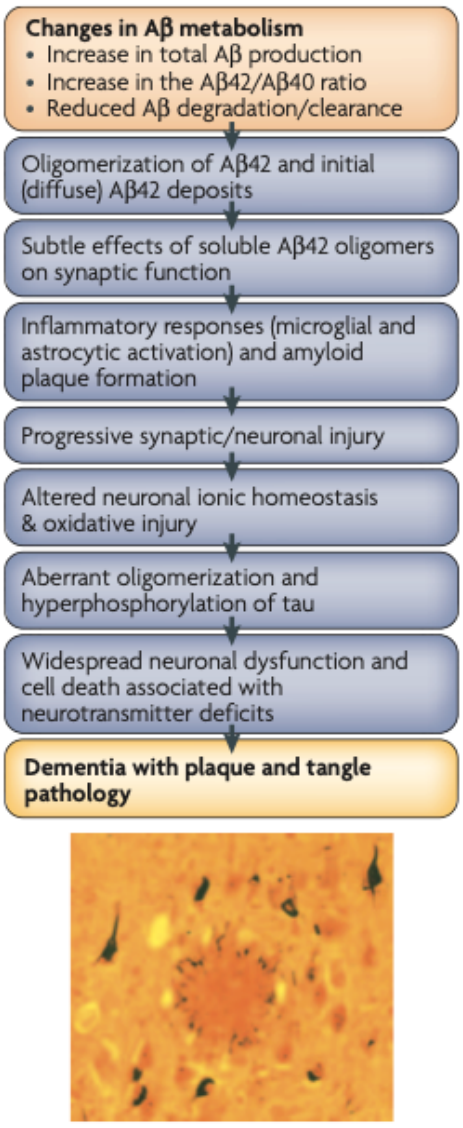

Figure 2.1: The amyloid cascade hypothesis

Figure from Haas and Selkoe, 2007.

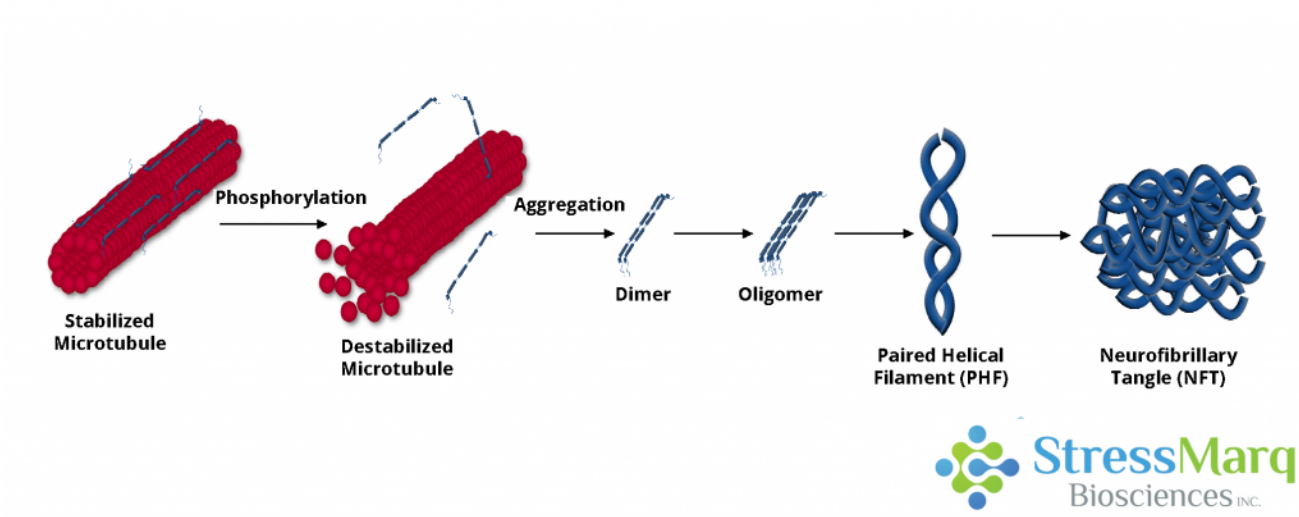

Figure 2.2: The tau hypothesis.

Figure from Knox (2022).

2.4 Treatments

2.4.1 Approved drug treatments

Currently, there are four approved drug treatments for AD in the UK and Europe: Donepezil, Galantamine, Rivastigmine and Memantine. With the exception of Memantine, these medications are all acetylcholinesterase (AChE) inhibitors. This approach is based on the observation that there is a premature loss of cholinergic neurons in the brains of AD patients (Bartus et al., 1982). Furthermore, acetylcholine levels decrease in regions such as the cerebral cortex and hippocampus as AD progresses, which are directly associated with amyloid deposition (Amenta et al., 2001). These medications are primarily used in mild to moderate AD cases and have varying degrees of effectiveness.

Donepezil is the most recently prescribed, first available in tablets and oral solution on the UK market in 2004. It has been shown to have various biological functions that influence the progression of AD, including enhancing cerebral blood flow, reducing APP levels, and influencing AChE expression (Jacobson & Sabbagh, 2008). The cognitive effects of Donepezil have been studied using memory-based tasks, demonstrating significant improvement in task performance in both animal (Abe et al., 2003; Hernandez et al., 2006) and human studies (Birks & Harvey, 2018). Evidence demonstrates that a daily dose of 5mg or 10mg improves cognition

and daily function in patients with mild to moderate AD, although there were no differences in behavioural symptoms or quality of life measurements (Birks & Harvey, 2018).

Another widely used drug treatment is **Galantamine**. In addition to being an AChE inhibitor, it also acts as a nicotinic receptor agonist, which responds to acetylcholine. A meta-analysis examining the impact of galantamine on various neuropsychological tests found significant improvements after 8-28 weeks of use (Jiang et al., 2015). However, adverse side effects such as gastrointestinal problems have been noted, causing a high drop-out rate in multiple studies.

Rivastigmine is approved for all stages of AD, including severe AD. It is available via capsule, oral solution, and skin patch. Apart from its AChE inhibitory function, Rivastigmine also acts as a butyrylcholinesterase (BuChE) inhibitor. The combination of both AChE and BuChE inhibition was considered because research has shown that higher BuChE activity in the medial temporal cortex is connected to slower cognitive decline, and levels of BuChE in AD patients are increased by up to 165% (Perry et al., 2003). A randomised trial found that Rivastigmine decreased the CSF activity of both inhibitors compared with Donepezil and Galantamine, although these CSF markers were not correlated with any clinical outcomes such as neuropsychological scores or Aβ and tau changes (Parnetti et al., 2011).

N-Methyl-D-Aspartate (NDMA) receptor antagonists, such as **Memantine**, represent another approach to treating AD. This rationale is based on the fact that glutamate receptors, particularly the NDMA type, are overactive and toxic, leading to neuronal damage and death. Memantine binds to these receptors, reducing their impact, and is mostly used to treat moderate to severe AD patients (Jarvis & Figgitt, 2003). A randomised control trial found that memantine-treated patients performed significantly better on some cognitive tests compared to placebo, though not on behavioural and lifestyle tests (Grossberg et al., 2013).

Given the complexity of AD, a single drug class may not be able to address all cognitive deficiencies. Thus, numerous studies have investigated combining these medications. A recent meta-analysis of 54 trials demonstrated that the combination of Donepezil and Memantine was more effective in improving cognition, daily activities, and neuropsychiatric symptoms than placebo, or either drug alone (Guo et al., 2020). However, the cost-effectiveness of combination therapy is disputed, and the risks of combining medications include increased

adverse events, drug interactions and patient noncompliance. To address these issues, a combination drug was released in the US in 2017, containing a fixed-dose combination of Donepezil and Memantine, named Namzaric™ (Boinpally et al., 2015). So far, the drug has been well received, demonstrating good cognitive and dementia behaviour improvements compared with placebo, representing a potential option for the treatment of patients with moderate to severe AD (Greig, 2015).

Overall, these drug treatments have shown some changes to AD patient's cognition; however, there is no evidence that they alter the course of the underlying dementing process. Many patients have a temporary reduction in symptoms, though the effects are not long lasting and can diminish after a few years of starting treatment; 1 year with Memantine (Reisberg et al., 2006) and 3 years for AChE inhibitors (Farlow et al., 2005; Pirttilä et al., 2004; Winblad et al., 2006). Therefore, it is important for physicians to manage the expectations of AD patients. It has been suggested that continuing treatment with the addition of a healthy diet, exercise and regular social contact is currently the best way to manage AD symptoms (Farlow et al., 2008).

2.4.2. Aβ plaques and tau deposition treatments

The initial focus of most treatment was the removal of Aβ plaques. Following the amyloid cascade hypothesis, Aβ clearance became the prime target for the development of new AD drug therapies. In 1999, the enzyme BACE1, crucial for Aβ production, was discovered (Vassar et al., 1999). Consequently, BACE1 inhibitors became a focus of many drug trials. For instance, in 2012, Eli Lilly announced that a BACE1 drug had successfully passed Phase 1 by reducing CSF Aβ40 and Aβ42 levels. However, due to adverse effects, the trial was halted and did not pass Phase 2. This outcome has been consistent across other BACE1 trial, none of which have passed Phase 3 of clinical trials.

Another avenue for Aβ clearance is immunotherapy, which is considered one of the most promising strategies in AD drug development. This approach involves creating antibodies that targets and reduce Aβ plaques. Recent Aβ-targeting therapies have shown encouraging results, leading to the FDA approval of two new AD drugs – **Aducanumab and Lecanemab**. These are monoclonal antibody drugs, designed to selectively target and reduce Aβ plaques in the brain. The first approved therapy, Aducanumab was initially halted during Phase 3 clinical trials for lack of demonstrated benefits, but this decision was redacted, and it became available

in June 2021. Administered intravenously every four weeks and monitored using PET scans, interim analysis from the PRIME study has indicated that Aducanumab decreased Aβ and slowed cognitive decline in AD patients compared to placebo (Sevigny, Chiao, et al., 2016). These results are promising; however, the drug is considered controversial as there remains an overall lack of sufficient evidence to support its efficacy. Issues with clinical trial design and analysis have been highlighted, and further investigation of Biogen's publicly available data does not support the conclusion that Aducanumab has clinical benefits (Knopman et al., 2021).

The Clarity AD study investigated Lecanemab and found that patients taking the drug had lower brain amyloid levels and a 27% reduction in cognitive and functional decline compared to placebo (Van Dyck et al., 2023). However, this decision was also controversial as routine MRI showed adverse side effects in patients taking Lecanemab (21% and 9% in the placebo group), and women and participants under the age of 65 did not show an improvement (Knopman & Hershey, 2023). Moreover, the significant slowing of cognitive decline reported in clinical trials may not be clinically meaningful, raising questions about the real-world effectiveness of the drug (Lansdall et al., 2023).

Another antibody drug targeting Aβ plaques, **Donanemab**, has shown promising results in Phase 3 clinical trials. The TRAILBLAZER study found that Donanemab improved cognition and daily life abilities compared to placebo (Mintun et al., 2021). However, specific cognitive measures such as the Clinical Dementia Rating (CDR) and Mini Mental State Examination (MMSE) did not show any difference between Donanemab and placebo, and PET and MRI scans yielded no significant differences. As such, an extension to the TRAILBLAZER study is currently ongoing to further examine the drug's efficacy.

Given the somewhat disappointing results of Aβ-targeted treatments, the focus has recently shifted to targeting tau protein. Tau has been more strongly associated with dementia symptoms than amyloid, suggesting that targeting tau may be a more effective treatment for AD (Lansdall, 2014; Sandusky-Beltran & Sigurdsson, 2020). However, tau-focused treatments are still in their early stages due to the greater complexity involved in developing a tau protein medication compared to anti-amyloid therapy (Pluta & Ułamek-Kozioł, 2020). Approaches to prevent tau protein build-up include modifications to the post-translational changes and microtubule destabilisation, prevention of tau accumulation, and immunotherapy (AADvac 1 vaccine) reported effective immunity against tau, though concerns about efficacy and adverse events

were noted (Novak et al., 2017). A follow-up study demonstrated slower hippocampal atrophy and less cognitive decline in patients administered with the drug, indicating that active immunotherapy might be a safe way to reduce tau pathology (Novak et al., 2018). **Gosuranemab**, the first monoclonal anti-tau antibody generated from familial AD patient stem cells, was tested in a Phase 1 clinical trial but halted due to significant brain atrophy in patients (Boxer et al., 2019). Following this, the PASSPORT and TauBasket trials were conducted to test intravenous infusion of Gosuranemab compared to placebo, but were also prematurely terminated in 2019.

Currently, the most advanced anti-tau monoclonal antibody for the treatment of AD is **Semorinemab**. Recent data analysis found that it did not slow clinical AD progression compared to placebo, as judged by tau PET and structural MRI (Teng et al., 2022). Despite this, other Phase 2 studies are testing Semorinemab in patients with moderate AD. Additionally, there is a growing body of literature on novel tau-targeting therapies studied in animal models, which have shown promising results on brain pathology and clinical symptoms.

In conclusion, opinions about the current treatments for AD are divided. The majority of prescribed drugs are AChE inhibitors, which appear to enhance clinical and daily functioning but do not impede the progression of the disease. Treatments centred on Aβ clearance, such as Aducanumab and Lecanemab, were considered promising but remain controversial and have divided clinical opinion. Tau has drawn attention as a potential next step in AD treatment due to its stronger correlation with cognitive deterioration (Hoskin et al., 2019). However, future treatments for AD will need to consider several critical points, including better understanding of the blood-brain-barrier (BBB) medication transport pathway, increasing sensitivity in clinical change assessments, and using more sensitive tests to identify tau and Aβ pathologies during therapy testing (Hoskin et al., 2019). Diagnosing patients in the preclinical stages of AD is crucial, as significant slowing of disease progression requires early intervention. Brain imaging techniques may help detect early signs of AD, allowing for tracking disease progression and identifying novel treatments. Techniques like MEG and EEG could be particularly effective in studying AD pathology due to the relationship between amyloid and tau pathology and synaptic dysfunction (Mucke & Selkoe, 2012; M. Wu et al., 2021). This will be discussed further in the following section.

2.5 Imaging techniques

Human non-invasive imaging offers a multitude of approaches to study the physiological and anatomical alterations with AD. These techniques have significantly contributed to our understanding of the neuropathological alterations in the brain linked to AD. Since AD has no cure, early diagnosis is crucial for benefiting patients individually and increasing the likelihood effective therapies. This section discusses MRI, fMRI and MEG as imaging modalities for AD, their key findings, and how they relate to neuropathology.

2.5.1. Magnetic Resonance Imaging (MRI)

Since its introduction in the early 1990s, MRI has seen an enormous increase in interest. Previously, imaging techniques such as CT and MRI were mainly used to rule out surgical interventions for memory problems. However, MRI-derived measurements are now acknowledged as crucial markers for AD and are utilised in clinics to aid in the diagnosis process and monitor the disease's progression in clinical trials (McKhann et al., 2011). MRI is an accessible method of identifying large-scale pathological alterations in vivo. Given the depth of information available in a MRI scan, several methods can be used to extract information about the structure and function of the brain.

MRI uses strong magnetic fields and radiofrequency pulses to generate images of the brain without ionising radiation. Signals from hydrogen protons in water and fat allow differentiation between brain tissue types, with contrasts such as T1 and T2 highlighting structural properties (for review see Jezzard & Clare, 2001).

In this thesis, structural MRI scans were used to study cortical and subcortical brain regions. This information is described in Chapter 3 and 4.

2.5.1.2 Structural MRI and AD

Measuring brain atrophy, or tissue volumes, is a primary focus of structural MRI studies in AD. The primary cause of this atrophy is thought to be the loss of neurons. Indeed, strong associations between autopsy-derived neuronal counts and MRI subcortical volumes suggest the high reliability of MRI estimations (Bobinski et al., 1999). The earliest region to display atrophy in AD is the medial temporal lobe (MTL), which includes the entorhinal cortex and hippocampus (Braak & Braak, 1991). One of the most common MRI markers used in clinical

research in AD is hippocampal volume. Many studies have found a reduced volume of the hippocampus in patients with AD or MCI compared with healthy controls (Barnes et al., 2009; Henneman et al., 2009; Shi et al., 2009). Additionally, increased atrophy of the hippocampus has shown to be a good predictor for patients that progress from MCI to AD, and those who did not (Franko et al., 2013; Korf et al., 2004). Thus, MRI-based measures of hippocampal atrophy are regarded as valid markers of disease state and are an important component of the clinical assessment and diagnosis of AD (Frisoni et al., 2010). Interestingly, longitudinal MRI studies of the hippocampus in asymptomatic patients who later developed AD showed that hippocampal volumes are reduced by 10% three years before receiving their diagnosis (Chan et al., 2003). This suggests that medial temporal lobe atrophy begins several years before diagnosis.

Importantly, brain atrophy detected using MRI is correlated with amyloid and tau deposition. For example, Jack Jr et al. (2008) investigated cortical reuptake of an amyloid-PET tracer and structural MRI measurements of the hippocampus in cognitively normal, MCI and AD patients. They found that AD patients had high amyloid load and low hippocampal volumes, MCI patients had mixed results, and cognitively healthy controls had low amyloid load and larger hippocampal volumes. These results were also correlated with cognitive scores, with MRI data showing stronger correlations than PET data. Similar results have been reported with CSF t-tau and p-tau measurements, showing that AD patients with smaller hippocampal volumes had higher tau levels (de Souza et al., 2012). Additional research has revealed distinct topographies for the burden of tau and amyloid. For instance, de Flores et al. (2022) examined MTL subregions to assess two distinct MTL networks: posterior-medial (PM) and anterior-temporal (AT), utilising longitudinal structural MRI and PET data. The findings indicated that amyloid deposition was higher in the PM network, whereas tau accumulation was more pronounced in the AT network. Functionally, these networks are thought to support different aspects of memory. The PM network is associated with spatial and contextual memory processing, whereas the AT network is more involved in item and semantic memory. Therefore, the observation that the MTL has a very high tau-to-amyloid ratio, particularly in the AT network, suggests that tau pathology in this region may occur independently of amyloid and could contribute directly to the early memory deficits in AD.

Overall, structural MRI is a powerful tool for detecting AD-related brain atrophy, particularly through measurements of hippocampal volume, which can provide valuable information for diagnosing and monitoring disease progression. However, its clinical use remains limited due to its challenges in complex data processing interpretation outside of research settings. While structural MRI plays a crucial role in understanding cerebral atrophy in AD, it is limited in its ability to capture functional changes, which may emerge earlier in the disease process.

2.5.2 Functional MRI (fMRI)

Functional MRI (fMRI) detects changes in blood flow within the brain by measuring Blood Oxygen Level Dependent (BOLD) activity. The BOLD signal arises from differences in the magnetic properties of haemoglobin depending on its oxygenation state. Fully oxygenated haemoglobin (HbO_2) is diamagnetic, making it indistinguishable from the surrounding brain tissue in a magnetic field. In contrast, deoxygenated haemoglobin is paramagnetic, which creates local magnetic field inhomogeneities and alters the MR signal. These signals are linked to neuronal activity, as most active brain regions consume more oxygen, promoting an increase in blood flow to replenish oxygen levels. This BOLD response forms the basis of fMRI, enabling researchers to infer patterns of neural activity and brain function (Glover, 2011; Logothetis, 2008). Importantly, evidence has shown that the BOLD response correlates with local field potentials (LFPs), reflecting the summed synaptic input and processing of neural populations. For example, Ekstrom et al. (2009) combined fMRI with intracranial EEG in the medial temporal lobe, and showed that BOLD fluctuations corresponded closely with LFPs, particularly in the gamma band. Such studies provide validation of fMRI, supporting its utility for both task-based paradigms and the analysis of spontaneous fluctuations in resting-state scans.

This thesis examines resting-state fMRI and its relation to AD pathology. This information is described in Chapter 6.

2.5.2.1 fMRI and AD

AD is associated with altered patterns of functional connectivity, as demonstrated by both resting-state and task-based fMRI studies. Most task-based fMRI research on AD focuses on variations of memory encoding tasks to explore disease-related differences. For instance, Han et al. (2007) used a verbal paired-associate encoding task in participants with or without the

APOE e4 allele and found that individuals with the e4 allele showed greater activation in several right hemisphere regions, despite similar structural metrics in grey matter and hippocampal volume. Similarly, in a study using a memory encoding task contrasting novel and familiar items, Trivedi et al. (2006) reported reduced activation in the hippocampus and MTL in APOE e3/4 carriers compared to e3/3 carriers, further highlighting functional connectivity differences related to AD risk.

In addition to memory encoding, fMRI has also been used to examine attentional processing in AD. One study comparing visual attention in AD patients and healthy controls found that the AD group showed reduced activation in both parietal lobes and the left frontal region during a visual search task. In contrast, increased activation was observed in the right frontal lobe and right occipito-temporal regions during a conjunction task, suggesting altered attentional strategies in AD (Hao et al., 2005). Furthermore, these attentional differences in AD have been linked to increasing levels of AD pathology, as measured by CSF biomarkers and PET imaging (Gordon et al., 2015).

The most well-known resting-state network is the DMN, which is associated with mind-wandering, autobiographical memory, and passive thought (Buckner et al., 2008). Additionally, the DMN plays a role in various memory processes such as episodic and semantic memory functions (Smallwood et al., 2021). The DMN includes several brain regions such as the parietal cortices, MTL, hippocampus, and thalamus. Given its role in episodic memory, the DMN is particularly relevant to AD research. Indeed, altered functional connectivity of the DMN has been observed in patients with MCI and AD (Binnewijzend et al., 2012; Greicius et al., 2004; Sorg et al., 2007; K. Wang et al., 2007), as well as in young carriers of the APOE4 gene (Filippini et al., 2009). In addition to the DMN, other resting-state networks, such as the dorsal and ventral attention networks, have also been found to be disrupted in AD (Fox et al., 2006; Li et al., 2012).

fMRI measures have also been shown to be associated with amyloid and tau burden. For example, studies have found a relationship between PET amyloid tracer uptake levels and connectivity in the DMN (Hedden et al., 2009; Mormino et al., 2011), demonstrating that higher amyloid burden is linked to reduced functional connectivity. Similar patterns have also been shown in tau-PET studies, where functional connectivity networks show an overlap with tau pathology networks (Hoenig et al., 2018). Furthermore, the presence of the APOE e4 allele

enhances this effect (Jann et al., 2024). This has also been shown in task-based fMRI where participants were tested on their episodic memory, and results demonstrated heightened activation during encoding with high Aβ levels (Mormino et al., 2012).

In overview, both resting-state and task-based fMRI studied have shown that AD is associated with alterations in functional connectivity. Importantly, fMRI findings have been linked to underlying AD pathology, suggesting that functional brain changes detectable with fMRI may serve as a good indicator of AD. However, BOLD fMRI reliability in the older population is not well researched, therefore is not currently recommended for clinical use (Aramadaka et al., 2023). In addition, fMRI is limited in its temporal resolution compared to other methods, such as MEG and EEG, which is discussed in more detail below.

2.5.3 Magnetoencephalography (MEG)

The use of MEG research in dementia has increased recently as efforts focus on detecting AD as early as possible in its pre-clinical stage. Early intervention may offer the best chance of therapeutic success, making this stage a major area of interest. Unlike structural MRI, MEG provides direct, millisecond-level resolution on large-scale brain activity and networks, which may be sensitive to the precursors of AD. This non-invasive method of measuring neuronal activity at different frequencies with minimal effort from subjects during resting-state scans, an essential factor given the older demographic typically involved in AD research.

MEG records the brain's electrophysiological responses by detecting changing in magnetic fields originating from neuronal activity. Neurons generate electric signals, creating surrounding magnetic signals. These signals primarily arise from the sum of excitatory postsynaptic potentials of large populations of pyramidal cells that are spatially aligned in the cortex. MEG uses highly sensitive sensors called SQUIDs (Superconducting Quantum Interference Device) to capture these patterns, typically employing magnetometers and gradiometers. Magnetometers measure magnetic fields directions, whereas gradiometers measure the local spatial derivative of the magnetic field, effectively reducing environmental noise. A central concept in MEG research is the study of neuronal oscillations, which is the rhythmic fluctuations in neural activity that reflect synchronised communication across networks. Oscillations can be characterised by multiple components, most commonly their frequency (how fast they cycle, in Hz), and amplitude or power (their strength).

Oscillations are broadly divided into frequency bands, each associated with cognitive functions: delta (<4Hz, deep sleep states), theta (4-8Hz, memory encoding and navigation), alpha (8-13Hz, attention and inhibition), beta (13-30Hz, sensorimotor processing and maintenance of cognitive states), and gamma (>30Hz, higher cognitive functions). Compared with EEG, MEG is less distorted by external factors such as CSF, skull thickness and skin (de Jongh et al., 2005), and offers better spatial resolution (Hedrich et al., 2017). Thus, MEG provides a direct link to neural activity, enabling the study of changes in oscillations (both frequency and amplitude) in both normal ageing and neurodegeneration.

2.5.3.1 MEG and AD

The power spectrum, showing the absolute or relative contribution to a signal from various frequency bands, is the most widely used technique for assessing MEG signals. Since its introduction in 1967, Welch's periodogram (Welch, 1967) has remained a fundamental technique for frequency analysis (see Chapter 5.1.1 for further details). MEG allows AD investigation through various methods, from functional connectivity and brain network assessments to spectral and single-channel estimations.

First, time-series analysis shows that AD patients have higher relative and absolute power in the delta and theta frequency bands (slow rhythms) and lower power in alpha, beta and gamma (frequency bands (fast frequency bands) compared to general ageing (de Haan et al., 2008; Fernández et al., 2002; Koelewijn et al., 2017). A comprehensive review by Engels et al. (2017) confirmed this general slowing patterns, and their summary of regional findings (see Figure 2.3) highlights that these alterations are not uniform across the brain. In particular, increases in delta and theta power are most commonly observed in temporal and parietal cortices, while alpha reductions are especially marked in posterior regions, including the occipital lobe. Beta power decreases appear more widespread, but with notable involvement of parietal areas. Additionally, Engels et al. (2017) also summarises functional connectivity changes, with reduced connectivity within posterior hubs and between temporo-parietal regions, alongside evidence of increased connectivity in frontal networks. Beyond spectral changes, peak alpha frequency has been identified as a sensitive marker, with AD patients showing a clear reduction relative to healthy controls (Garcés et al., 2013; Montez et al., 2009). Collectively, these findings indicate that AD is characterised by a combination of spectral slowing and network-level disconnection.

Second, examining the functional connectivity within and between brain regions is another method for studying AD with MEG. Although fMRI can also be used, MEG's superior temporal resolution and direct measurement of neuronal activity has expanded this area of study. Studies generally show lower functional connectivity in AD than controls. For example, Stam et al. (2006) found lower connectivity in the left fronto-temporal/parietal regions in the alpha and beta bands in AD patients. However, as most data is correlation-based, it is unclear whether these results indicate interactions between different brain regions. To address this, a recent study used general linear models (GLMs) and time-series for 90 regions of interest (ROIs) to compare functional connectivity between AD patients and controls, finding reduced global functional connectivity in the alpha and beta bands in AD patients. Interestingly, in the majority of ROIs the beta band proved to be the most reproducible (Schoonhoven et al., 2022).

Additionally, task-based MEG research reveals differences in brain activity between AD patients and controls. It has been demonstrated that whereas task-based networks and resting-state networks have a strong correlation, their functions differ slightly (Cole et al., 2021; Di et al., 2013). MEG research uses a wide range of tasks, from simple button-press and auditory tasks to intricate cognitive examinations. For example, Kurimoto et al. (2012) found significant differences in oscillatory activity during a visual memory task between AD patients and controls, such that patients showed decreased beta and gamma frequencies and beta event-related desynchronisation (ERD). Group differences are also observed in the "oddball" paradigm, where patients recall a set of letters previously shown among a set of targets and distractors, with hippocampal volume correlating with left parietal and temporal lobe activity. (Güntekin et al., 2013; Maestu et al., 2003). Thus, task-based MEG can be used to reveal differences between AD patients and controls, though fewer studies use task compared with resting-state.

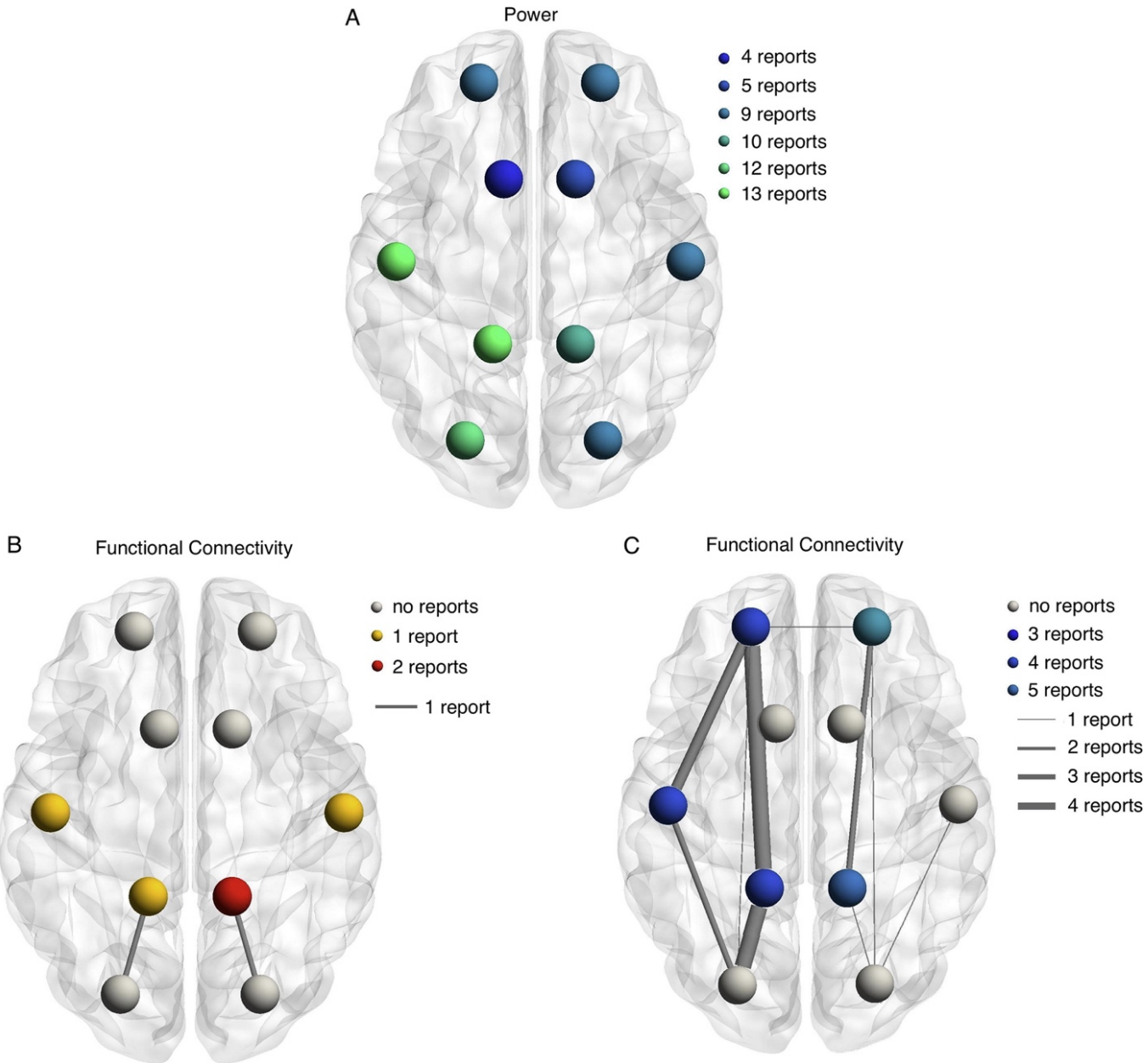

Figure 2.3 Overview of regional MEG findings in AD.
A) Oscillatory slowing. **B)** Increased functional connectivity within (dots) and between (lines) brain areas. **C)** Decreased functional connectivity within (dots) and between (lines) brain areas. The colours of the dots and the size of the lines indicate the number of instances reported.
Figure from Engels et al. (2017).

2.5.3.2 MEG and neuropathology in AD

To better understand the fundamentals of what the MEG signal signifies in terms of AD neuropathology, studies have begun to investigate the link between oscillatory activity and amyloid and tau accumulations. A recent study by Ranasinghe et al. (2020) analysed MEG functional maps in the delta, theta, and alpha frequency bands in both controls and likely AD patients, with amyloid and tau deposition evaluated using PET scans. The results indicated that the occipital and posterior temporoparietal cortices exhibited hyposynchronous alpha oscillations, while the frontal and anterior temporoparietal cortices had hypersynchronous delta-theta oscillations. Interestingly, alpha hyposynchrony was strongly correlated with tau deposition and was modulated by the degree of tau tracer uptake measured by PET. In contrast, delta-theta hypersynchrony was associated with both amyloid and tau depositions and PET tracer uptake. Additionally, MMSE scores correlated with reduced alpha synchrony but not with delta-theta synchrony. These findings suggest that tau, Aβ, and cognitive decline are specifically linked to abnormalities in neuronal synchronisation in the alpha and delta-theta bands. This aligns with other studies showing that higher levels of CSF t-tau and p-tau are correlated with reduced oscillatory power in EEG spectrums (Canuet et al., 2015; Kramberger et al., 2013).

Since alpha was uniquely linked to tau deposition, measuring alpha synchrony with MEG may be a useful technique in tau-specific clinical trials to assess treatment efficacy and course. Supporting this, Ranasinghe et al. (2021) investigated abnormalities in MEG synchrony in the alpha and delta-theta bands using NFT density at autopsy. The findings showed a significant correlation between NFT burden and alpha deficits (i.e., lower alpha synchrony was related with more NFTs) after controlling for the time between MEG scan and death using linear mixed models. In contrast, NFT burden was not linked to deficiencies in delta-theta synchrony. Therefore, these results suggest that decreases in the alpha band are sensitive markers of the neurodegenerative consequences linked to tau deposition in AD. This body of research has contributed to the understanding of the critical relationship between neuropathology and alpha hyposynchrony, although it contains some limitations such as small sample size and inconsistent inclusion of AD patients with atypical phenotypes.

Overall, MEG is a potential valuable tool in AD research. Studies have shown clear oscillatory differences between AD patients and controls, which relate to cerebral atrophy, cognitive scores and the underlying neuropathology. These findings support the idea that MEG is

sensitive enough to identify functional and regional abnormalities in AD. However, more research is needed that allows us to determine the exact relationship between MEG activity, cognition and the neural sources of these affected networks. It is therefore of interest to study multiple frequency bands in relation to cerebral atrophy, cognitive decline and Aβ and tau accumulation in both cross-sectional and longitudinal data.

This thesis examines oscillatory variations in resting-state MEG. This information is described in Chapter 5.

2.5.4 Issues with AD diagnostic criteria and sample sizes

Typically, the sample sizes in MEG studies examining AD are small. In a recent review by Engels et al. (2017), the average population size was 20 AD patients (range: 5 – 36) and 19 controls (range: 5 – 26). This lack of statistical power limits the ability to compare results with a healthy ageing population. Additionally, a well-known problem in this field is that populations are often not homogenous, with a lack of diversity and irregularities of male/female ratios. These pragmatic concerns hinder the effectiveness of the research, despite the fact they provide valuable insights into AD degeneration. Therefore, future research should aim to create a larger, well-balanced cohorts.

Moreover, it is likely that patients with mixed forms of dementia, those who were misdiagnosed, or those who diagnoses lacked amyloid and tau CSF/PET have been included in AD research. Since cognitive tests and structural brain imaging are the primary methods used to diagnose AD, most research studies involve participants with "probable AD/ MCI" but without pathologic indicators for AD. Consequently, this can complicate data interpretation since differences between groups may not exclusively result from AD cognitive impairments. Thus, it is crucial to consider these limitations and limit the inclusion of AD patients without confirmed amyloid and tau assessments.

From a practical perspective, recruiting AD patients into research studies is challenging (for an overview see Watson et al., 2014). For example, most patients seeking care for memory concerns initially see an outpatient primary care physician. A study has found that clinicians face various obstacles in referring patients, such as lack of time, diagnostic tools, proximity to research centres, and patient comorbidities (Galvin et al., 2009). Additionally, most AD

research requires the participation of a study partner, which is someone who knows the participant well and can provide information about their cognitive functioning and daily activities. Although most participants include their spouses or good friends as study partners, recent data from the Alzheimer's Association suggests an increase in the amount of older people with dementia living alone (Alzheimer's Association, 2019). Furthermore, to maintain good retention rates, it is crucial to take patients' time needs into account and ensure that the study visits is manageable.

One study that aims to address some of these limitations is the New Therapeutics in Alzheimer's Disease (NTAD) study. This study provides data from exclusively biomarker-positive MCI and AD patients (N=69) and biomarker-negative healthy controls (N=35). The creation of this cohort involved careful considerations of sample size numbers, study visit scheduling, and recruitment tactics. Detailed information is provided in Chapter 3.

2.6 Summary

This chapter has assessed the neuropathological process that define AD, reviewed the current available therapies, and highlighted significant MRI and MEG studies in AD research. MRI data has been fundamental in enhancing our understanding of cerebral atrophy associated with AD. However, unlike MRI and fMRI, MEG provides a direct link to synaptic function with excellent temporal resolution, which is crucial for understanding the underlying mechanical alterations associated with cognitive decline. It has been demonstrated that MEG markers are related to amyloid and tau pathology distinctively. Nonetheless, the neurophysiological signatures in AD and their relationship to amyloid, tau, cerebral atrophy, and cognitive decline need more further exploration. More information is needed on how each frequency band is associated with AD neuropathology and cognitive decline in a well-established AD cohort. Additionally, there are discrepancies in the literature about the inclusion of AD patients, as the majority of cohorts include patients with "probable AD" without confirmed tau and Aβ positivity, along with different phenotypes that are not representative of the general population. The most distinctive biomarkers related to amyloid and tau pathology include MRI structural alterations in the medial temporal cortex, fMRI alterations in the DMN, and MEG alterations in the theta and alpha frequency bands. Going forward, the subsequent chapters will explore these biomarkers and examine which can be used earliest in the disease.

This thesis aims to expand on these ideas by investigating the relationship between cognitive measures and the build-up of tau and amyloid in connection to multi-modal data (MRI and MEG) using the NTAD study data. Specifically, I will focus on:

1. Distinctions in the brain between AD and normal ageing.
2. Investigating whether resting-state MEG is a reliable marker for AD.
3. Evaluating whether longitudinal effects can be derived from MEG oscillatory differences.
4. Investigating whether resting-state fMRI yields similar results to MEG.
5. Assessing the relationships between neuroimaging modalities, neuropathology, and cognitive measures.

Chapter 3: The New Therapeutics in Alzheimer's Disease (NTAD) Study

3.1 Introduction

The New Therapeutics in Alzheimer's Disease (NTAD) study is a multi-centre (The University of Cambridge, The University of Oxford, and Cardiff University), multi-modal study established by Dementias Platform UK and supported by Alzheimer's Research UK and industry partners Johnson & Johnson, Lilly, and AstraZeneca. The study aims to identify sensitive biomarkers for next-generation experimental medicine studies by integrating various brain imaging techniques, cognitive assessments, and in-depth amyloid, tau, and blood testing, thereby creating a rich and informative dataset.

As discussed in Chapter 2, synaptic and neuronal changes associated with AD may be the most sensitive and earliest precursors of cognitive decline which are impaired before other common detection methods such as MRI (Samson-Dollfus et al., 1997). While PET scans and lumbar puncture provide information on the presence of amyloid and tau in the brain, these methods do not offer insights into synaptic function. Currently, there are limited options to assess synaptic function *in vivo*, therefore methods such as MEEG offer a new avenue to measure the neurophysiological properties involved in AD. As such, NTAD offers longitudinal data from 104 participants, including biomarker-positive individuals with a diagnosis of MCI or AD, and neurologically healthy controls.

This chapter provides an overview of the most relevant methodological aspects of the NTAD study examined in this thesis.

3.2 Methods

The study received ethical approval from the Health Research Authority and Research Ethics Committee (18/EE/0042). Approval was also obtained from the Administration of Radioactive Substances Advisory Committee (ARSAC) for the PET scan radioactive tracer administration and exposure. The full protocol outlining further details has been published by Lanskey et al. (2022). A substantial amount of my DPhil work focussed on the screening, recruitment, and collecting and curating of data. The total number of participants screened and recruited as part of this DPhil is shown in Figure 3.1. Other contributions are outlined in Appendix 1.

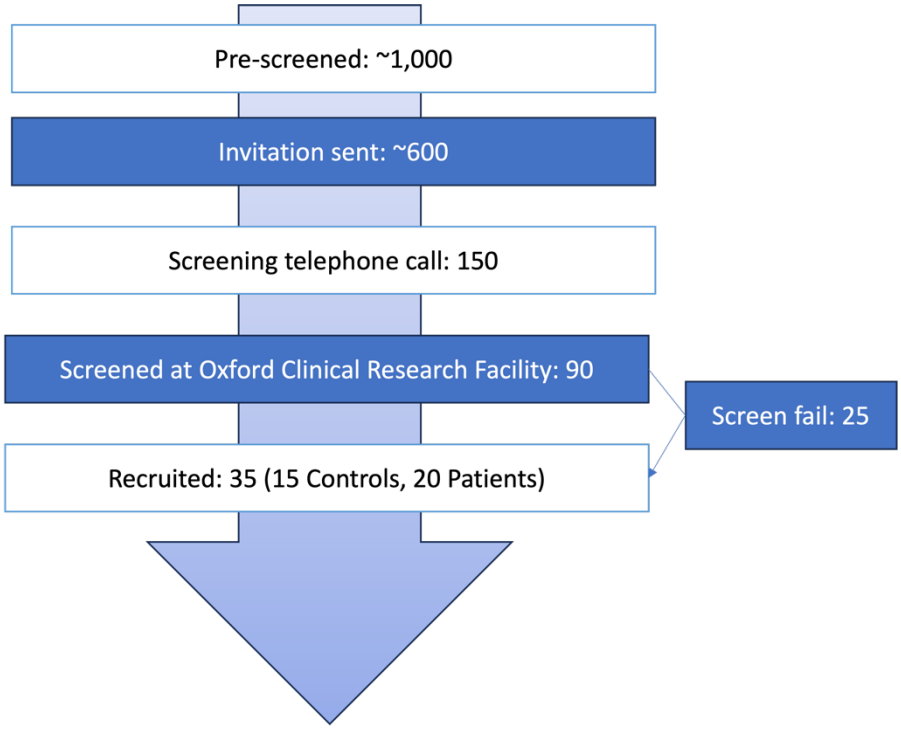

Figure 3.1. Participant flow chart of screening and recruitment numbers at the Oxford site as part of this DPhil project.
Recruitment sources were local memory clinics, the Clinical Research Network and Join Dementia Research. Pre-screening comprised of electronic screening of medical records. Invitations were sent to those who appeared eligible from their records. Those who remained eligible and interested after a screening telephone call were further screened at the Oxford Clinical Research Facility as described in in Section 3.2.1. Screen fails were mostly due to contradicting neuropathology results (i.e., patients with negative amyloid/tau ratio).

3.2.1 Participants

Potential participants aged 50-85 years old were recruited via the following methods: (1) advertisements in local memory clinics, (2) the Join Dementia Research (JDR) registry, and (3) electronically screened by the Clinical Research Network (CRN). For those contacted by the CRN, only patients who had not opted out of the 'Research Interest List' were contacted to take part. Those who expressed an interest in taking part were emailed or posted the participant information sheet and study partner information sheet.

Participants were either neurologically healthy volunteers with no history of memory issues, or patients diagnosed with MCI or AD. Patients had a Mini Mental State Examination (MMSE) score cut-off of > 18 and Clinical Dementia Rating (CDR) = 0.5 – 1. For healthy controls the score cut-offs were MMSE > 24 and CDR = 0. All participants had to be able to provide informed consent, had a study partner, and be able to undergo the visits outlined below.

Exclusion criteria included patients who were unable to give informed consent; those with MRI or MEG contraindications; a history of psychiatric conditions that may affect cognition; currently taking part in an experimental drug study; and those who could not undergo amyloid testing via lumbar puncture or PET scanning. Any uncertainly regarding eligibility was discussed with the principal investigator for the relevant site. See Appendix 2, table 1 for full details on inclusion and exclusion criteria. Patients who had AB/tau negative results were excluded as part of the NTAD study, though this group will be investigated further in a new project entitled Synaptic Health in Neurodegeneration (SHINE) as they represent an interesting group whose biomarker profile may offer further insights into the neurodegenerative processes distinct from typical AD pathology.

The total number of participants in each group across visits is shown in Table 3.1.

3.2.2 Overall study procedure

NTAD is a 2-year repeated-measures, observational-design study. Study visits were carried out at two sites: The University of Cambridge and The University of Oxford, each in partnership with their local NHS Hospital Trusts. There were two visits involved in the screening process carried out in the Addenbrookes Hospital, Cambridge or at the Warneford Hospital, Oxford. Screening visits took approximately 2 hours each. Subsequently, there were 2-3 baseline visits at the Wolfson Brain Imaging Centre (WBIC, Cambridge), or the Oxford Centre for Human Brain Activity (OHBA, Oxford). Baseline visits took approximately 3 hours each. An optional baseline visit included a test-retest session for a subset of patients who repeated the MEEG scan 2-4 weeks after the first visit. Patients were asked to return for a repeat assessment at 12-months (including clinical interview, MEEG, MRI and neuropsychological assessments), and at 24-months (clinical and neuropsychological assessments only). The full schedule of events for controls and patients can be seen in Appendix 2, tables 2 and 3.

3.2.3 Screening visits

All potential participants underwent a detailed screening visit to assess eligibility conducted by a medically qualified clinician, research nurse, and research assistant. After written, informed consent, the clinician administered a clinical interview which covered: demographics, medical history, family history of dementia, medication review, lifestyle factors, a physical

examination, and covid vaccination history. The remaining clinical assessments were administered by the research team. This included the CDR, Addenbrooke's Cognitive Exam - Revised (ACE-R), State-Trait-Anxiety-Inventory (STAIT), Geriatric Depression Scale (GDS), and Pittsburgh Sleep Quality Index (PSQI). The study partner was asked to complete the Instrumental Activities of Daily Living (iADL) and Mild Behavioural Impairment Checklist (MBI-C). All participants had their vital signs (temperature, pulse, blood pressure), hip and waist circumference, height and weight measurements taken. Blood sampling was completed at the first screening visit.

If biomarker status was unknown from recent clinical or research assessments, participants underwent a lumbar puncture or amyloid PET scan. The decision to perform either was based on medical contraindications and/or personal preference.

3.2.3.1 Lumbar puncture

CSF was collected via lumbar puncture administered by a Neurologist at the Clinical Research Facility at the Addenbrookes Hospital, Cambridge or at the Warneford Hospital, Oxford. Participant's blood results and current medication list were screened to ensure there were no contraindications to lumbar puncture. A local anaesthetic and spinal needle were used for collection of ~10ml CSF in two separate specimen bottles. 5ml were sent for analysis at The Institute for Neurology, London and 5ml were sent for storage at the BioRepository Laboratory, Cambridge. CSF was analysed using enzyme-linked immunosorbent assay (ELISA) for Aβ42, t-tau, and p-tau. A small number of samples also included Aβ40 analysis. A tau/Aβ40 ratio >1 and/or p-tau >57 was used to determine amyloid status, unless otherwise stated by a Principal Investigator.

A total of 25 controls and 31 patients (18 MCI patients, 13 AD patients) had a lumbar puncture.

3.2.3.2 PET Scan

PET scans were collected using the GE Signa PET/MR scanner at the Wolfson Brain Imaging Centre, Cambridge, or the GE Discovery PET/CT scanner at the Churchill Hospital, Oxford. Either of the following amyloid tracers were administered intravenously, depending on availability: Florbetaben (2.9 - 3.6 mSv), Florbetapir (2.8 - 3.5 mSv) and Flutemtamol (4.8 – 5.9mSv). Once the tracer was administered, participants were asked to wait in a dimmed room with limited stimulation for one hour before the PET scan began. The cerebellum was used as

the reference structure. A SUVR value > 1.19 was used to determine amyloid status, unless otherwise stated by a Principal Investigator.

A total of 7 controls and 35 patients (17 MCI patients, 18 AD patients) had a PET scan.

3.2.3.3 Blood testing

Blood samples were collected from all participants by a Research Nurse during the screening visit at the Clinical Research Facility. A clinician reviewed the results for safety and eligibility. Specific to this thesis, 59 participant's blood samples (15 controls, 24 MCI patients and 20 AD patients) were analysed for measure plasma levels of p-tau (p-tau181). Additional analyses, such as APOE genotyping and p-tau217, is due to be conducted in the future.

3.2.4 Baseline visits

Participants completed MEEG and MRI scans, along with a battery of neuropsychological assessments. Baseline visits were conducted over two or three sessions, depending on the participant's preference. The additional MEEG scan was repeated 2-4 weeks after the baseline visit.

3.2.4.1. MEEG acquisition

MEEG data were collected simultaneously in a magnetically shielded room. In Cambridge, both the Elekta VectorView and MEGIN Triux Neo scanner with 204 planar gradiometers and 102 magnetometers was used with either a 70 or 64 EasyCap channel BrainCap. At Oxford, the MEGIN Triux Neo scanner was used with an EasyCap 60 channel BrainCap for all data collection using the same gradiometer/magnetometer setup. All data was collected at 1000Hz. Standard fiducial points, 60 EEG electrode locations and <100 additional head points were digitised using a Polhemus Fastrak. 5 head position indicator (HPI) coils were continuously measured during the recording. Electrooculogram (EOG) was measured with electrodes placed above and below the left eye, and on each temple. Two electrodes placed on each wrist recorded electrocardiogram (ECG) data.

During the MEEG scan, participants either rested or performed simple tasks, responding using a button box. They were provided headphones and, if necessary, non-magnetic glasses. Tasks were performed in the following order: (1) audio-visual task, (2) auditory mismatch-negativity task, (3) scene-repetition task, (4) cross-model oddball task, (5) eyes-open resting state, where

participants were asked to fixate on a cross, relax and clear their mind, and (6) eyes-closed resting state, where participants were asked to keep their eyes closed, relax, clear their mind, and try not to fall asleep. Further task details can be found in Appendix 3.

The eyes-open resting state, and eyes-closed resting state are analysed in this thesis (Chapter 5).

3.2.4.2. MRI acquisition

MRI scans were collected using a 3T Siemens PRISMA scanner at either the Cambridge MRC Cognition and Brain Science Unit, or Oxford Centre for Human Brain Activity. Scans consisted of: (1) T1-weighted structural scan, (2) T2 FLAIR scan, (3) T2*-weighted image, (4) T2-weighted with fat saturation scan, (5) diffusion weighted imaging, (6) quantitative susceptibility mapping sequence, (7) resting-state functional MRI (fMRI) scan, (8) hippocampal subfield image, and (9) an arterial spin labelling (ASL) sequence.

T1-weighted structural MRI data (Chapters 4 & 5) and resting-state fMRI data (Chapter 6) are considered in this thesis.

Table 3.2: Total number of participants across activity and visits.

Numbers represent the total number of participants that completed each visit. Only patients were invited for the two-week and annual visits. The two-week visit included MEG only.

Group	Visit Time Point	MRI	MEG	Cognitive assessments
Controls	Baseline	35	35	35
MCI	Baseline	36	35	36
	Two-week	-	15	-
	Annual	26	25	27
AD	Baseline	34	32	35
	Two-week	-	5	-
	Annual	24	21	28

3.2.4.3. Neuropsychological assessments

The neuropsychological test battery was conducted in a private, quiet testing room in one session with breaks as needed. The tests consisted of the Repeatable Battery of the Assessment of Neuropsychological Status (RBANS), Digit span forwards and backwards, Free and Cued Selective Reminding Test (FCSRT), Logical Memory Test, National Adult Reading Test (NART), Digit symbol test, Trails making test, Logical Memory Test Delayed, Cambridge Neuropsychological Test Automated Battery (CANTAB), and Four Mountains task.

3.2.5 Annual visits

Participants in the patient group were asked to repeat the MEEG scan, MRI scan, neuropsychological assessments, clinical interview, and blood collection at 12 months post-baseline. The clinical and neuropsychological assessments were also repeated at 24 months.

3.3 Discussion

This chapter provided a methodological overview of the key aspects of the NTAD study that will be examined in this thesis, while also highlighting the unique value that NTAD offers to the AD research community. A crucial strength of the NTAD cohort is its strict recruitment criteria, which only include biomarker-positive patients and biomarker-negative controls, as well as other important aspects. This approach ensures a well-characterised sample that enhances the reliability of findings by reducing potential confounds from individuals with mixed of uncertain pathology. The NTAD study provides a rich and comprehensive dataset for analysis, encompassing a wide range of clinical and research cognitive scores, lumbar puncture results, blood biomarkers, and multiple MRI measures, including structural and functional imaging. NTAD also includes MEG recordings across multiple tasks, offering valuable and novel insights into neural activity patterns in AD. Additionally, NTAD offers longitudinal data in patients, as well as important test re-test measures of the MEG data. This dataset complements other large-scale studies, such as The Deep and Frequent Phenotyping (DFP) study, where scanning protocols were designed to align as closely as possible, enabling cross-cohort comparisons and validation of results.

This thesis will use the NTAD data to investigate the structural and functional alterations in AD, with the overall aim of identifying the most sensitive and reliable measures for detecting the early-AD related changes. Within the NTAD cohort, participants were clinically classified

as having either MCI or AD based on the criteria described above. MCI participants in general showed cognitive impairment with relatively preserved daily functioning, whereas those diagnosed with AD demonstrated more pronounced cognitive decline and greater impairment in everyday activities. Given these differences, Chapter 4 will examine group-specific patterns, but in subsequent chapters the MCI and AD groups will be combined into a single 'patient' group to improve statistical power and to focus on shared disease features, as all individuals included were biomarker-positive.

Chapter 4: Brain structure, Pathology and Cognitive Decline in AD

Structural MRI and cognitive testing play a crucial role in both the diagnosis and understanding of AD, providing key insights into brain atrophy and cognitive decline (McKhann et al., 2011). Given the growing emphasis on identifying early biomarkers, research suggests that by the time cognitive impairment becomes apparent, potential significant brain pathology may have already developed (Ikonomovic et al., 2003). As a result, the exploration of alternatives to cognitive assessments is a critical area of investigation. This chapter examines AD-related structural and pathological markers using MRI and lumbar puncture results, while also evaluating the range of cognitive tests available in the NTAD cohort, including both clinical and research-based assessments.

4.1 Introduction

Individuals experiencing cognitive concerns typically first consult their general practitioner (GP), who plays a crucial role in determining whether further testing for dementia is necessary. If warranted, the GP may refer the patient to secondary care for additional assessments, including brain imaging, blood tests, and cognitive assessments. These tests not only aid in diagnosing dementia, but also help rule out other potential causes of cognitive impairment, such as bleeding or tumours. Given the challenges of differentiating AD-related cognitive decline from normal ageing, particularly in the early stages, using these diagnostic tools is essential for an accurate and timely diagnosis.

Structural MRI is a powerful tool for assessing disease state and is widely recognised as a valid biomarker in the clinical assessment of AD (Frisoni et al., 2010). As discussed in Chapter 2, numerous studies have reported reductions in grey matter volume and hippocampal atrophy in AD patients (Barnes et al., 2009; Henneman et al., 2009; Shi et al., 2009). Moreover, these structural changes have been linked to amyloid and tau pathology, further reinforcing their relevance as disease markers (de Souza et al., 2012; Jack Jr et al., 2008). When available, imaging is encouraged in the diagnostic process. In fact, at least one of the following markers is often required for a dementia diagnosis: medial temporal lobe atrophy, tempoparietal hypometabolism, or abnormal amyloid/tau markers, highlighting the critical role of structural imaging in identifying AD (Dubois et al., 2007). Out of the various MRI biomarkers for AD, hippocampal volume is the most well-established (Modrego, 2006). Even in the mild dementia

stage, hippocampal atrophy is evident, with volume reductions of 15-30% compared to healthy controls (Van Der Flier et al., 2005). This reflects the value of structural MRI as a useful tool in AD. Given that the NTAD study described in Chapter 3 is relatively new and these markers have yet to be fully explored within this cohort, this chapter first aims to validate the cohort by examining whether the cognitive scores and structural MRI findings align with typical markers of AD. Following this, the analysis extends to evaluating the predictive performance of specific markers and the potential utility of research-based tests in detecting early-AD related changes.

In addition to structural MRI, cognitive assessments play a crucial role in the clinical diagnosis of AD. Several screening tests are available to clinicians, with the choice of test often influenced by geographical location and GP preference. The most frequently used tool for the initial assessment of MCI and AD is the MMSE. This test is favoured due to its quick administration and ability to track overall cognitive performance across multiple domains (Folstein et al., 1975). A more comprehensive alternative is the ACE, which provides a broader evaluation of cognitive function and allows for the calculation of both MMSE and ACE scores (Mioshi et al., 2006). Although reports have suggested that the MMSE can be biased by factors such as age, race, education, and socioeconomic status, it remains widely used in both clinical and research settings (Borson et al., 2005). Alternatives to the MMSE, such as the Mini-Cognitive Assessment Instrument (Mini-Cog) GP assessment of cognition (GPCOG), and Montreal Cognitive Assessment (MOCA), are popular because due to their similar sensitivity and specificity to MMSE, with fewer biases (Ismail et al., 2010). However, these tests are more complex and take longer to administer than the MMSE, which can limit their use in clinics due to resource constraints. Indeed, a review of cognitive test use in primary care found that only 20% of referral letters mentioned a cognitive score, suggesting that either the test was not completed or the score did not influence the referral decision (Fisher & Larner, 2007). This may be due to a lack of resources of confidence in the test used, suggesting that the current tests do not meet the needs of GPs and primary care physicians.

Better cognitive tests are needed for the detection of early AD, especially within research and clinical trial settings. For any test to be useful, it must be applicable to the whole population (i.e., unbiased) and target the earliest cognitive impairments associated with AD. Examples of such research tests include the Repeatable Battery for the Assessment of Neuropsychological Status (RBANS) (Randolph et al., 1998), Cambridge Neuropsychological Test Automated

Battery (CANTAB), and the Four Mountains (Chan et al., 2016). These have all demonstrated strong diagnostic accuracy and serve as valuable screening tools for detecting cognitive deficits associated with AD. For example, the Four Mountains test assesses spatial memory and has shown 100% diagnostic sensitivity and 78% specificity for detecting early AD in MCI patients, with a Receive Operating Characteristic (ROC) curve of 0.93 (Chan et al., 2016). Spatial navigation deficits are among the earliest cognitive impairments in AD, as the entorhinal cortex and, subsequently, the hippocampus – the brain regions affected earliest by the disease – play a crucial role in spatial orientation and memory (Braak & Braak, 1991; O'Keefe & Dostrovsky, 1971). Research has begun to adapt these spatial navigation tests into games, aiming to make screening both engaging and widely accessible. Examples include the Sea Hero Quest (Coutrot et al., 2018) and Spatial Performance Assessment for Cognitive Evaluation (SPACE) game (Colombo et al., 2024). While these gamified approaches show promise for large-scale cognitive screening in real-world populations, their applicability in clinical settings remains unknown.

4.1.1 Objectives

Given that the NTAD cohort includes measures of brain structure, pathology, and cognitive function, the objects of this analysis were to:

1. Validate the cohort by examining whether expected differences in brain structure and cognitive performance are observed between biomarker-positive MCI and AD patients, and healthy controls.
2. Assess the relationships between structural MRI markers, pathological biomarkers, and cognitive scores.
3. Explore the utility of research-based cognitive tests in comparison to traditional assessment methods for detecting early AD-related changes.

4.2 Methods

4.2.1 Participants

Of 162 participants screened, 2 were ineligible due to MRI contraindications, 5 were ineligible due to medical contraindications, 21 were ineligible due to LP or PET results, 5 were ineligible due to cognitive score results, 20 were withdrawn due to an inability/want to complete all tasks, and 3 had a change of diagnosis after enrolment. Therefore, a total of 106 participants (35 healthy controls, 71 patients) are included in the NTAD cohort.

Demographics of the participants are shown in Table 4.1.

4.2.2 Structural measurements

Of 106 participants in the NTAD cohort, 1 participant was unable to complete the MRI scan for their baseline visit and 21 patients could not complete the annual MRI scan. In addition, 1 annual scan contained excessive movement and was excluded from analysis. Therefore, the baseline results focus on 105 participants (35 controls, 70 patients) and the annual results focus on 50 patients (26 MCI patients, 24 AD patients).

Details of the baseline structural measurements are shown in Table 4.1.

4.2.2.1 Automated segmentation of tissue type and hippocampus using FSL

Prior to segmentation, all images were processed using the FMRIB Software Library (FSL: Woolrich et al., 2009; https://fsl.fmrib.ox.ac.uk/fsl/fslwiki/FSL). Images were then reoriented to standard Montreal Neurological Institute (MNI) space, cropped, and bias field corrected. FMRIB's Linear Registration Tool (FLIRT; Jenkinson et al. 2001; https://fsl.fmrib.ox.ac.uk/fsl/fslwiki/FLIRT) was used to register to standard space and brain extraction was performed using BET (Smith et al., 2002; https://fsl.fmrib.ox.ac.uk/fsl/fslwiki/BET). From here, subcortical structure volumes were derived using FMRIB's Integrated Registration and Segmentation Tool (FIRST; Patenaude et al., 2011; http://fsl.fmrib.ox.ac.uk/fsl/fslwiki/FIRST). All images were visually inspected to ensure accurate brain extraction. The grey matter (GM), white matter (WM) and cerebral spinal fluid (CSF) volumes were extracted using FMRIB's Automated Segmentation Tool (FAST; https://fsl.fmrib.ox.ac.uk/fsl/docs/#/structural/fast). The structure of the left and right hippocampus was saved as a mesh and labelled, and a voxel count was used to estimate the

total hippocampal volume. Finally, in order to allow for a direct comparison between each participant's volume (hippocampal volume, GM, WM, etc.), they were normalised using the individuals brain volume to create a percentage as follows: $(\frac{Normalised\ brain\ volume}{Total\ brain\ volume}) * 100$.

4.2.3 Neuropsychological assessments

The results section includes results from selected neuropsychological tests available from the NTAD study, focusing on well-established clinical assessments of global cognition such as the MMSE and ACE-R. These tests were chosen for their frequent use in diagnostic processes and their strong foundation in the literature. In addition, these clinical tests were compared with research-based assessments of episodic and spatial memory to further explore the effectiveness of neuropsychological testing. The specific research-based tests in this analysis are: i) the Four Mountains, ii) FCSRT, a verbal episodic memory assessment (Buschke, 1984), iii) the Logical Memory test, with focus on the delayed memory retention score (Wechsler, 1999) and, iv) the RBANS visuospatial and delayed memory index scores, selected as a replacement for the Rey figure recall test of non-verbal episodic memory (Randolph et al., 1998).

From the NTAD cohort, all participants completed the baseline neuropsychological tests described above. During the annual follow-ups, 16 patients did not complete the annual tests. Therefore, the baseline neuropsychological scores include 106 participants (35 controls, 69 patients) and annual scores include 55 participants (27 MCI patients, 28 AD patients).

Details of the baseline neuropsychological scores are shown in Table 4.1.

4.3.4.1 Four Mountains test

The Four Mountains test (4MT) is a non-verbal test of allocentric spatial memory, which is the ability to encode and recall spatial relationships between objects from a viewpoint-independent perspective. The task requires participants to view a sample of a mountainous landscape and then, after a brief delay, identify the same scene from a different viewpoint among four options. The correct choice relies on the ability to mentally rotate the scene and match topographical features, a cognitive operation that strongly engages the hippocampus. The 4MT has been shown to be a sensitive measure of hippocampal function, for example in a study by Hartley et al. (2007) on developmental amnesia patients, individuals with selective bilateral hippocampal damage performed at change level on the task, despite intact general intelligence and

recognition memory. A visual example of the 4MT trial is shown in Figure 4.1. Total test time for participants is 10-15 minutes, which makes it an ideal candidate for a clinical alternative to traditional neuropsychological assessments. For analysis, scores were calculated as a percentage of correct responses.

From the NTAD cohort, 87 participants completed the 4MT (33 controls, 31 MCI patients, 23 AD patients).

4.2.4 Neuropathology

During the screening visits, participants undertook either a PET scan or lumbar puncture which were detailed in Chapter 3.2.3. This thesis concentrates solely on the lumbar puncture/CSF results.

Details of the neuropathological values are shown in Table 4.7.

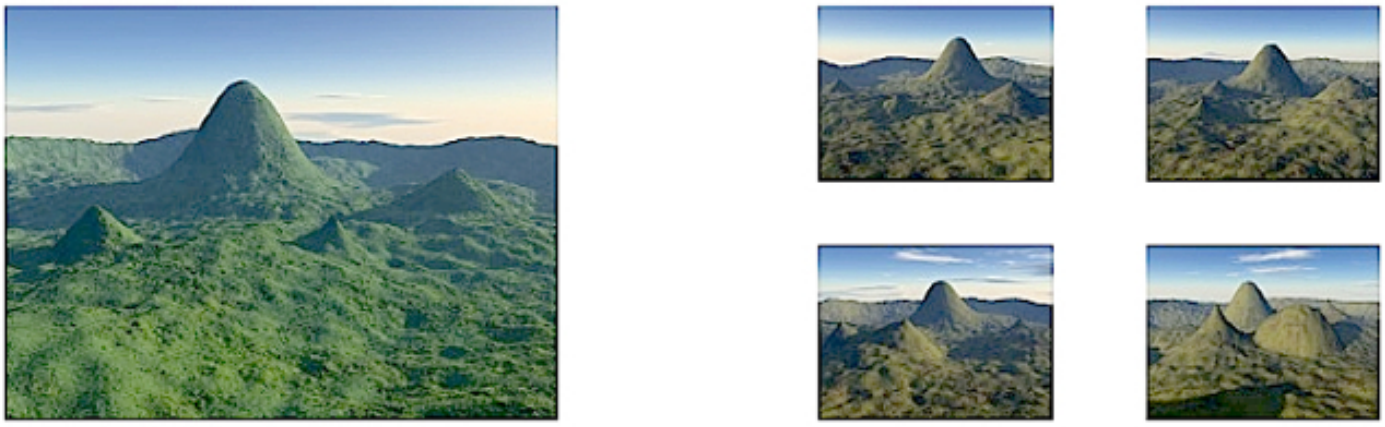

Figure 4.1 Visual representation of the 4MT.
A landscape (left) is shown for 8 seconds and after a 2 second delay the same landscape from a rotated viewpoint is shown alongside 3 foil images. Participants are asked to identify the previously viewed landscape (right, correct answer is top left image).

3.2.6 Statistics

Variables were analysed using JASP (Version 0.14.1). Analysis of variance (ANOVA) and Tukey correction for post-hoc tests were used to compare the baseline demographic variables, cognitive scores, brain volumes and neuropathological measures between controls, MCI, and AD patients. Homogeneity of variances was assessed using the Levene's test. A paired samples t-test was used to investigate the differences between baseline and annual scores.

Separate linear regression models were used to compare the predictability of brain structures, neuropsychological scores, and neuropathology measures, adjusting for age, sex, and years in education. The specific predictors and outcomes for each model are detailed within the relevant analyses. Residuals were visually inspected for linear assumptions. Paired t-tests were used to compare baseline and annual neuropsychological scores. $p < 0.05$ was considered significant for all analyses.

4.3 Results

4.3.1 Demographics

Results demonstrated a significant difference in age between the control and patient group ($F_{(2,103)}$ = 12.07, p < .001). Post hoc comparisons using Tukey's correction indicated significant age differences between controls and MCI patients *(*t(4.79), p < .001) and between controls and AD patients (t(3.85), p < .001). There was no significant difference in age between MCI and AD patients (t(0.85), p = 0.67).

Additionally, ANOVA revealed a significant difference in education levels among the groups ($F_{(2,103)}$= 5.46, p < .05). Tukey's post hoc test revealed a significant difference between controls and MCI patients (t(3.27), p < .05). However, no significant differences were found between controls and AD patients (t(2.1), p < .05) or between MCI and AD patients (t(1.17), p < .05).

4.3.2 Baseline results

4.3.2.1 Brain structure analysis

A one-way ANOVA revealed a significant effect of group on total brain volume (($F_{(2,100)}$= 3.46, p < .005), grey matter volume ($F_{(2,102)}$= 21.73, p < .001) and white matter volume (($F_{(2,102)}$ = 19.06, p < .001).

Furthermore, a one-way ANOVA demonstrated a significant effect of group on left hippocampal volume ($F_{(2,102)}$= 29.75, p < .001) (Figure 4.2A) and right hippocampal volume ($F_{(2,102)}$) = 31.33, p < .001) (Figure 4.2B). Tukey's post hoc test indicated that the left hippocampus was significantly smaller in the AD group compared to the MCI group (t(2.4), p < .05) and controls (t(7.54), p < .001). The MCI group also had a significantly smaller left hippocampal volume compared to controls (t(5.1), p < .001).

A similar pattern was observed for the right hippocampus where significant differences were found between the AD and MCI patients (t(2.71), p < .05), AD patients and controls (t(7.79), p < .001), and between MCI patients and controls (t(5.06), p < .001).

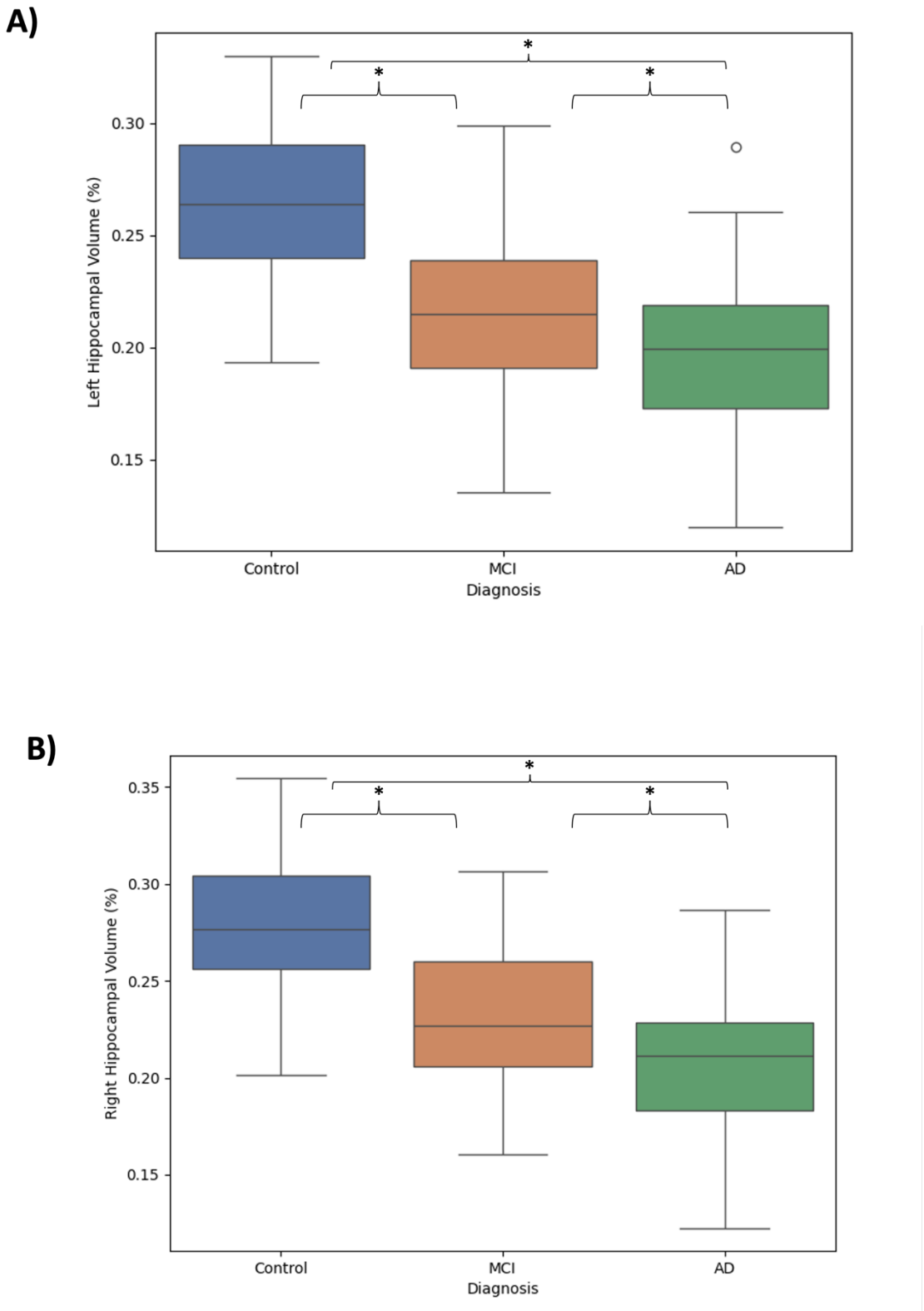

Figure 4.2. Group differences in baseline hippocampal volumes (%).

A boxplot showing the baseline group differences in **A)** left hippocampal volume, and **B)** right hippocampal volume. Controls are shown in blue, MCI patients shown in orange and AD patients in green. * denotes a significant association.

Table 4.1: Baseline demographic, brain volumes and neuropsychological assessments for the control and patient groups.

Values represent the mean (standard deviation). P values are results of one-way ANOVA. T values are results of Tukey post-hoc results for MCI and AD group differences. Brain tissue volumes are expressed as percentages of whole brain volumes.

	Controls (N=35)	**Patients (N=70)**		**P**	**T**
		MCI (*n*=35)	**AD**(*n*=35)		
Demographics					
Age (years)	66.5 (8.7)	75.1 (6.1)	72.95 (7.9)	< .001	0.461
Education (years)	16.4 (3.4)	13.7 (3.9)	14.7 (3.4)	0.006	0.473
Sex (F/M)	21/14	17/19	19/16	0.496	0.825
Neuropsychological assessments					
MMSE	29.1 (0.9)	26.3 (2.4)	23.2 (3.5)	< .001	< .001
ACE-R total score /100	93.7 (5.1)	79.9 (8.8)	65.9 (12.5)	< .001	< .001
ACE Attention /18	17.8 (0.5)	16.5 (1.6)	14.3 (2.8)	< .001	< .001
ACE Fluency /14	11.7 (2.7)	9 (3.3)	7.6 (1.9)	< .001	0.145
ACE Language /26	25.2 (1.9)	24.3 (2.4)	21.9 (3.5)	< .001	0.002
ACE Memory /26	23.4 (2.3)	15.6 (4.6)	10.6 (3.5)	< .001	< .001
ACE Visuospatial /16	15.5 (0.8)	14.5 (1.8)	11.9 (3.8)	< .001	< .001
Four Mountains (% correct)	70.3 (18.0)	47.3 (18.6)	37.1 (15.9)	< .001	0.109
FCSRT Delayed (free) / 48	33.5 (6.5)	16.7 (11.1)	12.1 (9.3)	< .001	0.155
FCSRT Delayed (total) / 48	47.8 (1.0)	39 (10.3)	35 (12.5)	< .001	0.093
RBANS Visuospatial index	110.9 (12.9)	78 (20.9)	61 (12.7)	< .001	< .001
RBANS Memory index	113 (16.0)	95 (18.7)	77 (20.3)	< .001	< .001

	Controls (N=35)	**Patients (N=67)**			
		MCI (*n*=35)	**AD**(*n*=32)		
Brain volumes					
Whole brain (mm^3)	1.422e+6 (1.5e+5)	1.366e+6 (1.2e+5)	1.339e+6 (1.3e+5)	0.035	0.686
Grey matter (%)	40.7 (1.8)	39 (2.0)	37.4 (2.1)	< .001	0.009
White matter (%)	38.2 (2.0)	35.7 (1.7)	35.9 (1.7)	< .001	0.888
Left hippocampus (%)	0.265 (0.04)	0.22 (0.04)	0.19 (0.04)	< .001	0.048
Right hippocampus (%)	0.277 (0.04)	0.23 (0.04)	0.20 (0.04)	< .001	0.021

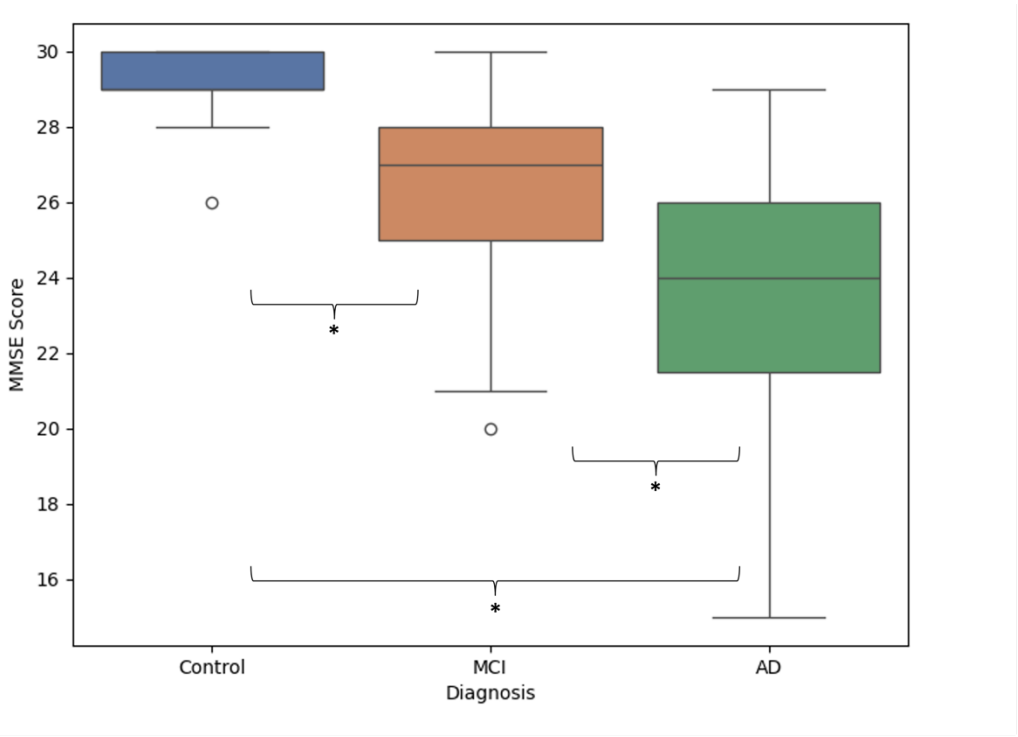

Figure 4.3. Baseline group differences in baseline MMSE score.
A boxplot showing the baseline group differences in MMSE score. Controls are shown in blue, MCI patients shown in orange and AD patients in green. * denotes a significant association.

As expected, MMSE scores significantly differed across groups, consistent with findings in the literature. A one-way ANOVA revealed a significant effect of group on MMSE score ($F_{(2,100)}$= 50.4, $p < .001$ (Figure 4.3). Tukey's correction demonstrated a significant difference between controls and MCI patients ($t(4.93)$, $p < .001$) and AD patients ($t(10.01)$, $p < .001$). There was also a significant difference between MCI and AD patients ($t(5.24)$, $p < .001$).

As shown in Table 4.1, a one-way ANOVA also revealed a significant effect of group on all cognitive scores, including ACE sub-scores, Four Mountains, FCSRT, and RBANS.

4.3.2.2 Brain structure and neuropsychological assessment analysis

Multiple linear regression analyses were conducted to examine whether cognitive scores commonly used in clinical practice predicted brain structure, with hippocampal volume as the outcome measure and age and years of education as covariates. Left and right hippocampi volumes were averaged together for analysis.

Results indicated that MMSE significantly predicted total hippocampal volume ($F_{(1,100)}$= 66.4, $p < .001$) and ACE-R total score ($F_{(1,100)}$ = 76, $p < .001$). (Figure 4.4).

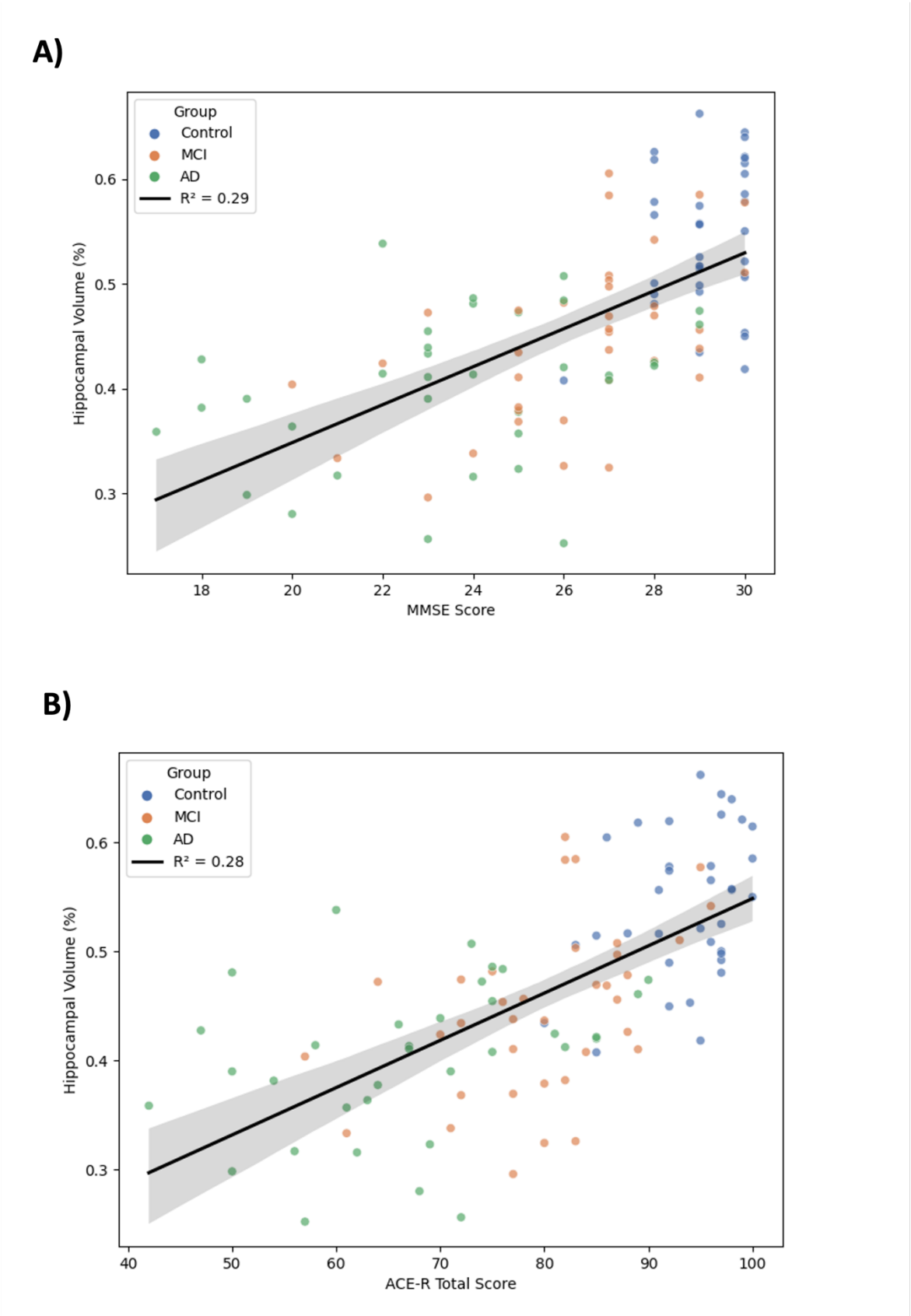

Figure 4.4. Scatterplots of total hippocampal volume (%) and cognitive test scores. Scatterplots showing the association between hippocampal volume and **A)** MMSE, and **B)** ACE-R total scores. Controls are shown in blue, MCI patients shown in orange and AD patients in green.

This section of the analysis broadens the focus to include a wider variety of neuropsychological assessments, aiming to better understand their relationship with brain structures. Due to the high multicollinearity among cognitive measures, each variable was z-scored, and separate linear regression models were computed. In these models, brain volumes served as the predicted variable, and the resulting R^2 and standardised beta coefficients were compared to evaluate the relative predictive strength of each cognitive measure.

Separate linear regression models examining the total hippocampal volume and neuropsychological assessments revealed that the ACE-R memory score was the most influential of hippocampal volume, followed by the RBANS Visuospatial index score (Table 4.2). This suggests that the hippocampus plays a crucial role in both memory and visuospatial ability.

Table 4.2. Results of individual linear regression analyses for baseline neuropsychological assessments (predictor) and total hippocampal volume (%).

Variable	R	R^2	β	t	*p*
ACE-R Attention	0.551	0.303	0.551	6.60	< .001
ACE-R Fluency	0.432	0.187	0.433	4.79	< .001
ACE-R Language	0.396	0.157	0.396	4.31	< .001
ACE-R Memory	0.667	**0.445**	**0.665**	8.95	< .001
ACE-R Visuospatial	0.385	0.149	0.391	4.18	< .001
MMSE	0.634	0.402	0.635	8.24	< .001
RBANS Visuospatial	0.654	0.428	0.648	8.34	< .001
RBANS Memory	0.504	0.254	0.491	5.69	< .001
FCSRT Total	0.524	0.274	0.560	5.7	< .001
Four Mountains (%)	0.506	0.256	0.513	5.35	< .001

The Four Mountains test (4MT) was explored in detail in this chapter as part of the broader objective to evaluate novel cognitive measures that may be sensitive to early AD pathology. While traditional cognitive assessments are well-established in clinical settings, this thesis aims to investigate whether alternative tests, such as the 4MT, offer improved sensitivity or complementary insights into early cognitive decline. Therefore, the 4MT is included here based on the hypothesis that performance on this task is strongly linked to hippocampal integrity and may be able to detect early AD-related spatial memory impairments. Details on the 4MT can be found in Section 4.3.4.1.

A one-way ANOVA revealed a significant effect of group on 4MT performance ($F(2,82) = 15.26$, $p < .001$). Tukey post-hoc analysis indicated that controls scored significantly higher than both MCI patients ($t(3.34) = p < .001$) and AD patients ($t(4.97)$, $p < .001$). No significant difference was observed between the MCI and AD patients ($t(1.07)$, $p = 0.54$). (Figure 4.5).

It was hypothesised that hippocampal volume would be the most predictive of 4MT performance compared to other brain volumes. Given the strong associations among brain measures, separate linear regressions were performed. Results showed that the right hippocampal volume was the strongest predictor of 4MT performance, followed by grey matter and the left hippocampus (Table 4.3).

A linear regression with 4MT as the predictor variable showed that it significantly predicted hippocampal volume ($F_{(1,86)} = 30.29$, $p < .001$) (Figure 4.6).

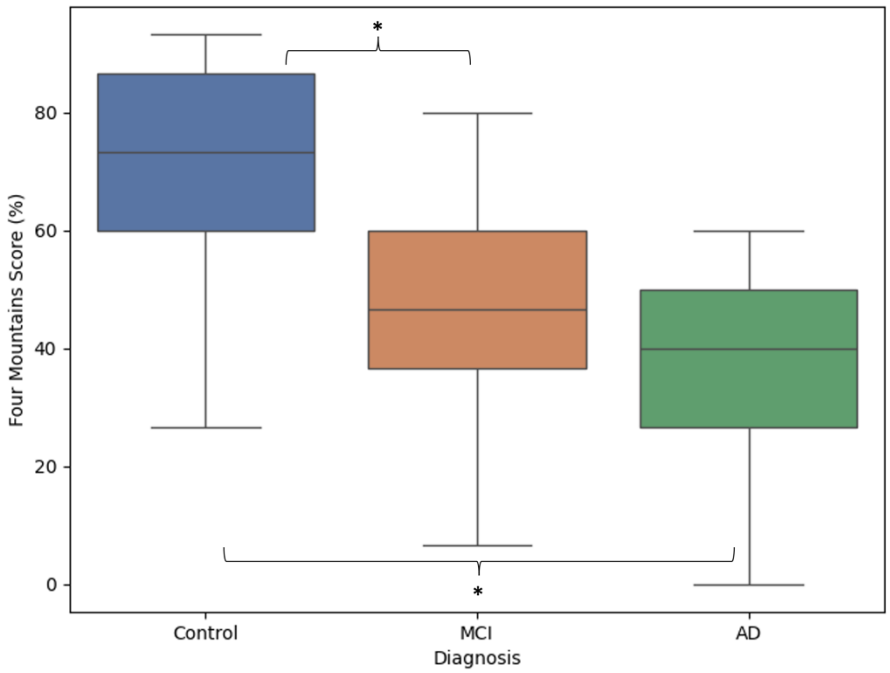

Figure 4.5. Baseline group differences in Four Mountains score.
A boxplot showing the baseline group differences in 4MT score. Controls are shown in blue, MCI patients shown in orange and AD patients in green. * denotes a significant association.

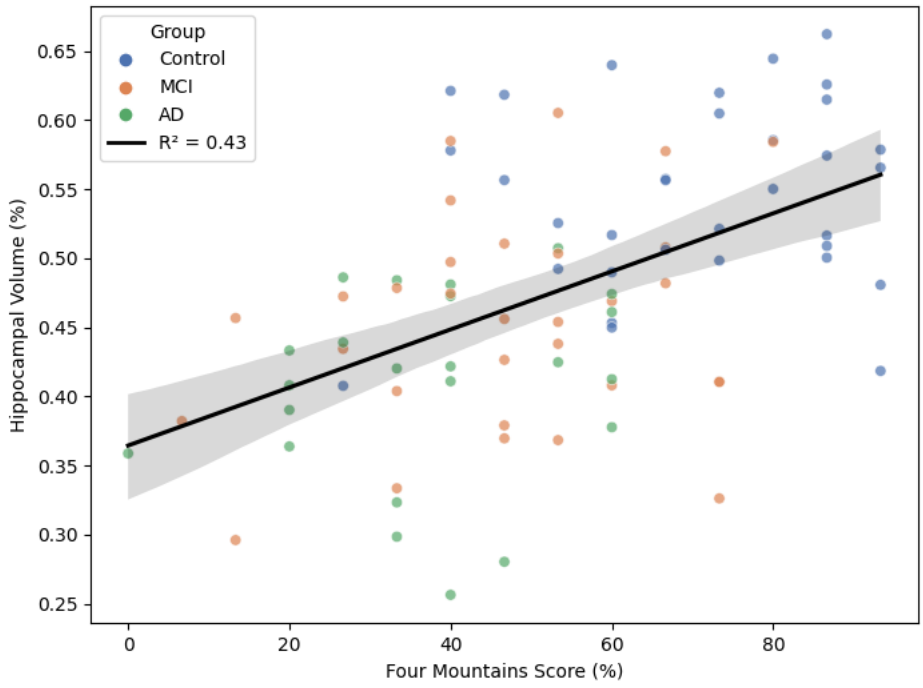

Figure 4.6. Scatterplot of total hippocampal volume and Four Mountains score.
Scatterplot showing the association between hippocampal volume and Four Mountains score. Controls are shown in blue, MCI patients shown in orange and AD patients in green.

Table 4.3. Results of individual linear regression analyses for brain volume measures (predictor) and Four Mountains score.

Variable	R	R^2	β	t	*p*
Total brain volume	0.274	0.075	0.260	2.6	0.01
Grey matter (%)	0.486	0.236	0.489	5.07	< .001
White matter (%)	0.445	0.198	0.450	4.53	< .001
Left hippocampal volume (%)	0.470	0.221	0.475	4.83	< .001
Right hippocampal volume (%)	0.508	**0.258**	**0.515**	5.34	< .001

4.3.2.3 Neuropathology analysis

A one-way ANOVA revealed a significant effect of group on CSF Aβ/tau ratio ($F_{(2,50)}$= 24.83, $p < .001$), t-tau ($F_{(2,50)}$= 13.91, $p < .001$), p-tau ($F_{(2,50)}$ = 16.95, $p < .001$), plasma p-tau181 ($F_{(2,50)}$= 18.59, $p < .001$), and Aβ42 ($F_{(2,52)}$ = 18.05, $p < .001$). There was no significant effect of group on Aβ40 values (Table 4.7).

Tukey correction was used to compare the patient groups in more detail. Results showed a significant difference of CSF Aβ/tau ratio between controls and MCI patients ($t(6.57), p < .001$) and between controls and AD patients ($t(4.9), p < .001$). No significant difference was observed between MCI and AD patients, which was expected as recruitment focused on MCI patients with positive AD pathology (Figure 4.7A). Similar results were found for CSF p-tau (Figure 4.7B), CSF t-tau (Figure 4.7C) and plasma p-tau181 (Figure 4.7D), suggesting that these neuropathological measures can successfully differentiate between controls and patients with AD pathology.

To investigate the relationship between neuropathology markers and memory scores, separate linear regression models were examined and R^2 effect sizes and beta values were compared to assess the predictability of neuropathology from cognitive scores.

Interestingly, the Four Mountains test was the most predictive for CSF Aβ/tau ratio and CSF p-tau levels (Table 4.4, Table 4.5). However, the RBANS Visuospatial score was most predictive for plasma p-tau181 (Table 4.6).

Table 4.4. Results of separate linear regression models for neuropsychological tests (predictor) and CSF Aβ/tau ratio.

Variable	R	R^2	β	t	*p*
ACE-R Attention	0.363	0.132	-0.368	2.79	.007
ACE-R Fluency	0.296	0.088	-0.300	2.216	0.031
ACE-R Language	0.228	0.052	-0.232	1.68	0.1
ACE-R Memory	0.259	0.211	-0.460	3.69	< .001
ACE-R Visuospatial	0.297	0.088	-0.303	2.22	0.031
MMSE	0.363	0.132	-0.368	2.78	0.008
RBANS Visuospatial	0.589	0.347	-0.612	4.9	< .001
RBANS Memory	0.534	0.285	-0.566	4.37	< .001
FCSRT (Total)	0.391	0.153	-0.365	2.82	.007
Four Mountains (%)	0.602	**0.363**	**-0.610**	4.9	< .001

Table 4.5. Results of separate linear regression models for neuropsychological tests (predictor) and CSF p-tau.

Variable	R	R^2	β	t	*p*
ACE-R Attention	0.298	0.089	-0.311	2.32	0.03
ACE-R Fluency	0.325	0.106	-0.333	2.46	0.017
ACE-R Language	0.206	0.043	-0.213	1.51	0.138
ACE-R Memory	0.351	0.123	-0.352	2.57	0.01
ACE-R Visuospatial	0.229	0.052	-0.262	1.68	0.099
MMSE	0.282	0.080	-0.301	2.1	0.041
RBANS Visuospatial	0.485	0.235	-0.526	3.9	< .001
RBANS Memory	0.406	0.165	-0.457	3.1	.003
FCSRT Total	0.365	0.133	-0.318	2.6	.013
Four Mountains (%)	0.56	**0.354**	**-0.617**	4.8	< .001

Table 4.6. Results of separate linear regression models for neuropsychological tests (predictor) plasma p-tau181.

Variable	R	R^2	β	t	*p*
ACE-R Attention	0.314	0.099	-0.314	2.5	0.015
ACE-R Fluency	0.164	0.027	-0.163	1.25	0.216
ACE-R Language	0.162	0.026	-0.162	1.24	0.219
ACE-R Memory	0.504	0.254	-0.503	4.4	< .001
ACE-R Visuospatial	0.279	0.077	-0.277	2.181	0.033
MMSE	0.416	0.173	-0.416	3.45	< .001
RBANS Visuospatial	0.614	**0.377**	**-0.579**	5.6	< .001
RBANS Memory	0.356	0.127	-0.339	2.72	.009
FCSRT Total	0.492	0.242	-0.475	3.96	< .001
Four Mountains (%)	0.527	0.278	-0.527	4.16	< .001

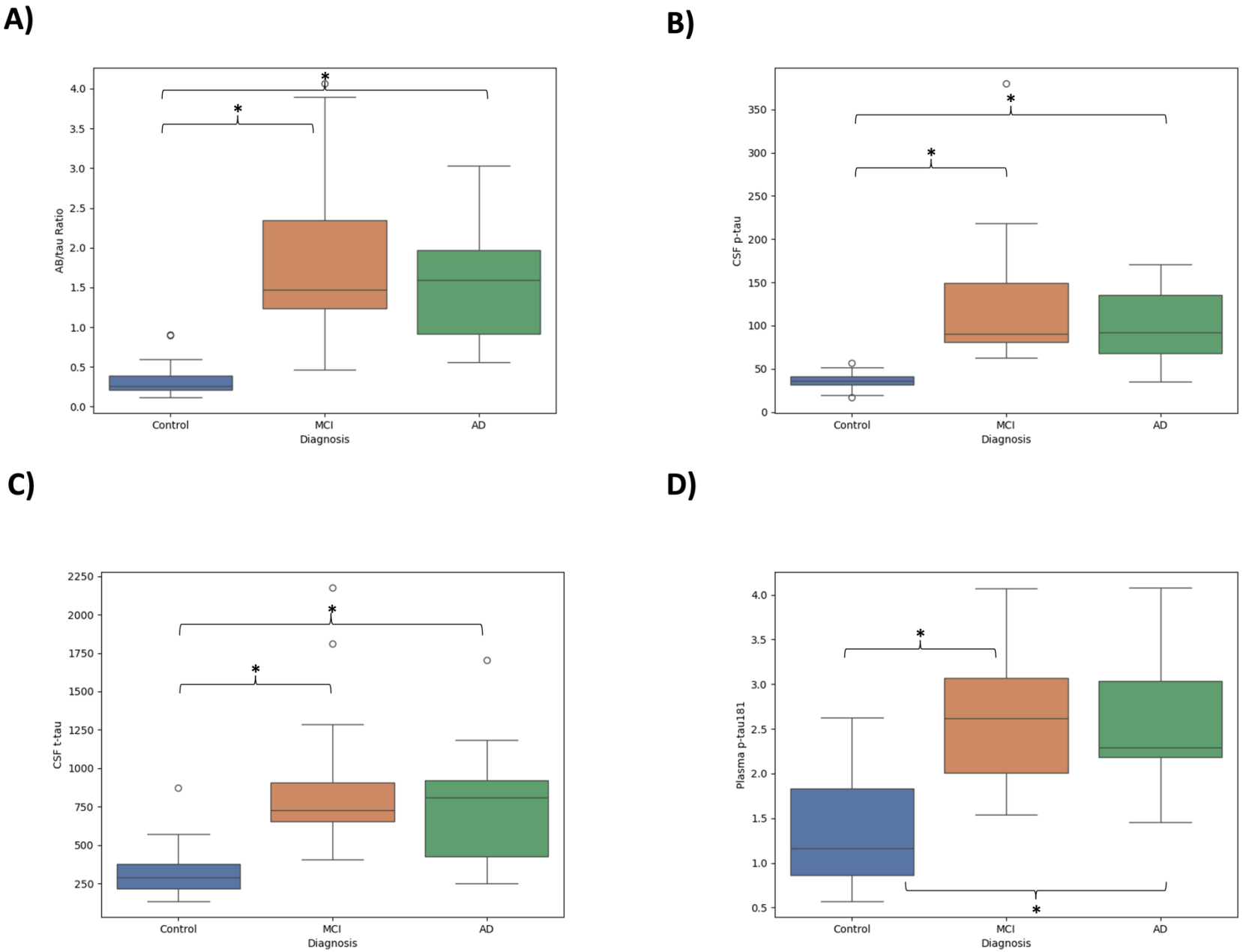

Figure 4.7. Baseline group differences in neuropathology measurements.
Boxplots showing the group differences in **A)** CSF Aβ/tau ratio. **B)** CSF p-tau. **C)** CSF t-tau. **D)** Plasma p-tau181. * = $p < .05$.

Table 4.7: Baseline CSF neuropathology measures for the control and patient groups.

Values represent the mean (standard deviation). P values are results of one-way ANOVA. Participants had various CSF analysis completed depending on lab availability. Aβ40 values are not displayed due to a small number of data available (N=5).

	Controls (N=20)	**Patients (N=29)**		**P**
		MCI (*n=17*)	**AD** (*n*=12)	
CSF tau/Aβ ratio				
Aβ42/tau ratio	0.35 (0.22)	1.91 (1.04)	1.63 (0.79)	< .001
	Controls (N=35)	**Patients (N=31)**		
		MCI (*n*=18)	**AD** (*n*=13)	
CSF Aβ42				
Aβ42	1020.76 (405.42)	544.28 (222.26)	479.31 (137.81)	< .001
	Controls (N=23)	**Patients (N=31)**		
		MCI (*n*=18)	**AD** (*n*=13)	
CSF Tau				
CSF p-tau	36.69 (9.98)	127.33 (79.53)	94.53 (41.88)	< .001
CSF t-tau	327.81 (163.35)	891.34 (470.0)	763.77 (407.15)	< .001
	Controls (N=15)	**Patients (N=44)**		
		MCI (*n*=24)	**AD** (*n*=20)	
Plasma pTau181				
p-tau181	1.33 (0.62)	2.57 (0.66)	5.44 (0.73)	< .001

4.3.3 Annual results

The following results focus on the patient group (MCI and AD patients) only as healthy controls did not complete the annual visits. Details of the annual structural measurements and neuropsychological scores are shown in Table 4.8.

Paired samples t-test revealed a significant difference between baseline and annual visits for all cognitive scores, except for ACE Fluency, ACE Memory, and Four Mountains scores. Additionally, all brain volume measurements, except for total brain volume, were significantly different between baseline and annual scans (Table 4.8).

Table 4.8: Annual brain volumes and neuropsychological assessments for the patient group.

Values represent the delta value (Δ) of the difference between baseline and annual scores. Negative values mean the score decreased over time, and positive values mean the score increased from baseline to follow-up. P values are results of paired samples t-test for MCI and AD patients combined.

	Patients (N=55)		**P**
	MCI Δ(*n*=27)	**AD** Δ(*n*=28)	
Neuropsychological assessments			
MMSE	-1.2	2.8	< .001
ACE-R total score /100	-2.4	-8.7	< .001
ACE Attention /18	-0.9	-2.6	< .001
ACE Fluency /14	+0.3	-0.8	.435
ACE Language /26	-0.7	-4.5	< .001
ACE Memory /26	+0.1	-1.7	.777
ACE Visuospatial /16	+3.8	-7.9	0.002
Four Mountains (% correct)	-3.22	-0.81	.193
FCSRT Delayed (free) /48	-3.22	-0.81	< .001
FCSRT Delayed (total) /48	-5.52	-6.21	< .001
RBANS Visuospatial index	+18.77	+13.88	< .001
RBANS Memory index	-31.50	-30.04	< .001

	Patients (N=47)		
	MCI (*n*=26)	**AD**(*n*=21)	
Brain volumes			
Whole brain (mm^3)	-7,000	+21,000	.101
Grey matter (%)	-0.6	+0.1	< .001
White matter (%)	-0.3	0	.004
Left hippocampus (%)	-0.01	+0.01	< .001
Right hippocampus (%)	-0.01	0	< .001

4.4 Discussion

This chapter presented an in-depth examination of the NTAD study, focusing on baseline measures of neuropsychological assessments, brain structure measurements and neuropathology markers. The primary aim of the results was to validate key structural and neuropsychological differences in the NTAD cohort, investigate potential relationships between these differences and neuropathological markers, and identify variables for subsequent analysis. The results revealed significant and expected structural, cognitive, and neuropathological differences between biomarker-positive patients and biomarker-negative controls. Additionally, clinical cognitive tests were compared to research-based assessments for AD through multiple linear regression models.

As expected, AD patients exhibited a considerable decrease in hippocampal volume compared to both MCI patients and healthy controls. The difference in total hippocampal volume between controls and MCI patients was 4.98%, while the difference between MCI and AD patients was 2.7%. Additionally, differences in MMSE scores, total ACE-R scores, and all sub-scores of the ACE-R exam were observed between controls and patients. These structural and neuropsychological differences support the validity of the NTAD as it demonstrates a clear distinction between healthy controls and biomarker-positive patients, aligning with findings from other research (Barnes et al., 2009; Henneman et al., 2009; Shi et al., 2009). Notably, the ACE-R memory score was the strongest predictor of hippocampal volume, indicating that hippocampal size correlates with memory function.

This analysis is one of the first to investigate MRI hippocampal volumes with ACE-R sub-scores in MCI and AD patients. Related evidence comes from FDG-PET research in AD patients, which has investigated the neural correlates of ACE sub-scores. In a study by Cabrera-Martín et al. (2023), the memory domain was the only sub-score associated with the parahippocampal gyrus and hippocampal regions. These PET findings suggest a specific link between hippocampal integrity and memory-related ACE performance, which is consistent with neuropathological evidence of hippocampal function (Braak & Braak, 1991), and supports the rationale for our MRI-based analysis in the NTAD cohort.

The Four Mountains score was investigated in detail, as this thesis is focused on exploring alternative measures for AD that could be utilised within a clinical setting. Previous research

has shown that the Four Mountains is designed to reflect the role of the hippocampus in spatial memory and can identify AD in its earliest stages (Chan et al., 2016). Therefore, this thesis conducted exploratory analysis of the test within the NTAD cohort, alongside comparisons with other tests of spatial and episodic memory such as the FCSRT and RBANS. Overall, controls scored much higher on the Four Mountains test than MCI and AD patients, with average scores of 70%, 47% and 37%, respectively. Moreover, in line with previous research, a positive association was found between Four Mountains and total hippocampal volume ($r = 0.441$), meaning that a larger hippocampus corresponds to a higher Four Mountains score (Chan et al., 2016). Taken together, these results indicate that the 4MT is a sensitive test for spatial memory ability which declines with the progression of the diagnosis.

Results further found that the right hippocampus was more strongly associated with the Four Mountains score than the left hippocampus, likely due to bilateral differences in hippocampal function as demonstrated by Ezzati et al. (2016), who found that the right hippocampus was more strongly associated with spatial memory, whereas the left hippocampus was associated with verbal episodic memory. These results support the idea that the Four Mountains test is sensitive to hippocampal changes and can detect differences between controls and patients. Although the effect sizes for the Four Mountains test were not as strong as for the MMSE or ACE-R, fewer participants were included in this analysis. Nevertheless, the results remain intriguing and in line with previous research, therefore this variable will be included in further analyses investigating the relationship between MEG measures and AD pathology.

Neuropathological measures, including Aβ/tau ratio, Aβ40, Aβ42, t-tau, p-tau, and plasma-tau181, were compared between groups. Results showed significant differences between controls and patients for all measures except Aβ40,with MCI and AD patients showing similar profiles. Given the NTAD's cohort screening for Aβ pathology, these findings were expected. Interestingly, when neuropathological measures were compared to cognitive test scores, it was found that the Four Mountains test was most predictive of performance on Aβ/tau ratio and p-tau measures. This result is intriguing, as Aβ/tau ratio and p-tau are believed to be strongly associated with cognitive deficits and the neuropathological changes characteristic of AD. This suggests that the Four Mountains test may be more predictive of neuropathological alterations in AD and could potentially detect these changes earlier than other commonly used measures, such as the MMSE and ACE-R. This is in line with earlier research by Coughlan et al. (2023),

who examined the relationship between Aβ42 and p-tau and the Four Mountains performance in the European Prevention for Alzheimer's Disease (EPAD) cohort. They found that Aβ42 and p-tau levels were significantly associated with lower scores on the Four Mountains test. Furthermore, the correlation between p-tau and spatial scores were mediated through the entorhinal cortex, suggesting that tau pathology, rather than amyloid deposition, has a stronger association with cognitive decline and clinical presentation.

An important aspect of the neuropathology measures investigated in the NTAD cohort was plasma p-tau, as it is a relatively new approach to assessing AD pathology without requiring a lumbar puncture. Previous research has demonstrated that plasma p-tau181 is predictive of MCI to AD conversion and cognitive decline (Kivisäkk et al., 2023; Smirnov et al., 2022), highlighting its potential as a reliable biomarker for earlier detection. Our results revealed a significant difference in plasma p-tau181 levels between controls and patients, supporting its role in distinguishing individuals with AD pathology. However, there was substantial overlap in scores between groups, suggesting that while plasma levels are a useful biomarker, it may not yet provide the same level of diagnostic precision as CSF-based tau measurements. Further analysis using multiple linear regression showed that plasma p-tau181 levels were most strongly predicted by the RBANS visuospatial index score, suggesting a potential link between plasma tau burden and visuospatial cognitive function. Given the ease of access and less invasive nature of plasma biomarkers, plasma p-tau181 will be included in later analyses to assess its utility in detecting AD-related changes. Future research should also explore alternative plasma tau markers, such as p-tau217, which has shown strong potential for distinguishing AD with a specificity compared to CSF-based measures (Ashton et al., 2024). Data on p-tau217 will soon be available within the NTAD cohort, allowing for a comprehensive evaluation of plasma-based biomarkers in AD. In the meantime, levels of Aβ/tau ratio, CSF p-tau and plasma p-tau181 will be included in later analyses to further test their utility in early detection of AD.

Overall, this chapter has outlined and analysed the NTAD study, confirming the validity of the NTAD cohort through the expected anatomical and cognitive differences between patients and controls. Additionally, intriguing findings from the Four Mountains test and neuropathology measures support recent research and provide novel insights into the relationship between hippocampal function, spatial memory, and AD pathology. These results emphasise the

potential of novel cognitive assessments in detecting early AD-related changes, reinforcing the need for further exploration. The analysis comparing MCI and AD patients revealed that, while there were differences in cognitive scores and structural measurements, neuropathology levels were similar across the two groups. Going forward, this thesis will combine MCI and AD patients into a single patient group for further analysis. Future investigations will focus on resting-state MEG and fMRI to better understand the neural mechanisms underlying AD. By examining connectivity patters and neural oscillatory activity in relation to cognitive and neuropathology this research will provide a more comprehensive understanding of how structural and functional brain changes contribute to cognitive decline. Key variables identified in this analysis, including well-known clinical measures such as the Aβ/tau ratio, MMSE score, and hippocampal volume, alongside research-based variables such as the Four Mountains test and p-tau, and plasma p-tau levels, will form the core set of variables for subsequent investigations. While these measures provide the primary focus for analyses, later chapters will also include exploratory analyses encompassing all brain volume metrics and ACE sub-scores to capture potential additional associations and patterns.

Chapter 5: Resting-state MEG: Linking oscillatory activity to MRI, cognitive scores, and neuropathology.

Over the last decade, research into the use of MEG in clinical applications has increased rapidly. In the field of AD research, studies have found frequency-wide alterations in the power spectra of resting-state data, indicating a slowing in brain activity in AD patients (Engels et al., 2017). However, these AD-related changes are not always consistent as they are limited by small sample sizes and the lack of biomarker status. In this chapter, I examine the resting-state MEG data from the NTAD cohort using a novel General Linear Modelling (GLM) approach and discuss its relationship to structural measures, neuropathology, and cognition.

5.1 Introduction

The most notable alteration associated with AD in non-invasive oscillatory data, such as MEG and EEG, is that patients with AD have increased delta and theta power, and decreased alpha and beta power compared with controls (de Haan et al., 2008; Fernández et al., 2002; Koelewijn et al., 2017). The second most common finding in MEEG research is occipital alpha showing, whereby AD patients exhibit a decrease in alpha peak frequency. These alterations have been linked to alterations in cognitive scores (Fernández et al., 2006) as well as accumulations of tau and amyloid (Ranasinghe et al., 2022). The majority of these data were gathered through the use of resting-state scans, which measure the brain's spontaneous oscillations during periods of rest – when there is no task. Even in these restful states, neuronal activity remains active across various brain regions.

Numerous studies that have looked at data from resting states have identified specific brain networks that are especially prominent during rest. The most well-known of these is the DMN which has been demonstrated to be altered in MCI patients (Garcés et al., 2014). The DMN is known to be extremely active during an idle state and to deactivate during task execution (Raichle et al., 2001). Clinically, the use of resting-state paradigms is advantageous due to its ease of acquisition for both participant effort and time. Moreover, the resting-state metrics obtained during these scans have shown to be reliable in the healthy population (Lew et al., 2021).

However, it remains unclear whether resting-state data should be obtained with eyes open, or eyes closed. This consideration is important when investigating alpha power as it is well documented that this decreases when the eyes are open (Berger, 1929; Cohen, 1968). This reduction in alpha power when the eyes are open is referred to as alpha reactivity (Westmoreland & Klass, 1998) . Previous research has found that individuals with AD exhibit reduced alpha reactivity compared to controls, with this decrease correlating with the severity of cognitive impairment (Babiloni et al., 2010; Fonseca et al., 2011). Schumacher et al. (2020) explored alpha reactivity using EEG in AD patients and patients with Lewy body dementia (LBD) in comparison to healthy controls. Their findings revealed that both AD and LBD patients exhibited diminished alpha reactivity compared to controls, with a more pronounced reduction in LBD patients. While not specific to AD, these results suggest that alpha reactivity is a marker of interest in neurodegenerative disorders. Thus, both eyes open and eyes closed conditions will be explored in this chapter, in addition to alpha peak frequency and alpha reactivity.

To date, healthy age-related differences in oscillatory activity are generally consistent. Oscillatory power in the lower frequency bands (delta and theta) are high in early life and decrease through adolescence, with delta continuing to decline and theta showing a potential increase in older age due to cognitive decline (Gasser et al., 1982; Musaeus et al., 2018). The higher frequency bands (alpha and beta) increase with age, peaking in early adulthood, then gradually decline in older age (Babiloni, Binetti, et al., 2006; Klimesch, 1999). In AD patients, these patterns are further altered, with delta and theta activity being higher and alpha and beta activity being lowered compared to healthy older adults (Garcés et al., 2013; Montez et al., 2009; Van der Hiele et al., 2007).

However, most studies include MCI and AD patients with unknown clinical biomarker status, which is crucial when making inferences about AD-specific brain changes. Clinical biomarkers refer to amyloid and tau deposition and neurodegeneration, measured by CSF, PET and MRI . From participant identification to monitoring analytical outcomes, biomarkers are integral to the design of most therapeutic drug studies. Most research relies on the National Institute of Neurological and Communicative Disorders and Stroke, the Alzheimer's Disease and Related Disorders Association, or the National Institute on Aging-Alzheimer's Association criteria for the diagnosis of AD in their participants. Recent research, however, indicates that some

individuals included in these studies may not have AD due to insufficient biomarker evidence. For example, recent studies have found that 15-25% of patients with a clinical diagnosis of AD failed to show abnormal amyloid levels as measured by CSF or PET (Landau et al., 2016; Sevigny, Suhy, et al., 2016). Thus, while this research has been important for our understanding of the brain alterations in AD, relying on clinical diagnosis alone may be insufficient and the use of biomarker status is essential when discussing an early marker of risk for developing AD. As discussed in Chapter 3, the NTAD study that we analyse in this work pays considerable attention to the diagnosis and biomarker status of its participants.

This biomarker-confirmed status in the NTAD study provides a foundation for exploring how MEG-derived resting-state measures relate to established clinical indicators of disease, including brain volumes, neuropathology measures, and neuropsychological scores. Previous studies have reported associations between MEG oscillatory features and clinical indicators of AD. For instance, reduced alpha power and lower peak frequency have been linked to smaller hippocampal volumes (López et al., 2014), while increases in delta/theta activity have been related to greater amyloid and tau deposition (Maestú et al., 2019). Moreover, MEG alterations, particularly in the alpha and beta bands, have been correlated with poorer cognitive performance (Garcés et al., 2013). However, many of these studies are constrained by small sample sizes or the absence of biomarker-confirmed diagnoses. Therefore, the present analysis will explore whether key clinical and research measures of AD can predict MEG oscillatory activity, which is a key focus of this thesis.

To further understand these electrophysiological differences between patients and controls, we can examine the underlying neural activity using frequency-domain analyses. The peaks of oscillations and the general spectral shape can be determined by using the time-average periodogram, which employs the Fourier Transform for the estimation of power spectra (Welch, 1967). While the statistical methods for these analyses have not significantly changed over decades, there have been considerable advances in the field. The power spectrum and suggested framework for data analysis included in this thesis are explained below.

5.1.1. The Power Spectrum

In general, the study of oscillatory brain activity can be described in distinct frequency bands, including 2-4Hz (delta), 4-8Hz (theta), 8-13Hz (alpha), 13-30Hz (beta) and >30Hz (gamma and high gamma). Each of these frequencies can be somewhat attributed to different types of

functional activity. For instance, alpha is linked to a relaxed concentration state, while beta and gamma are linked to focused attention, high-level cognition and memory recall. The lower frequency bands, delta and theta, are related with a thoroughly relaxed and sleep state.

These oscillations reflect the synchronised activity of large populations of neurons doing computations in the brain, changing on very fine spatial and temporal timescales. When neurons communicate with each other, they send small pulses of electricity called action potentials. The timing of these action potentials is crucial to ensure effective communication. Therefore, the synchronisation of firing between neurons ensures that the signal arrives from the pre-synaptic terminal to the post-synaptic terminal at the right time. Although the signal from the individual local field potentials (LFPs), also known as post-synaptic potentials or dendritic currents, is very small, cortical neurons tend to fire in a synchronised manner. This synchronisation produces thousand or even millions of LFPs at a given time that are often spatially aligned. As a result, these inputs into the neurons generate a summation of electrical and magnetic signals that can be detected from outside the skill using MEEG (Proudfoot et al., 2014). Therefore, we use MEG to measure oscillations from thousands of millions of synchronised neurons. Since MEG is a direct measure of neuronal communication, this thesis is interested in how this communication degrades over the lifetime and in conditions such as AD.

The most common method for quantifying this MEG signal is the power spectrum, which shows the absolute or relative contribution to a signal from a variety of frequency bands. The way in which we estimate this is by using Welch's periodogram (Welch, 1967). This involves taking the whole dataset recording, segmenting this into two second sliding windows, performing a Fourier Transform on these sliding windows, and then averaging across all of these to create the frequency power spectrum (Figure 5.1). This results in a power spectrum which shows the magnitude of each frequency for each sensor – a stronger contribution indicated by a higher magnitude. This approach is still widely used in MEG and EEG signal processing software packages and is considered the core method for frequency analysis.

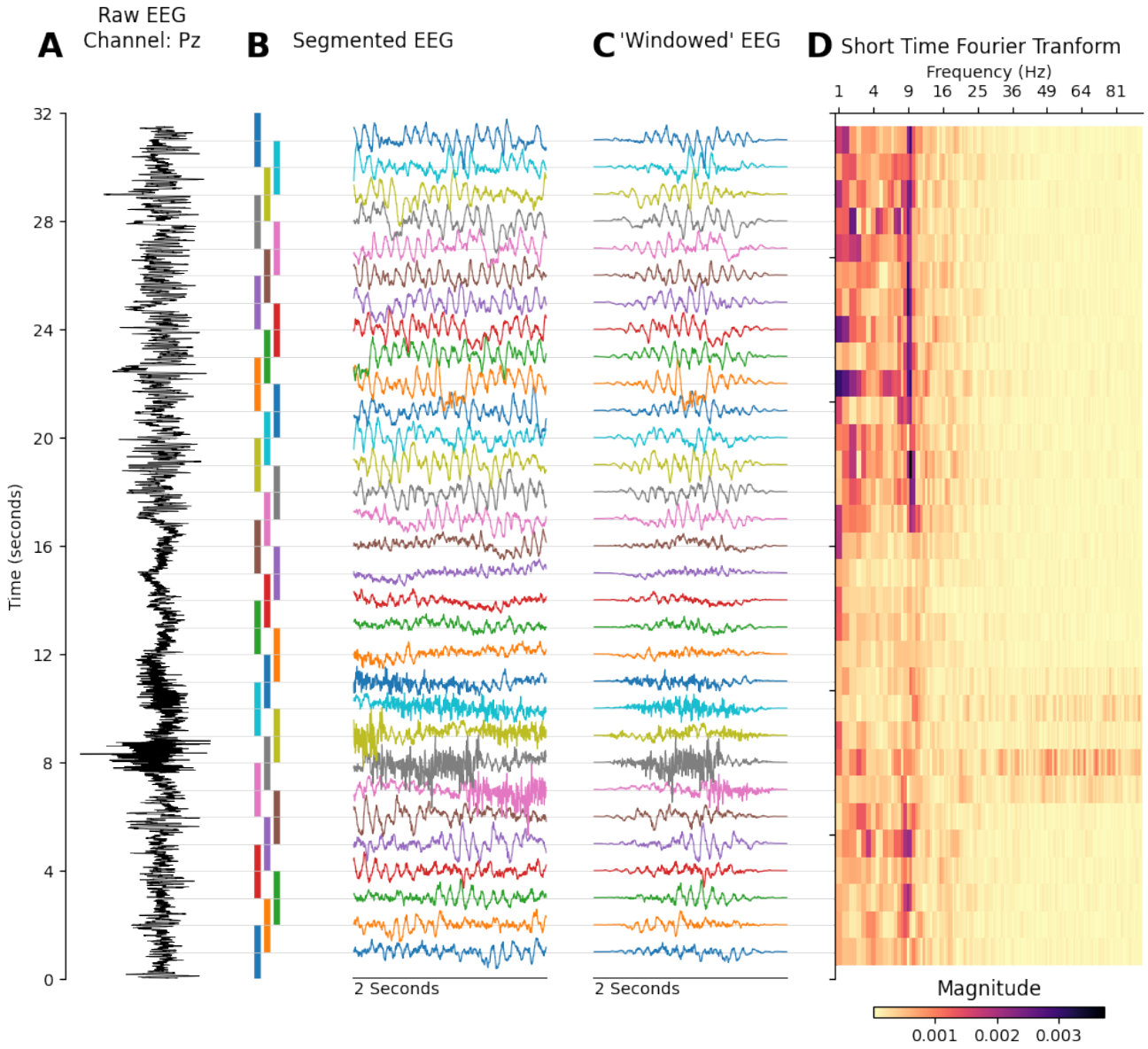

Figure 5.1. Welch's method for spectrum estimation.

A) Raw data of a 32-second segment of pre-processed EEG time-course data from sensor Pz. B) Time-course data segmented into 2-second sliding windows with 50% overlap. C) Windowed data edited using a tapper Hann window function to smooth out the edges of the segments. D) Short time-Fourier transform performed on each sliding window segment.

Each column of this matrix is the dependent variable to be described by the first-level GLM as described in section 5.1.2.

Figure from (Quinn et al., 2024).

5.1.2 The GLM-Spectrum

Welch's method of estimating a power spectrum has remained largely unchanged since 1967 although there has been a large evolution in statistics such as non-parametric permutations, multiple regressions, etc. In particular, Welch's periodogram uses averaging of the spectral content from multiple time segments to create a time-averaged power spectrum. Here, we instead propose using a GLM to estimate the power spectrum instead of using simple averaging, which we refer as the *GLM-Spectrum*. This has many benefits, such as the flexibility to do advanced modelling and significance testing using non-parametric statistics. This method has been outlined in our recent paper (Quinn et al., 2024), and will be described below.

5.1.2.1 First-level GLM

The "first-level" GLM (-Spectrum) analysis involves modelling the data for each participant's MEG data. As with the standard Welch's periodogram, the data is segmented into two second windows with a one second overlap, and a short time Fourier transform (STFT) is performed on each segment. However, unlike the simple averaging in the standard Welch's periodogram, we specify a GLM (multiple regression), in which the STFT data is modelled using multiple regressors. Specific regressors can be included in the GLM design matrix as predictors to describe the change over time at each frequency band in the data. These regressors can include anything that was measured during the time of the recording – for example, eye blinks, heart rate, etc. Thus, this information will be fitted into the model in a way which best describes the STFT data. Note that the first-level GLM is fitted, and the GLM-Spectrum estimated, for each frequency band/bin separately.

5.1.2.2 Group-level GLM

From here, the GLM-spectra estimated by the first-level GLMs are included as the dependant variable in a "group-level" analysis, in which another GLM is used to describe the between-subject variability. This is done by concatenating the parameter estimates (i.e., the GLM-spectra) from the first-level GLM over sessions/subjects, and fitting a group-level GLM to explain what varies between sessions or subjects. The group-level design matrix contains regressors that model the variability across participants, e.g., group membership and demographic measures such as age and sex. Note that once again, the group-level GLM is fitted, and the group-level GLM-Spectrum estimated for each frequency bin/band separately.

5.1.2.3 Permutation tests

Appropriate contrasts in the group-level GLM represent GLM-spectra of interest. These undergo non-parametric permutations, where permutations modify the design matrix to support a null-hypothesis, and then the GLM-spectra are recalculated to obtain the null distribution of the observed data. The observed group average GLM-spectra t-stats are then contrasted with this null distribution, and it is considered significant if it exceeds a predefined threshold, such as p=0.05. Additionally, we permute the columns of the design matrix that are directly related to the relevant controls whilst the remaining regressors are fixed. The number of permutations carried out are defined by the user.

5.2.3 Objectives

By using this GLM design method with the data collected from NTAD, this analysis aims to deepen our understanding of AD-related oscillatory differences in resting-state MEG data. The specific objectives were to determine if:

1. Whole-brain power spectra varies between biomarker-confirmed MCI/AD patients and healthy controls.
2. Differences between patients and controls are reliable and repeatable.
3. Whether alpha reactivity differs between patients and controls.
4. Assess the relationships between MEG, cognitive scores, and pathological biomarkers.

This analysis is conducted solely in sensor space using the GLM-Spectrum approach described above.

5.2 Methods

5.2.1 Participants

Of 104 participants in the NTAD study, 35 controls and 67 patients completed the baseline resting-state scan. From these participants, 20 patients completed the two-week scan, and 46 patients completed the annual resting-state scan. Demographics of these participants are presented in Chapter 3.

5.2.2 MEG acquisition

MEG data were acquired at the Oxford Centre for Human Brain Activity, Oxford and Wolfson Imaging Centre, Cambridge using the details described in Chapter 3.2.4. For the resting-state eyes open scan, participants were seated in the scanner and asked to keep their eyes open and fixated on a black cross presented on a grey background on a projector screen located one meter in front of them. Participants were asked to blink normally and keep as still as possible for the 5-minute scan. For the resting-state eyes closed scan, the projector screen was turned off and participants were asked to close their eyes and try not to fall asleep. Simultaneous EOG, ECG and eye tracking data were acquired during the recording. Only the EOG and ECG data was used as part of this thesis.

5.2.2 MEG pre-processing

MEG data were pre-processed using MNE Python and OHBA Software Library (OSL) (Quinn et al., 2022). The raw data were firstly Maxfiltered using move compensation and a temporally extended signal space separation (tSSS) algorithm (Taulu & Simola, 2006). A benefit of using tSSS is the removal of large participant artefacts such as dental material (Hillebrand et al., 2013), which are particularly common in the older population. Next, OSL batch-pre-processing (van Es et al., 2024) was used to crop the first 40 seconds from the data, bandpass filter the data between 0.1Hz and 175Hz and apply a notch filter in increments of 50Hz. Bad channels were automatically identified in the magnetometers and gradiometers and the data was re-sampled to 400Hz. Bad segments were detected and removed from the data by identifying outlier variance across channels. Independent Component Analysis (ICA) was applied to automatically identify non-neuronal signals such as eye blinks and heart rate– this was computed by correlating the data with the EOG and ECG channels obtained simultaneously with the MEG recording. Components with a correlation over r=.5 were automatically rejected and removed from the data. From here, manual artefact checking of the ICA was completed. If no components in the EOG or ECG domain were identified, manual rejection of eyeblinks and

cardiac components was undertaken by examining the spatial topography and time course. On average, 3 components (ECG and EOG combined) were removed from each dataset. Lastly, the signal variance from both magnetometers and gradiometers were standardised. This resulted in an estimate of power spectral density (PSD) for each participant; an estimate of power at each frequency (189 frequencies, 0 - 175Hz) for each sensor (204).

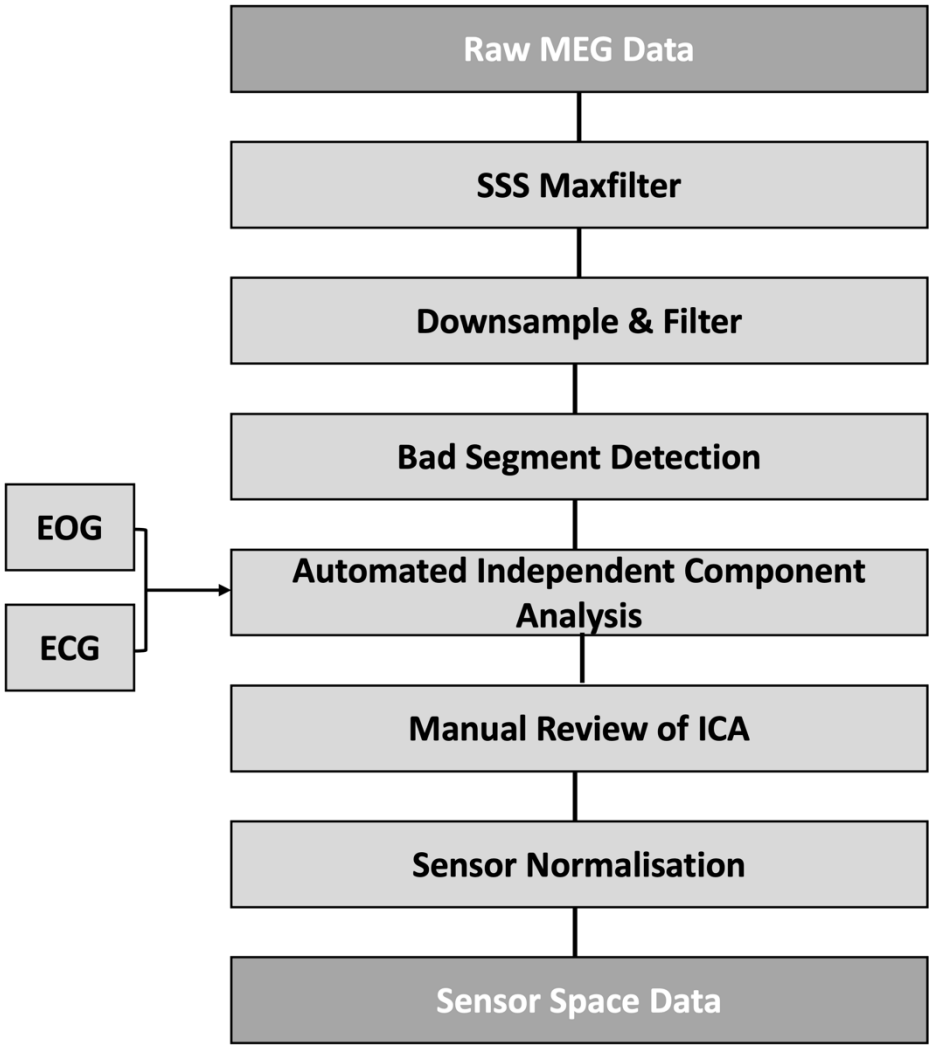

Figure 5.2. Schematic of the MEG data pre-processing pipeline.

Figure based on and adapted from Quinn et al. (2018).

5.2.4 Analysis

5.2.4.1 GLM first-level

The GLM design matrix specifies the regressors used in the first-level model. It includes a constant regressor, followed by a non-zero mean regressor derived from the V-EOG data which were filtered within the 3-20Hz frequency range to act as a confounding variable. For this analysis, data from the 204 planar gradiometers was used. This is because it has been shown that gradiometers are less affected by environmental noise and are more interpretable (Gross et al., 2013; Hansen et al., 2010). The data from the 204 gradiometers were combined and averaged within each of the 102 locations using a mean method, to generate a single gradient map, resulting in a total of 102 sensors. This combined data was used to compute the power spectrum between 1 and 95Hz with a segment length of 2 seconds. The parameter estimate for each participant's PSD is summarised by the Contrast of Parameter Estimate (COPE) value. As mentioned earlier, separate GLMs and corresponding COPEs are estimated for each frequency bin/band. We refer to the combination of the COPEs across frequency bins at a given location (e.g., sensor) as the "COPE-spectra".

Note that upon visual inspection of the data, an unknown artefact was present in the data from 26-30Hz. As such the analysis only focussed on frequencies up to 25Hz.

5.2.4.2 GLM group-level

The group-level analysis uses the COPE-spectra from the first-level results as the dependent variable to describe between-subject variability. The group-level design matrix included categorical regressors for the control and patient groups, as well as parametric regressors for well-known covariates age, sex, scanner, and education, which were all z-transformed to normalise variance to ensure that the parameter estimates were comparable.

To account for variability in cognitive scores between groups, two approaches to including MMSE were explored: 1) z-transforming the MMSE score separately for each group and including these as two regressors in the design matrix, and 2) demeaning the MMSE score across the whole sample and using it as a single regressor. Both approaches produced similar results, however the group specific MMSE scores were used in the final analysis (Figure 5.3). A contrast was used to define the estimate mean across all participants and a second to estimate the difference between controls and patients. Independent t-tests were specified between each covariate for baseline data, and paired t-tests for the two-week and annual data.

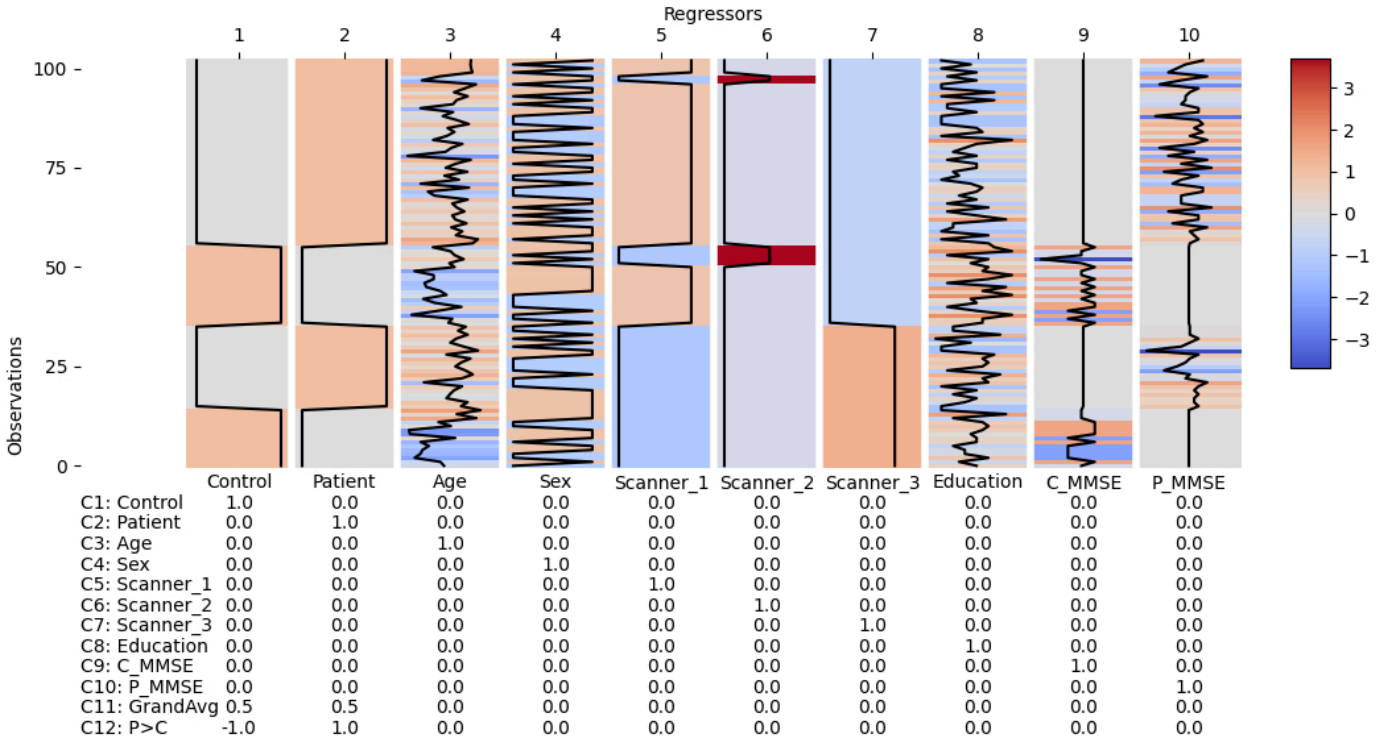

Figure 5.3. Group-level GLM.

This shows 10 regressors that were specified in the model, and 12 contrasts (11 main effects and 1 differential contrast)

5.2.4.3 Interclass correlation coefficient analysis

To measure the reliability/consistency of the baseline measurements, interclass correlation coefficient (ICC) analysis was conducted. This analysis uses the ICC to assess the reliability and consistency of baseline and two-week measurements. ICC was chosen over a paired t-test because the goal with the two-week measurements data is not to compare differences between two conditions, but to evaluate how closely related the repeated measurements are within the same participants. Unlike a paired t-test, which tests for statistical differences, ICC quantifies the degree of similarity between repeated measurements, making it more appropriate for assessing the baseline and two-week data. The analysis was conducted using the Pingouin software package (Vallat, 2018), with a specific focus on ICC3 results. ICC3 was chosen as the model includes raters that are fixed, so the goal is to assess the consistency of scores between measurements rather than absolute agreement. ICC estimates were interpreted as follows: 0 – 0.25 indicates poor reliability, 0.26 -0.5 indicates moderate reliability, 0.51 – 0.75 indicates good reliability, and 0.76 – 1 indicates excellent reliability.

5.2.4.4 Paired test GLM

For the comparison between baseline and annual data, a specialised GLM model was implemented to account for the paired nature of the data. A single regressor captured the differences from baseline to annual scans (Annual Follow-up > BaseLine, or AF>BL), along with separate subject-specific regressors for each subject (Figure 5.4). By including these subject-specific regressors, we controlled for the between-subject variability, allowing us to focus on within-subject changes over time. The resulting AF>BL COPEs were then tested for normality using the Shaprio-Wilk test (p> .05). If normally distributed, a paired t-test was applied; otherwise, a Wilcoxon Signed-Rank test was used.

5.2.4.5 Alpha peak frequency analysis

To determine the alpha peak frequency and its corresponding amplitude from each participant's spectral power, the Fitting Oscillations & One-Over F (FOOOF; (Donoghue et al., 2020) package was used. Firstly, the 1/f component of the spectrum was removed to enable a clearer view of the oscillatory peaks. Following this, the highest peak within a specified frequency range (5 – 15Hz) and sensor location (occipital channels) was identified, representing a typical alpha peak frequency range. In cases where no peak was identified, the corresponding participant was excluded from the FOOOF analysis.

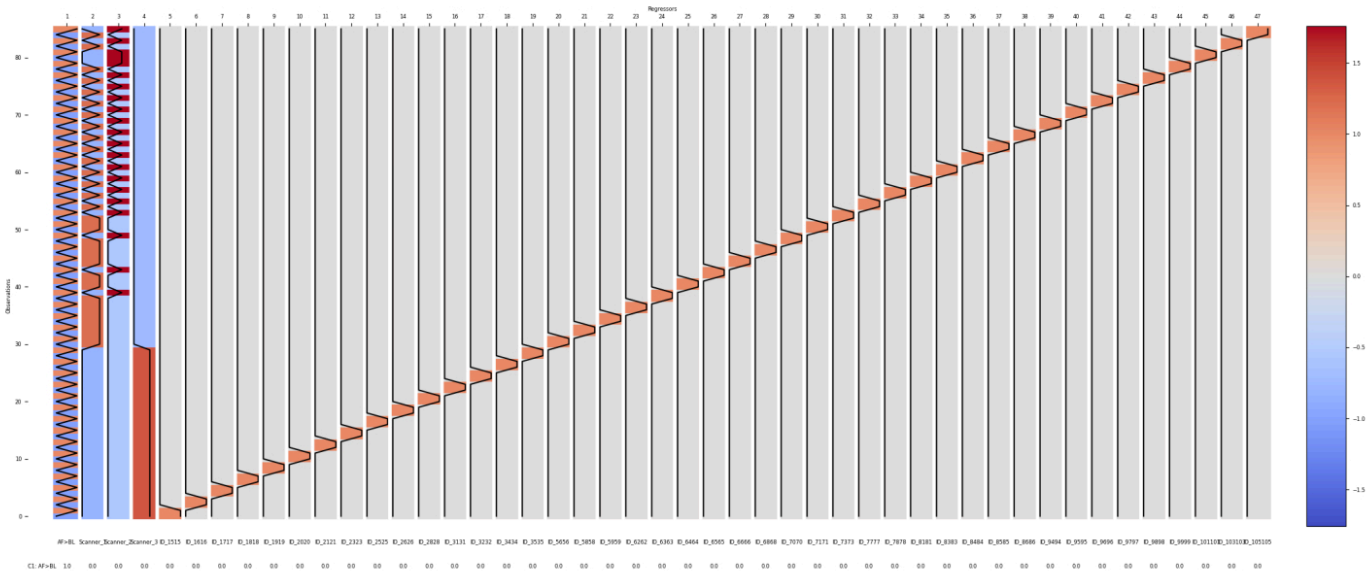

Figure 5.4. Paired test GLM (Baseline vs. Annual)

This shows one regressor for AL>BL differences, three scanner regressors, and the individual subject regressor. The single contrast C1: AF>BL shown, computes a COPE corresponding to a paired test comparing Annual Follow-up and BaseLine.

5.2.4.6 Alpha power and reactivity analysis

Alpha power was calculated as the relative power within a frequency range centred around each participant's individual alpha peak, in the occipital channels. The frequency range was defined as +-2Hz around the alpha peak frequency, which was identified from the eyes-closed condition. Individual alpha peak frequency was used, instead of the standard alpha frequency band, to account for the shift in alpha peak between controls and patients (Babiloni et al., 2015; Garcés et al., 2013; Montez et al., 2009). The eyes-closed alpha peak frequency was used to match previous literature (Fonseca et al., 2011; Schumacher et al., 2020).

Alpha reactivity was calculated as:

$$alpha\ reactivity = \left(\frac{alpha\ power\ eyes\ closed - alpha\ power\ eyes\ open}{alpha\ power\ eyes\ closed}\right)$$

This calculation represents the change in alpha power between eyes-closed and eyes-open conditions, with a larger number indicating greater alpha reactivity.

5.2.4.7 Statistics

Statistical significance between GLM contrasts was determined using non-parametric permutation testing of the observed differences between a specific contrast of interest defined in the GLM model. One thousand permutations were conducted to determine the maximum statistic across both spatial sensors and frequency bands within each individual analysis. Significant clusters of sensors, where the observed differences between controls and patients were greater than expected chance, were identified using a 95% threshold. This means that clusters were considered statistically significant if they fell into the top 5% of the permutation distribution. To account for variance in the different contrasts, permutation testing was conducted on the t-stats instead of the COPE values. To account for multiple comparisons, the maximum statistic for each main effect and contrast was computed across each frequency band and sensor. A result was considered statistically significant if it exceeded the 95th percentile of the null distribution. A visual representation of the permutation testing will be shown as a red bar in the plots below.

Individual alpha peak frequency and alpha reactivity were compared using independent t-tests or Mann-Whitney U tests depending on whether the data was normally distributed. Multiple

linear regressions were used between alpha peak frequency and hippocampal volume and neuropathology measures, accounting for age, sex, and years in education.

Separate linear regression models were used to compare the predictability of brain structure, neuropathology measures, and clinical scores on the MEG measures. The specific predictors and outcomes for each model are detailed within the relevant analyses.

5.2.4.8 Software and dependencies

All analyses in the following chapter were carried out in Python 3.8 with the following dependencies: numpy (Harris et al., 2020), Matplotlib (Hunter, 2007), MNE python (Gramfort et al., 2013), OSL (https://github.com/OHBA-analysis/osl), and glmtools (https://pypi.org/project/glmtools/).

Code for data pre-processing and statistical analysis can be found at: https://git.fmrib.ox.ac.uk/jpitt/ntad.

5.3 Results

5.3.1 Resting-state eyes-open

5.3.1.1 Whole cohort

Out of the 104 participants in the NTAD cohort, 1 was unable to complete the resting-state eyes-open scan. Therefore, the results were computed on 103 participants (35 healthy controls, 68 patients).

The average power spectra across all frequencies and participants for each virtual sensor is shown in Figure 5.5, based on the grand average contrast from the group-level design matrix presented in Figure 5.3. As in typical resting-state data, there is a general decline in spectral power with increasing frequency, except for an alpha peak at approximately 9Hz and some beta increases from approximately 15-25Hz.

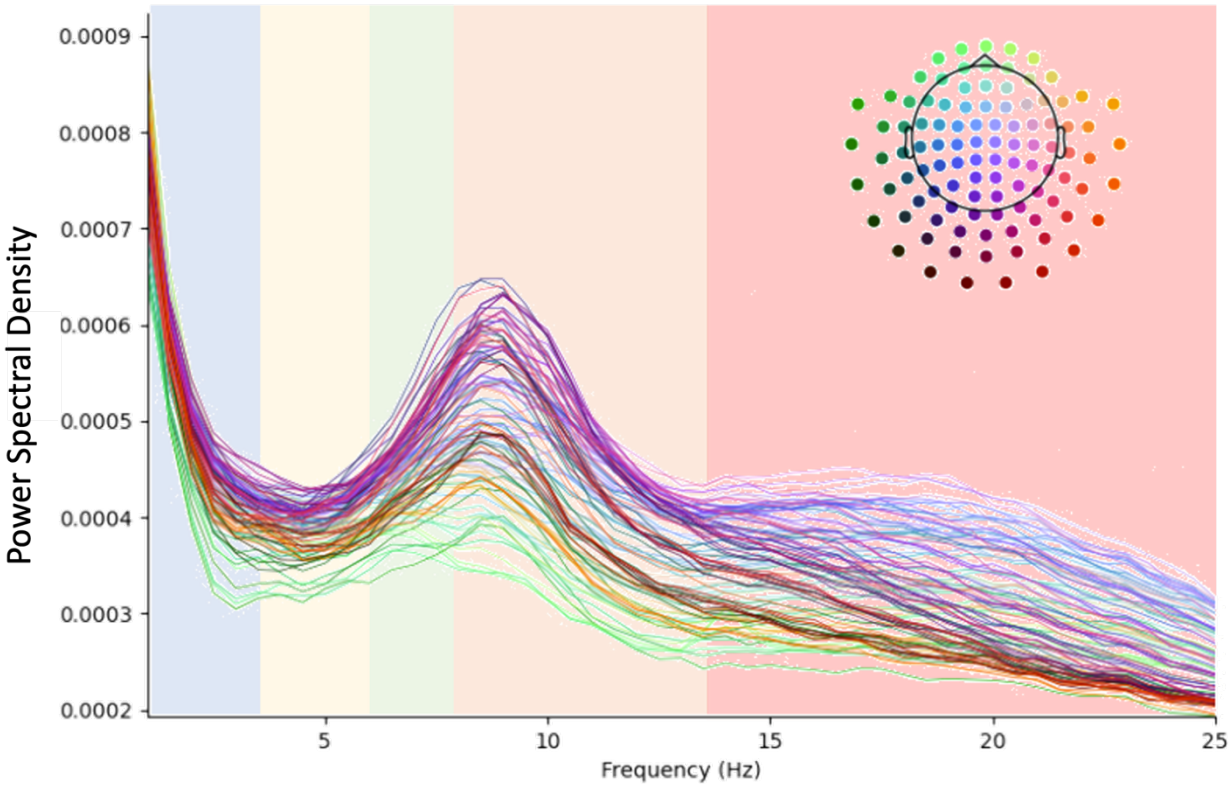

Figure 5.5. Whole cohort power spectra (resting-state eyes-open)**.**

Mean power spectra of all participants, over all sensors and frequencies for resting-state eyes-open data. Topography of sensors is shown by colour. Coloured bars represent the frequency band cut-offs (Delta: 1-4Hz, Theta: 4-8Hz, Alpha: 8-13Hz, Beta: 13-30Hz).

5.3.1.2 Patients vs. Controls

This cross-sectional analysis focused on whether there were any global differences in sensor-space power spectra between the patient and controls groups in the resting-state eyes-open condition, serving as a foundation for subsequent longitudinal investigations. The average topographies for each frequency are shown in Figure 5.6A, with the marked sensors indicating where there is a significant change in power at any frequency after non-parametric permutation testing. Figure 5.6B shows the power spectral density averaged over all sensors for the patients versus controls contrast.

Notably, the group-level GLM contrast (P>C from Figure 5.3) revealed that, after permutation testing, patients exhibited an increase in theta power and a decrease in alpha and beta power. These group differences support the idea that AD patients show unique power spectra differences that are not solely the result of ageing. No significant differences were observed in the delta frequency band. There was an additional visual difference in alpha peak frequency that was analysed separately (Section 5.3.3).

The observed patient versus controls significant differences within the theta, alpha and beta frequency bands were used to define clusters for subsequent analysis. The clusters were generated by averaging over the frequencies that had a significant value across all sensors. Multiple comparisons were controlled for using the permutation testing in the group-level GLM contrast (patients > controls). These clusters will be used to assess the reliability of the observed differences and to examine any changes in activity over time, providing a means to track the progression of alterations within these frequency bands.

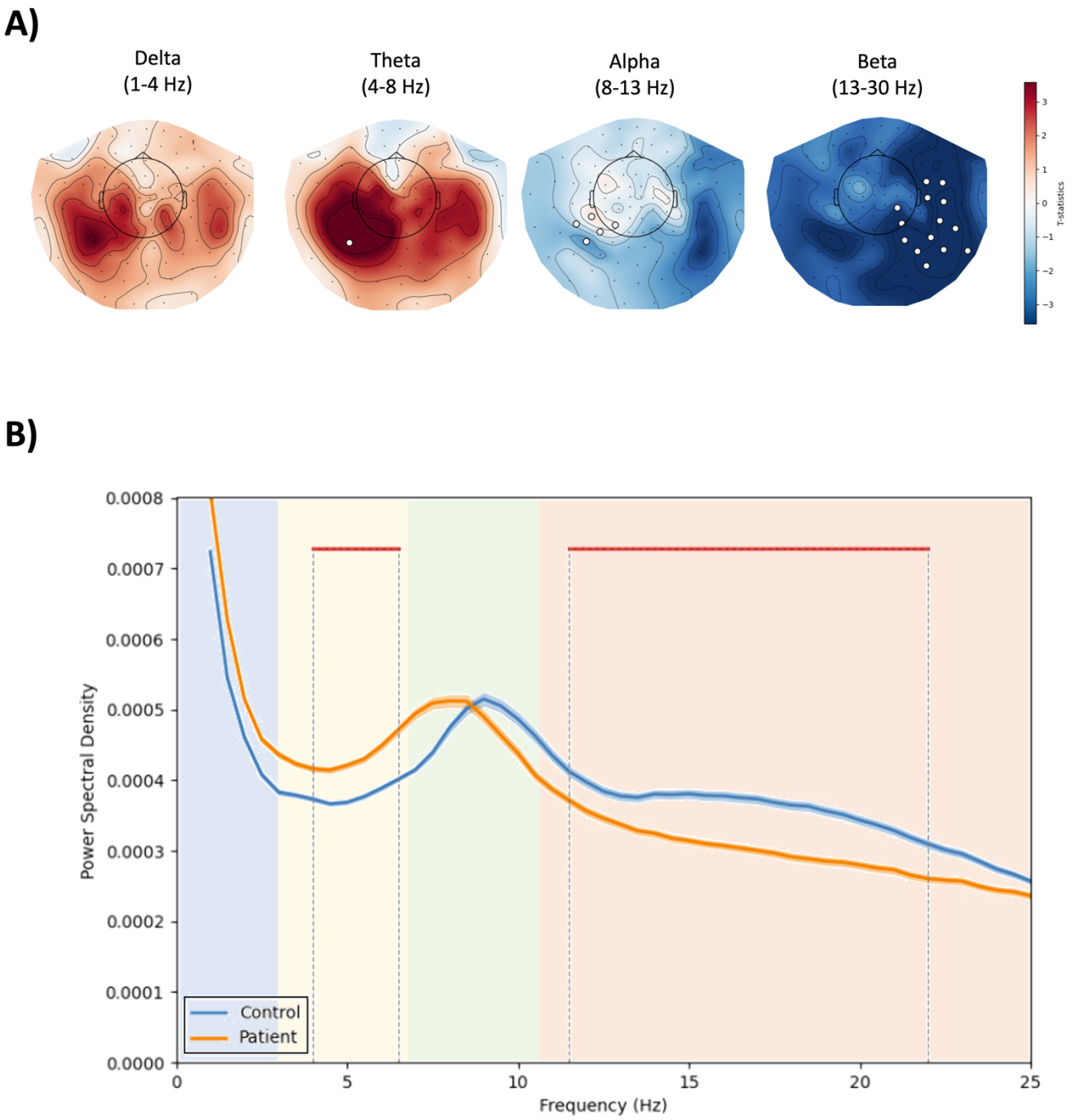

Figure 5.6. Cross-sectional statistical analysis of sensor-space MEG data for the Patient>Control group contrast across delta, theta, alpha, and beta frequencies (resting-state eyes-open).

A) Topography maps for each frequency. Red indicates increased power in patients, and blue indicates decreased power in patients. Marked sensors indicate significant changes in power after non-parametric permutation testing (95% significance threshold). Units displayed are t-statistics.

B) Mean power spectral density of controls and patients, over all sensors. The red bars indicate the frequencies that survived non-parametric permutation testing (95% significance threshold). Shaded areas represent the standard error.

5.3.1.3 Test re-test reliability

This analysis focussed on whether the baseline results were reliable and consistent over time. These results are on patient-only data as healthy controls did not complete any two-week scans. Of the 21 patients that completed the two-week scan, 1 was unable to complete the resting-state scans due to discomfort. Therefore, the test re-test reliability data was computed on 20 patients (15 MCI, 5 AD).

Each participant's power spectra from their first-level GLM were recalculated, with the power for each sensor averaged within the two frequency clusters identified in Figure 5.6B (Frequency Cluster 1: 4 – 6.5Hz and Frequency Cluster 2: 11.5 – 22Hz). Note that here in the results, these clusters are referred to as 'Frequency Clusters'; however, in the discussion, they will be referred to by their respective frequency bands for ease of understanding.

The topographies for Frequency Cluster 1 and Frequency Cluster 2 are shown in Figure 5.7A. Figure 5.7B displays the ICC values across all frequencies. Results demonstrated that ICC values exhibit lower reliability in the lower frequency bands (delta and theta) compared to the higher frequency bands (alpha and beta). This suggests that the alpha and beta frequency bands are more consistent within participants, and therefore may be better suited for tracking disease progression due to their high reliability.

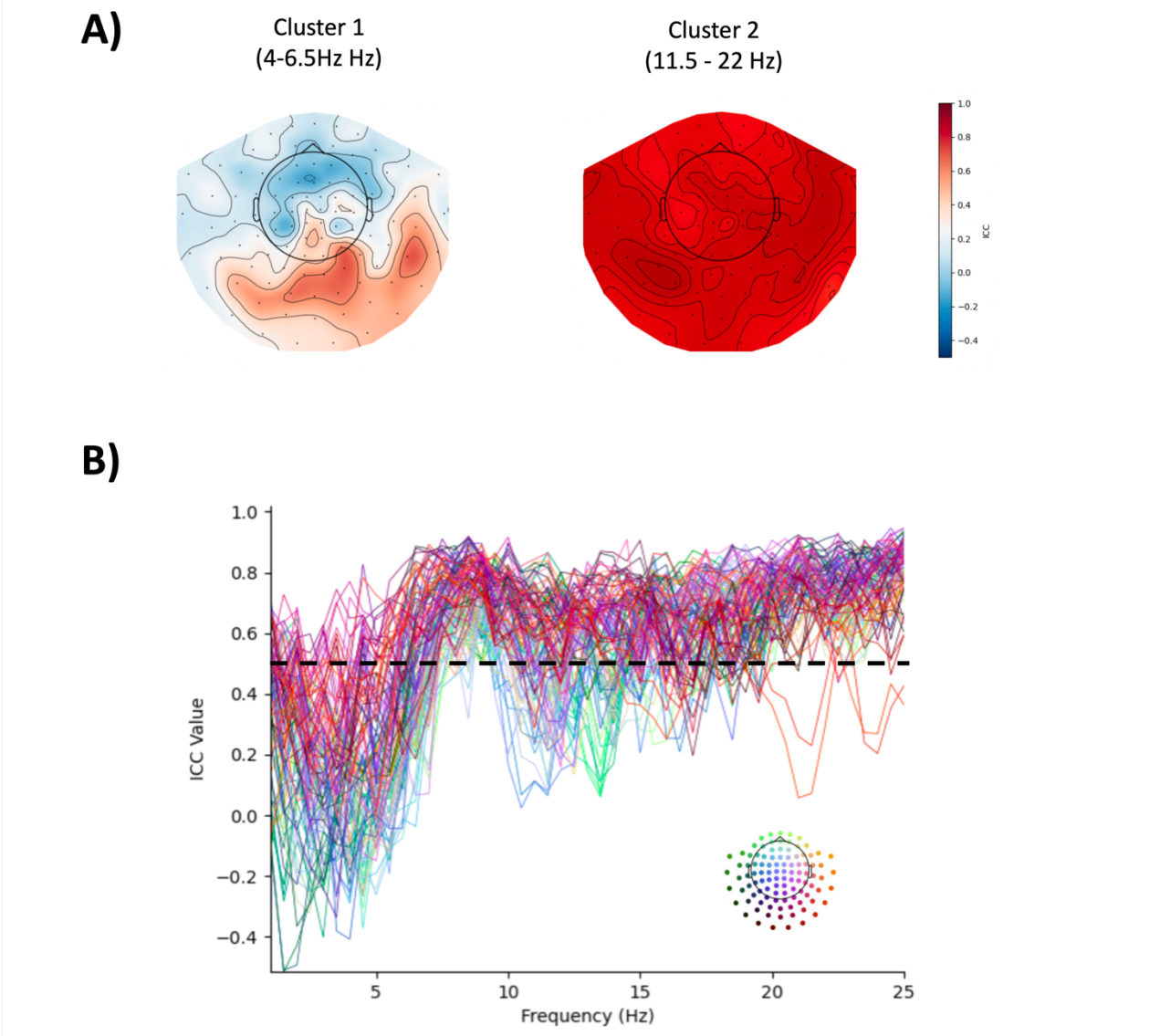

Figure 5.7. ICC results for baseline vs. two-week data (resting-state eyes-open).
A) Topography maps for each sensor in Frequency Cluster 1 (left) and Frequency Cluster 2 (right). Red indicates excellent/good reliability between baseline and two-week data, and blue indicates poor/no reliability between baseline and two-week data. Units displayed are ICC3 values.
B) ICC3 values for all frequencies and sensors. ICC values above 0.5 are considered good reliability, as indicated by the black line. Topography of sensors is shown by colour.

5.3.1.4 Annual results

This analysis focused on the follow-up MEEG scan conducted at 12-months to assess potential cognitive and neural declines over the course of a year. Like the test-retest analyses, these results are based solely on patient data as healthy controls did not complete the follow-up MEEG scan. From the 51 participants who completed the annual follow-up MEEG scan, 3 were unable to complete the resting-state eyes-open scan. Therefore, the annual results included in this GLM model were computed on 44 patients (25 MCI, 23 AD).

Using the same pre-defined Frequency Clusters as used in the test-retest analyses (see Figure 5.6B and 5.7A), each participants first-level GLM was recalculated separately for each sensor using the PSD averaged over the specified Frequency Cluster ranges (4.5 – 6Hz and 11.5 – 22Hz). This data was then input into a group-level paired-GLM design (Figure 5.3) to compare baseline and annual follow-up data.

The results show a significant difference in Frequency Cluster 2 ($t(2.32)$, $p = .02$), but no significant difference in Frequency Cluster 1 ($t(0.28)$, $p < .05$) (Figure 5.8).

The same analysis was then carried out, now within the two Frequency Clusters, but instead separately for each frequency bin <25Hz. This revealed a significant paired difference in beta band frequencies (Figure 5.9).

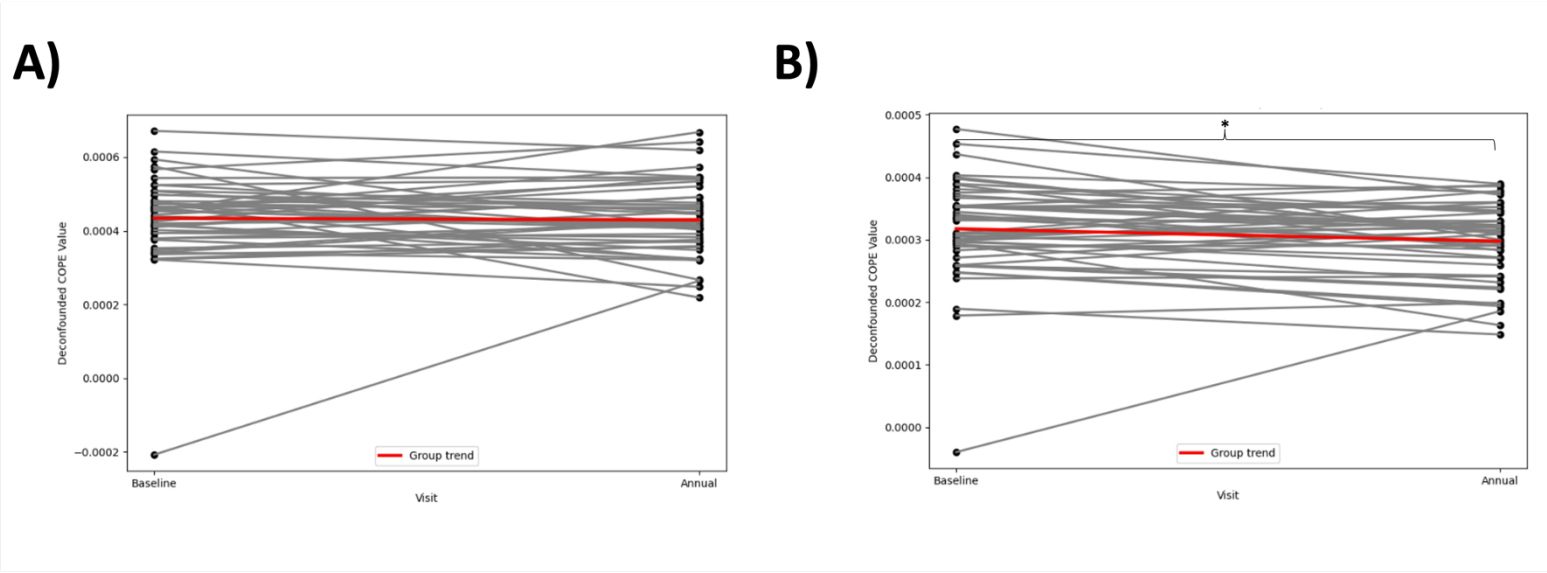

Figure 5.8. Frequency cluster subject-paired t-test analysis between baseline and annual follow-up scans (resting-state eyes-open).
Individual COPE values are shown for each participant (black) at baseline and annual follow-up scans for **(A)** Frequency Cluster 1 (4.5 – 6Hz) and **(B)** Frequency Cluster 2 (11.5 – 22Hz). Red bar represents the group mean trend between visits. * = $p < .05$.
Individual COPE values for each participant were extracted prior to the group-level GLM, therefore these values were deconfounded using the same regressors (age, sex, scanner, education, MMSE) to conduct this analysis.

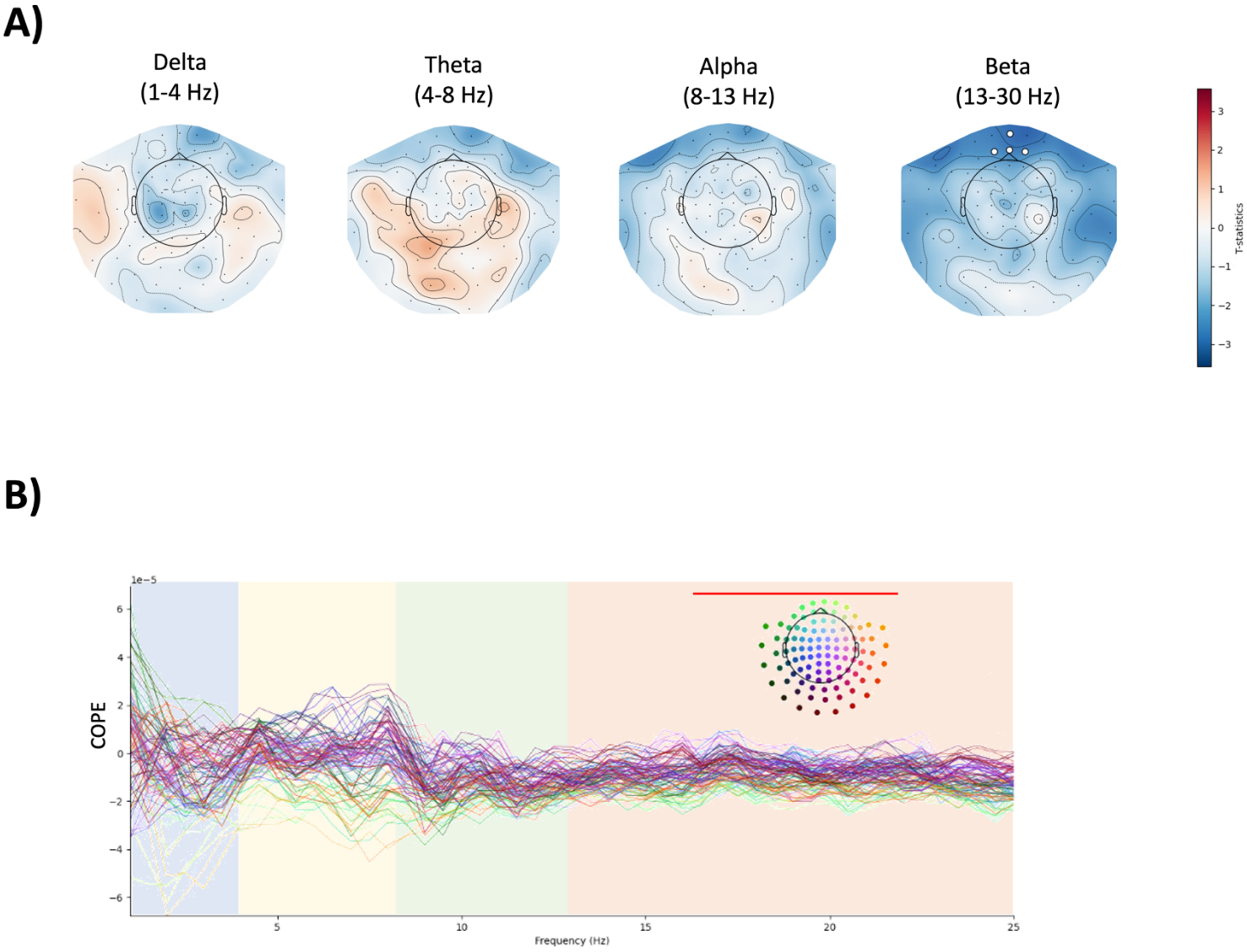

Figure 5.9. Frequency-wide subject paired t-test analysis between baseline and annual follow-up scans (resting-state eyes-open).

A) Topography maps of paired t-statistics for the Annual>Baseline contrast of power spectral density averaged within four frequency bands. Red indicates increased power in annual follow-up data, and blue indicates decreased power in annual follow-up data. Marked sensors are those that survived permutation testing (95% threshold). Units displayed are t-statistics.

B) Annual-Baseline contrast of the power spectral density (PSD). Each line is the PSD for a different sensor, with the line colours indicating where the sensor is in the topography (inset). The red line indicates the frequencies that survived permutation testing (95% threshold). Coloured bars represent the frequency band cut-offs.

5.3.2 Resting-state eyes-closed

5.3.2.1 Whole cohort

Out of the 104 participants in the NTAD cohort, 5 were unable to complete the resting-state eyes-closed scan. Therefore, the results included in this GLM model were computed on 99 participants (35 healthy controls, 64 patients).

The average power spectra across all frequencies and participants for each virtual sensor is shown in Figure 5.10, based on the grand average contrast from the group-level design matrix presented in Figure 5.3. Similarly to the resting-state eyes-open data, all participants showed a general decline in spectral power with increasing frequency except for an alpha peak at approximately 9Hz and some beta increases from 15-25Hz.

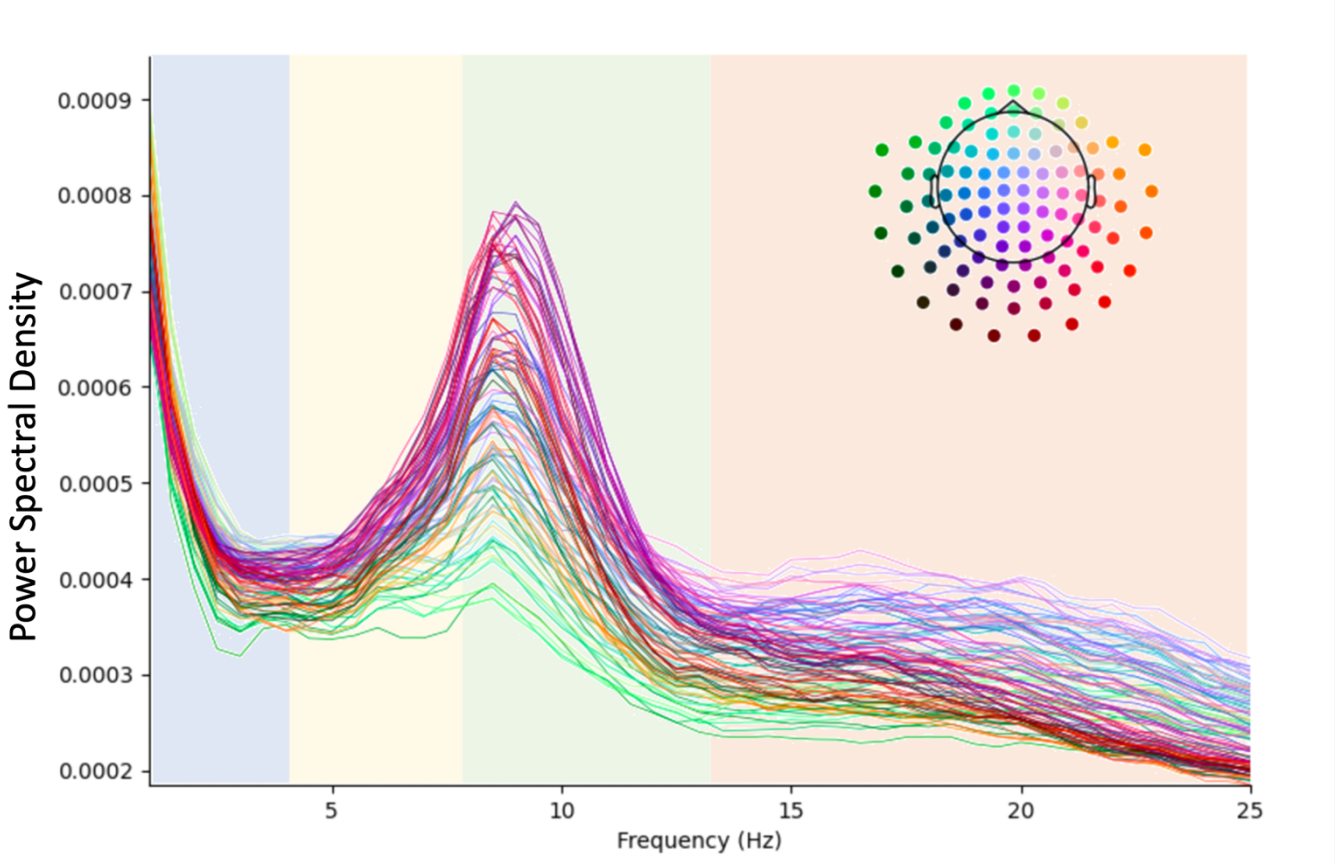

Figure 5.10. Whole cohort power spectra (resting-state eyes-closed)**.**

Mean power spectra of all participants, over all sensors and frequencies for resting-state eyes-closed data. Topography of sensors is shown by colour. Coloured bars represent the frequency band cut-offs (Delta: 1-4Hz, Theta: 4-8Hz, Alpha: 8-13Hz, Beta: 13-30Hz).

5.3.2.2 Patients vs. Controls

The average topographies for each frequency are shown in Figure 5.11A, with the marked sensors indicating where there is a significant change in power at any frequency following non-parametric permutation testing. Figure 5.10B shows the power spectral density averaged over all sensors for the patients versus controls contrast using the group-level design matrix shown in Figure 5.3.

The group-level GLM contrast (P>C from Figure 5.3) revealed that, after permutation testing, patients exhibited an increase in delta and theta power. No significant differences were observed in the alpha or beta frequency bands. The additional alpha analyses can be found in Section 5.3.3.

The observed patient versus controls significant differences with the theta band was used to define a single cluster for subsequent analysis. This was created by averaging across the frequency band for all sensors and analysed for both test re-test reliability and annual change.

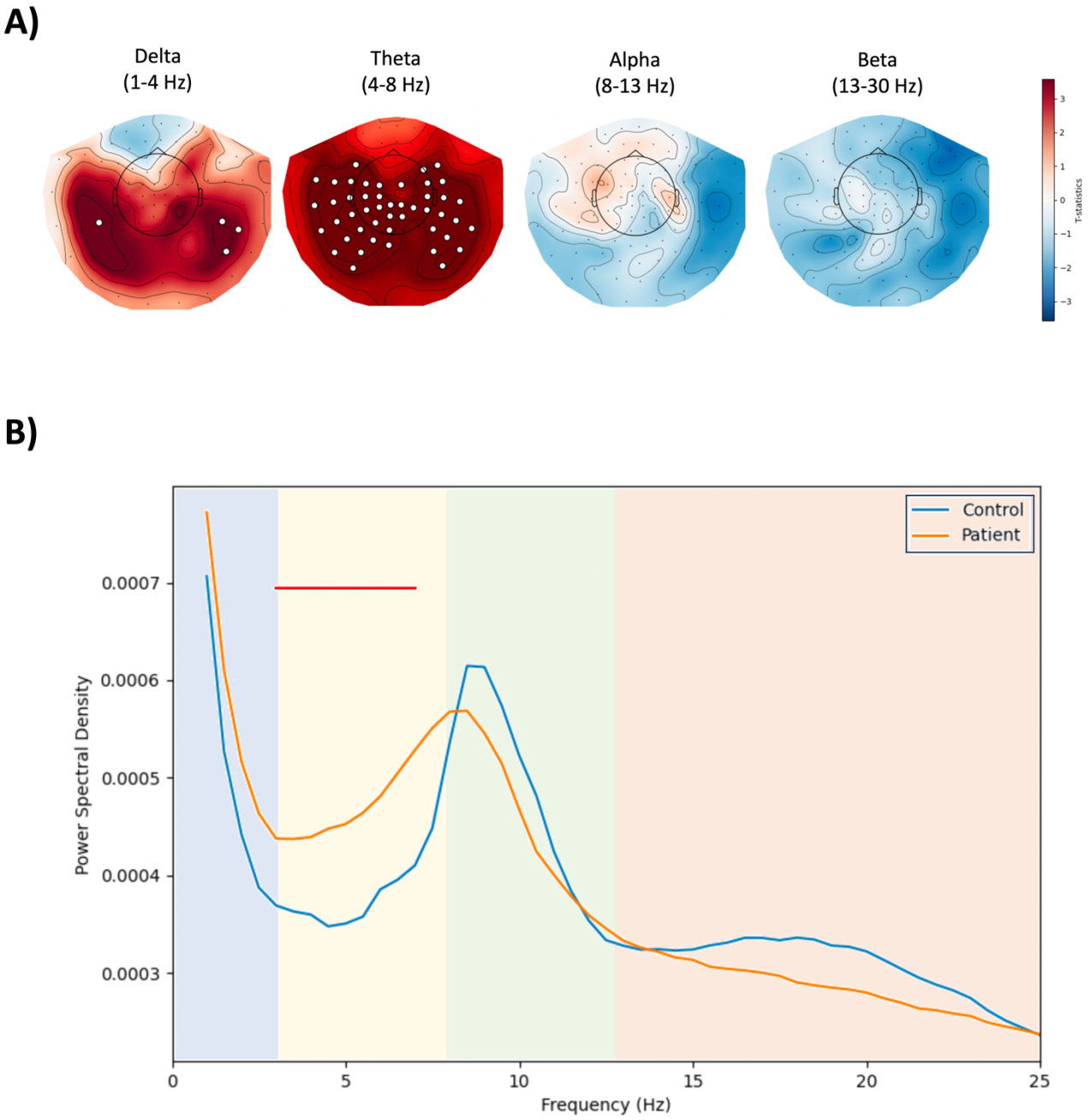

Figure 5.11. Cross-sectional statistical analysis of sensor-space MEG data for the Patient>Control group contrast across delta, theta, alpha, and beta frequencies (resting-state eyes-closed).

A) Topography maps for each frequency. Red indicates increased power, and blue indicates decreased power. Marked sensors indicate significant changes in power after non-parametric permutation testing (95% significance threshold). Units displayed are t-statistics.

B) Mean power spectral density of controls and patients, over all sensors. The red bar indicates the frequency that survived non-parametric permutation testing (95% significance threshold). Shaded areas represent the standard error. The variability within group is extremely low in this analysis.

5.3.2.3 Test re-test reliability

Of the 21 patients that completed the two-week scan, 2 were unable to complete the resting-state eyes-closed scan due to discomfort. Therefore, the test re-test reliability data presented below was computed on 19 patients (14 MCI, 5 AD).

Each participant's power spectra from their first-level GLM were recalculated, with the power for each sensor averaged within the frequency cluster identified in Figure 5.11B (Frequency Cluster 1: 3-7Hz). Note that here in the results, these clusters are referred to as 'Frequency Clusters'; however, in the discussion, they will be referred to by their respective frequency bands for ease of understanding.

The topographies for Frequency Cluster 1 are shown in Figure 5.12A. Figure 5.12B displays the ICC values across all frequencies. Results demonstrated that ICC values were more variable than the eyes-open data, with the highest reliability appearing within the theta band (7-10Hz). The delta band shows poor reliability across most sensors, and the alpha and beta bands display good reliability in the temporal and occipital sensors only.

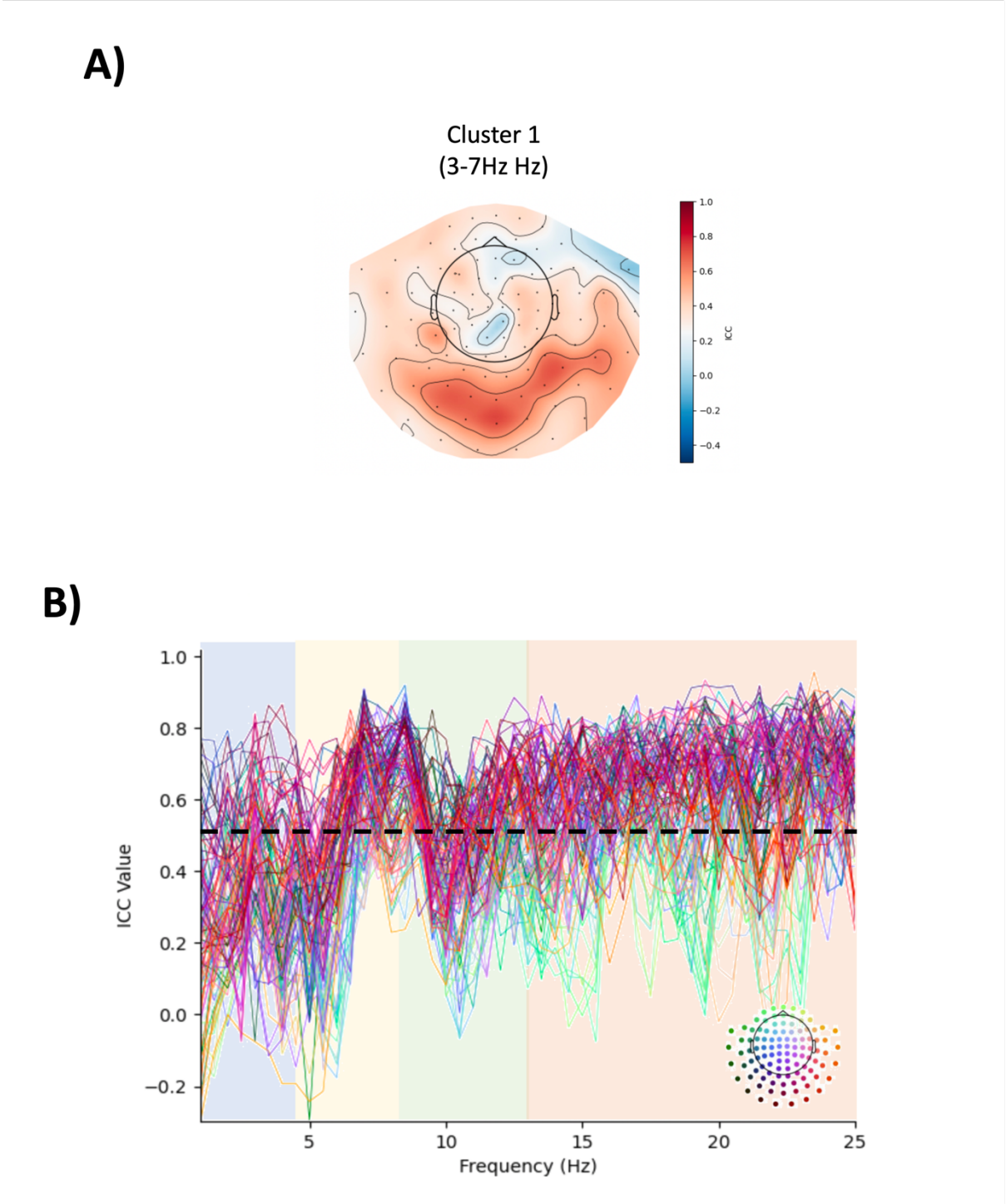

Figure 5.12. ICC results for baseline vs. two-week data (resting-state eyes-closed).
A) Topography maps for each sensor in Frequency Cluster 1. Red indicates excellent/good reliability between baseline and two-week data, and blue indicates poor/no reliability between baseline and two-week data. Units displayed are ICC3 values.
B) ICC3 values for all frequencies and sensors. ICC values above 0.5 are considered good reliability, as indicated by the black line. Topography of sensors is shown by colour.

5.3.2.4 Annual results

From the 51 participants who completed the annual MEEG scan, 6 were unable to complete the resting-state eyes-closed scan. Therefore, the annual follow-up results included in this GLM model were computed on 44 patients (24 MCI, 20 AD).

Using the same pre-defined Frequency Cluster as used in the test-retest analyses (see Figure 5.11B and 5.12A), each participants first-level GLM was recalculated separately for each sensor using the PSD averaged over the specified Frequency Cluster range (3 – 7Hz). This data was then input into a group-level paired-GLM design (Figure 5.4) to compare baseline and annual data follow-up data.

The results show no significant difference in Frequency Cluster 1 between baseline and annual data (t(0.77, $p > .05$) (Figure 5.13).

The same analysis was then carried out, not within the Frequency Cluster, but instead separately for each frequency bin <25Hz. This revealed no significant paired differences (Figure 5.14).

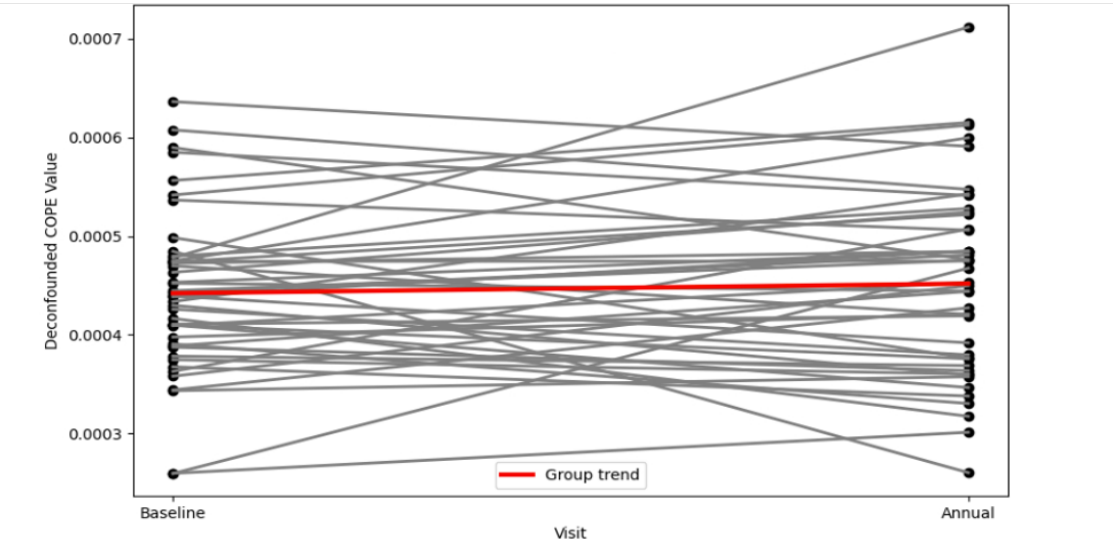

Figure 5.13. Frequency cluster subject-paired t-test analysis between baseline and annual follow-up scans (resting-state eyes-closed).
Individual COPE values are shown for each participant (black) at baseline and annual follow-up scans, following deconfounding with respect to the group-level GLM, for Frequency Cluster 1 (3-7Hz). Red bar represents the group mean trend between visits.
Individual COPE values for each participant were extracted prior to the group-level GLM, therefore these values were deconfounded using the same regressors (age, sex, scanner, education, MMSE) to conduct this analysis.

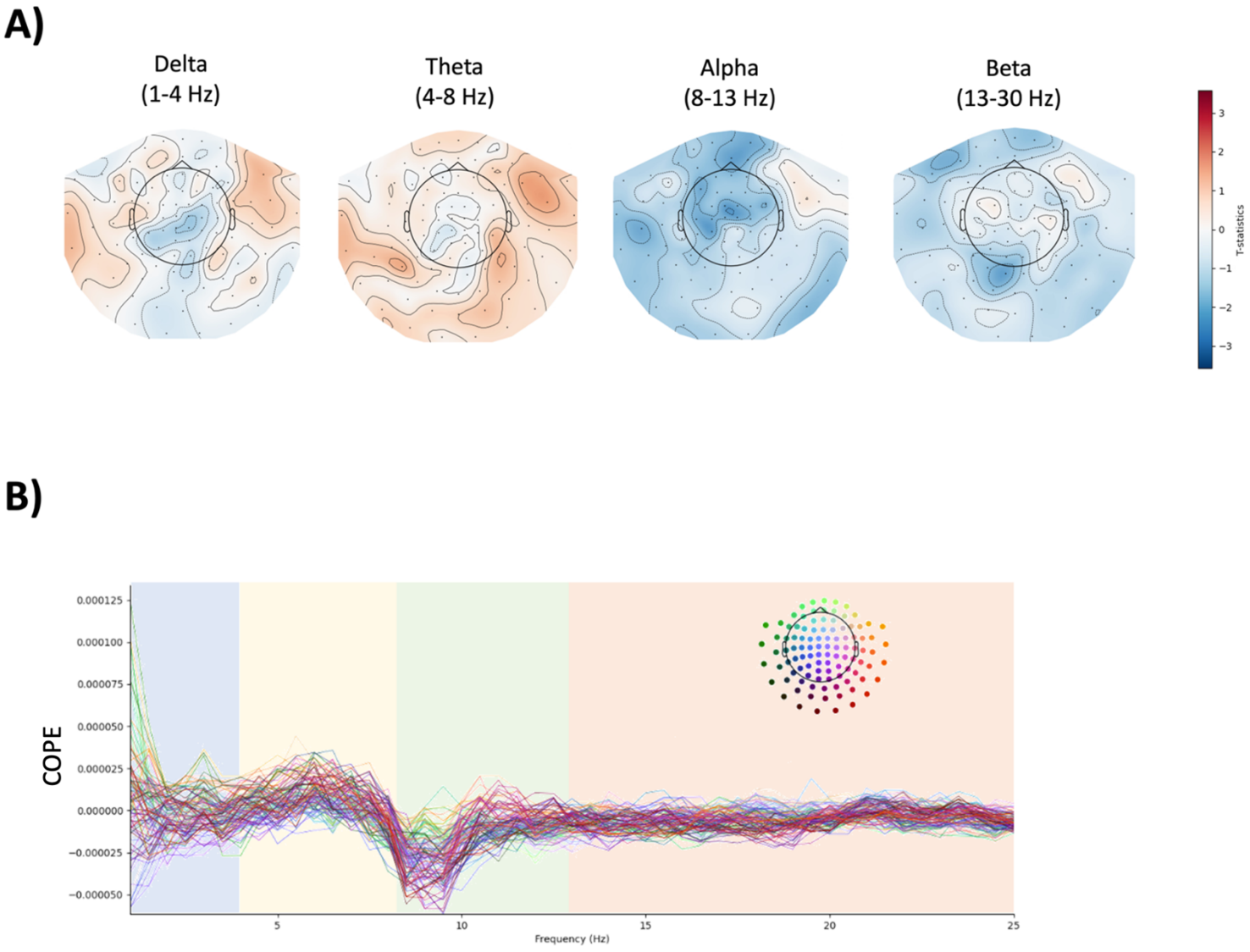

Figure 5.14. Frequency-wise subject paired t-test analysis between baseline and annual follow-up scans (resting-state eyes-closed).

A) Topography maps of paired t-statics for Annual>Baseline contrast for contrast of power spectral density averaged within four frequency bands. Red indicates increased power in annual follow-up data, and blue indicates decreased power in annual data. Units displayed are t-statistics.

B) Annual-Baseline contrast of the power spectral density (PSD). Each line is the PSD for a different sensor, with the line colours indicating where the sensor is in the topography (inset). Coloured bars represent the frequency band cut-offs.

5.3.3 Alpha Power

5.3.3.1 Alpha peak frequency

Observations of the spectral power in Figure 5.6B and Figure 5.11B suggested a potential shift in alpha peak frequency between patients and controls. As such, the alpha peak frequency and amplitude were calculated for baseline, two-week and annual scans for both eye conditions (Table 5.1).

A cross-sectional independent samples t-test of baseline data confirmed a significant difference between patients and controls for alpha peak frequency in the eyes-open condition (t(4.912), $p < .001$) (Figure 5.15A) and eyes-closed condition (t(1.956), $p = .05$) (Figure 5.15C). There was also a significant difference in alpha peak amplitude between controls and patients in the eyes-closed condition (t(2.273), $p < .02$) (Figure 5.15D), but not for the eyes-open condition (t(0.584), $p = 0.561$) (Figure 5.15B). This demonstrates that in the eyes-open condition, patients exhibit a slower alpha peak compared to controls, while in the eyes-closed condition, patients show a slower and lower alpha peak compared to controls.

Table 5.1 shows that there was no significant difference in a longitudinal subject-paired t-test between patients' alpha peak frequency, amplitude over a two-week or over a one-year period (i.e., annual follow-up).

5.3.3.2 Alpha power

Alpha power was calculated using the individual peak frequency from each participant in the occipital channels +-2Hz. Table 5.1 demonstrates that cross-sectional, independent t-tests between patients and controls revealed no significant difference in alpha power in neither the eyes-open (t(97) = 1.397, $p > .05$) or eyes-closed (t(97) = 1.57, $p > .05$) condition.

A longitudinal subject paired t-test revealed a significant difference in mean alpha power from baseline to annual follow-up scans in the eyes-open condition (t(39)= 2.466, $p = .018$), with a small effect size (Cohen's d = 0.39) (Figure 5.16A) and eyes-closed condition (t(39) = 2.513, $p = .016$) , with a small effect size (Cohen's d = 0.397) (Figure 5.16B). There were no significant differences between baseline and two-week in both eye conditions (Table 5.1).

5.3.3.3 Alpha Reactivity

Alpha reactivity was calculated as described in Section 5.3.4.4. Cross-sectional, independent t-tests demonstrated no significant difference in alpha reactivity between controls and patients (Table 5.1).

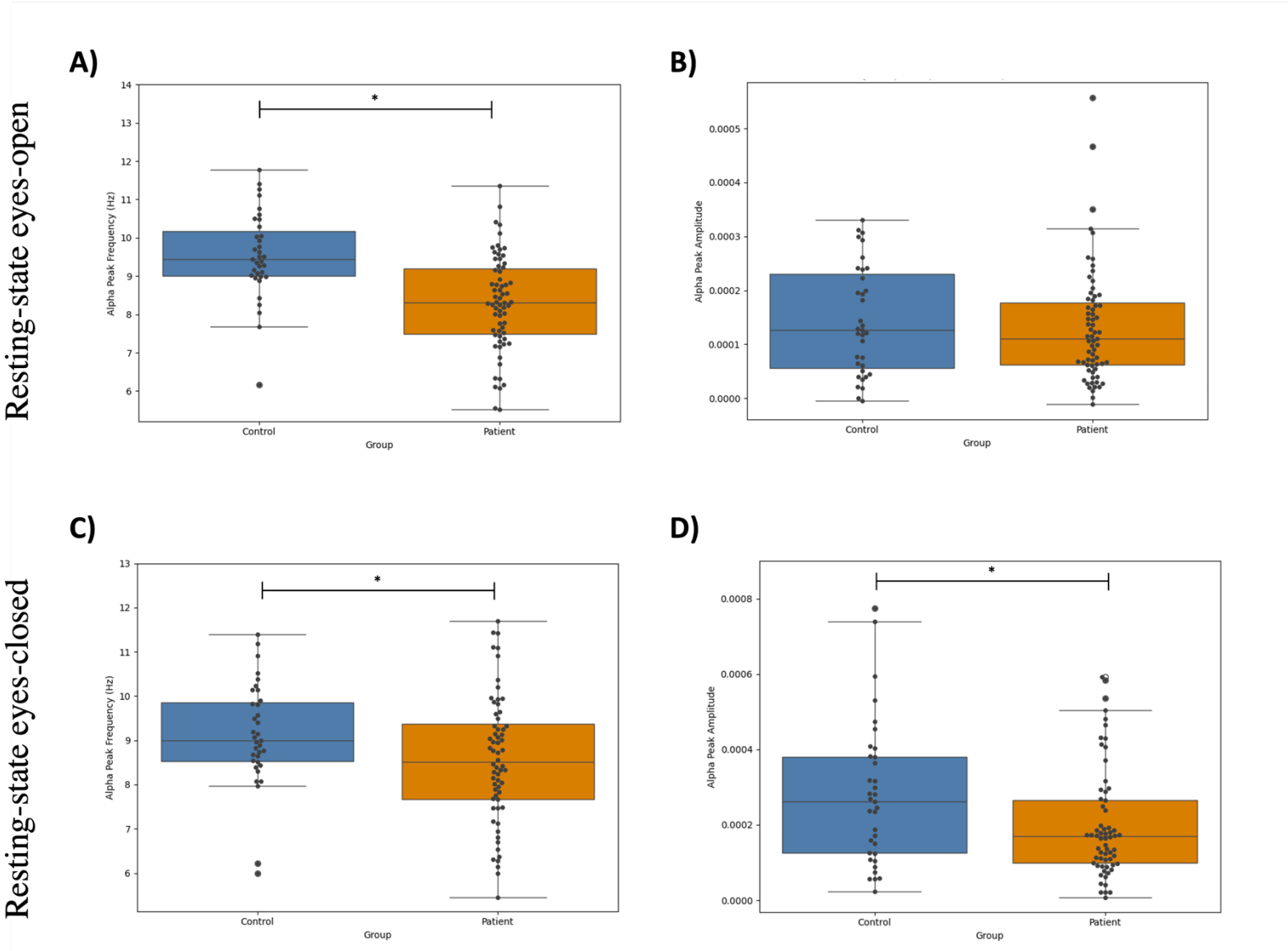

Figure 5.15. Cross-sectional alpha peak frequency and amplitude analysis. Group comparisons of the alpha peak frequency and amplitude for the eyes-open condition **(A&B, respectively)** and eyes-closed condition **(C&D, respectively).** Controls are shown in blue, and patients are shown in orange. Individual participant results are shown in black, with the standard deviation as bars. * = $p < .05$.

Table 5.1. Alpha peak and power values for baseline, two-week and annual visits for controls and patients.

Values represent the mean (standard deviation). Controls did not complete the two-week and annual scans. P values are results of paired t-tests for patients only. BL = baseline. TW = two-week. AF = annual follow-up. * indicates $p > .05$.

	Baseline		**Two-week**	**Annual**	**P**	**P**
	Controls (N = 35)	**Patients** (N = 67)	**Patients** (N = 20)	**Patients** (N = 46)	BL vs. TW	BL vs. AF
Alpha peak frequency (eyes-open)	9.538 (1.1)	8.3 (1.3)	9.14 (1.42)	8.29 (1.3)	0.179	0.134
Alpha peak amplitude (eyes-open)	1.4e-4 (1e-4)	1.31e-4 (1.1e-4)	1.29e-4 (9.2e-5)	1.38e-4 (1.26e-4)	0.989	0.913
Alpha power (eyes-open)	3.3263-4 (9.03e-5)	3.51e-4 (1.27e-4)	2.89e-4 (8.37e-5)	3.05e-4 (9.3e-5)	0.376	***0.018**
Alpha peak frequency (eyes-closed)	9.124 (1.2)	8.57 (1.4)	8.57 (1.43)	8.21 (1.29)	.199	0.182
Alpha peak amplitude (eyes-closed)	2.8e-4 (1.933-4)	2e-4 (1.5e-4)	1.79e-4 (1.62e-4)	2.25e-4 (1.43e-4)	0.989	0.551
Alpha power (eyes-closed)	4.15e-4 (1.68e-4)	3.66e-4 (1.39e-4)	3.21e-4 (1.29e-4)	3.24e-4 (1.18e-4)	0.297	***0.016**
Alpha reactivity (%)	0.09 (0.378)	-0.031 (0.427)	0.047 (0.55)	0.322 (1.2)	0.554	0.301

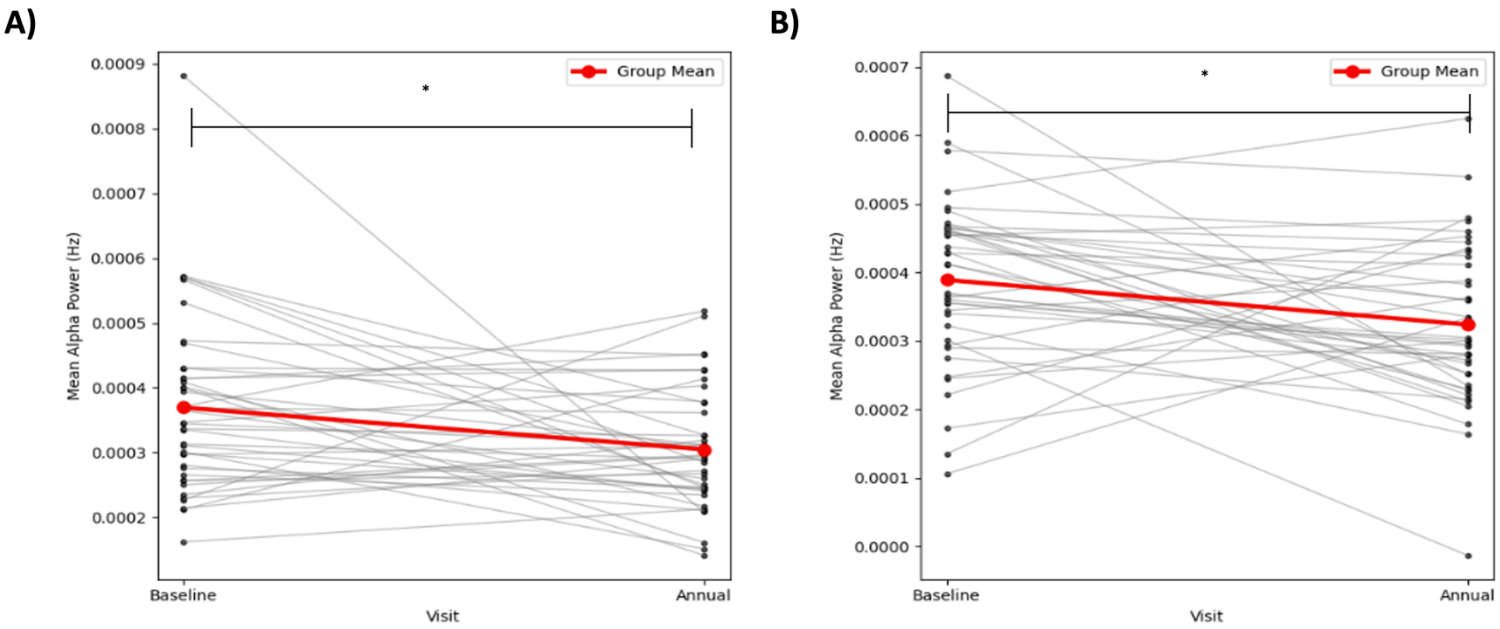

Figure 5.16. Alpha power subject paired-test analysis between baseline and annual follow-up scans.

Comparisons of the mean alpha power (averaged over all sensors) between baseline and annual visit for the eyes-open **(A)** and eyes-closed **(B)** conditions. Individual participant results are shown in black, with the group mean trend in red. * = $p < .05$.

5.3.4 Comparison with clinical measures of AD

This section focuses on the relationship between the identified MEG resting-state measures and clinical indicators of neurodegeneration in AD such as brain volume measure, neuropathology measures, and neuropsychological scores. The key MEG metrics included in this analysis are: 1) mean power in Frequency Cluster 1 (eyes-open), 2) mean power in Frequency Cluster 2 (eyes-open), 3) mean power in Frequency Cluster 1 (eyes-closed), and 4) alpha peak frequency (eyes-open), and 5) alpha peak frequency (eyes-closed). It is important to note that only the baseline values (i.e., not annual follow-up measurements) will be utilised in these analyses, as only baseline neuropathology data is available in the NTAD cohort.

5.3.4.1 Brain structure analysis

A multiple linear regression was performed using the hippocampal volume as the dependent variable with regressors for each of the five MEG metrics.

Table 5.2 shows that eyes-open Frequency Cluster 1,2 and alpha peak frequency were significantly associated with hippocampal volume. The eyes-closed metrics were not associated with the hippocampal volume.

As the previous chapters have highlighted the importance of the hippocampal volume in AD research, Figures 5.17 and 5.18 illustrate the associations between hippocampal volume and alpha peak frequency, and the Frequency Clusters in the eyes-open conditions. These MEG metrics were chosen based on the results shown in Table 5.2.

Table 5.2. Results of a multiple linear regression model for hippocampal volume (predictor) with MEG metrics.

Hippocampal volume		
	t	***p***
Frequency Cluster 1 (eyes-open)	3.169	**0.002**
Frequency Cluster 2 (eyes-open)	2.683	**0.009**
Frequency Cluster 1 (eyes-closed)	1.576	0.119
Alpha peak frequency (eyes-open)	2.584	**0.011**
Alpha peak frequency (eyes-closed)	1.163	0.248

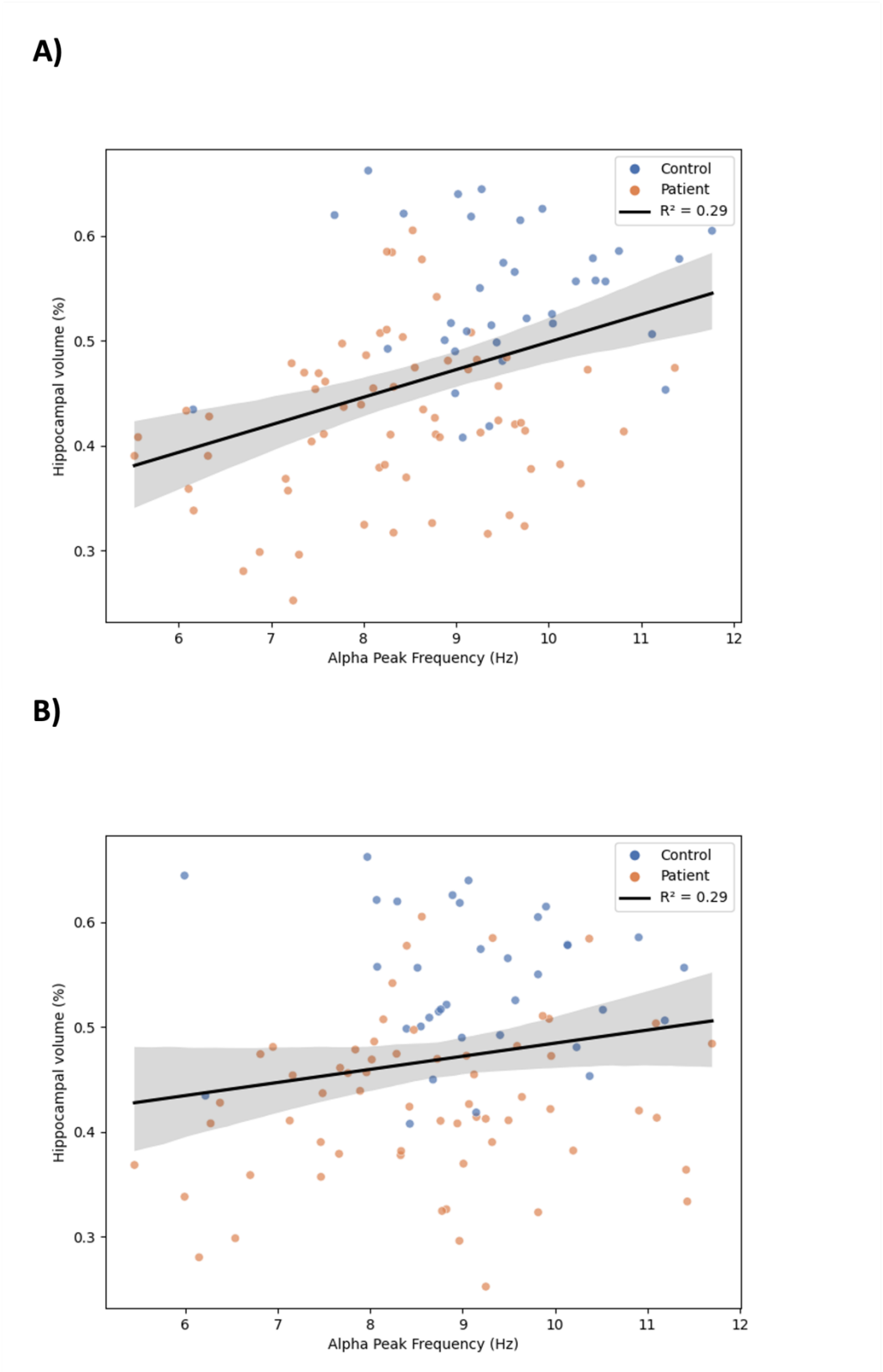

Figure 5.17. Alpha peak frequency and hippocampal volume analysis.
Alpha peak frequency (Hz) and hippocampal volume (%) regressions for the eyes-open **(A)** and eyes-closed **(B)** conditions, accounting for age, sex, and years in education. Controls are shown in blue, and patients are shown in orange. Larger hippocampal volumes denote increased pathology, whilst larger alpha peak frequency values denote decreased pathology.

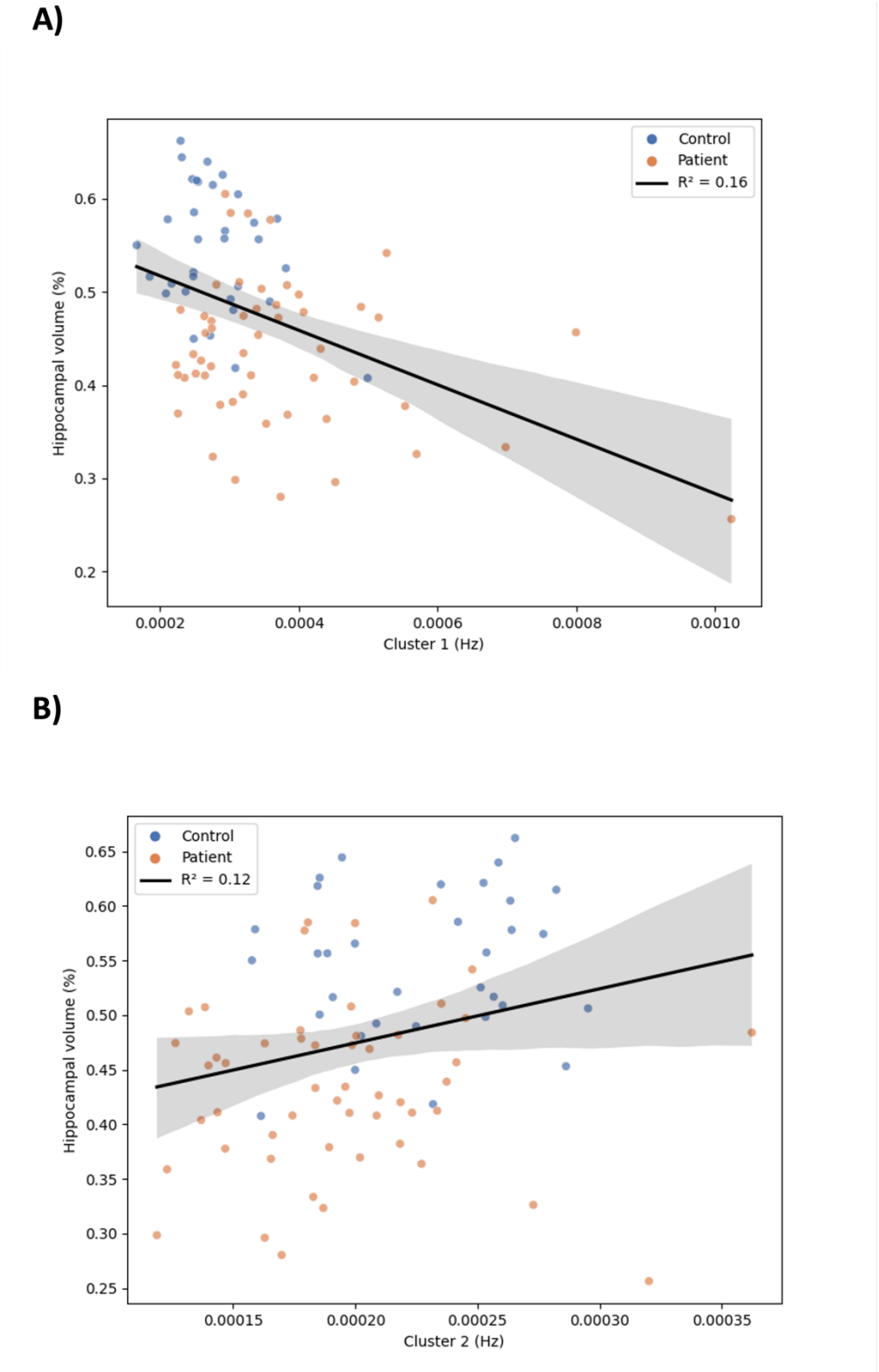

Figure 5.18. Hippocampal volume and eyes-open Frequency Cluster analysis. Hippocampal volume (%) regressions for Frequency Cluster 1 (4-6.5Hz) **(A)** and Frequency Cluster 2 (11.5-22Hz) **(B)** conditions. Controls are shown in blue, and patients are shown in orange. Lower hippocampal volume implies greater pathology. Lower values in Frequency Cluster 1 implies greater cognition, whilst higher values in Frequency Cluster 2 imply greater cognition.

5.3.4.2 Neuropathology analysis

Separate group-level, multiple linear regression models were performed using Aβ/tau ratio, p-tau, and plasma p-tau 18 as dependent variables, with regressors for each of the five MEG metrics.

Table 5.3 revealed significant associated between eyes-open alpha peak frequency and both the Aβ/tau ratio and p-tau measures. Additionally, Frequency Cluster 1 (eyes-open) was significantly associated with the Aβ/tau ratio. Plasma p-tau 181 demonstrated significant associations with Frequency Cluster 2 (eyes-open) and the eyes-closed Frequency Cluster 1. Notably, the eyes-closed alpha peak frequency did not show any associations with the neuropathology measures.

Figure 5.19 illustrates the associations between alpha peak frequency and the significant neuropathology associates shown in Table 5.3, specifically the Aβ/tau ration and p-tau. Additionally, Figure 5.20 demonstrates the associations between plasma p-tau181, and the significant frequency clusters identified in Table 5.3.

Table 5.3. Results of separate multiple linear regression models for Aβ/tau ratio, p-tau, and plasma p-tau181 (predictors) with the MEG metrics.

Aβ/tau ratio		
	t	***p***
Frequency Cluster 1 (eyes-open)	2.150	**0.037**
Frequency Cluster 2 (eyes-open)	1.133	0.263
Frequency Cluster 1 (eyes-closed)	0.299	0.766
Alpha peak frequency (eyes-open)	3.334	**0.002**
Alpha peak frequency (eyes-closed)	1.319	0.194
p-tau		
	t	***p***
Frequency Cluster 1 (eyes-open)	1.265	0.212
Frequency Cluster 2 (eyes-open)	0.604	0.549
Frequency Cluster 1 (eyes-closed)	0.782	0.438
Alpha peak frequency (eyes-open)	2.395	**0.021**
Alpha peak frequency (eyes-closed)	0.930	0.357
Plasma p-tau181		
	t	***p***
Frequency Cluster 1 (eyes-open)	1.166	0.249
Frequency Cluster 2 (eyes-open)	2.337	**0.024**
Frequency Cluster 1 (eyes-closed)	2.088	**0.042**
Alpha peak frequency (eyes-open)	0.700	0.488
Alpha peak frequency (eyes-closed)	1.125	0.266

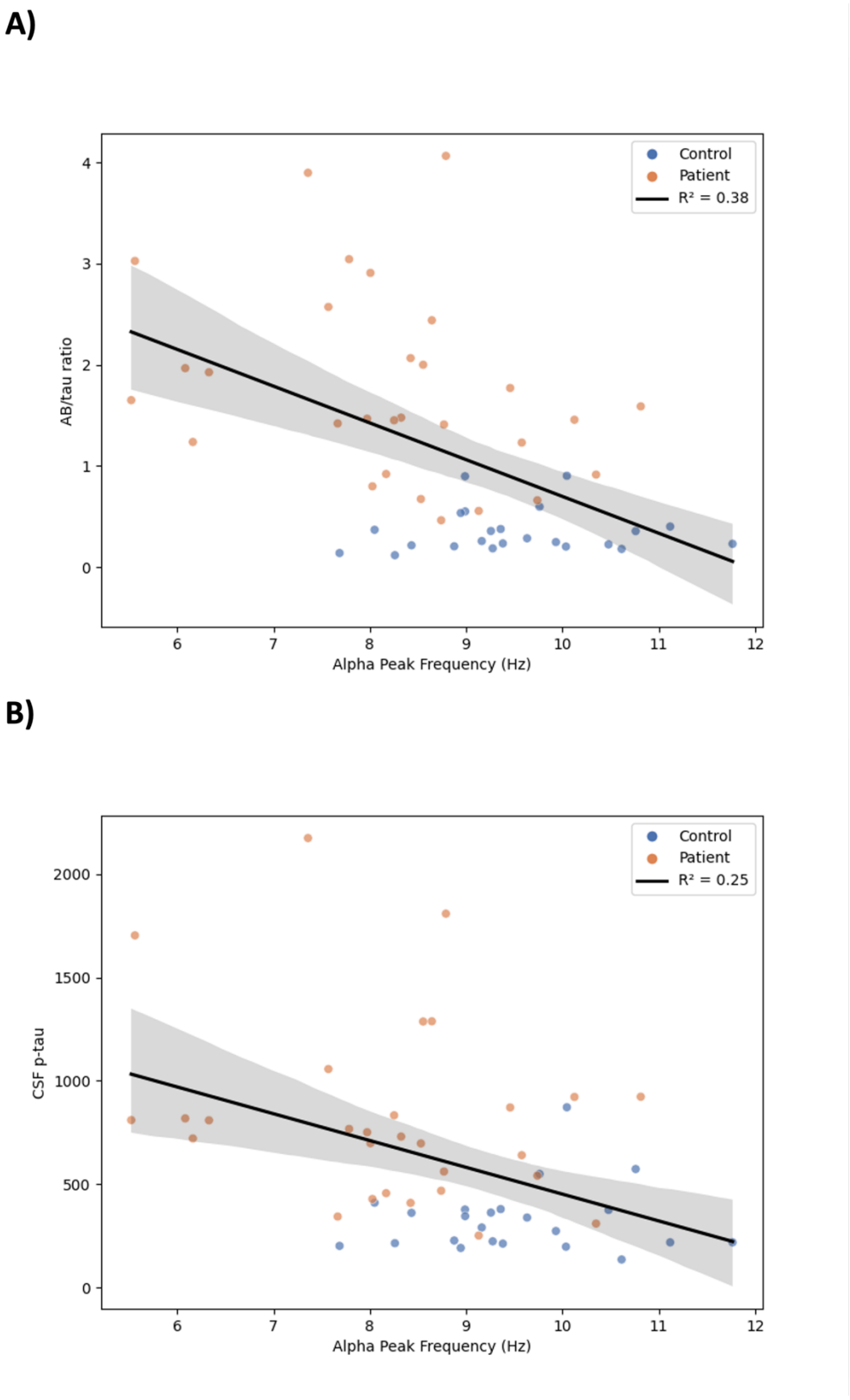

Figure 5.19: Alpha peak frequency and neuropathology analysis.
Linear regression analysis between alpha peak frequency eyes-open (Hz) and **(A)** Aβ/tau ratio and **(B)** p-tau. Controls are shown in blue, and patients are shown in orange. High Aβ/tau ratio and p-tau levels denotes greater pathology.

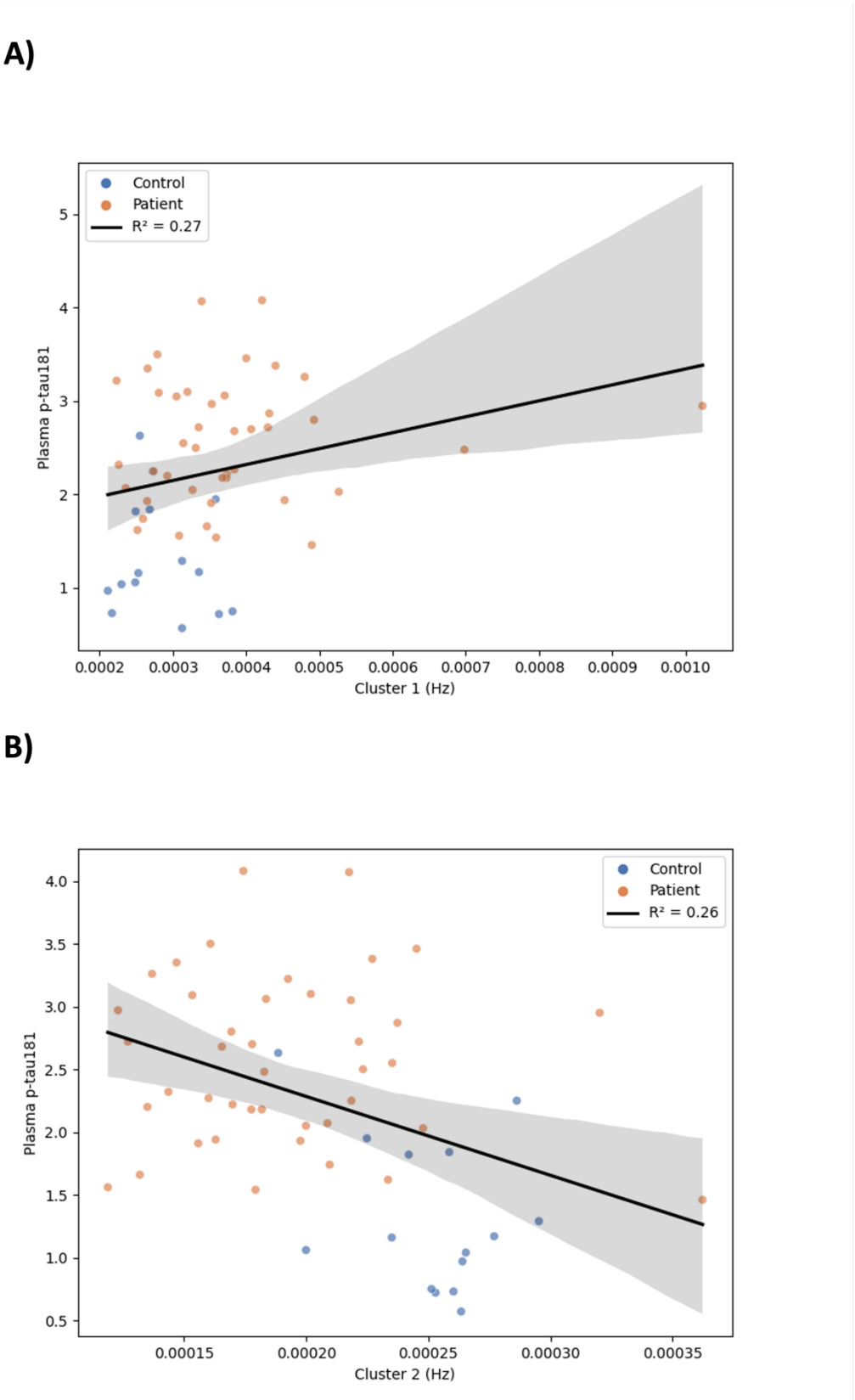

Figure 5.20: Plasma p-tau181 and significant Frequency Cluster analysis.
Linear regression analysis between plasma p-tau 181 and **(A)** Frequency Cluster 2 (eyes-open) and **(B)** Frequency Cluster 1 (eyes-closed). Controls are shown in blue, and patients are shown in orange. High plasma p-tau181 levels reflects greater pathology.

5.3.4.3 Neuropsychological assessment analysis

Separate group-level, multiple linear regressions were conducted using the MMSE score and the Four Mountains test as dependent variables, with regressors each of the five MEG metrics.

Table 5.4 revealed that the MMSE score had significant associated with both eyes-open clusters and the eyes-open alpha peak frequency. Similarly, the Four Mountains test demonstrated a significant association with Frequency Cluster 1 (eyes-open) and the eyes-open alpha peak frequency.

Figure 5.21 shows the significant associations between MMSE score and the MEG metrics identified in Table 5.4. Additionally, Figure 5.22 illustrates the Four Mountains score with the eyes-open Frequency Cluster 1 and alpha peak frequency.

However, it is important to note that the five MEG metrics were computed while controlling for MMSE score. As a result, although some significant associations between cognition and neural measures were observed, these associations may be reduced or impacted. The group-GLM was run without MMSE as a regressor, and the overall results were similar but future research could extend this by examining associations with cognition in models that do not include MMSE to determine whether stronger or additional effects emerge.

Table 5.4. Results of separate multiple linear regression models for MMSE and Four Mountains scores (predictors) with the MEG metrics.

MMSE		
	t	***p***
Frequency Cluster 1 (eyes-open)	4.138	**< .001**
Frequency Cluster 2 (eyes-open)	3.065	**0.003**
Frequency Cluster 1 (eyes-closed)	1.440	0.153
Alpha peak frequency (eyes-open)	2.796	**0.006**
Alpha peak frequency (eyes-closed)	1.352	0.180
Four Mountains		
	t	***p***
Frequency Cluster 1 (eyes-open)	3.794	**< .001**
Frequency Cluster 2 (eyes-open)	1.401	0.165
Frequency Cluster 1 (eyes-closed)	0.600	0.550
Alpha peak frequency (eyes-open)	2.992	**0.004**
Alpha peak frequency (eyes-closed)	1.272	0.207

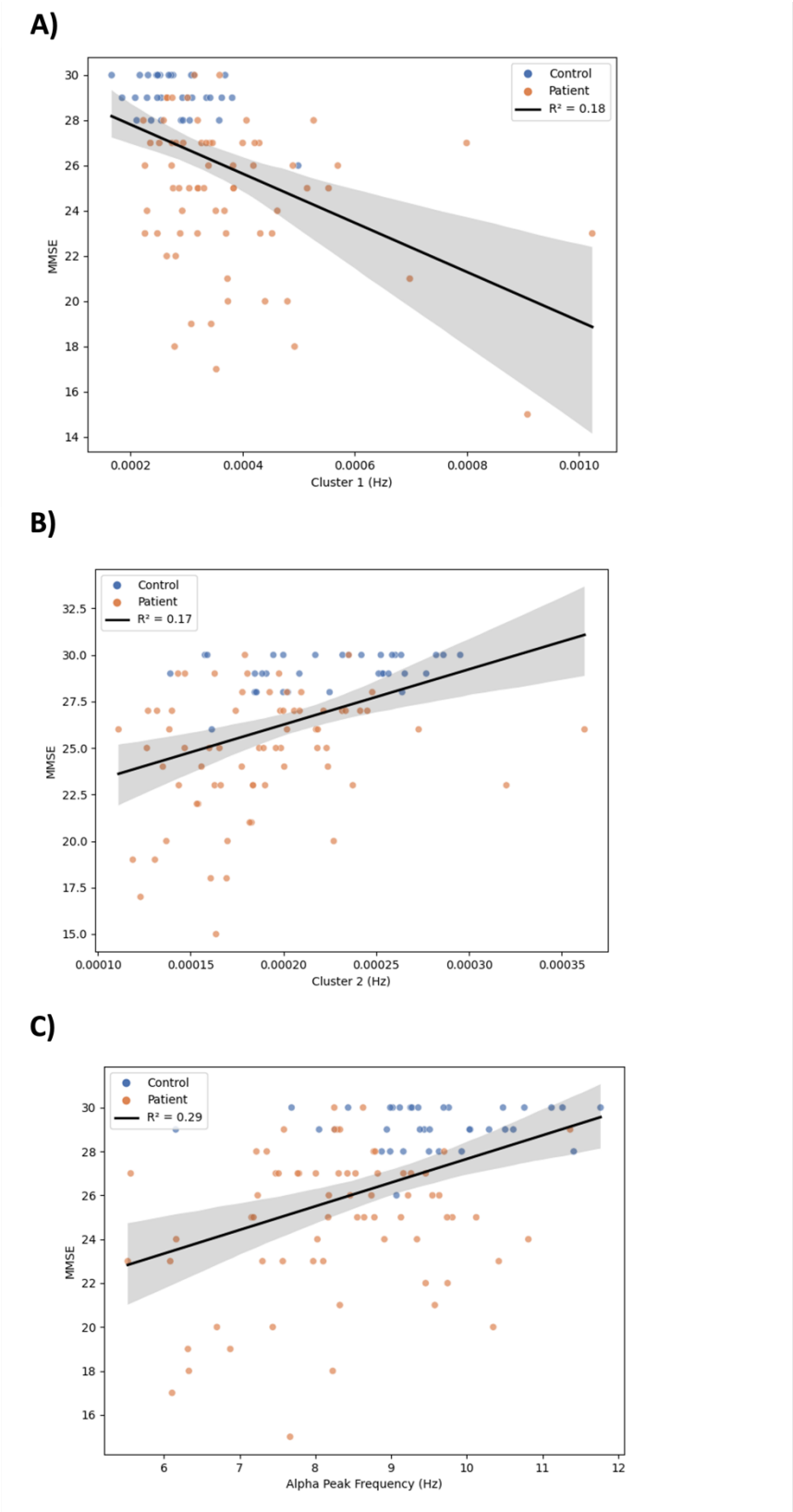

Figure 5.21: MMSE score and MEG metric analysis.
Linear regression analysis between MMSE score and **(A)** Frequency Cluster 1 (eyes-open), **(B)** Frequency Cluster 2 (eyes-open) and **(C)** alpha peak frequency (eyes-open). Controls are shown in blue, and patients are shown in orange. A lower MMSE score indicates poorer cognitive performance.

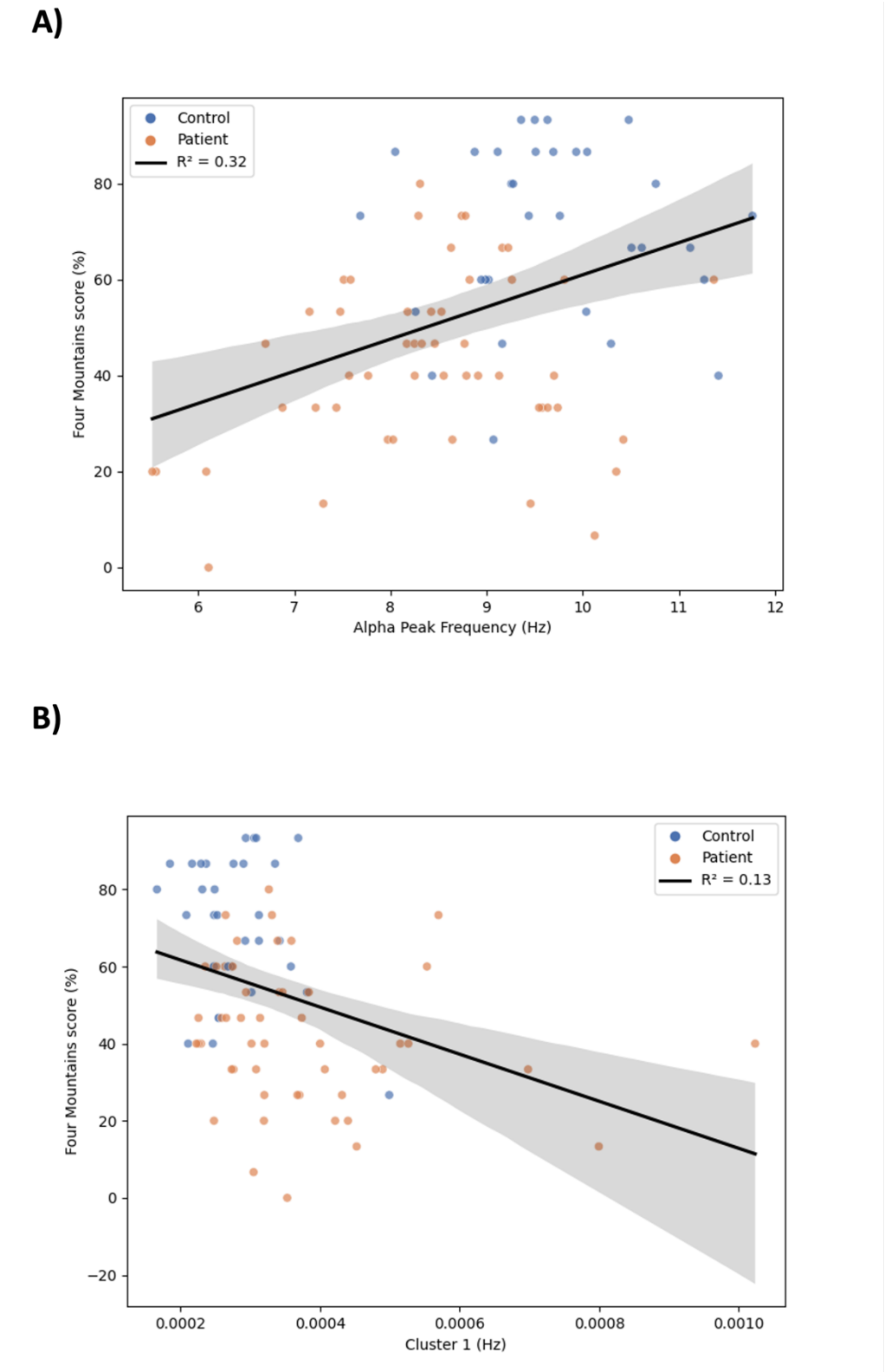

Figure 5.22: Four Mountains score and MEG metric analysis.
Linear regression analysis between the Four Mountains score and **(A)** alpha peak frequency (eyes-open) and **(B)** Frequency Cluster 1 (eyes-open). Controls are shown in blue, and patients are shown in range. A lower Four Mountains score indicates poorer cognitive performance.

5.4 Discussion

This chapter is among the first to investigate the relationship between sensor-space, electrophysiological measures with multiple measures of brain structure, neuropathology, and neuropsychological assessment in AD. The NTAD study offers a unique opportunity to study AD, as it is a longitudinal dataset containing multi-model neuroimaging data and comprehensive neuropathology and neuropsychological assessments.

Cross-sectional time-frequency analyses of the resting-state MEG NTAD data revealed a distinct spectral pattern in biomarker-positive MCI and AD patients compared to healthy aging controls. In the eyes-open condition, patients showed an increase in theta band activity, a decrease in alpha/beta band activity, and a shift in the alpha peak frequency. In the eyes-closed condition, patients exhibited an increase in theta band activity, a shift in alpha peak frequency, and a decrease in alpha peak amplitude. ICC was used to assess the test re-test reliability of these results between baseline and two-week data, revealing good to excellent reliability in both eye conditions for the higher frequency bands (alpha and beta), while the lower frequency bands (delta and theta) showed poor reliability. Notably, the eyes-open condition demonstrated greater reliability across a larger number of sensors.

Longitudinal subject-paired analysis on AD patients revealed annual differences in the beta frequency band during the eyes-open condition as well as alpha power across both eyes-open and eyes-closed conditions. These findings suggest that spectral changes in these measures may be sensitive to disease progression.

5.4.1 Cross-sectional analysis

The cross-sectional spectral differences observed between patients and controls in the NTAD cohort are largely consistent with previous research. In general, AD patients exhibit increased power in slower rhythms (delta and theta) and decreased power in faster rhythms (alpha and beta) compared with healthy controls (for review see Engels et al., (2017)). Specifically, a common observation in MEEG studies is a posterior slowing of alpha and beta power in AD patients compared with controls (Garcés et al., 2013; Koelewijn et al., 2017; Moretti et al., 2007). This finding is in line with the results in this chapter as results revealed decreased beta power in patients, distinct from the control group. This supports the notion that AD is characterised by specific electrophysiological alterations beyond the effects of normal aging.

Notably, the reduction in beta power was observed exclusively in the eyes-open condition, whereas in the eyes-closed condition, the differences between AD patients and controls were confined to the theta frequency band. These results suggest that spectral abnormalities associated with AD may vary based on the resting-state condition, which could explain some variance in overall MEEG findings in AD research and is an important factor for consideration in future studies. However, it is important to note that although the observed beta differences were not statistically significant, the eyes-closed condition was trending towards a similar distinction in the beta band. Indeed, the eyes-closed condition analysis included slightly fewer participants, which may have influenced the statistical outcomes. Nonetheless, further differences between eyes open and closed condition, as discussed below, highlight the relevance of including both paradigms to capture a comprehensive view of AD-related electrophysiological changes.

5.4.2 Alpha reactivity

Surprisingly, no significant differences were found in alpha reactivity between patients and controls. This contrasts with previous literature, which has often reported significant alterations in alpha reactivity among AD patients compared with controls and other neurodegenerative diseases (Babiloni et al., 2010; Fonseca et al., 2011; Schumacher et al., 2020), although these studies primarily utilised EEG data rather than MEG data. This discrepancy could imply that the calculation of alpha reactivity may be different when assessed by MEG, such as the specific analysis techniques used in MEG, the positioning of participants within the MEG helmet, or differences in spatial resolution between sensor and source space analysis. Future research could benefit from repeating this analysis in source-space and without standardisation to investigate this further.

5.4.3 Annual results

Longitudinal annual alterations were found in the mean alpha power in both eye eyes open and closed conditions, and beta frequency in the eyes-open condition. However, results revealed no significant association between MEG metrics and cognitive decline, as denoted by the annual change in MMSE score. While the annual changes in mean alpha power were observed, their small effect sizes indicate that these changes may not map directly onto cognitive outcomes. Importantly, structural and cognitive changes were detected in the annual results presented in Chapter 4, indicating that this timeframe can capture some disease-related progression. The absence of corresponding associations with MEG measures may therefore

suggest that electrophysiological alterations follow a different trajectory from structural and cognitive decline. These findings highlight the need for longer follow-up periods to clarify how MEG measures evolve over time.

5.4.4 Relationship between electrophysiological and clinical measures

Analysis focused on the relationship between these measures and clinical markers of AD identified in Chapter 4, specifically hippocampal volume, the Aβ/tau ratio, p-tau, plasma p-tau181, and the neuropsychological assessments of MMSE and Four Mountains. This analysis revealed significant associations between hippocampal volume and the theta, alpha/beta eyes-open frequency clusters, as well as eyes-open alpha peak frequency. Additionally, the eyes-open alpha peak frequency showed significant relationships with the Aβ/tau ratio and p-tau measures. Finally, the MMSE and Four Mountains tests were both significantly associated with the eyes-open frequency clusters and alpha peak frequency.

Recent research investigating the relationship between neurophysiology and clinical markers has shown that alpha hyposynchrony was modulated by a tau tracer uptake in PET scans. In contrast, delta/theta hypersynchrony was modulated by both tau and Aβ tracer uptake (K. G. Ranasinghe et al., 2020). This is in line with results presented in this chapter, as the Aβ/tau ratio was associated with both the theta and alpha frequency bands, whereas p-tau was only associated with alpha peak frequency. In addition, it was found that alpha synchronisations demonstrated associations with MMSE score (K. G. Ranasinghe et al., 2020, 2022). This is similar to results presented in this chapter, as associations were found between MMSE score and the alpha measures from the frequency clusters and peak frequency. Taken together, these results suggest that spectral measures offer valuable insights into the structural and neuropathological changes associated with AD, as well as their relationship with neuropsychological assessments.

Specifically, the significant associations between the eyes-open alpha peak frequency and established biomarkers such as the Aβ/tau ratio and p-tau suggest its potential utility in monitoring disease progression. Notably, the eyes-closed metrics showed little to no significant associations with any of the clinical measures. This lack of association may indicate that the eyes-open condition is more sensitive to capturing changes related to cognitive function and structural alterations in AD, which will be discussed further below.

Brain structure analysis revealed a significant association between hippocampal volume and alpha peak frequency, as well as the frequency clusters in the theta and alpha/beta frequency bands in the eyes-open data. This suggests that MEG metrics are able to capture important features related to AD-related neurodegeneration such as hippocampal atrophy. This is similar to previous literature which has shown progressive atrophy of the hippocampal correlates with decreased alpha power (Babiloni et al., 2009; Moretti et al., 2007). It is important, therefore, to explore the functional relationship between hippocampal volume and resting alpha rhythms. In humans, the cholinergic pathways that drive thalamocortical and cortico-cortical loops generate alpha oscillations in the 8-10.5 Hz range (Klimesch et al., 1998; Ricceri et al., 2004; Rossini et al., 1991). This has been shown in a MEG study that administered scopolamine (cholinergic antagonist) prior to scanning, and found a characteristic alteration of cortical alpha and theta rhythms (Osipova et al., 2005). Furthermore, it has been found that abnormal alpha rhythms in AD patients were modulated by long-term cholinergic therapy (Babiloni, Cassetta, et al., 2006). These findings suggest that the present findings may reflect cholinergic alterations manifesting as altered alpha power. As both structural and functional measures worsen with diagnosis and cognitive decline – and considering that structural markers may emerge too late in the disease process (Long & Holtzman, 2019; Price & Morris, 1999) - this demonstrates the potential of electrophysiological data, such as MEG, to identify AD-related changes earlier than structural imaging alone, making it a promising tool for early diagnosis and intervention.

5.4.5 Eyes open and closed conditions

Our results showed a distinct difference between the eyes-open and eyes-closed conditions. This finding is somewhat expected, as it is known that electrophysiological responses are influenced by sensory stimuli. Specifically, alpha activity tends to be more prominent during eyes-closed resting states and decreases with visual stimulation. This phenomenon was first documented by Berger (Adrian & Matthews, 1934), who observed that alpha activity in the occipital region was reduced when participants were exposed to light. This reduction in alpha activity suggests that visual stimulation plays a role in modulating cortical dynamics and it has been proposed that alpha suppression reflects the widespread communication between cortical and thalamo-cortical interactions, facilitating information processing (Gevins et al., 1997).

Differences in eyes-open and eyes-closed conditions have also been observed in studies of AD. For example, in a whole-brain source-space assessment of oscillatory activity in healthy young controls, older controls, and AD patients, it was found that results were highly similar for eyes-

open and closed resting state only in the ageing analysis (Koelewijn et al., 2017). While healthy controls typically demonstrated consistent patterns of brain activity over age in these conditions, the presence of neurodegeneration changes led to altered neural dynamics depending on the eye condition.

The eyes-open condition appeared to reveal more differences between AD patients and controls, consistent with the findings of this chapter. In particular, the eyes-open measures showed stronger associations with clinical markers of neurodegeneration, such as hippocampal volume and lumbar puncture metrics. By contrast, the eyes-closed condition may have produced fewer clinical associations due to potential confounds like drowsiness or sleep, which are especially relevant in spectral analysis (Strijbis et al., 2022). Additionally, test-retest reliability was higher in the eyes-open condition, with greater intraclass correlation (ICC) values observed across more sensors. This may reflect the reduced likelihood of confounds like drowsiness in the eyes-open state. Overall, these findings emphasize the importance of considering eye conditions when analysing resting-state MEEG data. Baseline estimates of electrophysiological measures can vary significantly depending on whether eyes are open or closed, particularly in the context of AD research.

5.4.6 Limitations and future research plans

A limitation to this chapter is the absence of younger controls in the analysis, which could have provided a more comprehensive understanding of spectral changes across the lifespan. Future plans could include the addition of the Cam-CAN dataset, which contains similar MEG data for 700 adults with ages 18-80. In the meantime, the observed group differences between the controls and patients are reassuring, as they demonstrate deviations from patterns associated with healthy ageing. Many neuroimaging studies in the dementia field tend to have relatively small sample size, so the NTAD cohort represents a robust dataset for this type of research. It is also important to note that this analysis was not aimed to assess specificity. The NTAD study includes only MCI and AD patients, and for this analysis, the focus was on this clinical group. Future research can build on these findings by including comparisons with biomarker-negative MCI patients and other neurodegenerative diseases. However, the extensive inclusion criteria in the NTAD study increases confidence that the patients included in this analysis are highly probable AD cases, minimising the risk of misdiagnosed participants influencing the results.
Furthermore, another limitation is that controls were not included in the annual follow-up, preventing direct longitudinal comparisons between patients and healthy individuals. Including

a control group would allow for a clearer distinction between disease-related changes and normal ageing effects, and this could be addressed in future research.

5.4.7 Summary

Overall, this chapter introduced a GLM approach to the analysis of MEG which allowed the addition of critical covariates such as age, sex, years in education, scanner location, and MMSE score. This allowed the analysis to focus on the specific input of MEG metrics in the context of clinical applications. The results revealed clear cross-sectional differences between AD patients and healthy controls, with patients showing increased theta and decreased alpha/beta power in the eyes-open condition, and theta increases in the eyes-closed condition. The robustness of these spectral differences was confirmed through test-retest reliability analysis, with stronger reliability in eyes-open data, ensuring the reliability of MEG metrics for clinical applications. Longitudinally, annual alterations in alpha and beta band power were observed, and while these changes did not directly correlate with cognitive decline, they may still play a role in explaining the progression of AD-related neurodegeneration over time.

The stronger associations found between eyes-open MEG data and key AD biomarkers – such as hippocampal volume, Aβ/tau ratio, p-tau, and cognitive measures – further suggest that MEG may be sensitive to early-stage AD changes. However, cognitive decline, as measures by changes in MMSE score over one year, was not associated with MEG metrics in this study. This finding suggests MEG may capture functional changes related to AD that are not immediately reflected in cognitive scores.

Future research should further explore the utility of MEG in source-space analysis, which could yield deeper insights into localised brain regions affected by AD. Additionally, extending the follow-up period beyond one year may be necessary to capture the gradual nature of cognitive decline in AD.

In summary, this chapter highlighted the potential use of MEG, particularly in the eyes-open condition, to capture electrophysiological signatures associated with AD pathology. In the next chapter, I will build on these results by providing a detailed comparison of resting-state MEG and fMRI to further investigate the capability of MEG in detecting functional changes in AD.

Chapter 6: A comparison of resting-state MEG and fMRI in AD

This thesis has thus far explored the relationship between resting-state MEG and AD-related changes in cognition, amyloid/tau pathology, and brain structure. In contrast, functional MRI is a widely utilised neuroimaging technique that consistently reveals alterations in resting-state networks in dementia patients (Beckmann et al., 2005; Damoiseaux et al., 2006). Studies investigating the DMN and Dorsal Attention Network (DAN) using fMRI have demonstrated its association with Aβ and tau accumulations in early AD, highlighting its potential as a biomarker. In this chapter, resting-state fMRI data from the NTAD cohort are examined and compared with the MEG findings from the previous chapter to provide a comprehensive view of how each modality contributes to our understanding of AD and their potential as early biomarkers.

6.1 Introduction

Functional MRI (fMRI) is a widely used neuroimaging technique that reflects brain activity by detecting changes in blood flow, known as the BOLD signal. By measuring BOLD responses across distinct brain regions, fMRI can be used to assess functional connectivity and compare patterns of brain activity between healthy aging individuals and those with conditions such as AD. One of the major advantages of fMRI is its spatial resolution. Early studies showed that fMRI could show distinct borders between the visual areas, revealing what we would expect to see from animal neurophysiology (Engel et al., 1994). In addition to task-based fMRI, where participants engage in specific tasks during scanning, resting-state fMRI offers a valuable method for evaluating brain networks that remain active during rest.

Several approaches are commonly used to analyse resting-state fMRI data, including seed-based analysis, independent component analysis (ICA) and region of interest analysis. Seed-based analysis examines the functional connectivity of a predefined brain region by correlating its time series with those of all other regions, producing a functional connectivity map. Similarly, region of interest analysis is hypothesis-driven and involves defining specific regions using brain atlases or prior research to create a connectivity map. In contrast, ICA is a data-driven method that decomposes the BOLD signal into distinct time courses and spatial maps by identifying patterns of synchronous neural activity. Unlike seed-based and region of interest analysis, ICA does not rely on predefined regions, making it advantageous for

capturing whole-brain connectivity. However, ICA's effectiveness depends heavily on thorough data cleaning to minimise noise components that could obstruct true neural signals (Griffanti et al., 2014).

Several key resting-state networks have been identified using fMRI (Beckmann et al., 2005; Damoiseaux et al., 2006), including the DMN. The DMN is comprised of multiple brain regions such as the bilateral parietal cortex, posterior cingulate cortex, medial temporal cortex, hippocampus, and thalamus. This network is thought to support processes like mind-wandering, autobiographical memory, and passive thought (Buckner et al., 2008). The DMN's involvement in episodic memory makes it particularly relevant in AD research, as dysfunction within this network has been linked to the early cognitive decline characteristic of the disease. The functional connectivity of the DMN has been shown to be altered in the early stages of MCI and AD (Binnewijzend et al., 2012; Greicius et al., 2004; Sorg et al., 2007; K. Wang et al., 2007), with differences also observed in young carriers of the APOE4 gene – a genetic risk factor for AD (Filippini et al., 2009).

Beyond the DMN, other resting-state brain networks have also been found to be disrupted in AD, including networks associated with attentional control such as the dorsal attention network (DAN) and ventral attention network (VAN) (Fox et al., 2006; Li et al., 2012). The DAN, which includes the intraparietal sulcus and frontal eye fields, is thought to be involved in top-down attention to locations or features (i.e., spatial attention). In contrast, the VAN is thought to play a role in detecting unattended stimuli and initiating shifts in attention (Vossel et al., 2014). AD-related changes have also been found in regions such as the amygdala (Z. Wang et al., 2016), motor (Agosta et al., 2010; Vidoni et al., 2012), and language (Weiler et al., 2014).

6.1.2 The comparison of fMRI and MEG measures

Functional connectivity refers to the measurement of how neural activity in one brain region correlates with activity in another. It has become a key approach in fMRI analysis for investigating large-scale brain networks and has been reliably used to identify resting-state networks (Noble et al., 2019). Additionally, fMRI functional connectivity has been shown to be high stable across participants and scans (Buckner et al., 2009; Damoiseaux et al., 2006), as well as across different resting-state conditions, including eyes closed and eyes open with or without a fixation cross (Fransson, 2005). For MEG and EEG, resting-state functional connectivity measures have typically focussed on the correlations in amplitude time courses,

referred to as amplitude-envelope correlation (AEC), which results in similar patterns as fMRI (Bruns et al., 2000). However, the reliability of MEG functional connectivity is not as well established (Jin et al., 2011). Additionally, the MEG signal itself differs between eyes-open and eyes-closed resting-state conditions (Barry et al., 2007), and as shown earlier in this thesis (Chapter 5), the reliability of the MEG signal also varies between these conditions. Nonetheless, it has been suggested that electrophysiological and fMRI data are complementary (Nentwich et al., 2020).

Specifically, studies investigating the relationship between M/EEG and the fMRI BOLD signal have compared responses recorded from both modalities across different sessions. While results have shown that oscillatory activity can spatially align with the BOLD signal (Singh et al., 2002), this relationship varies across frequency bands. For example, lower frequencies bands such as alpha and beta often exhibit a negative correlation with the BOLD signal (Mukamel et al., 2005; Zumer et al., 2010), whereas findings for the gamma frequency band are more complex, with some studies reporting a positive correlation (Logothetis et al., 2001) and others showing no clear relationship (Adjamian et al., 2004). A recent review of the relationship between age related changes in functional connectivity in dementia with fMRI and M/EEG data highlighted the different potential biomarkers offered by each modality (P. Ranasinghe & Mapa, 2024). For fMRI, these included disruptions in large-scale networks such as the DMN and fronto-parietal network. MEG and EEG studies showed alpha and beta power reductions and altered inter-regional coherence. By integrating these approaches, researchers may gain a more comprehensive understanding of brain-related changes, even if they yield different results. This chapter will be investigating some of the same measures included in this review, including fMRI brain networks and MEG sensor-space frequency analysis, but will do so within the same cohort rather than across studies.

Given the differences in data acquisition and analysis between these modalities, it is unsurprising that fMRI and MEG often yield distinct results. Nonetheless, understanding the unique insights each modality offers is crucial, particularly in the context of neurological diseases such as AD, where one method may prove superior in detecting early brain changes associated with the disease. This chapter focuses on the fMRI results from the same NTAD participants investigated in the previous chapter's MEG analysis. This approach offers two key advantages: first, it allows us to evaluate the contribution of fMRI data to the NTAD analysis; and second, it enables a direct comparison with the MEG findings to assess whether the two

modalities reveal similar or distinct patterns. Since this thesis has explored the potential for MEG to offer a more sensitive measure of AD-related changes than MRI, this comparative analysis is essential for determining the relative strengths of each technique in detecting early AD-related alterations.

6.1.3 Objectives

This analysis uses the ICA method to understand brain-related changes associated with AD using resting-state fMRI data. The specific objectives were to:

1. Determine whether brain network components differ between biomarker-positive MCI/AD patients and healthy controls.
2. Assess whether ICA-derived components correlate with cognitive and neuropathological measures.
3. Examine the relationship between group differences observed in resting-state fMRI and MEG findings.

6.2 Methods

6.2.1 Participants

Of 104 participants in the NTAD study, data for both the resting-state MEG and fMRI baseline scans were available for 24 controls and 57 patients (30 MCI, 27 AD). 2 participants were excluded for excessive movement during the fMRI scan (>1.5mm), as determined by the absolute motion. Therefore, results are based on 23 controls and 56 patients (30 MCI, 26 AD). Demographics of these participants are presented in Table 6.1. As in Chapter 5, MCI and AD patients are combined into a single 'patient' group for this analysis.

6.2.2 MEG analysis

The resting-state eyes-open MEG data is analysed in this chapter to ensure consistency with the corresponding fMRI data, which was also acquired with participants' eyes open. Detailed parameters for MEG data acquisition are described in Chapter 5.2. Only baseline data is included in this analysis.

MEG data was pre-processed to sensor space and analysed as described in Chapter 5.3. The identified Frequency Clusters and alpha peak frequency are included in this analysis.

6.2.3 fMRI analysis

6.2.3.1 fMRI acquisition

Data were acquired at the Oxford Centre for Human Brain Activity (Oxford) and Wolfson Imaging Centre (Cambridge) using the details described in Chapter 3.2.4. Resting-state fMRI scans included 200 T2*-weighted echo planar imaging volumes with the following parameters: TE = 30ms, TR = 1500ms, flip angle = 90 degrees, acquisition matrix = 64x64, number of slices = 54, slice thickness = 3mm, voxel size = 3mm isotropic, acquisition time = 5 minutes 50 seconds. Participants were asked to look at a fixation cross presented on the screen, blink normally and keep as still as possible. Only baseline fMRI data is included in this analysis.

6.2.3.2 fMRI pre-processing

As the data was collected with reverse phase-encoded blips, this resulted in a pair of images with distortions in opposite directions. As such, the images were merged along the time dimension, and FSL's *topup* was applied using information about the phase-encoding direction (x-axis) and total readout time (0.028ms). FSL's *topup* was used to estimate and correct

susceptibility-induced distortions in the fMRI data (Andersson et al., 2003). Following this, *applytopup* was used to correct the main fMRI file by applying the calculated distortion field using a Jacobian transformation, ensuring spatial accuracy in the corrected images.

Pre-processing was performed using FSL's FEAT (Woolrich et al., 2001). This included high-pass temporal filtering, motion correction, brain extraction, spatial smoothing and affine registration to the individual's structural scan using FLIRT (Jenkinson et al., 2002; Jenkinson & Smith, 2001) and boundary-based registration (Greve & Fischl, 2009). Registration from structural to standard (MNI) space was conducted using FNIRT.

Independent Component Analysis was applied to each dataset using MELODIC (Multivariate Exploratory Linear Optimized Decomposition; Beckmann et al., 2005). This was performed to identify a set of independent components, each with its own time series. These components represent either neuronal signals or noise-related artefacts (e.g., motion, cardiac, or scanner-induced artefacts). To minimise noise in the data, FMRIB's ICA-based X-noiseifier (FIX) was used to identify and regress out non-neuronal components (Griffanti et al., 2014; Salimi-Khorshidi et al., 2014). FIX is designed to automatically classify ICA components as signal or noise, but its effectiveness depends on prior training using manually labelled scans. To optimise FIX, a study-specific training model was developed, tailored to the NTAD scan parameters. A total of 10 controls (5 from the Oxford site and 5 from the Cambridge site) and 10 patients (5 Oxford, 5 Cambridge) were randomly selected for manual artefact cleaning and labelling as "Signal", "Unknown", or "Unclassified Noise". This model was then applied across the whole dataset. Finally, this pre-processed and "fixed" (clean) data was transformed into MNI space using FNIRT.

6.2.3.3. Independent Component Analysis

The pre-processed "fixed" functional data was used to create a group-level ICA to show patterns of connectivity across participants that was used to identify the resting-state networks of interest. A threshold of 25 components was selected and the results were visually inspected for sensible spatial topography and plausible anatomical location, to select components likely representing meaningful resting-state networks.

The dual regression technique was used to test the group effect (Beckmann et al., 2005; Filippini et al., 2009). Subject-specific time series were derived by regressing the group-level

ICA spatial maps onto each participant's pre-processed functional data, while applying a brain mask (MNI) to constrain the analysis to relevant voxels. From here, each participant's time series was regressed into their pre-processed functional data, resulting in subject-specific spatial maps. Each participant's spatial map was then split into the 25 components identified as part of the group-level ICA, and concatenated to create a 4D file that was used in a General Linear Model (GLM) to investigate differences between controls and patients. An example of the DMN component, based on its characteristic spatial pattern consistent with the literature, is shown in Figure 6.1.

The GLM design matrix was setup to specify each explanatory variable of interest and their contrasts. This included regressors for the group differences of age and education. There were no sex differences. Furthermore, to ensure that differences in functional connectivity were not driven by structural differences, each participant's grey matter (GM) maps were included as a regressor (Figure 6.2) . This was calculated using FSL's *feat_gm_preprare*.

For the comparison between clinical measurements and MEG metrics, the mean beta values were extracted from voxels showing statistically significant effects using a binary mask generated with *fslmeants*. These voxels were defined by thresholding a group-level statistical map at $p < .05$, corrected for multiple comparisons across space, highlighting regions with significant functional connectivity differences. The maps were obtained during dual regression, which first regresses group-level ICA spatial components against each participant's fMRI data to obtain participant-specific time courses (temporal regression), and then regresses these time courses back onto the fMRI data to produce participant-specific spatial maps (spatial regression). Significant voxels from these maps were used as masks, and the mean beta values within each mask provide a summary measure of functional connectivity for each participant, which was then compared with clinical measures.

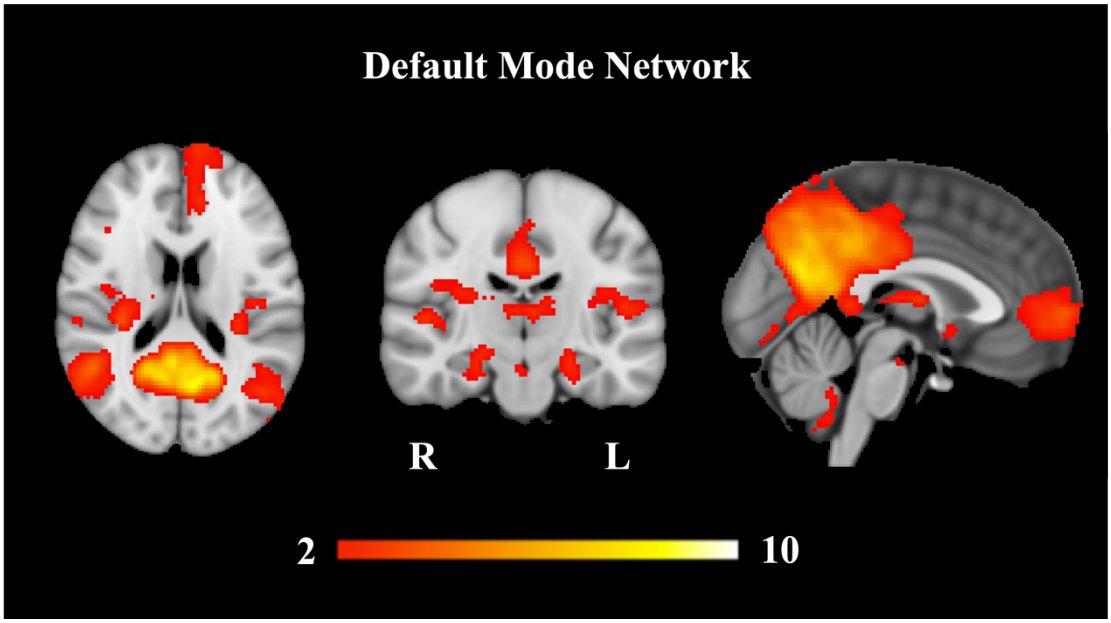

Figure 6.1: The Default Mode Network

Example of the default mode network component derived from the 4D file created as part of the group-ICA. Z > 2 for visualisation. R = right hemisphere, L = left hemisphere.

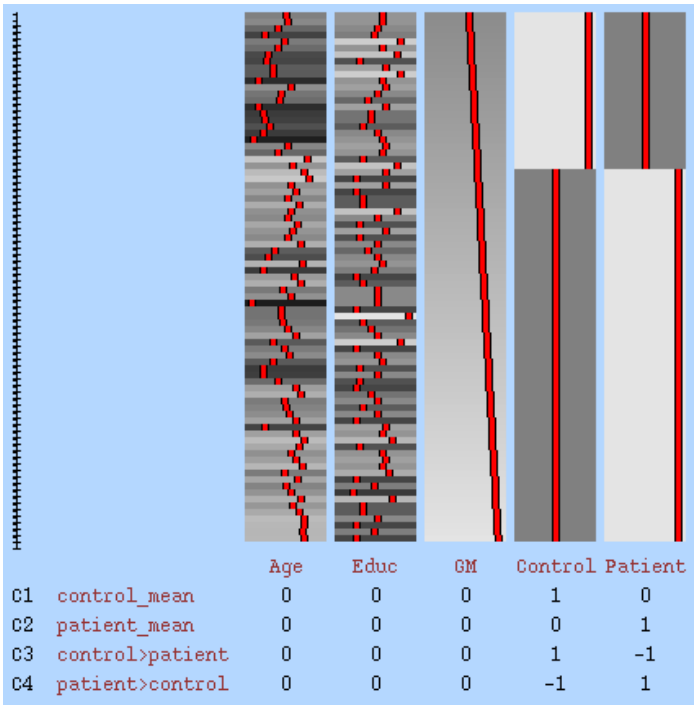

Figure 6.2. fMRI group-level GLM design

This shows 5 regressors that were specified in the model, and 4 contrasts (2 main effects and 2 differential contrasts).

6.2.4 Statistical analysis

Statistical significance between GLM contrasts was determined by non-parametric permutation testing. FSL's *randomise* was used to apply three thousand permutations across voxels for each component analysis. Significant differences between controls and patients were identified at a 95% threshold, meaning that differences were considered statistically significant if they fell into the top 5% of the permutation distribution. Results presented are the corrected p values, accounting for multiple comparisons across voxels. *fsl-cluster* was used to determine the cluster with the highest number of statistically significant voxels for visualisation purposes. Only the functional connectivity *within* a region was analysed. In this context, a region refers to a statistically significant ICA component that formed a spatially coherent pattern.

Non-imaging variables were analysed using JASP (Version 0.14.1). Independent samples t-tests were used to compare differences in the demographic variables (age, sex, education, MMSE) and absolute MRI motion. Pearson's correlations and multiple linear regression models using the mean beta values within the binary mask were used to investigate the relationship between the ICA components and the clinical score measurements, as well as the relationship between fMRI and MEG metrics. Pearson's correlations were included in this analysis to provide an initial assessment of the strength and direction of relationships between variables, while linear regressions were used to explore the predictability of the fMRI measures, allowing comparisons with the methods used in Chapter 5.

6.3 Results

6.3.1 Demographic and absolute movement

Baseline demographic, MMSE score and absolute motion for the participants analysed in this chapter are presented in Table 6.1. There was a significant difference in age, education and MMSE score between controls and patients. There were no significant differences in sex or MRI absolute motion.

6.3.2 fMRI ICA Analysis

ICA analysis of the fMRI data revealed significant differences between controls and patients in four components for the group-level GLM contrast (C>P from Figure 6.2). These included a motor/pre-motor component (Figure 6.3A), DAN (Figure 6.3B), a language component (Figure 6.3C), and the DMN (Figure 6.3D), suggesting that controls have significantly higher functional connectivity in these areas than patients.

6.3.3 Comparison of ICA and clinical measures

This section focuses on the relationship between the identified fMRI components and the clinical measures of AD such as neuropsychological analysis scores and neuropathology measures. Only the baseline values (i.e., data acquired at the first time point) will be utilised in these analyses, as only baseline neuropathology data is available in the NTAD cohort. In addition to the measures highlighted in Chapter 4, this analysis included the AD as an exploratory measure to provide a broader assessment of cognitive function.

Table 6.1. Baseline demographic, MMSE score, and absolute motion (MRI) for the control and patient groups.

Values represent the mean (s.d). P values are results of an independent samples t-test.

	Controls (N=23)	**Patients (N=56)**	**P**
Demographics			
Age (years)	65.04 (7.62)	73.48 (7.48)	< .001
Education (years)	16.63 (3.02)	14.51 (3.61)	0.014
Sex (F/M)	9/15	28/29	0.344
MMSE (/30)	29.17 (0.82)	25 (2.98)	< .001
MRI Absolute motion (mm)	0.227 (0.198)	0.329 (0.08)	0.070

Pearson's correlation analysis was conducted for each participant group (i.e., controls and patients) separately, as well as the overall group. First, for the **Aβ/tau ratio**, a significant correlation for the overall group was found with DMN ($r(42) = 0.4$, $p < .05$) the DAN ($r(42) = 0.604$, $p < .05$), motor network ($r(42) = 0.37$, $p < .05$), and language network ($r(42) = 0.49$, $p < .05$). The patient group was significantly correlated with the DAN only ($r(42) = 0.41$, $p = 0.04$). No significant correlations were observed between the control group's fMRI components and Aβ/tau ratio. (Figure 6.4).

Additionally, for **CSF p-tau**, significant relationships on the overall group were found with the DAN ($r(42) = 0.346$, $p < .05$), as well as with the motor ($r(42) = 0.366$, $p < .05$) and language network ($r(42) = 0.346$, $p < .05$). No significant correlation was found for the control and patient group separately (Figure 6.5).

Similarly, significant correlations were observed for the overall group between **plasma p-tau181** and functional connectivity: with DMN ($r(43) = 0.311$, $p < .05$) the DAN ($r(43) = 0.367$, $p < .05$), motor network ($r(43) = 0.325$, $p < .05$), and the language network ($r(43) = 0.37$, $p < .05$). No significant correlation when looking at the control and patient group separately (Figure 6.6).

A significant relationship was also observed between the functional connectivity of all four components and the **MMSE score** for the overall group. Specifically, DMN ($r(78) = 0.308$, $p < .05$), DAN ($r(78) = 0.424$, $p < .05$), motor network ($r(78) = 0.36$, $p < .05$), and language network ($r(78) = 0.32$, $p < .05$) were all significantly related to MMSE performance. No significant correlations were found for the control and patient group separately (Figure 6.7).

Interestingly, a multiple linear regression model revealed that DMN functional connectivity was most strongly associated with the ACE attention score, compared to the other sub-scores of the ACE and MMSE. The ACE memory and MMSE score were also significant (Table 6.2). No significant associations were found between the DAN, motor or language components and the ACE and MMSE scores.

Additionally, multiple linear regression models of the Four Mountains score (predictor) and ICA components revealed that the only significant association was the DAN for the overall group ($t(2.292, p < .05)$; however, this relationship was weak ($R^2 = 0.082$) (Figure 6.8).

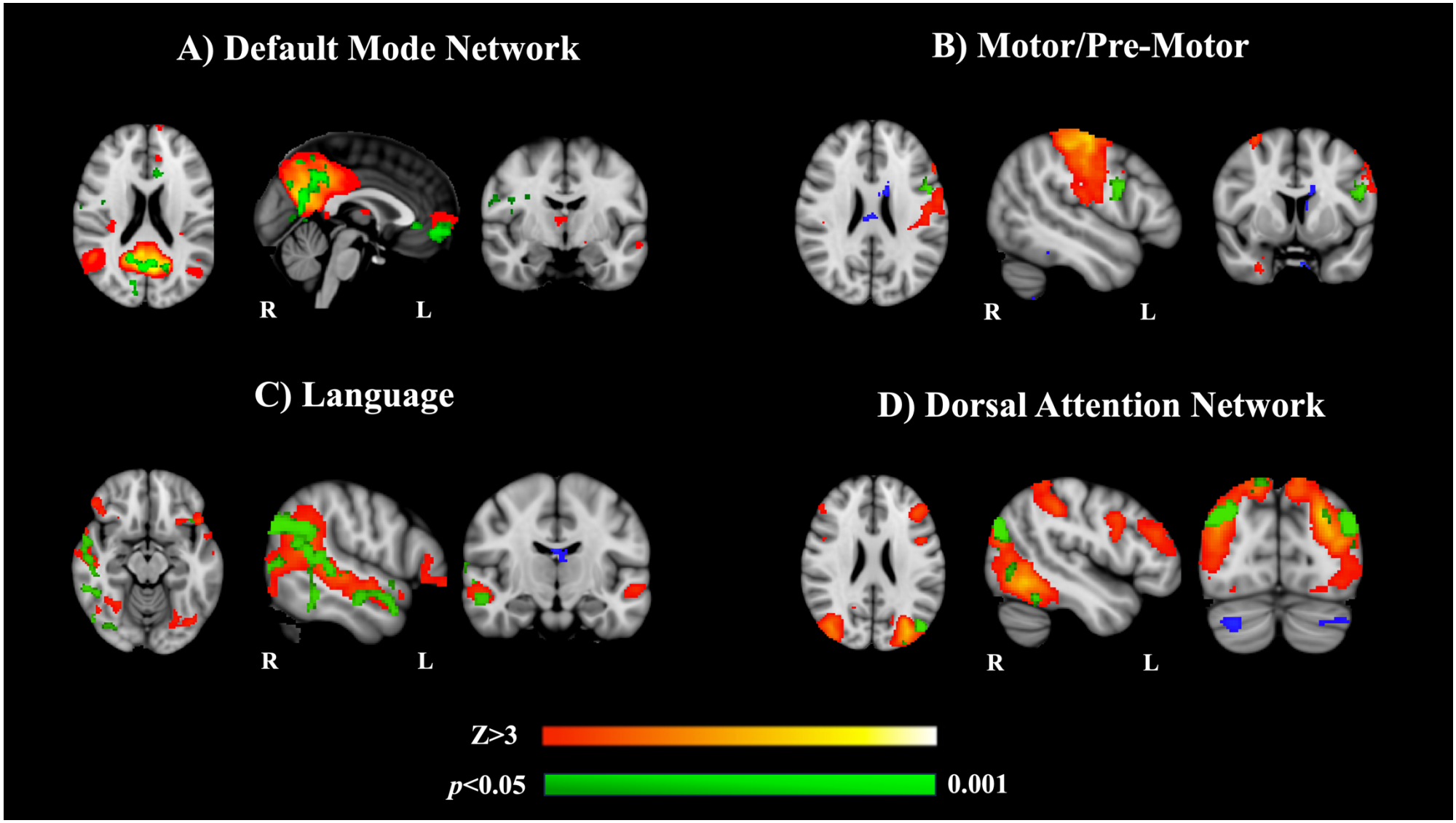

Figure 6.3. ICA Results (C>P).

ICA results of the four components that showed significant differences between controls and patients following 3000 permutations. Images shown are corrected p-values and thresholded using z > 3 (red/yellow) with a significance threshold of $p < .05$ (green). R and L = right and left hemisphere respectively.

Table 6.2. Results of a multiple linear regression model for DMN functional connectivity (predictor) and ACE sub-scores.

DMN Functional Connectivity			
	t	**β**	***p***
ACE Attention	4.003	1.011	**< .001**
ACE Fluency	0.239	-0.005	0.812
ACE Language	1.453	-0.117	0.150
ACE Memory	2.008	0.211	**0.048**
ACE Visuospatial	0.761	0.181	0.449
MMSE	2.499	-0.891	**0.015**

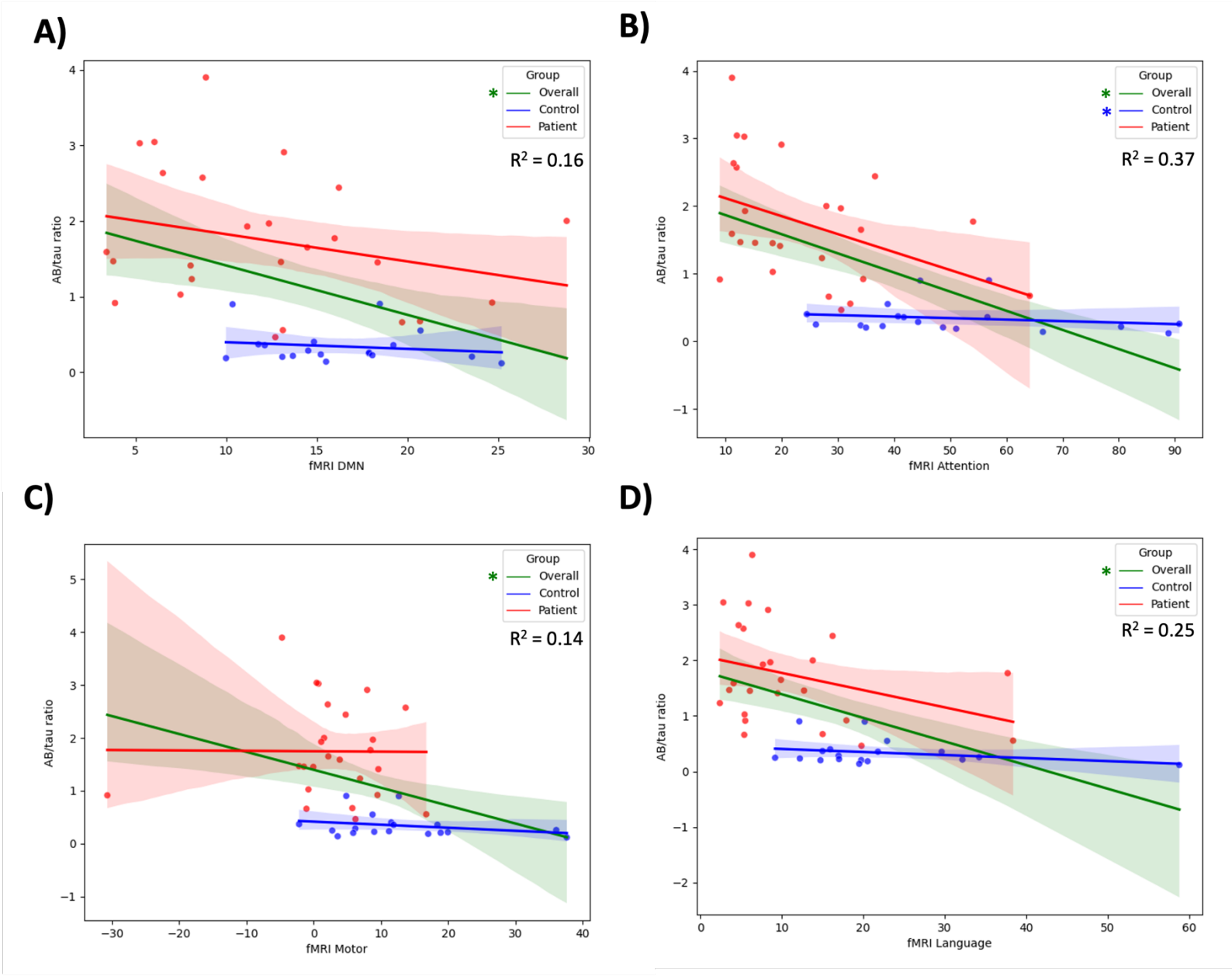

Figure 6.4. ICA components and Aβ/tau analysis.
The relationship between the Aβ/tau ratio and the mean beta values of functional connectivity within the A) DMN, B) dorsal attention network C) motor/pre-motor, and D) language components. Controls are shown in blue, patients shown in red. The overall regression for controls and patients combined is shown in green. Shaded areas represent the confidence intervals. The R^2 value is shown for the overall regression. * denotes a significant association.

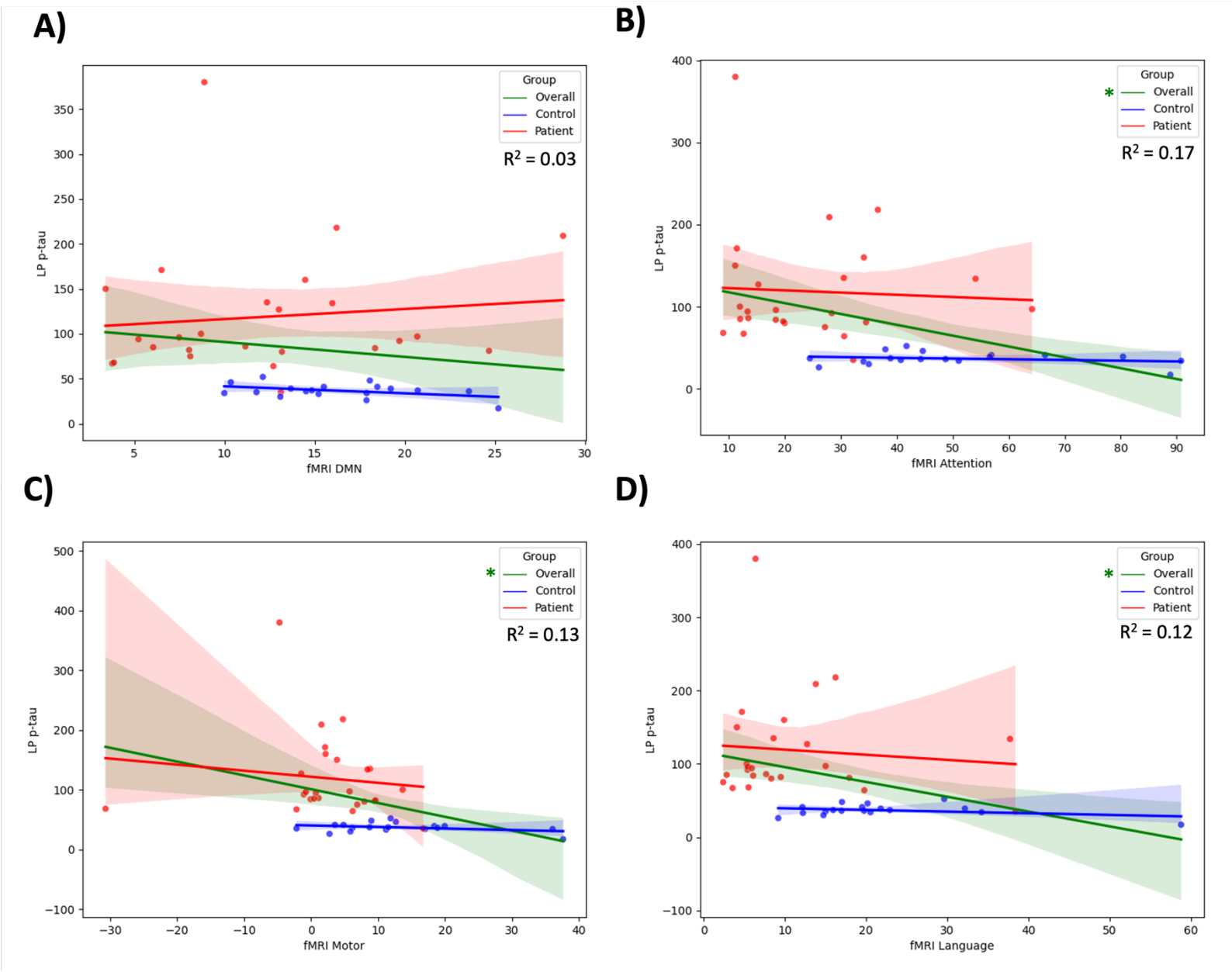

Figure 6.5. ICA components and CSF p-tau analysis.
The relationship between CSF p-tau and the mean beta values of functional connectivity within the A) DMN, B) dorsal attention network C) motor/pre-motor, and D) language components. Controls are shown in blue, patients shown in red. The overall regression for controls and patients combined is shown in green. Shaded areas represent the confidence intervals. The R^2 value is shown for the overall regression. * denotes a significant association.

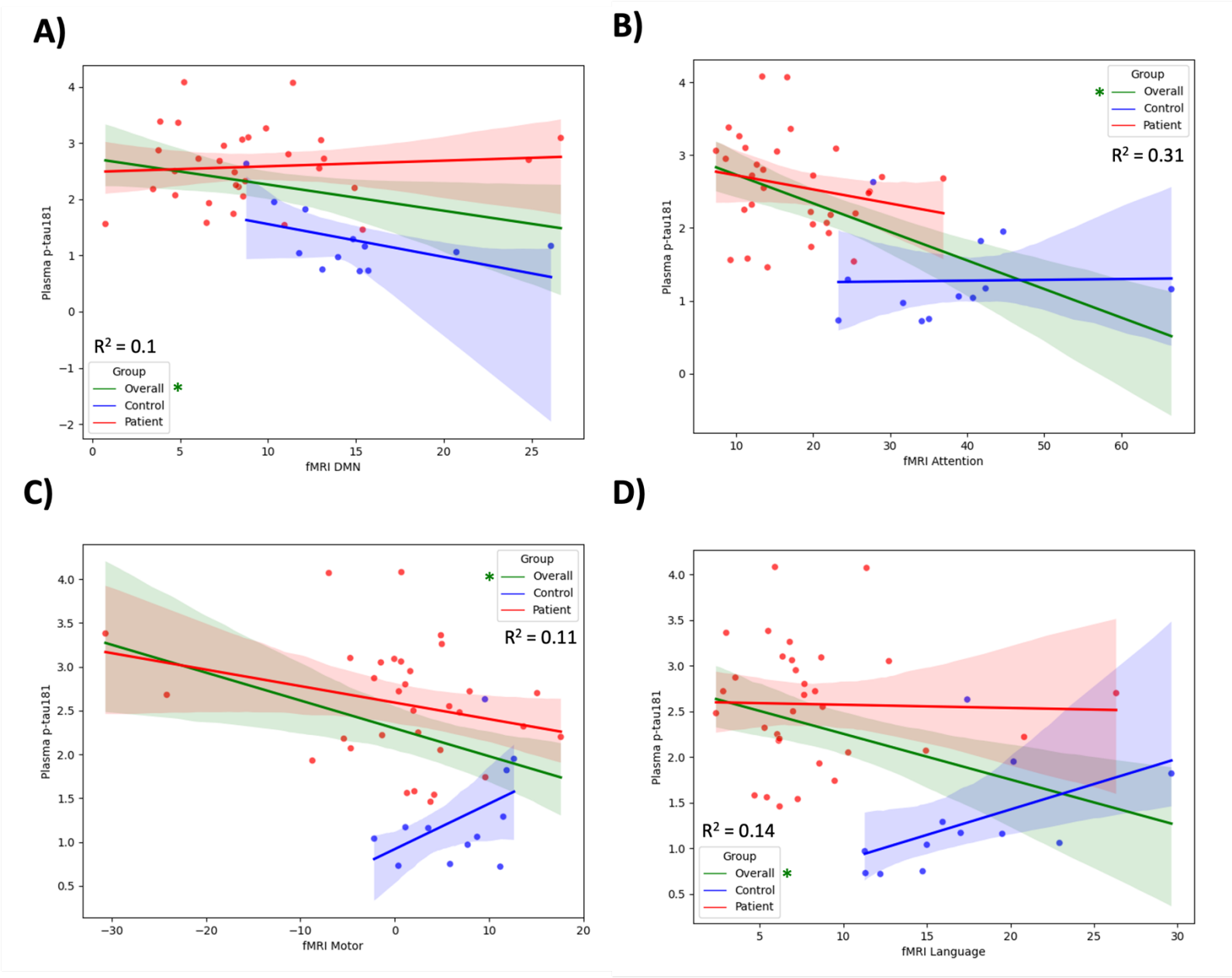

Figure 6.6. ICA components and plasma p-tau analysis.
The relationship between plasma p-tau181 and the mean beta values of functional connectivity within the A) DMN, B) dorsal attention network C) motor/pre-motor, and D) language components. Controls are shown in blue, patients shown in red. The overall regression for controls and patients combined is shown in green. Shaded areas represent the confidence intervals. The R^2 value is shown for the overall regression. * denotes a significant association.

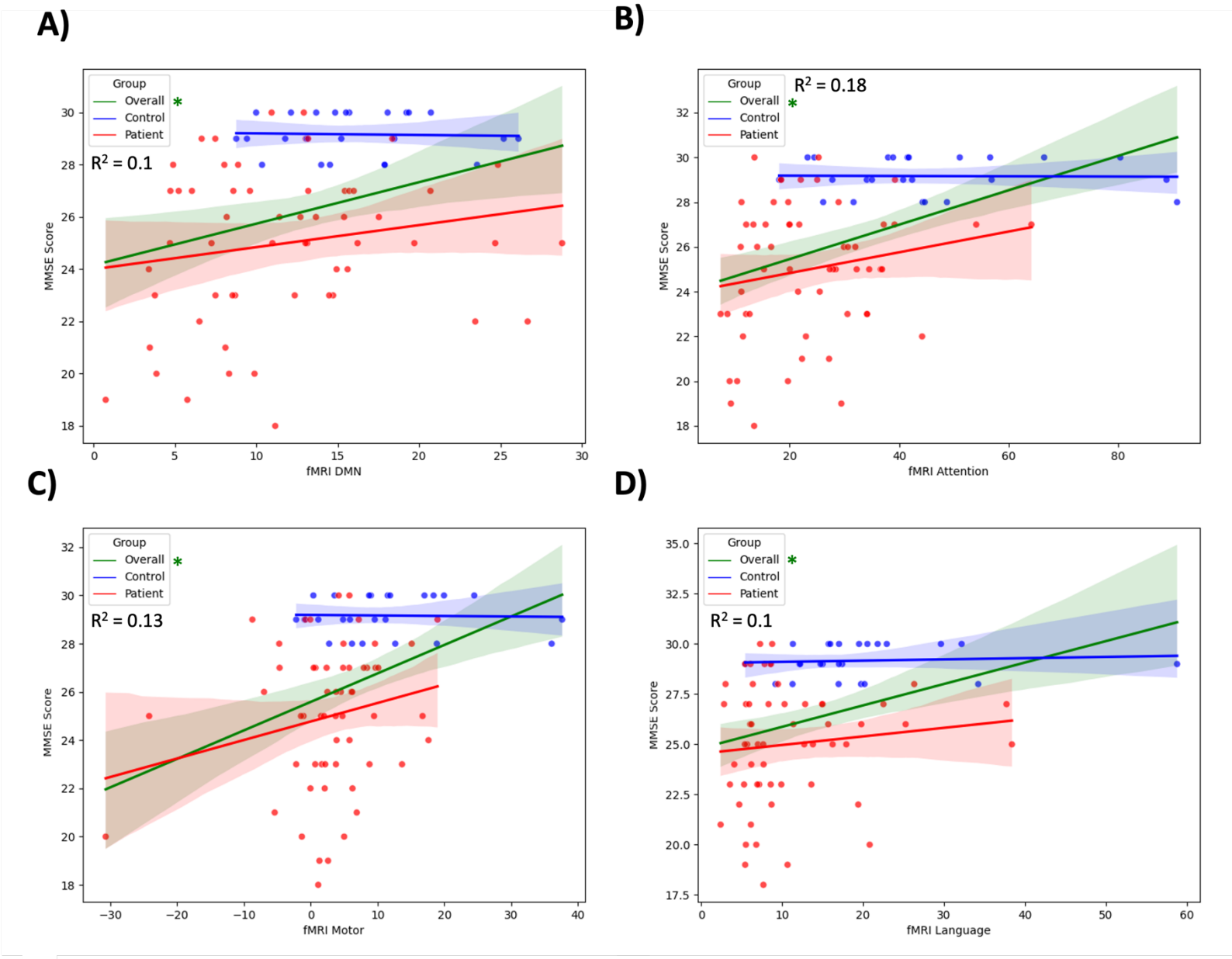

Figure 6.7. ICA components and MMSE score analysis.
The relationship between the MMSE score and the mean beta values of functional connectivity within the A) DMN, B) dorsal attention network C) motor/pre-motor, and D) language components. Controls are shown in blue, patients shown in red. The overall regression for controls and patients combined is shown in green. Shaded areas represent the confidence intervals. The R^2 value is shown for the overall regression. * denotes a significant association.

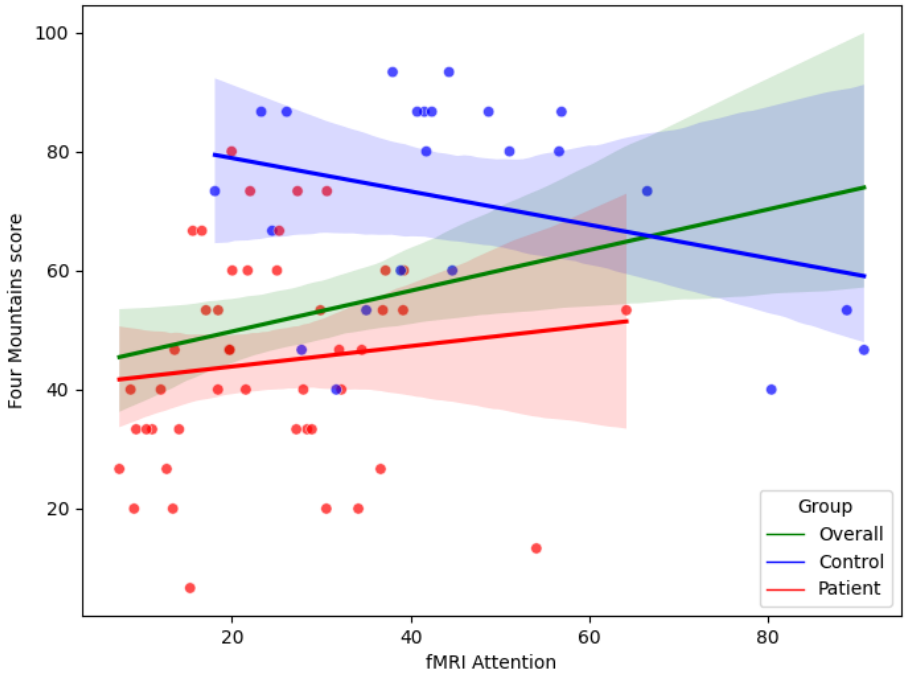

Figure 6.8. Dorsal attention network and 4MT.
The relationship between the Four Mountains (4MT) score (predictor) and dorsal attention network mean beta values of functional connectivity. Controls are shown in blue, patients shown in red. The overall regression for controls and patients combined is shown in green (R^2 = 0.082).

6.3.4 Comparison of fMRI and MEG metrics

This section focuses on exploring the relationship between the fMRI ICA components and the MEG metrics identified in Chapter 5. Specifically, this was an exploratory analysis aimed at investigating how similar the patterns of activity observed in fMRI and MEG are, and whether these two modalities capture related functional networks associated with similar cognitive and neural processes.

Separate multiple linear regression models for each fMRI-derived ICA component and the five MEG metrics identified in Chapter 5.3 revealed no significant associations between the variables for the overall group analysis. However, for the patient group there was a significant relationship between the fMRI-derived DAN and MEG-derived alpha peak frequency (eye-closed). For the control group, there were significant associations between the fMRI-derived DAN and language networks and MEG-derived alpha peak frequency (eyes-open) (Table 6.3).

Table 6.3. Results of a separate multiple linear regression models for fMRI ICA component and MEG metrics.

Results are shown for the overall group, and control and patients' group separately.

	Overall			Controls			Patients		
	t	**β**	***p***	**t**	**β**	***p***	**t**	**β**	***p***
Default Mode Network									
Alpha peak frequency (eyes-open)	1.126	0.088	0.264	1.382	-0.422	0.184	1.027	0.184	0.310
Alpha peak frequency (eyes-closed)	0.182	-0.072	0.856	1.161	0.319	0.261	0.410	-0.168	0.684
Frequency Cluster 1 (eyes-open)	1.643	-0.171	0.105	0.449	0.122	0.659	0.978	-0.240	0.333
Frequency Cluster 2 (eyes-open)	0.149	0.014	0.882	0.619	-0.103	0.544	0.043	0.090	0.966
Frequency Cluster 1 (eyes-closed)	0.267	0.068	0.791	0.270	0.023	0.790	0.160	0.073	0.874
Dorsal Attention Network									
Alpha peak frequency (eyes-open)	1.031	0.153	0.306	2.690	-0.673	**0.015**	1.037	0.177	0.305
Alpha peak frequency (eyes-closed)	1.508	-0.224	0.136	0.991	0.248	0.335	2.230	-0.403	**0.031**
Frequency Cluster 1 (eyes-open)	1.326	-0.168	0.189	0.160	-0.031	0.874	0.992	0.158	0.327
Frequency Cluster 2 (eyes-open)	0.840	0.113	0.404	1.248	-0.240	0.228	0.004	-0.006	0.997
Frequency Cluster 1 (eyes-closed)	0.674	-0.088	0.503	0.224	0.043	0.825	1.392	-0.218	0.171
Motor/Pre-Motor									
Alpha peak frequency (eyes-open)	0.329	0.050	0.744	0.985	-0.294	0.338	0.477	-0.087	0.635
Alpha peak frequency (eyes-closed)	0.196	0.030	0.845	0.655	0.195	0.521	0.255	0.049	0.800
Frequency Cluster 1 (eyes-open)	0.938	-0.122	0.352	0.409	0.093	0.687	0.399	0.068	0.692
Frequency Cluster 2 (eyes-open)	0.079	-0.011	0.937	1.232	-0.282	0.234	0.604	-0.111	0.549
Frequency Cluster 1 (eyes-closed)	0.457	-0.061	0.649	0.482	-0.110	0.636	0.327	-0.055	0.745
Language									
Alpha peak frequency (eyes-open)	0.572	0.087	0.569	2.315	-0.296	**0.033**	0.441	0.076	0.661
Alpha peak frequency (eyes-closed)	0.832	-0.128	0.409	1.439	0.096	0.167	1.537	-0.280	0.132
Frequency Cluster 1 (eyes-open)	0.217	0.028	0.829	0.587	-0.208	0.564	1.762	0.282	0.085
Frequency Cluster 2 (eyes-open)	0.812	0.112	0.420	0.966	0.276	0.347	0.427	0.074	0.672
Frequency Cluster 1 (eyes-closed)	0.469	-0.063	0.641	0.263	-0.282	0.796	0.611	-0.097	0.544

6.4 Discussion

This chapter investigated fMRI data within the NTAD cohort, aiming to replicate known DMN differences between controls and patients and examine their relationship with measures of neuropathology and neuropsychological assessments. Additionally, as a unique exploratory analysis, fMRI measures were compared with the MEG metrics identified earlier in this thesis to assess potential similarities between the two neuroimaging modalities.

Cross-sectional analysis of the resting-state fMRI data revealed significant differences between biomarker-positive MCI and AD patients and healthy aging controls in four fMRI ICA components; the DMN, DAN, motor/pre-motor, and language networks. These findings demonstrate that patients exhibit significantly lower functional connectivity in these networks compared with controls. Statistical analysis of neuropathology and neuropsychological assessment measures showed distinct relationships with these networks. The Aβ/tau ratio was associated with the DMN and DAN, while CSF p-tau was related to all networks except the DMN. Plasma p-tau181 and MMSE scores were associated with all four network components. Additionally, the Four Mountains test was examined across all four networks, and the DAN was the only fMRI ICA component associated with the score. Finally, an exploratory analysis comparing fMRI and MEG metrics revealed distinct associations with the fMRI ICA networks and the MEG alpha peak frequency measures when examining the patient and control group separately.

6.4.1 ICA Results

Using ICA, we found that patients exhibited significantly less functional connectivity in the DMN. This is similar to other studies that have reported DMN activity distinguishes AD from healthy ageing (Greicius et al., 2004; Jones et al., 2011), and studies investigating MCI to AD conversion have suggested the DMN as a potential clinical biomarker (Sperling et al., 2010). However, findings across studies are not always consistent, as differences may arise due to variability in AD diagnosis methods and data pre-processing steps (Eyler et al., 2019). Given that our analysis was conducted with the NTAD cohort, which includes participants with robust biomarker testing, as well as strict data cleaning and analysis protocols, we can be confident that the observed DMN differences between controls and patients are valid. Future research could build on this by examining MCI and AD subgroups separately to determine whether these differences are primarily driven by Aβ positivity or also reflects disease severity.

In addition to DMN alterations, ICA revealed reduced functional connectivity in other networks, including the DAN. Attentional impairment is thought to be an early clinical manifestation of AD and is included in most AD cognitive tests, though it is often less noticeable than memory impairments, which is typically the most recognised symptom of AD. The DAN is associated with working and episodic memory (Zhan et al., 2016), and has been previously shown to exhibit significant functional connectivity differences in MCI and AD patients using both task and resting-state fMRI methods (H. Wu et al., 2023; Zhang et al., 2015). Our results align with previous findings in resting-state fMRI, showing significant reduced functional connectivity in the DAN in patients compared to healthy controls.

Similarly, language production deficits can occur in the early stages of AD. As with attention, language deficits are often assessed in cognitive tests for AD, focussing on aspects such as naming, repetition, and comprehension. Our ICA results revealed distinct alterations in a language network, demonstrating that patients exhibit decreased functional connectivity in this area compared to healthy ageing controls. This finding aligns with previous studies that have shown that language functional connectivity is compromised in AD patients (Weiler et al., 2014). Both of these results were derived from ICA analysis rather than ROI or seed-based methods, highlighting that different analytic approaches can reveal complementary aspects of functional connectivity. Furthermore, these results were obtained from resting-state fMRI, whereas previous studies have used task-based methods focussed on attention and language. This distinction is important because it highlights the potential of resting-state fMRI as a tool for uncovering early network disruptions in AD, even in the absence of task-induced activation.

Motor symptoms are less commonly known in AD but can include a slowing of gait (the pattern of walking) (Masse et al., 2021), reduced grip strength (Buchman et al., 2007), poor balance (Yoon et al., 2020), and reduced manual dexterity (de Paula et al., 2016). Among these, gait disturbances are the most prevalent motor issue in AD, with up to 30% of MCI patients exhibiting abnormal gaits compared with controls and nonamnestic-MCI patients (Verghese et al., 2008). However, the neural mechanisms underlying these motor symptoms are not well known, and research in this area is complicated by the challenge of distinguishing them from signs of parkinsonism. Despite this, our resting-state fMRI ICA results revealed a significant difference in a motor/pre-motor network between patients and controls, indicating reduced functional connectivity in this brain region in AD patients. Other studies have also shown altered motor networks in AD patients, though these used a simple motor task such as a grip

task (Agosta et al., 2010; Vidoni et al., 2012). These findings suggest that even though motor symptoms are less commonly known in AD, there is evidence of disrupted brain activity in the motor-related network.

6.4.2 Associations with clinical measures

Correlation analyses revealed significant associations between functional connectivity and neuropathological biomarkers. Specifically, the Aβ/tau ratio was significantly correlated with all four ICA components. Plasma p-tau 181 and MMSE scores were also significantly associated with all four ICA components, whilst CSF p-tau was only associated with the DAN, motor, and language networks. However, it is important to highlight that these correlations were primarily observed in the combined group analysis; when examined separately in control and patient groups, most associations were no longer significant. This suggests that these relationships may be driven by overall group differences rather than within-group analysis. The only exception was the relationship between the Aβ/tau ratio and DAN functional connectivity, which remained significant when analysing the patient group independently.

Previous research has established a link between the DMN and amyloid and tau accumulation, with evidence suggesting that DMN structures are particularly vulnerable to amyloid deposition. Studies using fMRI and PET imaging have demonstrated that Aβ deposition is associated with disrupted functional connectivity within the DMN (Buckner et al., 2005; Sheline et al., 2010). CSF tau and p-tau levels have also been associated with the DMN. Using resting-state fMRI and PET scans, high level of tau pathology in the posteriomedial cortex and hyperconnectivity between temporal and parietal nodes of the DMN were found compared to healthy older controls (Putcha et al., 2022). Furthermore, greater tau burden has been found to be associated with lower functional connectivity in DMN regions in a group of participants that carry the Presinilin-1 E280A gene, meaning they are expected to develop early-onset AD (Guzmán-Vélez et al., 2022). Our results showed a significant association between the Aβ/tau ratio and DMN functional connectivity, however the absence of this relationship when the control and patient groups were analysed separately indicates that this relationship may be driven by broader group differences rather than a meaningful neuropathological marker of AD. Further investigation with a larger sample size is needed to help clarify this relationship.

Tau deposition patterns characteristic of AD has also been found in the DAN. For instance, when examining the spatial distribution of a tau PET tracer in the brains of prodromal and clinical AD patients, increased tau deposition was observed in the posterior cortical networks, including the DAN and higher visual networks, rather than the DMN as previously reported (Hansson et al., 2017). This finding is further supported by evidence from posterior cortical atrophy (PCA) patients, who also show significant tau accumulation in these regions. The DAN may play a crucial role in the early stages of AD, as it comprises key nodes involved in visuospatial attention – a cognitive domain often affected early in AD-related decline (Cronin-Golomb et al., 1991). Consistent with this, our finding that the Aβ/tau and DAN functional connectivity was the only one to remain significant in separate analyses, and that it was the only component to be related to the Four Mountains test, aligns with the notion that pathology may be particularly relevant to disease processes, suggesting that the DAN could serve as a more reliable network for AD detection than the other ICA networks identified in this analysis.

While tau deposition and functional connectivity changes in the DAN appear to be particularly relevant for detecting early AD-related pathology, cognitive performance in AD may still be more closely linked to DMN connectivity. Interestingly, although our analyses identified the DAN as a potentially reliable marker for AD, a multiple linear regression model revealed that DMN connectivity was most strongly associated with the ACE attention score, along with the ACE memory and MMSE scores. No such associations were found for the DAN, motor or language components. This suggests that while DAN dysfunction may reflect underlying pathology, DMN connectivity remains a stronger correlate of cognitive performance in AD, reinforcing previous findings that link DMN connectivity with MMSE scores (Grieder et al., 2018). Together, these findings suggest that the DAN may serve as a promising biomarker for early AD detection, while the DMN may better capture the clinical impact of disease progression.

6.4.3 Comparison of fMRI and MEG metrics

An exploratory analysis was conducted to investigate the association between the four fMRI ICA components and the five MEG metrics that showed significant differences between patients and controls. While no significant associations were found for the overall group analysis, distinct patterns emerged when examining the patient and control group separately. In the patient group, DAN functional connectivity was significantly associated with the eyes-closed alpha peak frequency measure. Conversely, in the control group, significant associations

were observed between both the DAN and language network with the eyes-open alpha peak frequency measure. These findings highlight the potential cross-over between fMRI and MEG. Previous studies have attempted to compare the fMRI BOLD signal with MEG oscillatory activity by examining responses recorded from both modalities in separate sessions. Findings suggest that oscillatory signatures spatially align with BOLD signal patterns, highlighting a meaningful correspondence between these measures (Singh et al., 2002). Notably, MEG studies have demonstrated a negative temporal correlation between BOLD and alpha/beta oscillations, suggesting that decreases in these frequency bands may coincide with increases in neural activity as reflected by the BOLD signal (Mukamel et al., 2005; Zumer et al., 2010). More specific to our results, a recent study by Tripathi & Somers (2023) investigated the relationship between functional connectivity within the DMN and DAN and peak alpha and beta frequencies in participants from the Human Connectome Project. Their findings revealed that the magnitude of the anticorrelation between the DMN and DAN was negatively associated with both peak alpha and beta frequencies. Interestingly, participants with either very high or very low alpha peak frequency exhibited stronger connectivity within and between these networks, suggesting a non-linear relationship. While our results examined the DMN and DAN separately and indicated that lower peak alpha frequency was linked to reduced connectivity, both studies point to a meaningful, yet complex, relationship between fMRI-derived connectivity and MEG oscillatory dynamics. Instead, both modalities offer unique complementary insights into brain activity rather than reflecting the same processes.

In the control group, the eyes-open alpha peak frequency showed associations with fMRI ICA components, specifically in the DAN and language networks. This suggests that this MEG metric may be the most robust and informative of the measures examined in this thesis. This is in line with the results presented in Chapter 5, where the eyes-open alpha peak was consistently associated with the Aβ/tau ratio, p-tau and cognitive scores compared to the other measures. Importantly, these associations between eyes-open alpha peak, as well as the other significant MEG metrics, were stronger than those observed in the fMRI data. For example, the overall group comparison of the eyes-open alpha peak frequency and MMSE showed an R^2 value of 0.29 whereas the fMRI components averaged an R^2 value of 0.13. Similarly, the association between p-tau and alpha peak frequency yielded an R^2 value of 0.25, compared to an average R^2 value of 0.11 for the fMRI components. Notably, the strongest association was observed between the eyes-open alpha peak frequency and performance on the Four Mountains test,

which demonstrated an R^2 value of 0.32, far exceeding the corresponding fMRI R^2 value of 0.082. The only exception to this pattern was the fMRI DAN association with the Aβ/tau ratio, which was comparable to the alpha peak frequency measure, further suggesting that the DAN may be the most relevant fMRI measure identified in this analysis. Nonetheless, the MEG metrics consistently demonstrated stronger associations with clinical and cognitive measure of AD, suggesting the idea that MEG may be more sensitive to detecting AD-related changes. One possible explanation for this is that the NTAD cohort included many patients in the early stage of their diagnosis, as per the inclusion criteria. Therefore, as MEG measures fast, dynamic neuronal activity directly, it may be better equipped to detect subtle, early-stage dysfunction than fMRI, which relies on a slower hemodynamic response. This suggests that MEG may be particularly valuable for identifying AD-related changes at the earliest stages of the disease when interventions are likely to be most effective.

6.4.4 Limitations and future research plans

This chapter is limited in its comparison of fMRI and MEG data, as the resting-state analysis did not include a full voxel-wise or timeseries analysis, nor did it incorporate a task-related comparison. Instead, this chapter focussed on the specific group difference comparisons. Future research could extend this work by conducting a more comprehensive analysis of the full resting-state fMRI and MEG timeseries, which could look at how each MEG frequency band is associated with fMRI data. Nonetheless, the observed group differences between controls and patients in this data are encouraging, as the findings highlight deviations in brain activity associated with AD. Future studies could expand on these results by including biomarker-negative patients from similar study protocols, such as the Deep and Frequent Phenotyping study, to further explore the underlying mechanisms of AD pathology.

6.4.5 Summary

Overall, this chapter investigated the resting-state fMRI data in the NTAD cohort to explore AD-specific differences in brain activity and to provide a basis for comparison with the MEG findings presented in this thesis. Given the focus of this thesis on the potential advantages of MEG as a biomarker tool, it was necessary to examine the fMRI data to identify group differences and establish a meaningful comparison. By directly comparing these fMRI results with MEG metrics, this analysis aimed to evaluate which technique may be more effective in detecting early-AD related changes.

Similar to previous research, the fMRI results revealed significantly lower functional connectivity in the DMN, dorsal attention, motor and language networks in patients compared to healthy controls. The comparison of these components with clinical measures demonstrated associations with the DMN and DAN with the Aβ/tau ratio, while CSF p-tau, plasma p-tau181 and MMSE scores were associated with all four networks. However, these relationships were complicated as the only surviving association when examining the control and patient groups separately was the DAN and Aβ/tau ratio.

The MEG metrics identified in this thesis were more strongly associated with the clinical measures than the fMRI ICA components, providing novel insight into the potential of MEG as a more sensitive marker in AD. The stronger associations found between sensor-space eyes-open resting-state MEG and key AD biomarkers – such as Aβ/tau ratio, p-tau and cognitive measures- suggest that MEG may be more sensitive to early-stage AD. This heightened sensitivity may be attributed to the NTAD cohort's inclusion of patients with early MCI or AD, a stage at which fMRI may struggle to detect subtle neural changes. Unlike the BOLD signal, MEG captures oscillatory brain activity, providing a more direct measure of neural function. As a result, MEG may be better equipped to detect the early neuronal disruptions that precede more overt functional connectivity changes in fMRI, reinforcing its potential as a more sensitive tool for identifying and tracking early AD-related changes.

Future research should examine the fMRI and MEG data in more detail, which could unveil a more detailed picture of the modalities. Additionally, the longitudinal fMRI data could be explored to investigate how this modality captures the decline of AD over time and how this compares to the longitudinal MEG results.

In summary, this chapter demonstrated that while both fMRI and MEG reveal AD-related changes in brain activity, MEG showed stronger associations with key biomarkers and cognitive measures, suggesting it may be more sensitive to early-stage AD. The next chapter will summarise the key findings from this thesis, discuss its limitations, and outline potential directions of future research.

Chapter 7: Discussion

This thesis presented a comprehensive analysis of multiple neuroimaging methods compared with cognitive and neuropathological measures, with the aim of exploring MEG as potential biomarker for AD. There were two overarching aims of this work. Firstly, it aimed to outline the neuropathology of AD and validate the NTAD cohort by exploring well-established clinical and research-based cognitive tests, informing subsequent analyses on key variables. Secondly, it aimed to explore power spectral differences in MEG between patients and controls, correlate these differences with pathological markers of AD, and compare them with fMRI measures. This summary chapter will answer the five questions outlined in Chapter 1 and discuss the implications of these findings.

Objective 1: To outline the neuropathology of AD and introduce the NTAD study

7.1 What do we know about the neuropathology of AD?

Chapter 2 outlined the neuropathology of AD, highlighting two key hypotheses: the amyloid cascade hypothesis, and the tau hyperphosphorylation hypothesis. The amyloid hypothesis proposes that Aβ accumulation initiates a pathological cascade, triggering the misfolding of proteins, the formation of NFTs, neuronal death and ultimately, cognitive decline. Aβ pathology can be assessed through CSF measurements of Aβ40 and Aβ42, its two main isoforms, or via amyloid-PET imaging. In contrast, the tau hypothesis suggests that when tau proteins become hyperphosphorylated and lose their stabilising role in the neuronal cytoskeleton, they form NFTs, leading to impaired synaptic transmission, synapse loss, and dementia. The long-standing debate over whether amyloid or tau pathology appears first remains, though emerging evidence suggests that the sequence may vary depending on brain region. Tau and p-tau can also be measured using CSF and PET imaging. More recently, the development of plasma-based assays offers a less invasive alternative, allowing amyloid and tau biomarkers to be detected through blood testing. These new tools are especially promising for clinical use, as they offer more accessible and scalable options for early diagnosis and monitoring.

While these biomarkers are essential for understanding AD-related changes, many studies fail to include them in recruitment criteria, resulting in the inclusion of participants with mixed of

uncertain diagnoses. Current therapies, largely targeting the cholinergic system, have limited effectiveness, while newer drugs aimed at Aβ clearance, such as Aducanumab and Lecanemab, remain controversial. The evolving role of biomarkers in diagnosis was also discussed, highlighting the ongoing debate around whether neuropathological changes alone are sufficient for diagnosis in the absence of cognitive symptoms. Present guidance suggests that individuals with amyloid or tau pathology but no cognitive impairment should be classified as "at risk".

Building on this, non-invasive imaging techniques such as MRI, fMRI and MEG were explored to better understand neuropathological alterations in the AD brain. Structural MRI measurements, such as hippocampal volume, are well-established markers of AD and, where available, are commonly used in clinical settings to support diagnosis. Functional brain activity measured with fMRI has revealed both resting-state and task-based differences between AD patients and healthy controls, highlighting functional disruptions in the AD brain. However, fMRI lacks the temporal resolution needed to capture fast neural dynamics. In contrast, MEG offers high temporal resolution, making it a promising tool for AD research. Prior studies were discussed that have shown MEG's sensitivity to regional and functional abnormalities, but the relationship between MEG activity, cognitive, and pathology still requires more research. To address this gap, the NTAD study was introduced as a platform for conducting this in-depth analysis.

7.2 What study cohort could be used to investigate MEG in AD?

Chapter 3 introduced the NTAD study, a multi-centre, multi-modal study aimed at identifying sensitive biomarkers for next-generation experimental medicine studies. A detailed overview of recruitment, screening and visit procedures was provided, emphasising the rigorous inclusion and exclusion criteria used to establish a well-characterised cohort. The NTAD study offers a rich dataset comprising of cognitive, neuropathological structural, and functional measures from biomarker-positive patients and biomarker-negative controls. It also represents a valuable resource for combining with other cohorts, such as Cam-CAN and DFP, particularly given the age mismatch between NTAD controls and patients, which could be mitigated through combined analyses. Participants underwent a comprehensive battery including clinical cognitive assessments, blood sampling, lumbar puncture or PET imaging, MEG and MRI scans, and multiple research-based cognitive tests. Patients also completed a MEG test-retest scan two to four week after baseline, along with follow-up assessments at 12 months and 24

months. This study complements other large-scale studies, such as DFP, with closely aligned scanning protocols to facilitate future cross-cohort comparisons and validation. Notably, data from the Oxford site were collected as part of this DPhil project. Overall, this chapter outlined the key methodological approaches underpinning the thesis.

Objective 2: To explore MEG signatures of AD and compare with fMRI

7.3 What distinguishes normal ageing from AD?

Chapter 4 presented the first analysis in this thesis, exploring cognitive and structural differences between AD patients and healthy ageing controls. The NTAD cohort was validated by examining MRI and cognitive measures. Standard clinical cognitive tests were compared with research-based assessments that may be more sensitive to early AD-related changes, including the Four Mountains Test, RBANS, and FCSRT. Of these, the Four Mountains Test showed the strongest associations with neuropathological markers (Aβ/tau ratio and p-tau), outperforming even established tools like the MMSE and ACE, as well as other memory-based tests. This suggests it may be a more sensitive predictor of early pathological changes in AD. However, poor performance on the 4MT may reflect memory problems, difficulties in matching viewpoints, or a combination of both. Future research could incorporate a perceptual baseline to help clarify whether observed effects are driven by hippocampal-dependent spatial processing or more general perceptual difficulties.

Chapter 4 also included a novel comparison of MRI data with specific cognitive subdomains, such as the ACE-R memory score, which showed the strongest association with hippocampal volume—supporting long-standing findings linking memory decline and hippocampal atrophy (Braak & Braak, 1991). However, as discussed in Chapter 2, early detection is essential for effective intervention, as AD pathology can precede symptoms by decades. The Four Mountains Test may therefore be a promising tool for earlier identification than currently used clinical assessments. MEG was introduced as a potential method for detecting early synaptic dysfunction, offering insight into neural dynamics before structural changes are evident. Based on the findings in Chapter 4, this analysis concludes by identifying key clinical and research-based variables to be carried forward into subsequent analyses. Future work could extend this analysis by incorporating additional brain regions, such as the entorhinal cortex, to provide a more comprehensive understand of the neural correlates of cognitive decline.

Chapter 5 introduced the power spectrum and GLM approach to MEG analysis, offering an in-depth investigation of the relationship between sensor-space electrophysiological measures and various measures of neurocognition. Cross-sectional results revealed a distinct profile in patients, characterised by increased theta activity, reduced alpha/beta power, and lower alpha peak frequency. Longitudinal analysis indicated alterations in alpha power across both eye conditions and reduced beta power in the eyes-open condition.

Clinical associations highlighted that the eyes-open MEG metrics were most informative. Significant correlations were observed between hippocampal volume and the theta and alpha/beta clusters, as well as alpha peak frequency. Alpha peak frequency was also associated with Aβ/tau ratio and p-tau levels. Cognitive associations showed that both MMSE and Four Mountains scores were significantly related to the eyes-open MEG measures, while eyes-closed metrics showed minimal associations. These findings suggest that the eyes-open condition is more reliable and sensitive to disease-related neural and cognitive changes.

7.4 Are MEG measures of AD reliable?

Chapter 4 included test re-test reliability of the MEG metrics from patient data, using ICC to assess the stability of spectral power measurements over time. Unlike traditional statistical methods such as a paired t-tests, which assess differences in mean values, ICC provides a more robust evaluation of consistency of individual measurements across repeated sessions. This is an essential requirement for any potential biomarker, which made this analysis particularly valuable in evaluating the reliability of MEG in AD research. The results indicated good to excellent reliability across the power spectrum, particularly in the alpha and beta frequency bands. Importantly, the eyes-open resting-state condition outperformed the eyes-closed condition, demonstrating higher reliability across a greater number of sensors. This suggested that the eyes-open condition may be more stable and suitable for longitudinal studies aiming to monitor disease progression or evaluate the efficacy of therapeutic interventions in AD.

7.5 Are there any differences between MEG and fMRI results?

Given the aim of MEG as a potential AD biomarker, it was essential to compare findings with fMRI data, a modality with established clinical relevance. Chapter 6 analysed resting-state fMRI from the same NTAD participants using ICA analysis, identifying group differences in four networks: the DMN, DAN, motor/premotor network, and a language network. The Aβ/tau ratio was linked to the DMN and DAN, while p-tau correlated with all except the DMN. Plasma

p-tau181 and MMSE were associated with all four networks. The Four Mountains test was uniquely associated with the DAN. Interestingly, the direction of this association differed between groups as controls with higher 4MT scores were linked to lower DAN activity, whereas in patients higher 4MT scores were linked to higher DAN activity. This reversal may reflect compensatory network recruitment in patients, whereby increased DAN connectivity supports preserved spatial memory performance, whereas in controls more efficient processing requires less DAN engagement. An exploratory analysis comparing MEG and fMRI metrics revealed distinct, modality-specific associations, with MEG showing stronger correlations with clinical measures. MEG metrics were more closely linked to key AD biomarkers, including the Aβ/tau ratio, p-tau levels, and cognitive test performance, suggesting greater sensitivity to early-stage AD. These findings supported the potential of MEG as a biomarker for AD, particularly for tracking disease progression and guiding the development of new therapeutic interventions.

7.6 Implications and future work

Results from this work demonstrate that MEG can successfully distinguish patients with AD pathology from healthy controls. In particular, the eyes-open condition revealed an increase in theta power and a decrease in the alpha/beta power in patients, while the eyes-closed condition showed increase in theta activity. These findings aligned with previous studies reporting elevated lower frequency power in AD (de Haan et al., 2008; Fernández et al., 2002; Koelewijn et al., 2017), suggesting that theta power might be the most sensitive to disease. However, it is important to note that test re-test reliability was lowest in the lower frequency bands across both eye conditions. This highlights a crucial distinction: the features most sensitive to AD may not be necessarily the most reliable across time, which has implications for their utility as stable biomarkers. Building on this, occipital alpha slowing was explored in this thesis, as it has been linked to alterations in cognitive scores (Fernández et al., 2006) and accumulations of tau and amyloid (Ranasinghe et al., 2022). Given the observed variability in MEG signal reliability across frequency bands, the alpha band emerged as a particularly promising target as it demonstrated higher test-retest reliability across a greater number of sensors, especially in the eyes-open condition. This suggests that alpha-related measures may offer greater stability and reproducibility for longitudinal monitoring, making them more suitable for use in clinical trials and experimental medicine. Importantly, results from this thesis showed that alpha peak frequency, particularly in the eyes-open condition, was significantly associated with multiple

markers of AD. Specifically, it was related to the Aβ/tau ratio, p-tau levels and hippocampal volumes, hallmarks of AD pathology. These findings support the notion that alpha peak frequency may serve as a valuable biomarker, offering both robust test-retest reliability and sensitivity to functional decline and underlying pathology. However, this is mainly limited to baseline data, as further research is required to establish its longitudinal utility.

As this body suggests that MEG may serve as a potential biomarker capable of detecting AD earlier than traditional methods like MRI, it is important to highlight that MEG is not merely reflecting the same information. Instead, MEG provides unique insights into functional brain dynamics, particularly neural oscillations and synaptic activity, that are not captured by structural imaging. To explore this further, we compared MEG and MRI metrics with neuropathological and cognitive measures. The results showed that MEG metrics were more strongly associated with neuropathological markers, such as the Aβ/tau ratio, while MRI metrics were more closely related to cognitive scores, including the MMSE and ACE memory score. The Four Mountains test was associated with both MEG and MRI measures (Table 7.1).

This suggest that MEG and MRI metrics are not simply overlapping measures but are capturing distinct aspects of AD, similarly to the comparison of fMRI data. Specifically, MEG appears to be more closely linked to underlying neuropathological changes, as reflected by stronger associations with the Aβ/tau ratio. To explore how these imaging modalities relate to cognition, the MMSE, ACE memory and Four Mountains test were included in the comparison. As expected, the ACE memory score showed stronger associations with hippocampal volume, a structural marker of memory, whereas the Four Mountains test was also significantly related with MEG measures. This highlights its potential clinical value as a tool for identifying AD at an earlier stage. Notably, the MEG metric most consistently associated with pathology was the eyes-open alpha peak frequency. This further supports the notion, as discussed earlier, that this specific MEG measure may be the most promising candidate for use as a clinical biomarker. Overall, the distinction between MEG and MRI underscores MEG's added value in detecting early, functional brain changes that may precede structural degeneration, offering a potentially more sensitive approach as an AD biomarker.

Looking ahead, the findings from this thesis support the potential role of MEG within the future of precision medicine. Precision, or personalised, medicine refers to an innovative approach to disease prevention and treatment that considers individual differences in genes, environment,

and lifestyle. In the context of AD, this means moving beyond a one-size-fits-all model to develop more personalised strategies for early detection, monitoring, and intervention. This idea was recently highlighted by Lu et al. (2023) who described precision medicine as a necessary shift towards more efficient and effective healthcare, and proposed a model that enhances the identification of biomarker-dependent drug trials. These ideas are being more accepted by national health system. For instance, the Australian government recently announcement $185 million to support advances in precision oncology, demonstrating the growing recognition of biomarker-driven strategies in medical research. Therefore, the future of precision medicine in AD could include MEG, with features such as the time series or alpha peak frequency incorporated into a patient's personalised biomarker profile.

Along these lines, MEG technology is advancing into the new space wearable systems, through the advancement of optically pumped magnetometers (OPMs) (Brookes et al., 2022). These wearable MEG systems offer significant advantages over traditional cryogenic MEG setups, including increased flexibility and reduced infrastructure requirements. Unlike EEG, MEG is less sensitive to distortions from the skull and scalp, making it a better option for precisely measuring neuronal activity. This innovation could help transition MEG into the clinical space, as it would be more accessible in smaller clinical settings such as memory clinics. This idea has been proposed in the field of epilepsy research, where it has been suggested that OPM-MEG could help expand the use of MEG to children with epilepsy who are unable to wear or tolerate standard MEG systems (Pedersen et al., 2022). More specifically in the context of AD, the clinical application of MEG may be limited by the challenged of recording from older adults, who often exhibit increased levels of movement and restlessness during scans, and standard MEG systems are highly sensitive to motion. OPM systems have demonstrated reliable data during movement (Roberts et al., 2019), however these systems still require significant further development to their current limitations, such as the weight of the helmet and heat generated by the systems.

Findings from this thesis suggest that MEG-derived markers, such as alpha peak frequency, show strong correlations with key AD biomarkers like the Aβ/tau ratio, p-tau levels, and cognitive measures. In principle, this raises the possibility that MEG could be used to enhance the sensitivity of early detection methods. However, it is important to recognise that MEG biomarkers, by design, are currently benchmarked against established markers like amyloid and tau. Thus, while MEG may correlate with these pathological markers, it cannot necessarily

surpass them diagnostically at this stage – rather, it offers an additional, non-invasive, and functional dimension to disease monitoring. To move forward into clinical translation, MEG markers must be reliably replicated across diverse cohorts and ideally adapted to more accessible EEG or OPM systems.

Given the data collection component of this thesis, it is important to discuss my experiences of interacting with participants and their families. Recruitment for this study proved particularly challenging. Filling willing participants was difficult, especially given the invasive lumbar puncture procedure, and many more screening phone calls and visits were required than the number of participants ultimately recruited. Additionally, a number of potential patients were excluded due to negative biomarker results, further limiting the pool of eligible participants.
The quality of data was heavily reliant on establishing a strong relationship and clear communication with participants from the very first contact. By creating these relationships, participants felt more at ease, enabling them to complete the visits and follow instructions effectively. For instance, by demonstrating the effect of movement of the MEG signal, participants were better able to understand the importance of staying still. Additionally, I used text on a screen when participants entered the MRI scanner to help them stay calm and provide clear instructions, especially when communication via the intercom was challenging. It was also important to involve the participant's family as much as possible, ensuring they felt comfortable with their relative's participation, particularly during more invasive procedures such as the lumbar puncture.

Future clinical studies should consider the burden placed on participant's during visits, as there were instances when participants could not complete all tasks. Specifically, while most participants were able to complete the resting-state scans (5 minutes), many could not finish the VAB task (15 minutes), as it was fast-paced and challenging. This consideration was also important when scheduling participants, as those who struggled more were given the opportunity to attend multiple shorter sessions, providing them with a more manageable, enjoyable experience. Overall, building strong relationships with participants and their families, while providing a consistent and familiar research team, not only helped with recruitment and data quality, but also made the experience more positive for everyone involved.

Table 7.1. Results of a separate multiple linear regression models for neuropathology measures and cognitive scores (predictors) with MRI and MEG metrics.

Aβ/tau ratio			
	t	**β**	***p***
Hippocampal volume (%)	0.718	-0.106	0.476
Frequency Cluster 1 (eyes-open)	2.104	0.285	**0.041**
Frequency Cluster 2 (eyes-open)	1.182	-0.160	0.244
Frequency Cluster 1 (eyes-closed)	0.287	0.036	0.775
Alpha peak frequency (eyes-open)	2.846	-0.510	**0.007**
Alpha peak frequency (eyes-closed)	1.047	0.172	0.301
MMSE			
	t	**β**	***p***
Hippocampal volume (%)	4.860	0.451	**< .001**
Frequency Cluster 1 (eyes-open)	1.772	-0.142	0.080
Frequency Cluster 2 (eyes-open)	1.936	0.181	0.056
Frequency Cluster 1 (eyes-closed)	0.669	-0.055	0.505
Alpha peak frequency (eyes-open)	1.772	0.185	0.080
Alpha peak frequency (eyes-closed)	0.924	-0.088	0.358
Four Mountains			
	t	**β**	***p***
Hippocampal volume (%)	3.125	0.333	**0.003**
Frequency Cluster 1 (eyes-open)	2.842	-0.287	0.006
Frequency Cluster 2 (eyes-open)	0.715	0.078	0.477
Frequency Cluster 1 (eyes-closed)	0.879	0.088	0.382
Alpha peak frequency (eyes-open)	2.312	0.276	**0.024**
Alpha peak frequency (eyes-closed)	1.074	-0.120	0.286
ACE Memory			
	t	**β**	***p***
Hippocampal volume (%)	5.521	0.501	**< .001**
Frequency Cluster 1 (eyes-open)	1.740	-0.144	0.085
Frequency Cluster 2 (eyes-open)	1.637	0.151	0.105
Frequency Cluster 1 (eyes-closed)	0.745	-0.061	0.458
Alpha peak frequency (eyes-open)	1.518	0.158	0.133
Alpha peak frequency (eyes-closed)	1.048	-0.102	0.298

7.7 Limitations

Limitations specific to each analysis were discussed in the relevant chapters. However, there are broader limitations surrounding both the use of MEG and the NTAD study that should be considered. Firstly, there are a few limitations to the NTAD study itself. For example, although significant effort to recruit as many participants as possible, this proved challenging due to the stringent inclusion criteria. As a result, the overall cohort size is slightly limited by its size, and ideally more participants would be included in the overall analysis and especially within the test re-test analysis. In addition, there was an age mismatch between controls and patients, as the patients were considerably older than the healthy controls. Another limitation is the lack of amyloid and tau measurements at the annual follow-up visit limited the ability to fully quantify changes in participant's clinical status beyond neuropsychological testing; such biomarker data would have provided valuable comparisons alongside the annual MEG and MRI scans. There was also missing neuropathology data at baseline, as tau quantification was not completed for all participants. Future studies should aim to perform consistent biomarker assessments across the entire cohort. Finally, a one-year interval between visits may not be sufficient to detect meaningful cognitive deterioration. Extending the follow-up period or including a two-year visit could have provided more sensitive measures of change.

Secondly, the results from this thesis should also be compared with other neurodegenerative diseases, such as non-biomarker positive MCI patients and other dementias. Non-biomarker positive MCI patients present with similar cognitive symptoms as early-stage AD but lack the characteristic amyloid or tau biomarkers. The clinical overlap between AD and non-biomarker positive MCI could mean that MEG data could be useful in distinguishing between the two conditions, but only if it demonstrates clear differences in neuronal activity. Including this comparison would help assess not only the sensitivity but also the specificity of MEG as a potential biomarker. Similarly, the inclusion of other dementias would help determine if MEG can differentiate between patients that may present with overlapping clinical symptoms. This work is currently ongoing, as other studies have included these additional participant profiles, For instance, the DFP study includes non-biomarker positive MCI patients , enabling direct comparisons with NTAD data, since the scanning protocols were deliberately designed to be closely aligned. Additionally, the follow-up study to NTAD, entitled Synaptic Health in Neurodegeneration (SHINE), includes participants with multiple diagnoses, such as Lewy body dementia and frontotemporal dementia. Future research should also include longitudinal follow-up of healthy controls, as this would allow a more direct comparison with patient

trajectories over time. These expanded analyses will be very informative in shaping the potential clinical application of MEG.

Finally, while MEG shows promise as a sensitive tool for detecting synaptic changes in AD, its use in clinical settings is constrained by the complexity of both data acquisition and analysis. The requirement for specialised, expensive equipment and technical expertise means that, at present, MEG remains primarily a research tool. Its proposed role as a biomarker for AD is therefore most applicable to academic studies, experimental medicine trials, and early-stage therapeutic research. Nonetheless, the potential remains for MEG to be integrated into clinical practice and personalised medicine in the future, provided that protocols become more standardised and accessible. A limitation of this thesis is that although the NTAD study included simultaneous MEEG recordings, the EEG results were not analysed. Future research should aim to directly compare MEG and EEG results to evaluate whether the biomarkers identified here can also be detected using EEG. If these findings generalise to EEG, incorporating such biomarkers into clinical practice would become a much more feasible goal. Additional analyses on the MEG data could also include the 1/f slope for AD diagnosis. This was removed in order to investigate the alpha peak, but as the 1/f slope reflects the balance of excitatory and inhibitory neural activity and has been linked to AD (Martínez-Cañada et al., 2023), including it in further analyses could provide complementary insights into how MEG is related to early disease-related changes.

7.8 Conclusion

In summary, this thesis has provided novel insights into synaptic health in AD and its relationship to cognition and neuropathology. The findings support the potential of MEG as a sensitive tool for detecting synaptic dysfunction, with alpha peak frequency emerging as a promising marker, due to its strong test-retest reliability and associations with key pathological markers including amyloid and tau. Exploratory analysis of the Four Mountains test revealed links with neuropathology, suggesting it may offer greater clinical utility than some standard cognitive assessments. Comparisons with structural and functional MRI demonstrated that MEG provides unique information rather than duplication existing modalities, capturing real-time neural oscillatory activity across multiple frequency bands and offering a richer, more dynamic view of brain function. Together, these results highlight MEG's potential as both a research tool and future clinical instrument for early diagnosis and evaluating therapeutic interventions.

References

Abe, Y., Aoyagi, A., Hara, T., Abe, K., Yamazaki, R., Kumagae, Y., Naruto, S., Koyama, K., Marumoto, S., & Tago, K. (2003). Pharmacological characterization of RS-1259, an orally active dual inhibitor of acetylcholinesterase and serotonin transporter, in rodents: Possible treatment of Alzheimer's disease. *Journal of Pharmacological Sciences*, *93*(4), 95–105.

Adjamian, P., Holliday, I. E., Barnes, G. R., Hillebrand, A., Hadjipapas, A., & Singh, K. D. (2004). Induced visual illusions and gamma oscillations in human primary visual cortex. *European Journal of Neuroscience*, *20*(2), 587–592.

Adrian, E. D., & Matthews, B. H. (1934). The Berger rhythm: Potential changes from the occipital lobes in man. *Brain*, *57*(4), 355–385.

Agosta, F., Rocca, M. A., Pagani, E., Absinta, M., Magnani, G., Marcone, A., Falautano, M., Comi, G., Gorno-Tempini, M. L., & Filippi, M. (2010). Sensorimotor network rewiring in mild cognitive impairment and Alzheimer's disease. *Human Brain Mapping*, *31*(4), 515–525.

Alzheimer's Association. (2019). 2019 Alzheimer's disease facts and figures. *Alzheimer's & Dementia*, *15*(3), 321–387.

Amenta, F., Parnetti, L., Gallai, V., & Wallin, A. (2001). Treatment of cognitive dysfunction associated with Alzheimer's disease with cholinergic precursors. Ineffective treatments or inappropriate approaches? *Mechanisms of Ageing and Development*, *122*(16), 2025–2040.

Andersson, J. L., Skare, S., & Ashburner, J. (2003). How to correct susceptibility distortions in spin-echo echo-planar images: Application to diffusion tensor imaging. *Neuroimage*, *20*(2), 870–888.

Andreasen, N., Sjögren, M., & Blennow, K. (2003). CSF markers for Alzheimer's disease: Total tau, phospho-tau and Aβ42. *The World Journal of Biological Psychiatry*, *4*(4), 147–155. https://doi.org/10.1080/15622970310029912

Apostolova, L. G., Green, A. E., Babakchanian, S., Hwang, K. S., Chou, Y.-Y., Toga, A. W., & Thompson, P. M. (2012). Hippocampal atrophy and ventricular enlargement in normal aging, mild cognitive impairment and Alzheimer's disease. *Alzheimer Disease and Associated Disorders*, *26*(1), 17.

Aramadaka, S., Mannam, R., Narayanan, R. S., Bansal, A., Yanamaladoddi, V. R., Sarvepalli, S. S., & Vemula, S. L. (2023). Neuroimaging in Alzheimer's disease for early diagnosis: A comprehensive review. *Cureus*, *15*(5).

Ashton, N. J., Brum, W. S., Di Molfetta, G., Benedet, A. L., Arslan, B., Jonaitis, E., Langhough, R. E., Cody, K., Wilson, R., & Carlsson, C. M. (2024). Diagnostic accuracy of a plasma phosphorylated tau 217 immunoassay for Alzheimer disease pathology. *JAMA Neurology*, *81*(3), 255–263.

Babiloni, C., Binetti, G., Cassarino, A., Dal Forno, G., Del Percio, C., Ferreri, F., Ferri, R., Frisoni, G., Galderisi, S., & Hirata, K. (2006). Sources of cortical rhythms in adults during physiological aging: A multicentric EEG study. *Human Brain Mapping*, *27*(2), 162–172.

Babiloni, C., Cassetta, E., Dal Forno, G., Del Percio, C., Ferreri, F., Ferri, R., Lanuzza, B., Miniussi, C., Moretti, D. V., & Nobili, F. (2006). Donepezil effects on sources of cortical rhythms in mild Alzheimer's disease: Responders vs. Non-Responders. *Neuroimage*, *31*(4), 1650–1665.

Babiloni, C., Del Percio, C., Boccardi, M., Lizio, R., Lopez, S., Carducci, F., Marzano, N., Soricelli, A., Ferri, R., & Triggiani, A. I. (2015). Occipital sources of resting-state alpha rhythms are related to local gray matter density in subjects with amnesic mild

cognitive impairment and Alzheimer's disease. *Neurobiology of Aging*, *36*(2), 556–570.

Babiloni, C., Frisoni, G. B., Pievani, M., Vecchio, F., Lizio, R., Buttiglione, M., Geroldi, C., Fracassi, C., Eusebi, F., Ferri, R., & Rossini, P. M. (2009). Hippocampal volume and cortical sources of EEG alpha rhythms in mild cognitive impairment and Alzheimer disease. *Neuroimage*, *44*(1), 123–135. https://doi.org/10.1016/j.neuroimage.2008.08.005

Babiloni, C., Lizio, R., Vecchio, F., Frisoni, G. B., Pievani, M., Geroldi, C., Claudia, F., Ferri, R., Lanuzza, B., & Rossini, P. M. (2010). Reactivity of cortical alpha rhythms to eye opening in mild cognitive impairment and Alzheimer's disease: An EEG study. *Journal of Alzheimer's Disease*, *22*(4), 1047–1064.

Baldeiras, I., Santana, I., Leitão, M. J., Gens, H., Pascoal, R., Tábuas-Pereira, M., Beato-Coelho, J., Duro, D., Almeida, M. R., & Oliveira, C. R. (2018). Addition of the Aβ42/40 ratio to the cerebrospinal fluid biomarker profile increases the predictive value for underlying Alzheimer's disease dementia in mild cognitive impairment. *Alzheimer's Research & Therapy*, *10*(1), 33. https://doi.org/10.1186/s13195-018-0362-2

Barage, S. H., & Sonawane, K. D. (2015). Amyloid cascade hypothesis: Pathogenesis and therapeutic strategies in Alzheimer's disease. *Neuropeptides*, *52*, 1–18.

Barnes, J., Bartlett, J. W., van de Pol, L. A., Loy, C. T., Scahill, R. I., Frost, C., Thompson, P., & Fox, N. C. (2009). A meta-analysis of hippocampal atrophy rates in Alzheimer's disease. *Neurobiology of Aging*, *30*(11), 1711–1723.

Barry, R. J., Clarke, A. R., Johnstone, S. J., Magee, C. A., & Rushby, J. A. (2007). EEG differences between eyes-closed and eyes-open resting conditions. *Clinical Neurophysiology*, *118*(12), 2765–2773.

Bartus, R. T., Dean III, R. L., Beer, B., & Lippa, A. S. (1982). The cholinergic hypothesis of geriatric memory dysfunction. *Science*, *217*(4558), 408–414.

Beckmann, C. F., DeLuca, M., Devlin, J. T., & Smith, S. M. (2005). Investigations into resting-state connectivity using independent component analysis. *Philosophical Transactions of the Royal Society B: Biological Sciences*, *360*(1457), 1001–1013.

Berger, H. (1929). Über das elektroenkephalogramm des menschen. *Archiv Für Psychiatrie Und Nervenkrankheiten*, *87*(1), 527–570.

Binnewijzend, M. A., Schoonheim, M. M., Sanz-Arigita, E., Wink, A. M., van der Flier, W. M., Tolboom, N., Adriaanse, S. M., Damoiseaux, J. S., Scheltens, P., & van Berckel, B. N. (2012). Resting-state fMRI changes in Alzheimer's disease and mild cognitive impairment. *Neurobiology of Aging*, *33*(9), 2018–2028.

Birks, J. S., & Harvey, R. J. (2018). Donepezil for dementia due to Alzheimer's disease. *Cochrane Database of Systematic Reviews*, *6*.

Blennow, K., Vanmechelen, E., & Hampel, H. (2001). CSF Total tau, Aβ42 and Phosphorylated tau Protein as Biomarkers for Alzheimer's Disease. *Molecular Neurobiology*, *24*(1–3), 087–098. https://doi.org/10.1385/MN:24:1-3:087

Blennow, K., & Zetterberg, H. (2018). Biomarkers for Alzheimer's disease: Current status and prospects for the future. *Journal of Internal Medicine*, *284*(6), 643–663. https://doi.org/10.1111/joim.12816

Bloom, G. S. (2014). Amyloid-β and tau: The trigger and bullet in Alzheimer disease pathogenesis. *JAMA Neurology*, *71*(4), 505–508.

Bobinski, M., De Leon, M., Wegiel, J., Desanti, S., Convit, A., Saint Louis, L., Rusinek, H., & Wisniewski, H. (1999). The histological validation of post mortem magnetic resonance imaging-determined hippocampal volume in Alzheimer's disease. *Neuroscience*, *95*(3), 721–725.

Boinpally, R., Chen, L., Zukin, S. R., McClure, N., Hofbauer, R. K., & Periclou, A. (2015). A novel once-daily fixed-dose combination of memantine extended release and donepezil for the treatment of moderate to severe Alzheimer's disease: Two phase I studies in healthy volunteers. *Clinical Drug Investigation*, *35*, 427–435.

Borson, S., Scanlan, J. M., Watanabe, J., Tu, S., & Lessig, M. (2005). Simplifying detection of cognitive impairment: Comparison of the Mini-Cog and Mini-Mental State Examination in a multiethnic sample. *Journal of the American Geriatrics Society*, *53*(5), 871–874.

Boxer, A. L., Qureshi, I., Ahlijanian, M., Grundman, M., Golbe, L. I., Litvan, I., Honig, L. S., Tuite, P., McFarland, N. R., & O'Suilleabhain, P. (2019). Safety of the tau-directed monoclonal antibody BIIB092 in progressive supranuclear palsy: A randomised, placebo-controlled, multiple ascending dose phase 1b trial. *The Lancet Neurology*, *18*(6), 549–558.

Braak, H., & Braak, E. (1991). Neuropathological stageing of Alzheimer-related changes. *Acta Neuropathologica*, *82*(4), 239–259.

Braak, H., & Del Tredici, K. (2014). *Neuroanatomy and pathology of sporadic Alzheimer's disease*.

Brookes, M. J., Leggett, J., Rea, M., Hill, R. M., Holmes, N., Boto, E., & Bowtell, R. (2022). Magnetoencephalography with optically pumped magnetometers (OPM-MEG): The next generation of functional neuroimaging. *Trends in Neurosciences*, *45*(8), 621–634.

Bruns, A., Eckhorn, R., Jokeit, H., & Ebner, A. (2000). Amplitude envelope correlation detects coupling among incoherent brain signals. *Neuroreport*, *11*(7), 1509–1514.

Buchman, A. S., Wilson, R. S., Boyle, P. A., Bienias, J. L., & Bennett, D. A. (2007). Grip strength and the risk of incident Alzheimer's disease. *Neuroepidemiology*, *29*(1–2), 66–73.

Buckner, R. L., Andrews-Hanna, J. R., & Schacter, D. L. (2008). The brain's default network: Anatomy, function, and relevance to disease. *Annals of the New York Academy of Sciences*, *1124*(1), 1–38.

Buckner, R. L., Sepulcre, J., Talukdar, T., Krienen, F. M., Liu, H., Hedden, T., Andrews-Hanna, J. R., Sperling, R. A., & Johnson, K. A. (2009). Cortical hubs revealed by intrinsic functional connectivity: Mapping, assessment of stability, and relation to Alzheimer's disease. *Journal of Neuroscience*, *29*(6), 1860–1873.

Buckner, R. L., Snyder, A. Z., Shannon, B. J., LaRossa, G., Sachs, R., Fotenos, A. F., Sheline, Y. I., Klunk, W. E., Mathis, C. A., & Morris, J. C. (2005). Molecular, structural, and functional characterization of Alzheimer's disease: Evidence for a relationship between default activity, amyloid, and memory. *Journal of Neuroscience*, *25*(34), 7709–7717.

Buschke, H. (1984). Cued recall in amnesia. *Journal of Clinical and Experimental Neuropsychology*, *6*(4), 433–440.

Canuet, L., Pusil, S., Lopez, M. E., Bajo, R., Pineda-Pardo, J. A., Cuesta, P., Galvez, G., Gaztelu, J. M., Lourido, D., Garcia-Ribas, G., & Maestu, F. (2015). Network Disruption and Cerebrospinal Fluid Amyloid-Beta and Phospho-Tau Levels in Mild Cognitive Impairment. *Journal of Neuroscience*, *35*(28), 10325–10330. https://doi.org/10.1523/JNEUROSCI.0704-15.2015

Chan, D., Gallaher, L. M., Moodley, K., Minati, L., Burgess, N., & Hartley, T. (2016). The 4 Mountains Test: A Short Test of Spatial Memory with High Sensitivity for the

Diagnosis of Pre-dementia Alzheimer's Disease. *Journal of Visualized Experiments*, *116*, 54454. https://doi.org/10.3791/54454

Chan, D., Janssen, J. C., Whitwell, J. L., Watt, H. C., Jenkins, R., Frost, C., Rossor, M. N., & Fox, N. C. (2003). Change in rates of cerebral atrophy over time in early-onset Alzheimer's disease: Longitudinal MRI study. *The Lancet*, *362*(9390), 1121–1122.

Chapleau, M., Iaccarino, L., Soleimani-Meigooni, D., & Rabinovici, G. D. (2022). The Role of Amyloid PET in Imaging Neurodegenerative Disorders: A Review. *Journal of Nuclear Medicine*, *63*(Supplement 1), 13S-19S. https://doi.org/10.2967/jnumed.121.263195

Cohen, D. (1968). Magnetoencephalography: Evidence of magnetic fields produced by alpha-rhythm currents. *Science*, *161*(3843), 784–786.

Cole, M. W., Ito, T., Cocuzza, C., & Sanchez-Romero, R. (2021). The functional relevance of task-state functional connectivity. *Journal of Neuroscience*, *41*(12), 2684–2702.

Colombo, G., Minta, K., Grübel, J., Tai, W. L. E., Hölscher, C., & Schinazi, V. R. (2024). Detecting cognitive impairment through an age-friendly serious game: The development and usability of the spatial performance assessment for cognitive evaluation (SPACE). *Computers in Human Behavior*, *160*, 108349.

Corder, E. H., Saunders, A. M., Strittmatter, W. J., Schmechel, D. E., Gaskell, P. C., Small, Gw., Roses, A., Haines, J., & Pericak-Vance, M. A. (1993). Gene dose of apolipoprotein E type 4 allele and the risk of Alzheimer's disease in late onset families. *Science*, *261*(5123), 921–923.

Cosentino, S. A., Stern, Y., Sokolov, E., Scarmeas, N., Manly, J. J., Tang, M. X., Schupf, N., & Mayeux, R. P. (2010). Plasma β-amyloid and cognitive decline. *Archives of Neurology*, *67*(12), 1485–1490.

Coughlan, G., DeSouza, B., Zhukovsky, P., Hornberger, M., Grady, C., & Buckley, R. F. (2023). Spatial cognition is associated with levels of phosphorylated-tau and β-amyloid in clinically normal older adults. *Neurobiology of Aging*, *130*, 124–134.

Coutrot, A., Schmidt, S., Pittman, J., Hong, L., Wiener, J., Hölscher, C., Dalton, R., Hornberger, M., & Spiers, H. (2018). Virtual navigation tested on a mobile app (Sea Hero Quest) is predictive of real-world navigation performance: Preliminary data. *BioRxiv*, 305433.

Cronin-Golomb, A., Corkin, S., Rizzo, J. F., Cohen, J., Growdon, J. H., & Banks, K. S. (1991). Visual dysfunction in Alzheimer's disease: Relation to normal aging. *Annals of Neurology: Official Journal of the American Neurological Association and the Child Neurology Society*, *29*(1), 41–52.

Daly, J., De Luca, F., Berens, S. C., Field, A. P., Rusted, J. M., & Bird, C. M. (2024). The effect of apolipoprotein E genotype on spatial processing in humans: A meta-analysis and systematic review. *Cortex*, *177*, 268–284.

Damoiseaux, J. S., Rombouts, S. A., Barkhof, F., Scheltens, P., Stam, C. J., Smith, S. M., & Beckmann, C. F. (2006). Consistent resting-state networks across healthy subjects. *Proceedings of the National Academy of Sciences*, *103*(37), 13848–13853.

de Flores, R., Das, S. R., Xie, L., Wisse, L. E., Lyu, X., Shah, P., Yushkevich, P. A., & Wolk, D. A. (2022). Medial temporal lobe networks in Alzheimer's disease: Structural and molecular vulnerabilities. *Journal of Neuroscience*, *42*(10), 2131–2141.

de Haan, W., Stam, C. J., Jones, B. F., Zuiderwijk, I. M., van Dijk, B. W., & Scheltens, P. (2008). Resting-state oscillatory brain dynamics in Alzheimer disease. *Journal of Clinical Neurophysiology*, *25*(4), 187–193.

de Jongh, A., de Munck, J. C., Gonçalves, S. I., & Ossenblok, P. (2005). Differences in MEG/EEG epileptic spike yields explained by regional differences in signal-to-noise ratios. *Journal of Clinical Neurophysiology*, *22*(2), 153–158.

de Paula, J. J., Albuquerque, M. R., Lage, G. M., Bicalho, M. A., Romano-Silva, M. A., & Malloy-Diniz, L. F. (2016). Impairment of fine motor dexterity in mild cognitive impairment and Alzheimer's disease dementia: Association with activities of daily living. *Revista Brasileira de Psiquiatria*, *38*(3), 235–238.

de Souza, L. C., Chupin, M., Lamari, F., Jardel, C., Leclercq, D., Colliot, O., Lehéricy, S., Dubois, B., & Sarazin, M. (2012). CSF tau markers are correlated with hippocampal volume in Alzheimer's disease. *Neurobiology of Aging*, *33*(7), 1253–1257.

Di, X., Gohel, S., Kim, E. H., & Biswal, B. B. (2013). Task vs. Rest—Different network configurations between the coactivation and the resting-state brain networks. *Frontiers in Human Neuroscience*, *7*, 493.

Dickson, D. W., Crystal, H. A., Mattiace, L. A., Masur, D. M., Blau, A. D., Davies, P., Yen, S.-H., & Aronson, M. K. (1992). Identification of normal and pathological aging in prospectively studied nondemented elderly humans. *Neurobiology of Aging*, *13*(1), 179–189.

Donix, M., Ercoli, L. M., Siddarth, P., Brown, J. A., Martin-Harris, L., Burggren, A. C., Miller, K. J., Small, G. W., & Bookheimer, S. Y. (2012). Influence of Alzheimer disease family history and genetic risk on cognitive performance in healthy middle-aged and older people. *The American Journal of Geriatric Psychiatry*, *20*(7), 565–573.

Donoghue, T., Haller, M., Peterson, E. J., Varma, P., Sebastian, P., Gao, R., Noto, T., Lara, A. H., Wallis, J. D., & Knight, R. T. (2020). Parameterizing neural power spectra into periodic and aperiodic components. *Nature Neuroscience*, *23*(12), 1655–1665.

Dronse, J., Fliessbach, K., Bischof, G. N., von Reutern, B., Faber, J., Hammes, J., Kuhnert, G., Neumaier, B., Onur, O. A., Kukolja, J., van Eimeren, T., Jessen, F., Fink, G. R., Klockgether, T., & Drzezga, A. (2017). In vivo Patterns of Tau Pathology, Amyloid-β Burden, and Neuronal Dysfunction in Clinical Variants of Alzheimer's Disease. *Journal of Alzheimer's Disease*, *55*(2), 465–471. https://doi.org/10.3233/JAD-160316

Dubois, B., Feldman, H. H., Jacova, C., DeKosky, S. T., Barberger-Gateau, P., Cummings, J., Delacourte, A., Galasko, D., Gauthier, S., & Jicha, G. (2007). Research criteria for the diagnosis of Alzheimer's disease: Revising the NINCDS–ADRDA criteria. *The Lancet Neurology*, *6*(8), 734–746.

Ekstrom, A., Suthana, N., Millett, D., Fried, I., & Bookheimer, S. (2009). Correlation between BOLD fMRI and theta-band local field potentials in the human hippocampal area. *Journal of Neurophysiology*, *101*(5), 2668–2678.

Engel, S. A., Rumelhart, D. E., Wandell, B. A., Lee, A. T., Glover, G. H., Chichilnisky, E.-J., & Shadlen, M. N. (1994). fMRI of human visual cortex. *Nature*, *369*(6481), 525–525.

Engels, M., Van der Flier, W., Stam, C., Hillebrand, A., Scheltens, P., & Van Straaten, E. (2017). Alzheimer's disease: The state of the art in resting-state magnetoencephalography. *Clinical Neurophysiology*, *128*(8), 1426–1437.

Eyler, L. T., Elman, J. A., Hatton, S. N., Gough, S., Mischel, A. K., Hagler, D. J., Franz, C. E., Docherty, A., Fennema-Notestine, C., & Gillespie, N. (2019). Resting state abnormalities of the default mode network in mild cognitive impairment: A systematic review and meta-analysis. *Journal of Alzheimer's Disease*, *70*(1), 107–120.

Ezzati, A., Katz, M. J., Zammit, A. R., Lipton, M. L., Zimmerman, M. E., Sliwinski, M. J., & Lipton, R. B. (2016). Differential association of left and right hippocampal volumes

with verbal episodic and spatial memory in older adults. *Neuropsychologia*, *93*, 380–385.

Fagan, A. M., Mintun, M. A., Mach, R. H., Lee, S., Dence, C. S., Shah, A. R., LaRossa, G. N., Spinner, M. L., Klunk, W. E., Mathis, C. A., DeKosky, S. T., Morris, J. C., & Holtzman, D. M. (2006). Inverse relation between in vivo amyloid imaging load and cerebrospinal fluid Aβ $_{42}$ in humans. *Annals of Neurology*, *59*(3), 512–519. https://doi.org/10.1002/ana.20730

Fagan, A. M., Roe, C. M., Xiong, C., Mintun, M. A., Morris, J. C., & Holtzman, D. M. (2007). Cerebrospinal fluid tau/β-amyloid42 ratio as a prediction of cognitive decline in nondemented older adults. *Archives of Neurology*, *64*(3), 343–349.

Farlow, M. R., Lilly, M. L., & ENA713 B352 Study Group mfarlow@ iupui. edu. (2005). Rivastigmine: An open-label, observational study of safety and effectiveness in treating patients with Alzheimer's disease for up to 5 years. *BMC Geriatrics*, *5*, 1–7.

Farlow, M. R., Miller, M. L., & Pejovic, V. (2008). Treatment Options in Alzheimer's Disease: Maximizing Benefit, Managing Expectations. *Dementia and Geriatric Cognitive Disorders*, *25*(5), 408–422. https://doi.org/10.1159/000122962

Farrer, L. A. (1997). Effects of Age, Sex, and Ethnicity on the Association Between Apolipoprotein E Genotype and Alzheimer Disease: A Meta-analysis. *JAMA*, *278*(16), 1349. https://doi.org/10.1001/jama.1997.03550160069041

Fernández, A., Maestú, F., Amo, C., Gil, P., Fehr, T., Wienbruch, C., Rockstroh, B., Elbert, T., & Ortiz, T. (2002). Focal temporoparietal slow activity in Alzheimer's disease revealed by magnetoencephalography. *Biological Psychiatry*, *52*(7), 764–770.

Filippini, N., MacIntosh, B. J., Hough, M. G., Goodwin, G. M., Frisoni, G. B., Smith, S. M., Matthews, P. M., Beckmann, C. F., & Mackay, C. E. (2009). Distinct patterns of brain

activity in young carriers of the APOE-ε4 allele. *Proceedings of the National Academy of Sciences*, *106*(17), 7209–7214.

Fisher, C., & Larner, A. (2007). Frequency and diagnostic utility of cognitive test instrument use by GPs prior to memory clinic referral. *Family Practice*, *24*(5), 495–497.

Folstein, M. F., Folstein, S. E., & McHugh, P. R. (1975). "Mini-mental state": A practical method for grading the cognitive state of patients for the clinician. *Journal of Psychiatric Research*, *12*(3), 189–198.

Fonseca, L. C., Tedrus, G. M., Fondello, M. A., Reis, I. N., & Fontoura, D. S. (2011). EEG theta and alpha reactivity on opening the eyes in the diagnosis of Alzheimer's disease. *Clinical EEG and Neuroscience*, *42*(3), 185–189.

Fox, M. D., Corbetta, M., Snyder, A. Z., Vincent, J. L., & Raichle, M. E. (2006). Spontaneous neuronal activity distinguishes human dorsal and ventral attention systems. *Proceedings of the National Academy of Sciences*, *103*(26), 10046–10051.

Franko, E., Joly, O., & Alzheimer's Disease Neuroimaging Initiative. (2013). Evaluating Alzheimer's disease progression using rate of regional hippocampal atrophy. *PloS One*, *8*(8), e71354.

Fransson, P. (2005). Spontaneous low-frequency BOLD signal fluctuations: An fMRI investigation of the resting-state default mode of brain function hypothesis. *Human Brain Mapping*, *26*(1), 15–29.

Frisoni, G. B., Fox, N. C., Jack, C. R., Scheltens, P., & Thompson, P. M. (2010). The clinical use of structural MRI in Alzheimer disease. *Nature Reviews Neurology*, *6*(2), 67–77.

Galvin, J. E., Meuser, T. M., Boise, L., & Connell, C. M. (2009). Predictors of physician referral for patient recruitment to Alzheimer disease clinical trials. *Alzheimer Disease and Associated Disorders*, *23*(4), 352.

Garcés, P., Pineda-Pardo, J. Á., Canuet, L., Aurtenetxe, S., López, M. E., Marcos, A., Yus, M., Llanero-Luque, M., Del-Pozo, F., & Sancho, M. (2014). The Default Mode Network is functionally and structurally disrupted in amnestic mild cognitive impairment—A bimodal MEG–DTI study. *NeuroImage: Clinical*, *6*, 214–221.

Garcés, P., Vicente, R., Wibral, M., Pineda Pardo, J. A., López, M. E., Aurtenetxe, S., Marcos, A., de Andrés, M. E., Yus, M., & Sancho, M. (2013). Brain-wide slowing of spontaneous alpha rhythms in mild cognitive impairment. *Frontiers in Aging Neuroscience*, *5*, 100.

Gasser, T., Bächer, P., & Möcks, J. (1982). Transformations towards the normal distribution of broad band spectral parameters of the EEG. *Electroencephalography and Clinical Neurophysiology*, *53*(1), 119–124.

Gevins, A., Smith, M. E., McEvoy, L., & Yu, D. (1997). High-resolution EEG mapping of cortical activation related to working memory: Effects of task difficulty, type of processing, and practice. *Cerebral Cortex (New York, NY: 1991)*, *7*(4), 374–385.

Glenner, G. G., & Wong, C. W. (1984). Alzheimer's disease: Initial report of the purification and characterization of a novel cerebrovascular amyloid protein. *Biochemical and Biophysical Research Communications*, *120*(3), 885–890.

Glover, G. H. (2011). Overview of functional magnetic resonance imaging. *Neurosurgery Clinics*, *22*(2), 133–139.

Gómez-Isla, T., Hollister, R., West, H., Mui, S., Growdon, J. H., Petersen, R. C., Parisi, J. E., & Hyman, B. T. (1997). Neuronal loss correlates with but exceeds neurofibrillary tangles in Alzheimer's disease. *Annals of Neurology: Official Journal of the American Neurological Association and the Child Neurology Society*, *41*(1), 17–24.

Gordon, B. A., Friedrichsen, K., Brier, M., Blazey, T., Su, Y., Christensen, J., Aldea, P., McConathy, J., Holtzman, D. M., & Cairns, N. J. (2016). The relationship between

cerebrospinal fluid markers of Alzheimer pathology and positron emission tomography tau imaging. *Brain*, *139*(8), 2249–2260.

Gordon, B. A., Zacks, J. M., Blazey, T., Benzinger, T. L., Morris, J. C., Fagan, A. M., Holtzman, D. M., & Balota, D. A. (2015). Task-evoked fMRI changes in attention networks are associated with preclinical Alzheimer's disease biomarkers. *Neurobiology of Aging*, *36*(5), 1771–1779.

Gramfort, A., Luessi, M., Larson, E., Engemann, D. A., Strohmeier, D., Brodbeck, C., Goj, R., Jas, M., Brooks, T., & Parkkonen, L. (2013). MEG and EEG data analysis with MNE-Python. *Frontiers in Neuroscience*, *7*, 70133.

Greicius, M. D., Srivastava, G., Reiss, A. L., & Menon, V. (2004). Default-mode network activity distinguishes Alzheimer's disease from healthy aging: Evidence from functional MRI. *Proceedings of the National Academy of Sciences*, *101*(13), 4637–4642.

Greig, S. L. (2015). Memantine ER/Donepezil: A Review in Alzheimer's Disease. *CNS Drugs*, *29*(11), 963–970. https://doi.org/10.1007/s40263-015-0287-2

Greve, D. N., & Fischl, B. (2009). Accurate and robust brain image alignment using boundary-based registration. *Neuroimage*, *48*(1), 63–72.

Grieder, M., Wang, D. J., Dierks, T., Wahlund, L.-O., & Jann, K. (2018). Default mode network complexity and cognitive decline in mild Alzheimer's disease. *Frontiers in Neuroscience*, *12*, 770.

Griffanti, L., Salimi-Khorshidi, G., Beckmann, C. F., Auerbach, E. J., Douaud, G., Sexton, C. E., Zsoldos, E., Ebmeier, K. P., Filippini, N., & Mackay, C. E. (2014). ICA-based artefact removal and accelerated fMRI acquisition for improved resting state network imaging. *Neuroimage*, *95*, 232–247.

Groot, C., Villeneuve, S., Smith, R., Hansson, O., & Ossenkoppele, R. (2022). Tau PET Imaging in Neurodegenerative Disorders. *Journal of Nuclear Medicine*, *63*(Supplement 1), 20S-26S. https://doi.org/10.2967/jnumed.121.263196

Gross, J., Baillet, S., Barnes, G. R., Henson, R. N., Hillebrand, A., Jensen, O., Jerbi, K., Litvak, V., Maess, B., & Oostenveld, R. (2013). Good practice for conducting and reporting MEG research. *Neuroimage*, *65*, 349–363.

Grossberg, G. T., Manes, F., Allegri, R. F., Gutiérrez-Robledo, L. M., Gloger, S., Xie, L., Jia, X. D., Pejović, V., Miller, M. L., & Perhach, J. L. (2013). The safety, tolerability, and efficacy of once-daily memantine (28 mg): A multinational, randomized, double-blind, placebo-controlled trial in patients with moderate-to-severe Alzheimer's disease taking cholinesterase inhibitors. *CNS Drugs*, *27*, 469–478.

Güntekin, B., Emek-Savaş, D. D., Kurt, P., Yener, G. G., & Başar, E. (2013). Beta oscillatory responses in healthy subjects and subjects with mild cognitive impairment. *NeuroImage: Clinical*, *3*, 39–46.

Guo, J., Wang, Z., Liu, R., Huang, Y., Zhang, N., & Zhang, R. (2020). Memantine, Donepezil, or Combination Therapy—What is the best therapy for Alzheimer's Disease? A Network Meta-Analysis. *Brain and Behavior*, *10*(11), e01831. https://doi.org/10.1002/brb3.1831

Haass, C., & Selkoe, D. J. (2007). Soluble protein oligomers in neurodegeneration: Lessons from the Alzheimer's amyloid β-peptide. *Nature Reviews Molecular Cell Biology*, *8*(2), 101–112. https://doi.org/10.1038/nrm2101

Hampel, H., & Teipel, S. J. (2004). Total and Phosphorylated Tau Proteins: Evaluation as Core Biomarker Candidates in Frontotemporal Dementia. *Dementia and Geriatric Cognitive Disorders*, *17*(4), 350–354. https://doi.org/10.1159/000077170

Han, S. D., Houston, W. S., Jak, A. J., Eyler, L. T., Nagel, B. J., Fleisher, A. S., Brown, G. G., Corey-Bloom, J., Salmon, D. P., & Thal, L. J. (2007). Verbal paired-associate learning by APOE genotype in non-demented older adults: fMRI evidence of a right hemispheric compensatory response. *Neurobiology of Aging*, *28*(2), 238–247.

Hansen, P., Kringelbach, M., & Salmelin, R. (2010). *MEG: An introduction to methods*. Oxford university press.

Hansson, O., Grothe, M. J., Strandberg, T. O., Ohlsson, T., Hägerström, D., Jögi, J., Smith, R., & Schöll, M. (2017). Tau pathology distribution in Alzheimer's disease corresponds differentially to cognition-relevant functional brain networks. *Frontiers in Neuroscience*, *11*, 167.

Hansson, O., Lehmann, S., Otto, M., Zetterberg, H., & Lewczuk, P. (2019). Advantages and disadvantages of the use of the CSF Amyloid β (Aβ) 42/40 ratio in the diagnosis of Alzheimer's Disease. *Alzheimer's Research & Therapy*, *11*(1), 34. https://doi.org/10.1186/s13195-019-0485-0

Hao, J., Li, K., Li, K., Zhang, D., Wang, W., Yang, Y., Yan, B., Shan, B., & Zhou, X. (2005). Visual attention deficits in Alzheimer's disease: An fMRI study. *Neuroscience Letters*, *385*(1), 18–23.

Hardy, J., & Allsop, D. (n.d.). *Amyloid deposition as the central event in the aetiology of Alzheimer's disease*.

Harris, C. R., Millman, K. J., Van Der Walt, S. J., Gommers, R., Virtanen, P., Cournapeau, D., Wieser, E., Taylor, J., Berg, S., & Smith, N. J. (2020). Array programming with NumPy. *Nature*, *585*(7825), 357–362.

Hartley, T., Bird, C. M., Chan, D., Cipolotti, L., Husain, M., Vargha-Khadem, F., & Burgess, N. (2007). The hippocampus is required for short-term topographical memory in humans. *Hippocampus*, *17*(1), 34–48.

Hedden, T., Van Dijk, K. R., Becker, J. A., Mehta, A., Sperling, R. A., Johnson, K. A., & Buckner, R. L. (2009). Disruption of functional connectivity in clinically normal older adults harboring amyloid burden. *Journal of Neuroscience*, *29*(40), 12686–12694.

Hedrich, T., Pellegrino, G., Kobayashi, E., Lina, J.-M., & Grova, C. (2017). Comparison of the spatial resolution of source imaging techniques in high-density EEG and MEG. *Neuroimage*, *157*, 531–544.

Henneman, W., Sluimer, J., Barnes, J., Van Der Flier, W., Sluimer, I., Fox, N., Scheltens, P., Vrenken, H., & Barkhof, F. (2009). Hippocampal atrophy rates in Alzheimer disease: Added value over whole brain volume measures. *Neurology*, *72*(11), 999–1007.

Hernandez, C. M., Gearhart, D. A., Parikh, V., Hohnadel, E. J., Davis, L. W., Middlemore, M. L., Warsi, S. P., Waller, J. L., & Terry, A. V. (2006). Comparison of galantamine and donepezil for effects on nerve growth factor, cholinergic markers, and memory performance in aged rats. *Journal of Pharmacology and Experimental Therapeutics*, *316*(2), 679–694.

Hesse, C., Rosengren, L., Andreasen, N., Davidsson, P., Vanderstichele, H., Vanmechelen, E., & Blennow, K. (2001). Transient increase in total tau but not phospho-tau in human cerebrospinal fluid after acute stroke. *Neuroscience Letters*, *297*(3), 187–190.

Hillebrand, A., Fazio, P., De Munck, J., & Van Dijk, B. (2013). Feasibility of clinical magnetoencephalography (MEG) functional mapping in the presence of dental artefacts. *Clinical Neurophysiology*, *124*(1), 107–113.

Hoenig, M. C., Bischof, G. N., Seemiller, J., Hammes, J., Kukolja, J., Onur, Ö. A., Jessen, F., Fliessbach, K., Neumaier, B., & Fink, G. R. (2018). Networks of tau distribution in Alzheimer's disease. *Brain*, *141*(2), 568–581.

Hoskin, J. L., Sabbagh, M. N., Al-Hasan, Y., & Decourt, B. (2019). Tau immunotherapies for Alzheimer's disease. *Expert Opinion on Investigational Drugs*, *28*(6), 545–554.

Hunter, J. D. (2007). Matplotlib: A 2D graphics environment. *Computing in Science & Engineering*, *9*(03), 90–95.

Ikonomovic, M. D., Mufson, E. J., Wuu, J., Cochran, E. J., Bennett, D. A., & DeKosky, S. T. (2003). Cholinergic plasticity in hippocampus of individuals with mild cognitive impairment: Correlation with Alzheimer's neuropathology. *Journal of Alzheimer's Disease*, *5*(1), 39–48.

Ingelsson, M., Fukumoto, H., Newell, K., Growdon, J., Hedley–Whyte, E., Frosch, M., Albert, M., Hyman, B., & Irizarry, M. (2004). Early Aβ accumulation and progressive synaptic loss, gliosis, and tangle formation in AD brain. *Neurology*, *62*(6), 925–931.

Ismail, Z., Rajji, T. K., & Shulman, K. I. (2010). Brief cognitive screening instruments: An update. *International Journal of Geriatric Psychiatry: A Journal of the Psychiatry of Late Life and Allied Sciences*, *25*(2), 111–120.

Jack, C. R., Petersen, R. C., Xu, Y., O'Brien, P. C., Smith, G. E., Ivnik, R. J., Tangalos, E. G., & Kokmen, E. (1998). Rate of medial temporal lobe atrophy in typical aging and Alzheimer's disease. *Neurology*, *51*(4), 993. https://doi.org/10.1212/WNL.51.4.993

Jack Jr, C. R., Andrews, J. S., Beach, T. G., Buracchio, T., Dunn, B., Graf, A., Hansson, O., Ho, C., Jagust, W., & McDade, E. (2024). Revised criteria for diagnosis and staging of Alzheimer's disease: Alzheimer's Association Workgroup. *Alzheimer's & Dementia*, *20*(8), 5143–5169.

Jack Jr, C. R., Barkhof, F., Bernstein, M. A., Cantillon, M., Cole, P. E., DeCarli, C., Dubois, B., Duchesne, S., Fox, N. C., & Frisoni, G. B. (2011). Steps to standardization and validation of hippocampal volumetry as a biomarker in clinical trials and diagnostic criterion for Alzheimer's disease. *Alzheimer's & Dementia*, *7*(4), 474–485.

Jack Jr, C. R., Lowe, V. J., Senjem, M. L., Weigand, S. D., Kemp, B. J., Shiung, M. M., Knopman, D. S., Boeve, B. F., Klunk, W. E., & Mathis, C. A. (2008). 11C PiB and

structural MRI provide complementary information in imaging of Alzheimer's disease and amnestic mild cognitive impairment. *Brain*, *131*(3), 665–680.

Jacobson, S. A., & Sabbagh, M. N. (2008). Donepezil: Potential neuroprotective and disease-modifying effects. *Expert Opinion on Drug Metabolism & Toxicology*, *4*(10), 1363–1369.

Janelidze, S., Mattsson, N., Palmqvist, S., Smith, R., Beach, T. G., Serrano, G. E., Chai, X., Proctor, N. K., Eichenlaub, U., & Zetterberg, H. (2020). Plasma P-tau181 in Alzheimer's disease: Relationship to other biomarkers, differential diagnosis, neuropathology and longitudinal progression to Alzheimer's dementia. *Nature Medicine*, *26*(3), 379–386.

Jann, K., Cen, S., Santos, M., Aksman, L., Wijesinghe, D., Zhang, R., Lynch, K., Ringman, J. M., Wang, D. J., & Alzheimer's Disease Neuroimaging Initiative. (2024). Effect of genetic risk on the relationship between rs-fMRI complexity and tau and amyloid PET in Alzheimer's disease. *Journal of Alzheimer's Disease*, *101*(2), 429–435.

Jarvis, B., & Figgitt, D. P. (2003). Memantine. *Drugs & Aging*, *20*, 465–476.

Jenkinson, M., Bannister, P., Brady, M., & Smith, S. (2002). Improved optimization for the robust and accurate linear registration and motion correction of brain images. *Neuroimage*, *17*(2), 825–841.

Jenkinson, M., & Smith, S. (2001). A global optimisation method for robust affine registration of brain images. *Medical Image Analysis*, *5*(2), 143–156.

Jezzard, P., & Clare, S. (2001). Principles of nuclear magnetic resonance and MRI. *Functional MRI: An Introduction to Methods*, *3*, 67–92.

Jiang, D., Yang, X., Li, M., Wang, Y., & Wang, Y. (2015). Efficacy and safety of galantamine treatment for patients with Alzheimer's disease: A meta-analysis of randomized controlled trials. *Journal of Neural Transmission*, *122*, 1157–1166.

Jin, S.-H., Seol, J., Kim, J. S., & Chung, C. K. (2011). How reliable are the functional connectivity networks of MEG in resting states? *Journal of Neurophysiology*, *106*(6), 2888–2895.

Jones, D., Machulda, M., Vemuri, P., McDade, E., Zeng, G., Senjem, M., Gunter, J., Przybelski, S., Avula, R., & Knopman, D. (2011). Age-related changes in the default mode network are more advanced in Alzheimer disease. *Neurology*, *77*(16), 1524–1531.

Kivisäkk, P., Carlyle, B. C., Sweeney, T., Trombetta, B. A., LaCasse, K., El-Mufti, L., Tuncali, I., Chibnik, L. B., Das, S., & Scherzer, C. R. (2023). Plasma biomarkers for diagnosis of Alzheimer's disease and prediction of cognitive decline in individuals with mild cognitive impairment. *Frontiers in Neurology*, *14*, 1069411.

Klimesch, W. (1999). EEG alpha and theta oscillations reflect cognitive and memory performance: A review and analysis. *Brain Research Reviews*, *29*(2–3), 169–195.

Klimesch, W., Doppelmayr, M., Russegger, H., Pachinger, T., & Schwaiger, J. (1998). Induced alpha band power changes in the human EEG and attention. *Neuroscience Letters*, *244*(2), 73–76.

Knopman, D. S., & Hershey, L. (2023). Implications of the Approval of Lecanemab for Alzheimer Disease Patient Care. *Neurology*, *101*(14), 610–620.

Knopman, D. S., Jones, D. T., & Greicius, M. D. (2021). Failure to demonstrate efficacy of aducanumab: An analysis of the EMERGE and ENGAGE trials as reported by Biogen, December 2019. *Alzheimer's & Dementia*, *17*(4), 696–701.

Koelewijn, L., Bompas, A., Tales, A., Brookes, M. J., Muthukumaraswamy, S. D., Bayer, A., & Singh, K. D. (2017). Alzheimer's disease disrupts alpha and beta-band resting-state oscillatory network connectivity. *Clinical Neurophysiology*, *128*(11), 2347–2357.

Kolanko, M. A., Win, Z., Loreto, F., Patel, N., Carswell, C., Gontsarova, A., Perry, R. J., & Malhotra, P. A. (2020). Amyloid PET imaging in clinical practice. *Practical Neurology*, *20*(6), 451–462. https://doi.org/10.1136/practneurol-2019-002468

Korf, E. S. C., Wahlund, L.-O., Visser, P. J., & Scheltens, P. (2004). Medial temporal lobe atrophy on MRI predicts dementia in patients with mild cognitive impairment. *Neurology*, *63*(1), 94. https://doi.org/10.1212/01.WNL.0000133114.92694.93

Kramberger, M. G., Kåreholt, I., Andersson, T., Winblad, B., Eriksdotter, M., & Jelic, V. (2013). Association between EEG abnormalities and CSF biomarkers in a memory clinic cohort. *Dementia and Geriatric Cognitive Disorders*, *36*(5–6), 319–328.

Kurimoto, R., Ishii, R., Canuet, L., Ikezawa, K., Iwase, M., Azechi, M., Aoki, Y., Ikeda, S., Yoshida, T., Takahashi, H., Nakahachi, T., Kazui, H., & Takeda, M. (2012). Induced oscillatory responses during the Sternberg's visual memory task in patients with Alzheimer's disease and mild cognitive impairment. *NeuroImage*, *59*(4), 4132–4140. https://doi.org/10.1016/j.neuroimage.2011.10.061

La Joie, R., Visani, A. V., Lesman-Segev, O. H., Baker, S. L., Edwards, L., Iaccarino, L., Soleimani-Meigooni, D. N., Mellinger, T., Janabi, M., & Miller, Z. A. (2021). Association of APOE4 and clinical variability in Alzheimer disease with the pattern of tau-and amyloid-PET. *Neurology*, *96*(5), e650–e661.

Landau, S. M., Horng, A., Fero, A., Jagust, W. J., Alzheimer's Disease Neuroimaging Initiative, Alzheimer's Disease Neuroimaging Initiative, Weiner, M., Aisen, P., Weiner, M., & Aisen, P. (2016). Amyloid negativity in patients with clinically diagnosed Alzheimer disease and MCI. *Neurology*, *86*(15), 1377–1385.

Lansdall, C. J. (2014). An effective treatment for Alzheimer's disease must consider both amyloid and tau. *Bioscience Horizons*, *7*, hzu002.

Lansdall, C. J., McDougall, F., Butler, L., Delmar, P., Pross, N., Qin, S., McLeod, L., Zhou, X., Kerchner, G., & Doody, R. (2023). Establishing clinically meaningful change on outcome assessments frequently used in trials of mild cognitive impairment due to Alzheimer's disease. *The Journal of Prevention of Alzheimer's Disease*, *10*(1), 9–18.

Lanskey, J. H., Kocagoncu, E., Quinn, A. J., Cheng, Y.-J., Karadag, M., Pitt, J., Lowe, S., Perkinton, M., Raymont, V., & Singh, K. D. (2022). New Therapeutics in Alzheimer's Disease longitudinal cohort study (NTAD): Study protocol. *BMJ Open*, *12*(12), e055135.

Leuzy, A., Mattsson-Carlgren, N., Palmqvist, S., Janelidze, S., Dage, J. L., & Hansson, O. (2022). Blood-based biomarkers for Alzheimer's disease. *EMBO Molecular Medicine*, *14*(1), e14408. https://doi.org/10.15252/emmm.202114408

Lew, B. J., Fitzgerald, E. E., Ott, L. R., Penhale, S. H., & Wilson, T. W. (2021). Three-year reliability of MEG resting-state oscillatory power. *NeuroImage*, *243*, 118516.

Lewczuk, P., Esselmann, H., Otto, M., Maler, J. M., Henkel, A. W., Henkel, M. K., Eikenberg, O., Antz, C., Krause, W.-R., Reulbach, U., Kornhuber, J., & Wiltfang, J. (2004). Neurochemical diagnosis of Alzheimer's dementia by CSF Aβ42, Aβ42/Aβ40 ratio and total tau. *Neurobiology of Aging*, *25*(3), 273–281. https://doi.org/10.1016/S0197-4580(03)00086-1

Li, R., Wu, X., Fleisher, A. S., Reiman, E. M., Chen, K., & Yao, L. (2012). Attention-related networks in Alzheimer's disease: A resting functional MRI study. *Human Brain Mapping*, *33*(5), 1076–1088.

Lim, Y. Y., Mormino, E. C., Alzheimer's Disease Neuroimaging Initiative, & Alzheimer's Disease Neuroimaging Initiative. (2017). APOE genotype and early β-amyloid accumulation in older adults without dementia. *Neurology*, *89*(10), 1028–1034.

Logothetis, N. K. (2008). What we can do and what we cannot do with fMRI. *Nature*, *453*(7197), 869–878.

Logothetis, N. K., Pauls, J., Augath, M., Trinath, T., & Oeltermann, A. (2001). Neurophysiological investigation of the basis of the fMRI signal. *Nature*, *412*(6843), 150–157.

Long, J. M., & Holtzman, D. M. (2019). Alzheimer Disease: An Update on Pathobiology and Treatment Strategies. *Cell*, *179*(2), 312–339. https://doi.org/10.1016/j.cell.2019.09.001

López, M. E., Bruna, R., Aurtenetxe, S., Pineda-Pardo, J. Á., Marcos, A., Arrazola, J., Reinoso, A. I., Montejo, P., Bajo, R., & Maestú, F. (2014). Alpha-band hypersynchronization in progressive mild cognitive impairment: A magnetoencephalography study. *Journal of Neuroscience*, *34*(44), 14551–14559.

Lu, C. Y., Terry, V., & Thomas, D. M. (2023). Precision medicine: Affording the successes of science. *NPJ Precision Oncology*, *7*(1), 3.

Maestu, F., Arrazola, J., Fernandez, A., Simos, P., Amo, C., Gil-Gregorio, P., Fernandez, S., Papanicolaou, A., & Ortiz, T. (2003). Do cognitive patterns of brain magnetic activity correlate with hippocampal atrophy in Alzheimer's disease? *Journal of Neurology, Neurosurgery, and Psychiatry*, *74*(2), 208.

Maestú, F., Cuesta, P., Hasan, O., Fernandéz, A., Funke, M., & Schulz, P. E. (2019). The importance of the validation of M/EEG with current biomarkers in Alzheimer's disease. *Frontiers in Human Neuroscience*, *13*, 17.

Mahley, R. W. (1988). Apolipoprotein E: cholesterol transport protein with expanding role in cell biology. *Science*, *240*(4852), 622–630.

Martínez-Cañada, P., Perez-Valero, E., Minguillon, J., Pelayo, F., López-Gordo, M. A., & Morillas, C. (2023). Combining aperiodic 1/f slopes and brain simulation: An

EEG/MEG proxy marker of excitation/inhibition imbalance in Alzheimer's disease. *Alzheimer's & Dementia: Diagnosis, Assessment & Disease Monitoring*, *15*(3), e12477.

Masse, F. A. A., Ansai, J. H., Fiogbe, E., Rossi, P. G., Vilarinho, A. C. G., de Medeiros Takahashi, A. C., & de Andrade, L. P. (2021). Progression of gait changes in older adults with mild cognitive impairment: A systematic review. *Journal of Geriatric Physical Therapy*, *44*(2), 119–124.

McKhann, G. M., Knopman, D. S., Chertkow, H., Hyman, B. T., Jack, C. R., Kawas, C. H., Klunk, W. E., Koroshetz, W. J., Manly, J. J., Mayeux, R., Mohs, R. C., Morris, J. C., Rossor, M. N., Scheltens, P., Carrillo, M. C., Thies, B., Weintraub, S., & Phelps, C. H. (2011). The diagnosis of dementia due to Alzheimer's disease: Recommendations from the National Institute on Aging-Alzheimer's Association workgroups on diagnostic guidelines for Alzheimer's disease. *Alzheimer's & Dementia*, *7*(3), 263–269. https://doi.org/10.1016/j.jalz.2011.03.005

Mehta, P., Pirttila, T., Patrick, B., Barshatzky, M., & Mehta, S. (2001). Amyloid β protein 1–40 and 1–42 levels in matched cerebrospinal fluid and plasma from patients with Alzheimer disease. *Neuroscience Letters*, *304*(1–2), 102–106.

Mintun, M. A., Lo, A. C., Duggan Evans, C., Wessels, A. M., Ardayfio, P. A., Andersen, S. W., Shcherbinin, S., Sparks, J., Sims, J. R., & Brys, M. (2021). Donanemab in early Alzheimer's disease. *New England Journal of Medicine*, *384*(18), 1691–1704.

Mioshi, E., Dawson, K., Mitchell, J., Arnold, R., & Hodges, J. R. (2006). The Addenbrooke's Cognitive Examination Revised (ACE-R): A brief cognitive test battery for dementia screening. *International Journal of Geriatric Psychiatry: A Journal of the Psychiatry of Late Life and Allied Sciences*, *21*(11), 1078–1085.

Modrego, P. J. (2006). Predictors of conversion to dementia of probable Alzheimer type in patients with mild cognitive impairment. *Current Alzheimer Research*, *3*(2), 161–170.

Montez, T., Poil, S.-S., Jones, B. F., Manshanden, I., Verbunt, J. P., van Dijk, B. W., Brussaard, A. B., van Ooyen, A., Stam, C. J., & Scheltens, P. (2009). Altered temporal correlations in parietal alpha and prefrontal theta oscillations in early-stage Alzheimer disease. *Proceedings of the National Academy of Sciences*, *106*(5), 1614–1619.

Moretti, D. V., Miniussi, C., Frisoni, G. B., Geroldi, C., Zanetti, O., Binetti, G., & Rossini, P. M. (2007). Hippocampal atrophy and EEG markers in subjects with mild cognitive impairment. *Clinical Neurophysiology*, *118*(12), 2716–2729. https://doi.org/10.1016/j.clinph.2007.09.059

Mormino, E. C., Brandel, M. G., Madison, C. M., Marks, S., Baker, S. L., & Jagust, W. J. (2012). Aβ deposition in aging is associated with increases in brain activation during successful memory encoding. *Cerebral Cortex*, *22*(8), 1813–1823.

Mormino, E. C., Smiljic, A., Hayenga, A. O., H. Onami, S., Greicius, M. D., Rabinovici, G. D., Janabi, M., Baker, S. L., V. Yen, I., & Madison, C. M. (2011). Relationships between beta-amyloid and functional connectivity in different components of the default mode network in aging. *Cerebral Cortex*, *21*(10), 2399–2407.

Morris, J. (1997). The challenge of characterizing normal brain aging in relation to Alzheimer's disease. *Neurobiology of Aging*, *18*(4), 388–392.

Morris, J. C., Roe, C. M., Xiong, C., Fagan, A. M., Goate, A. M., Holtzman, D. M., & Mintun, M. A. (2010). APOE predicts amyloid-beta but not tau Alzheimer pathology in cognitively normal aging. *Annals of Neurology*, *67*(1), 122–131.

Moscovitch, M., Nadel, L., Winocur, G., Gilboa, A., & Rosenbaum, R. S. (2006). The cognitive neuroscience of remote episodic, semantic and spatial memory. *Current Opinion in Neurobiology*, *16*(2), 179–190.

Mucke, L., & Selkoe, D. J. (2012). Neurotoxicity of amyloid β-protein: Synaptic and network dysfunction. *Cold Spring Harbor Perspectives in Medicine*, *2*(7).

Mukamel, R., Gelbard, H., Arieli, A., Hasson, U., Fried, I., & Malach, R. (2005). Coupling between neuronal firing, field potentials, and FMRI in human auditory cortex. *Science*, *309*(5736), 951–954.

Musaeus, C. S., Engedal, K., Høgh, P., Jelic, V., Mørup, M., Naik, M., Oeksengaard, A.-R., Snaedal, J., Wahlund, L.-O., & Waldemar, G. (2018). EEG theta power is an early marker of cognitive decline in dementia due to Alzheimer's disease. *Journal of Alzheimer's Disease*, *64*(4), 1359–1371.

Myers, R., Schaefer, E., Wilson, P., d'Agostino, R., Ordovas, J., Espino, A., Au, R., White, R., Knoefel, J., & Cobb, J. (1996). Apolipoprotein E element 4 association with dementia in a population-based study: The Framingham Study. *Neurology*, *46*(3), 673–677.

Nelson, P. T., Pious, N. M., Jicha, G. A., Wilcock, D. M., Fardo, D. W., Estus, S., & Rebeck, G. W. (2013). APOE-ε2 and APOE-ε4 correlate with increased amyloid accumulation in cerebral vasculature. *Journal of Neuropathology & Experimental Neurology*, *72*(7), 708–715.

Noble, S., Scheinost, D., & Constable, R. T. (2019). A decade of test-retest reliability of functional connectivity: A systematic review and meta-analysis. *Neuroimage*, *203*, 116157.

Novak, P., Schmidt, R., Kontsekova, E., Kovacech, B., Smolek, T., Katina, S., Fialova, L., Prcina, M., Parrak, V., & Dal-Bianco, P. (2018). FUNDAMANT: an interventional

72-week phase 1 follow-up study of AADvac1, an active immunotherapy against tau protein pathology in Alzheimer's disease. *Alzheimer's Research & Therapy*, *10*(1), 1–16.

Novak, P., Schmidt, R., Kontsekova, E., Zilka, N., Kovacech, B., Skrabana, R., Vince-Kazmerova, Z., Katina, S., Fialova, L., & Prcina, M. (2017). Safety and immunogenicity of the tau vaccine AADvac1 in patients with Alzheimer's disease: A randomised, double-blind, placebo-controlled, phase 1 trial. *The Lancet Neurology*, *16*(2), 123–134.

O'Keefe, J., & Dostrovsky, J. (1971). The hippocampus as a spatial map: Preliminary evidence from unit activity in the freely-moving rat. *Brain Research*.

Osipova, D., Ahveninen, J., Jensen, O., Ylikoski, A., & Pekkonen, E. (2005). Altered generation of spontaneous oscillations in Alzheimer's disease. *NeuroImage*, *27*(4), 835–841. https://doi.org/10.1016/j.neuroimage.2005.05.011

Palmqvist, S., Janelidze, S., Quiroz, Y. T., Zetterberg, H., Lopera, F., Stomrud, E., Su, Y., Chen, Y., Serrano, G. E., & Leuzy, A. (2020). Discriminative accuracy of plasma phospho-tau217 for Alzheimer disease vs other neurodegenerative disorders. *Jama*, *324*(8), 772–781.

Palmqvist, S., Zetterberg, H., Mattsson, N., Johansson, P., For the Alzheimer's Disease Neuroimaging Initiative, Minthon, L., Blennow, K., Olsson, M., For the Swedish BioFINDER study group, Hansson, O., Hansson, O., Minthon, L., Toresson, H., Nägga, K., Palmqvist, S., Stomrud, E., Johansson, P., Nilsson, C., Nilsson, M., … Spicer, K. (2015). Detailed comparison of amyloid PET and CSF biomarkers for identifying early Alzheimer disease. *Neurology*, *85*(14), 1240–1249. https://doi.org/10.1212/WNL.0000000000001991

Parnetti, L., Chiasserini, D., Andreasson, U., Ohlson, M., Hüls, C., Zetterberg, H., Minthon, L., Wallin, Å., Andreasen, N., & Talesa, V. (2011). Changes in CSF acetyl-and butyrylcholinesterase activity after long-term treatment with AChE inhibitors in Alzheimer's disease. *Acta Neurologica Scandinavica*, *124*(2), 122–129.

Pedersen, M., Abbott, D. F., & Jackson, G. D. (2022). Wearable OPM-MEG: A changing landscape for epilepsy. *Epilepsia*, *63*(11), 2745–2753.

Pirttilä, T., Wilcock, G., Truyen, L., & Damaraju, C. (2004). Long-term efficacy and safety of galantamine in patients with mild-to-moderate Alzheimer's disease: Multicenter trial. *European Journal of Neurology*, *11*(11), 734–741.

Pluta, R., & Ułamek-Kozioł, M. (2020). Tau protein-targeted therapies in Alzheimer's disease: Current state and future perspectives. *Exon Publications*, 69–82.

Portelius, E., Westman-Brinkmalm, A., Zetterberg, H., & Blennow, K. (2006). Determination of β-amyloid peptide signatures in cerebrospinal fluid using immunoprecipitation-mass spectrometry. *Journal of Proteome Research*, *5*(4), 1010–1016.

Price, J. L., & Morris, J. C. (1999). Tangles and plaques in nondemented aging and ?preclinical? Alzheimer's disease. *Annals of Neurology*, *45*(3), 358–368. https://doi.org/10.1002/1531-8249(199903)45:3<358::AID-ANA12>3.0.CO;2-X

Proudfoot, M., Woolrich, M. W., Nobre, A. C., & Turner, M. R. (2014). Magnetoencephalography. *Practical Neurology*, *14*(5), 336–343.

Putcha, D., Eckbo, R., Katsumi, Y., Dickerson, B. C., Touroutoglou, A., & Collins, J. A. (2022). Tau and the fractionated default mode network in atypical Alzheimer's disease. *Brain Communications*, *4*(2), fcac055.

Quinn, A. J., Atkinson, L. Z., Gohil, C., Kohl, O., Pitt, J., Zich, C., Nobre, A. C., & Woolrich, M. W. (2024). The GLM-Spectrum: A multilevel framework for spectrum analysis with covariate and confound modelling. *Imaging Neuroscience*, *2*, 1–26.

Quinn, A. J., van Es, M. W. J., Gohil, C., & Woolrich, M. W. (2022). *OHBA Software Library in Python (OSL)* (Version 0.1.1) [Computer software]. [object Object]. https://doi.org/10.5281/ZENODO.6875060

Quinn, A. J., Vidaurre, D., Abeysuriya, R., Becker, R., Nobre, A. C., & Woolrich, M. W. (2018). Task-Evoked Dynamic Network Analysis Through Hidden Markov Modeling. *Frontiers in Neuroscience*, *12*, 603. https://doi.org/10.3389/fnins.2018.00603

Raichle, M. E., MacLeod, A. M., Snyder, A. Z., Powers, W. J., Gusnard, D. A., & Shulman, G. L. (2001). A default mode of brain function. *Proceedings of the National Academy of Sciences*, *98*(2), 676–682.

Ranasinghe, K. G., Cha, J., Iaccarino, L., Hinkley, L. B., Beagle, A. J., Pham, J., Jagust, W. J., Miller, B. L., Rankin, K. P., & Rabinovici, G. D. (2020). Neurophysiological signatures in Alzheimer's disease are distinctly associated with TAU, amyloid-β accumulation, and cognitive decline. *Science Translational Medicine*, *12*(534), eaaz4069.

Ranasinghe, K. G., Petersen, C., Kudo, K., Mizuiri, D., Rankin, K. P., Rabinovici, G. D., Gorno-Tempini, M. L., Seeley, W. W., Spina, S., & Miller, B. L. (2021). Reduced synchrony in alpha oscillations during life predicts post mortem neurofibrillary tangle density in early-onset and atypical Alzheimer's disease. *Alzheimer's & Dementia*, *17*(12), 2009–2019.

Ranasinghe, K. G., Verma, P., Cai, C., Xie, X., Kudo, K., Gao, X., Lerner, H., Mizuiri, D., Strom, A., Iaccarino, L., La Joie, R., Miller, B. L., Gorno-Tempini, M. L., Rankin, K. P., Jagust, W. J., Vossel, K., Rabinovici, G. D., Raj, A., & Nagarajan, S. S. (2022). Altered excitatory and inhibitory neuronal subpopulation parameters are distinctly associated with tau and amyloid in Alzheimer's disease. *bioRxiv*, 2022.03.09.483594. https://doi.org/10.1101/2022.03.09.483594

Ranasinghe, P., & Mapa, M. S. (2024). Functional connectivity and cognitive decline: A review of rs-fMRI, EEG, MEG, and graph theory approaches in aging and dementia. *Exploration of Medicine*, *5*(6), 797–821.

Randolph, C., Tierney, M. C., Mohr, E., & Chase, T. N. (1998). The Repeatable Battery for the Assessment of Neuropsychological Status (RBANS): Preliminary Clinical Validity. *Journal of Clinical and Experimental Neuropsychology*, *20*(3), 310–319. https://doi.org/10.1076/jcen.20.3.310.823

Reisberg, B., Doody, R., Stöffler, A., Schmitt, F., Ferris, S., & Möbius, H. J. (2006). A 24-week open-label extension study of memantine in moderate to severe Alzheimer disease. *Archives of Neurology*, *63*(1), 49–54.

Ricceri, L., Minghetti, L., Moles, A., Popoli, P., Confaloni, A., De Simone, R., Piscopo, P., Scattoni, M. L., di Luca, M., & Calamandrei, G. (2004). Cognitive and neurological deficits induced by early and prolonged basal forebrain cholinergic hypofunction in rats. *Experimental Neurology*, *189*(1), 162–172.

Roberts, G., Holmes, N., Alexander, N., Boto, E., Leggett, J., Hill, R. M., Shah, V., Rea, M., Vaughan, R., & Maguire, E. A. (2019). Towards OPM-MEG in a virtual reality environment. *NeuroImage*, *199*, 408–417.

Rossini, P. M., Desiato, M., Lavaroni, F., & Caramia, M. (1991). Brain excitability and electroencephalographic activation: Non-invasive evaluation in healthy humans via transcranial magnetic stimulation. *Brain Research*, *567*(1), 111–119.

Salimi-Khorshidi, G., Douaud, G., Beckmann, C. F., Glasser, M. F., Griffanti, L., & Smith, S. M. (2014). Automatic denoising of functional MRI data: Combining independent component analysis and hierarchical fusion of classifiers. *Neuroimage*, *90*, 449–468.

Samson-Dollfus, D., Delapierre, G., Do Marcolino, C., & Blondeau, C. (1997). Normal and pathological changes in alpha rhythms. *International Journal of Psychophysiology*, *26*(1–3), 395–409.

Sandusky-Beltran, L., & Sigurdsson, E. (2020). Tau immunotherapies: Lessons learned, current status and future considerations. *Neuropharmacology*, *175*, 108104.

Schöll, M., Lockhart, S. N., Schonhaut, D. R., O'Neil, J. P., Janabi, M., Ossenkoppele, R., Baker, S. L., Vogel, J. W., Faria, J., Schwimmer, H. D., Rabinovici, G. D., & Jagust, W. J. (2016). PET Imaging of Tau Deposition in the Aging Human Brain. *Neuron*, *89*(5), 971–982. https://doi.org/10.1016/j.neuron.2016.01.028

Schoonhoven, D. N., Briels, C. T., Hillebrand, A., Scheltens, P., Stam, C. J., & Gouw, A. A. (2022). Sensitive and reproducible MEG resting-state metrics of functional connectivity in Alzheimer's disease. *Alzheimer's Research & Therapy*, *14*(1), 1–19.

Schumacher, J., Thomas, A. J., Peraza, L. R., Firbank, M., Cromarty, R., Hamilton, C. A., Donaghy, P. C., O'Brien, J. T., & Taylor, J.-P. (2020). EEG alpha reactivity and cholinergic system integrity in Lewy body dementia and Alzheimer's disease. *Alzheimer's Research & Therapy*, *12*, 1–12.

Serrano-Pozo, A., Qian, J., Monsell, S. E., Betensky, R. A., & Hyman, B. T. (2015). APOE ε2 is associated with milder clinical and pathological A lzheimer disease. *Annals of Neurology*, *77*(6), 917–929.

Sevigny, J., Chiao, P., Bussière, T., Weinreb, P. H., Williams, L., Maier, M., Dunstan, R., Salloway, S., Chen, T., & Ling, Y. (2016). The antibody aducanumab reduces Aβ plaques in Alzheimer's disease. *Nature*, *537*(7618), 50–56.

Sevigny, J., Suhy, J., Chiao, P., Chen, T., Klein, G., Purcell, D., Oh, J., Verma, A., Sampat, M., & Barakos, J. (2016). Amyloid PET screening for enrichment of early-stage

Alzheimer disease clinical trials: Experience in a phase 1b clinical trial. *Alzheimer Disease & Associated Disorders*, *30*(1), 1–7.

Sheline, Y. I., Raichle, M. E., Snyder, A. Z., Morris, J. C., Head, D., Wang, S., & Mintun, M. A. (2010). Amyloid plaques disrupt resting state default mode network connectivity in cognitively normal elderly. *Biological Psychiatry*, *67*(6), 584–587.

Shi, F., Liu, B., Zhou, Y., Yu, C., & Jiang, T. (2009). Hippocampal volume and asymmetry in mild cognitive impairment and Alzheimer's disease: Meta-analyses of MRI studies. *Hippocampus*, *19*(11), 1055–1064.

Singh, K. D., Barnes, G. R., Hillebrand, A., Forde, E. M., & Williams, A. L. (2002). Task-related changes in cortical synchronization are spatially coincident with the hemodynamic response. *Neuroimage*, *16*(1), 103–114.

Smallwood, J., Bernhardt, B. C., Leech, R., Bzdok, D., Jefferies, E., & Margulies, D. S. (2021). The default mode network in cognition: A topographical perspective. *Nature Reviews Neuroscience*, *22*(8), 503–513.

Smirnov, D. S., Ashton, N. J., Blennow, K., Zetterberg, H., Simrén, J., Lantero-Rodriguez, J., Karikari, T. K., Hiniker, A., Rissman, R. A., & Salmon, D. P. (2022). Plasma biomarkers for Alzheimer's disease in relation to neuropathology and cognitive change. *Acta Neuropathologica*, *143*(4), 487–503.

Sorg, C., Riedl, V., Muhlau, M., Calhoun, V. D., Eichele, T., Läer, L., Drzezga, A., Förstl, H., Kurz, A., & Zimmer, C. (2007). Selective changes of resting-state networks in individuals at risk for Alzheimer's disease. *Proceedings of the National Academy of Sciences*, *104*(47), 18760–18765.

Sperling, R. A., Dickerson, B. C., Pihlajamaki, M., Vannini, P., LaViolette, P. S., Vitolo, O. V., Hedden, T., Becker, J. A., Rentz, D. M., & Selkoe, D. J. (2010). Functional

alterations in memory networks in early Alzheimer's disease. *Neuromolecular Medicine*, *12*, 27–43.

Squire, L. R., Stark, C. E., & Clark, R. E. (2004). The medial temporal lobe. *Annu. Rev. Neurosci.*, *27*(1), 279–306.

Stam, C. J., Jones, B., Manshanden, I., Van Walsum, A. van C., Montez, T., Verbunt, J. P., de Munck, J. C., van Dijk, B. W., Berendse, H. W., & Scheltens, P. (2006). Magnetoencephalographic evaluation of resting-state functional connectivity in Alzheimer's disease. *Neuroimage*, *32*(3), 1335–1344.

Strijbis, E. M., Timar, Y. S., Schoonhoven, D. N., Nauta, I. M., Kulik, S. D., de Ruiter, L. R., Schoonheim, M. M., Hillebrand, A., & Stam, C. J. (2022). State changes during resting-State (Magneto) encephalographic studies: The effect of drowsiness on spectral, connectivity, and network analyses. *Frontiers in Neuroscience*, *16*, 782474.

Taulu, S., & Simola, J. (2006). Spatiotemporal signal space separation method for rejecting nearby interference in MEG measurements. *Physics in Medicine & Biology*, *51*(7), 1759.

Teng, E., Manser, P. T., Pickthorn, K., Brunstein, F., Blendstrup, M., Sanabria Bohorquez, S., Wildsmith, K. R., Toth, B., Dolton, M., Ramakrishnan, V., Bobbala, A., Sikkes, S. A. M., Ward, M., Fuji, R. N., Kerchner, G. A., Tauriel Investigators, Farnbach, P., Kyndt, C., O'Brien, T., … Weisman, D. (2022). Safety and Efficacy of Semorinemab in Individuals With Prodromal to Mild Alzheimer Disease: A Randomized Clinical Trial. *JAMA Neurology*, *79*(8), 758. https://doi.org/10.1001/jamaneurol.2022.1375

Thal, D. R., Rüb, U., Orantes, M., & Braak, H. (2002). Phases of Aβ-deposition in the human brain and its relevance for the development of AD. *Neurology*, *58*(12), 1791–1800.

Tripathi, V., & Somers, D. C. (2023). Default Mode and Dorsal Attention Network functional connectivity associated with alpha and beta peak frequency in individuals. *Biorxiv*, 2023–02.

Trivedi, M. A., Schmitz, T. W., Ries, M. L., Torgerson, B. M., Sager, M. A., Hermann, B. P., Asthana, S., & Johnson, S. C. (2006). Reduced hippocampal activation during episodic encoding in middle-aged individuals at genetic risk of Alzheimer's disease: A cross-sectional study. *BMC Medicine*, *4*, 1–14.

Vallat, R. (2018). Pingouin: Statistics in Python. *J. Open Source Softw.*, *3*(31), 1026.

Van Der Flier, W. M., van Straaten, E. C., Barkhof, F., Ferro, J., Pantoni, L., Basile, A.-M., Inzitari, D., Erkinjuntti, T., Wahlund, L. O., & Rostrup, E. (2005). Medial temporal lobe atrophy and white matter hyperintensities are associated with mild cognitive deficits in non-disabled elderly people: The LADIS study. *Journal of Neurology, Neurosurgery & Psychiatry*, *76*(11), 1497–1500.

Van der Hiele, K., Vein, A., Reijntjes, R., Westendorp, R., Bollen, E., Van Buchem, M., Van Dijk, J., & Middelkoop, H. (2007). EEG correlates in the spectrum of cognitive decline. *Clinical Neurophysiology*, *118*(9), 1931–1939.

Van Dyck, C. H., Swanson, C. J., Aisen, P., Bateman, R. J., Chen, C., Gee, M., Kanekiyo, M., Li, D., Reyderman, L., & Cohen, S. (2023). Lecanemab in early Alzheimer's disease. *New England Journal of Medicine*, *388*(1), 9–21.

van Es, M. W., Gohil, C., Quinn, A. J., & Woolrich, M. W. (2024). osl-ephys: A Python toolbox for the analysis of electrophysiology data. *arXiv Preprint arXiv:2410.22051*.

Vassar, R., Bennett, B. D., Babu-Khan, S., Kahn, S., Mendiaz, E. A., Denis, P., Teplow, D. B., Ross, S., Amarante, P., & Loeloff, R. (1999). β-Secretase cleavage of Alzheimer's amyloid precursor protein by the transmembrane aspartic protease BACE. *Science*, *286*(5440), 735–741.

Verberk, I. M., Thijssen, E., Koelewijn, J., Mauroo, K., Vanbrabant, J., De Wilde, A., Zwan, M. D., Verfaillie, S. C., Ossenkoppele, R., & Barkhof, F. (2020). Combination of plasma amyloid beta (1-42/1-40) and glial fibrillary acidic protein strongly associates with cerebral amyloid pathology. *Alzheimer's Research & Therapy*, *12*, 1–14.

Verghese, J., Robbins, M., Holtzer, R., Zimmerman, M., Wang, C., Xue, X., & Lipton, R. B. (2008). Gait dysfunction in mild cognitive impairment syndromes. *Journal of the American Geriatrics Society*, *56*(7), 1244–1251.

Vidoni, E. D., Thomas, G. P., Honea, R. A., Loskutova, N., & Burns, J. M. (2012). Evidence of altered corticomotor system connectivity in early-stage Alzheimer's disease. *Journal of Neurologic Physical Therapy*, *36*(1), 8–16.

Vlassenko, A. G., Benzinger, T. L. S., & Morris, J. C. (2012). PET amyloid-beta imaging in preclinical Alzheimer's disease. *Biochimica et Biophysica Acta (BBA) - Molecular Basis of Disease*, *1822*(3), 370–379. https://doi.org/10.1016/j.bbadis.2011.11.005

Vossel, S., Geng, J. J., & Fink, G. R. (2014). Dorsal and ventral attention systems: Distinct neural circuits but collaborative roles. *The Neuroscientist*, *20*(2), 150–159.

Wang, K., Liang, M., Wang, L., Tian, L., Zhang, X., Li, K., & Jiang, T. (2007). Altered functional connectivity in early Alzheimer's disease: A resting-state fMRI study. *Human Brain Mapping*, *28*(10), 967–978.

Wang, Z., Zhang, M., Han, Y., Song, H., Guo, R., & Li, K. (2016). Differentially disrupted functional connectivity of the subregions of the amygdala in Alzheimer's disease. *Journal of X-Ray Science and Technology*, *24*(2), 329–342.

Watson, J. L., Ryan, L., Silverberg, N., Cahan, V., & Bernard, M. A. (2014). Obstacles and opportunities in Alzheimer's clinical trial recruitment. *Health Affairs*, *33*(4), 574–579.

Wechsler, D. (1999). *Wechsler memory scale third UK E*.

Weiler, M., Fukuda, A., HP Massabki, L., M Lopes, T., R Franco, A., P Damasceno, B., Cendes, F., & LF Balthazar, M. (2014). Default mode, executive function, and language functional connectivity networks are compromised in mild Alzheimer s disease. *Current Alzheimer Research*, *11*(3), 274–282.

Weingarten, M. D., Lockwood, A. H., Hwo, S. Y., & Kirschner, M. W. (1975). A protein factor essential for microtubule assembly. *Proceedings of the National Academy of Sciences*, *72*(5), 1858–1862. https://doi.org/10.1073/pnas.72.5.1858

Welch, P. (1967). The use of fast Fourier transform for the estimation of power spectra: A method based on time averaging over short, modified periodograms. *IEEE Transactions on Audio and Electroacoustics*, *15*(2), 70–73.

Welge, V., Fiege, O., Lewczuk, P., Mollenhauer, B., Esselmann, H., Klafki, H.-W., Wolf, S., Trenkwalder, C., Otto, M., Kornhuber, J., Wiltfang, J., & Bibl, M. (2009). Combined CSF tau, p-tau181 and amyloid-β 38/40/42 for diagnosing Alzheimer's disease. *Journal of Neural Transmission*, *116*(2), 203–212. https://doi.org/10.1007/s00702-008-0177-6

Westmoreland, B. F., & Klass, D. W. (1998). Defective alpha reactivity with mental concentration. *Journal of Clinical Neurophysiology*, *15*(5), 424–428.

Winblad, B., Wimo, A., Engedal, K., Soininen, H., Verhey, F., Waldemar, G., Wetterholm, A.-L., Haglund, A., Zhang, R., & Schindler, R. (2006). 3-year study of donepezil therapy in Alzheimer's disease: Effects of early and continuous therapy. *Dementia and Geriatric Cognitive Disorders*, *21*(5–6), 353–363.

Wischik, C., Novak, M., Edwards, P., Klug, A., Tichelaar, W., & Crowther, R. (1988). Structural characterization of the core of the paired helical filament of Alzheimer disease. *Proceedings of the National Academy of Sciences*, *85*(13), 4884–4888.

Wisdom, N. M., Callahan, J. L., & Hawkins, K. A. (2011). The effects of apolipoprotein E on non-impaired cognitive functioning: A meta-analysis. *Neurobiology of Aging*, *32*(1), 63–74.

Woolrich, M. W., Ripley, B. D., Brady, M., & Smith, S. M. (2001). Temporal autocorrelation in univariate linear modeling of FMRI data. *Neuroimage*, *14*(6), 1370–1386.

Wu, H., Song, Y., Yang, X., Chen, S., Ge, H., Yan, Z., Qi, W., Yuan, Q., Liang, X., & Lin, X. (2023). Functional and structural alterations of dorsal attention network in preclinical and early-stage Alzheimer's disease. *CNS Neuroscience & Therapeutics*, *29*(6), 1512–1524.

Wu, M., Zhang, M., Yin, X., Chen, K., Hu, Z., Zhou, Q., Cao, X., Chen, Z., & Liu, D. (2021). The role of pathological tau in synaptic dysfunction in Alzheimer's diseases. *Translational Neurodegeneration*, *10*, 1–11.

Yasuno, F., Tanimukai, S., Sasaki, M., Hidaka, S., Ikejima, C., Yamashita, F., Kodama, C., Mizukami, K., Michikawa, M., & Asada, T. (2012). Association between cognitive function and plasma lipids of the elderly after controlling for apolipoprotein E genotype. *The American Journal of Geriatric Psychiatry*, *20*(7), 574–583.

Yoon, B., Choi, S. H., Jeong, J. H., Park, K. W., Kim, E.-J., Hwang, J., Jang, J.-W., Kim, H. J., Hong, J. Y., & Lee, J.-M. (2020). Balance and mobility performance along the Alzheimer's disease spectrum. *Journal of Alzheimer's Disease*, *73*(2), 633–644.

Zhan, Y., Ma, J., Alexander-Bloch, A. F., Xu, K., Cui, Y., Feng, Q., Jiang, T., Liu, Y., & Alzheimer's Disease Neuroimaging Initiative. (2016). Longitudinal study of impaired intra-and inter-network brain connectivity in subjects at high risk for Alzheimer's disease. *Journal of Alzheimer's Disease*, *52*(3), 913–927.

Zhang, Z., Zheng, H., Liang, K., Wang, H., Kong, S., Hu, J., Wu, F., & Sun, G. (2015). Functional degeneration in dorsal and ventral attention systems in amnestic mild

cognitive impairment and Alzheimer's disease: An fMRI study. *Neuroscience Letters*, *585*, 160–165.

Zumer, J. M., Brookes, M. J., Stevenson, C. M., Francis, S. T., & Morris, P. G. (2010). Relating BOLD fMRI and neural oscillations through convolution and optimal linear weighting. *Neuroimage*, *49*(2), 1479–1489.

Appendix 1 – Contributions to the NTAD study

Large multi-modal, multi-site studies are simply not possible without the effort of many individuals. The following section will outline the numerous individuals involved in the NTAD study that are relevant to this DPhil.

Contributions to the NTAD study

Professor James Rowe, Professor Kia Nobre, Professor Mark Woolrich, Professor Rik Hension, Professor Krish Singh, Dr John Isaac, Dr Vanessa Raymont, Dr Micharl Parkinton, Dr Giacomo Salvadore, Dr Stephen Lowe were involved in the design of the study across all sites. Local study coordinators and NHS research staff were involved in the study set-up.

Specific to the Oxford site, Dr Eduardo Ostinelli, Dr Katherine Smith and Dr Caroline Zangani undertook the detailed screening of all participants who entered the study. Mr Tony Thayanandan helped with the setup of the study, assisted with contractual aspects, and completed training for DPhil students and research assistants on the cognitive tests. My contributions involved the initial setup of the study at the Oxford site, recruiting patients, and organising and conducting all visits including screening, MEEG data collection, MRI data collection, and neuropsychological testing. Other DPhil students and research assistants who assisted with various baseline visits include Mr Oliver Kohl, Miss Lara Bolte, Dr Giedre

Cepukaityte and Mr Oscar Haines. The NTAD data in this thesis has been analysed independently and is the result of my own work.

Appendix 2 – NTAD inclusion criteria and schedule of events

Table 1. Group inclusion criteria and general exclusion criteria.

<table>
<tr><th colspan="2">Group specific inclusion criteria</th></tr>
<tr><th>Controls</th><th>Patients</th></tr>
<tr><td>• No history of memory issues
• CDR = 0
• MMSE > 24
• 50 – 85 years old
• Negative AD biomarker status
• Study partner available</td><td>• Diagnosis of MCI or AD
• CDR = 0.5 – 1
• MMSE >18
• 50 – 85 years old
• Positive biomarker status
• Able to provide informed consent
• Study partner available</td></tr>
<tr><th colspan="2">General exclusion criteria (both controls and patients)</th></tr>
<tr><td colspan="2">• Significant neurological disease, other than AD, that my affect cognition.
• Presence of any significant psychiatric disorder that could affect participation.
• Any clinically important abnormality that could compromise study participation.
• A clinically significant illness, medical or surgical procedure, or trauma within 30 days prior to screening or baseline.
• Known or suspected systemic infection.</td></tr>
</table>

- Medications affecting cognition, unless on a stable dose for >30 days prior to baseline
- Rosen Modified Hachinski Ischaemic score >= 4.
- History of seizure, expect febrile seizures or single provoked seizure.
- Head trauma resulting in protracted loss of consciousness, or serious infectious disease affecting the brain, within five years of screening and baseline.
- Participation in a clinical trial of an investigational medicinal product
- Impairment of vision or hearing that could affect study participation .
- Formal education <= 7 years.
- Inability to read and write fluently in English.
- Inability to walk 10 meters independently.
- Contraindications of blood sampling, lumbar puncture (e.g., spinal deformations), amyloid PET scan, MRI or MEEG recordings as judged by the Investigator.

Table 2. Schedule of events for controls.

Visit	1	2	3	4	5	6	7	8	9
Visit Type	Screening	Baseline	Baseline	Baseline	2 weeks	Annual follow up 1	Annual follow up 1	Annual follow up 1	Annual follow up 2
Time (Months)	-1	0	0	0	0.5	12	12	12	24
Procedures									
Screening	X								
Venepuncture	X								
Consent	X	X	X	X					
Clinical & Cognitive Measures									
Clinical interview	X								
Clinical assessments	X								
Neuropsychological assessments				X					
Imaging									
PET or CSF option	X								
MRI			X						
MEEG		X							

Table 3. Schedule of events for patients.

Visit	1	2	3	4	5	6	7	8	9

Visit Type	Screening	Baseline	Baseline	Baseline	2 weeks	Annual follow up 1	Annual follow up 1	Annual follow up 1	Annual follow up 2
Time (Months)	-1	0	0	0	0.5	12	12	12	24
Procedures									
Screening	X								
Venepuncture	X					X			
Consent	X	X	X	X	X	X	X	X	X
Clinical & Cognitive Measures									
Clinical interview	X					X			X
Clinical assessments	X					X			X
Neuropsychological assessments				X		X			X
Imaging									
PET or CSF option	X								
MRI			X					X	
MEEG		X			X		X		

Appendix 3 – MEG experimental task details.

During the MEG scan, participants completed tasks in the following order:

1. **Audio-visual task**

Participants fixated on a red, central fixation dot on the screen in front of them and were asked to press a button on the button box when they heard or saw something on the screen. Auditory stimuli comprised of tones (n=100) of 300Hz, 600Hz or 1200Hz which were presented for 300ms after an interval of 100ms. Visual stimuli comprised of a concentric black and white circle that appeared for 300ms after a delay of 3000ms. Filler trials (n=30) contained only the red fixation dot. The visual and auditory trials were randomly intermixed and 10 initial practice trials were shown to the participant to familiarise them to the task.

2. **Auditory mismatch-negativity task**

The roving auditory mismatch negativity task was designed to elicit error responses to deviant tones followed by rapid plasticity as predictions are updated. Participants passively watched a muted nature documentary and heard binaural, in-phase sinusoidal tones durations of 100ms and 500ms. Tone frequencies were the same within but different between blocks. Blocks ranged from 400Hz to 800Hz. The number of tones varied from 3 to 11 according to a truncated exponential distribution.

3. **Scene-repetition task**

Participants viewed a series of complex scenes (landscapes and cityscapes) and were asked to press a button on the button box when the scene contained a moon (n=26 different moon images). Target scenes containing the mood ensure attention but are not of interest. The main interest is the difference between initial and repeated presentation of non-target scenes. Each

scene is presented for 800ms and preceded by a fixation cross of 200ms. Scenes are pseudo-randomised.

4. Cross-model oddball task

This task was designed to assess hippocampal-dependent paired-associates learning. Participants were asked to learn associations between four visual objects and sounds. Trials comprised of 700ms visual, abstract 'object' and a 400ms sound, starting 300ms after trial onset. There was an initial training period (80 trials) with a 10-item assessment that followed the task, where participants heard a sound and was asked to report which of the four objects the sound was paired with most during the task. The main task had 770 bimodal trials and 40 unimodal trials, randomly intermixed. Bimodal trials consisted of standard, learnt object-sound pairs (n=670), standard objects paired with novel sounds (n=50), and mismatched pairs, where the object and sound are from different standard pairs (n=50). The participant completed the same 10-item assessment after the main task was completed.

5. Resting state (eyes-open), and 6. resting state (eyes-closed)

Participants were asked to clear their mind, relax, and stay awake with either (1) eyes-open or (2) eyes-closed. The eyes-open condition included a central fixation cross on the screen, and the screen was turned off during the eyes-closed condition.

Full MEG protocol details, including figures of each task, can be found at Lanskey et al. (2022).